

# **Inflammatory Gene Regulation in Chronic Prostatitis / Chronic Pelvic Pain Syndrome (CP/CPPS) and Prostate Cancer**

A thesis submitted in accordance with the assigned joint award doctoral program in fulfillment of the requirements for the degree of Doctor of Philosophy (PhD)

to the Faculties of Veterinary Medicine and Medicine  
of the Justus Liebig University Giessen

and the Faculty of Medicine, Nursing and Health Sciences  
of the Monash University Melbourne

Submitted by

Nils Martin Nesheim

born on 17 December 1986

in Frankfurt am Main, Germany

Gießen, 2020

From the  
Department of Urology, Pediatric Urology and Andrology  
of the Faculty of Medicine  
at the Justus-Liebig-University (JLU) Giessen

and the  
Department of Anatomy and Developmental Biology  
of the Faculty of Medicine, Nursing and Health Sciences  
at the Monash-University (MU) Melbourne

Supervision

*JLU Supervisor:* Prof. Dr. rer. nat. Undraga Schagdarsurengin, JLU Giessen

*JLU Supervisor:* Prof. Dr. med. Florian Wagenlehner, JLU Giessen

*JLU Co-Supervisor:* Prof. Dr. rer. nat. Martin Bergmann, JLU Giessen

*MU Supervisor:* Dr. Stuart Ellem, University of Southern Queensland

*MU Supervisor:* Prof. Gail Risbridger, MU Melbourne

Examination

*JLU Supervisors and Reviewers:* Prof. Dr. rer. nat. Undraga Schagdarsurengin and  
Prof. Dr. med. Florian Wagenlehner, JLU Giessen

*External Reviewer for JLU:* Prof. Dr. rer. nat. Susanne Füssel, Technical University, Dresden

*External Reviewer for MU:* Prof. Arunasalam Dharmarajan, Curtin University, Western Australia

*External Reviewer for MU:* Dr. Catherine McDermott, Bond University, Gold Coast, Queensland

Day of thesis defence:

10 February 2020

# **Copyright Notice**

## **Notice 1**

Under the Copyright Act 1968, this thesis must be used only under the normal conditions of scholarly fair dealing. In particular no results or conclusions should be extracted from it, nor should it be copied or closely paraphrased in whole or in part without the written consent of the author. Proper written acknowledgement should be made for any assistance obtained from this thesis.

## **Notice 2**

I certify that I have made all reasonable efforts to secure copyright permissions for third-party content included in this thesis and have not knowingly added copyright content to my work without the owner's permission.

# Declaration of Authorship

## Declaration (Monash-University)

This thesis is an original work of my research and contains no material which has been accepted for the award of any other degree or diploma at any university or equivalent institution. To the best of my knowledge and belief, this thesis contains no material previously published or written by another person, except where due reference is made in the text of the thesis.

## Erklärung zur Dissertation (Justus-Liebig-Universität)

Hiermit erkläre ich, dass ich die vorliegende Arbeit selbständig und ohne unzulässige Hilfe oder Benutzung anderer als der angegebenen Hilfsmittel angefertigt habe. Alle Textstellen, die wörtlich oder sinngemäß aus veröffentlichten oder nichtveröffentlichten Schriften entnommen sind, und alle Angaben, die auf mündlichen Auskünften beruhen, sind als solche kenntlich gemacht. Bei den von mir durchgeführten und in der Dissertation erwähnten Untersuchungen habe ich die Grundsätze guter wissenschaftlicher Praxis, wie sie in der „Satzung der Justus-Liebig-Universität Gießen zur Sicherung guter wissenschaftlicher Praxis“ niedergelegt sind, eingehalten sowie ethische, datenschutzrechtliche und tierschutzrechtliche Grundsätze befolgt. Ich versichere, dass Dritte von mir weder unmittelbar noch mittelbar geldwerte Leistungen für Arbeiten erhalten haben, die im Zusammenhang mit dem Inhalt der vorgelegten Dissertation stehen, oder habe diese nachstehend spezifiziert. Die vorgelegte Arbeit wurde weder im Inland noch im Ausland in gleicher oder ähnlicher Form einer anderen Prüfungsbehörde zum Zweck einer Promotion oder eines anderen Prüfungsverfahrens vorgelegt. Alles aus anderen Quellen und von anderen Personen übernommene Material, das in der Arbeit verwendet wurde oder auf das direkt Bezug genommen wird, wurde als solches kenntlich gemacht. Insbesondere wurden alle Personen genannt, die direkt und indirekt an der Entstehung der vorliegenden Arbeit beteiligt waren. Mit der Überprüfung meiner Arbeit durch eine Plagiatserkennungssoftware beziehungsweise ein internetbasiertes Softwareprogramm erkläre ich mich einverstanden.

Print Name: Nils Nesheim

Place, Date: \_\_\_\_\_ Berlin, 2 April 2020 \_\_\_\_\_ Signature: \_\_\_\_\_

# Zusammenfassung

Chronische Prostatitis/Chronisches Beckenschmerzen-Syndrom (CP/CPPS) ist eine chronisch entzündliche Erkrankung mit unklarer Ätiologie, hohem Leidensdruck und begünstigt im fortgeschrittenen Alter die Entstehung des Prostatakarzinoms (PCa). CP/CPPS und PCa gehen mit Veränderungen der Steroid-Sexhormone und der Immunantwort einher. Durch ausgiebige Charakterisierung des PCa Stroma konnte außerdem gezeigt werden, dass tumor-assoziierte Makrophagen (TAM), Mastzellen und krebsassoziierte Fibroblasten (CAF) den Krankheitsverlauf maßgeblich mitbestimmen. Der Einfluss stromaler Zellen auf CP/CPPS hingegen ist aufgrund des Mangels von Gewebe-Biopsien weniger gut verstanden.

In der vorliegenden Arbeit wurden Flüssig-Biopsien (Blut und Ejakulat) auf CP/CPPS-assoziierte Veränderungen von Östradiol (E2), Testosteron und ihrer Rezeptoren, der Östrogen-Rezeptoren ER $\alpha$  und ER $\beta$  (Gene: *ESR1*, *ESR2*) sowie des Androgen-Rezeptors (*AR*) untersucht. Um den Einfluss stromaler Zellen auf die Pathogenese von CP/CPPS und PCa zu untersuchen, wurden die Mastzell-Linien HMC-1 und LAD2, *in vitro* differenzierter Makrophagen (THP-1) und krebsassoziierte Fibroblasten (CAF) aus Prostataktomie-Gewebe charakterisiert.

Unsere Ergebnisse zeigten, dass CP/CPPS mit einer erhöhten E2-Konzentration im Seminalplasma (SP) sowie systemischer (Blut) und organ-spezifischer (Ejakulat) *ESR1* Herunterregulation assoziiert ist. Stratifizierung der CP/CPPS Patienten nach Alter konnte zudem herausstellen, dass Testosteron, E2 und ihre Rezeptoren (ER $\alpha$ , ER $\beta$  und AR) in älteren Patienten (>40 Jahre) herunterreguliert sind. Die Mastzell-Linien (HMC-1/LAD2) unterschieden sich maßgeblich im Hinblick auf die Expression von Östrogen-Rezeptoren (ER $\alpha$ /ER $\beta$ ), der basalen Expression inflammatorisch relevanter Gene und ihrer Antwort auf E2-Stimulation. Makrophagen-Polarisation mit konditioniertem Medium (CM) zeigte darüber hinaus, dass Mastzellen und primäre CAF die Makrophagen-Antwort beeinflussen. Mastzell CM unterdrückte Makrophagen-Expression von Transkripten der tumoriziden M1-Immunantwort (*TNF* und *HLA-DQAI*). CAF CM induzierte Makrophagen-Expression von Transkripten (*IL-1 $\beta$*  und *IL-10*) mit nachweislicher Assoziation zur Prostata-Karzinogenese. Unsere Co-Kultur Experimente legen nahe, dass Makrophagen die stromal/epitheliale Interaktion beeinflussen und die gerichtete Zellmigration stimulieren.

Unsere Studie trägt zum Verständnis vom Einfluss der Sexualhormone und stromaler Interaktionen auf chronisch entzündliche Erkrankungen der Prostata bei.

# Abstract

Chronic Prostatitis/Chronic Pelvic Pain Syndrome (CP/CPPS) is a chronic inflammatory disease with unclear etiology, high disease burden and increases the risk for prostate cancer (PCa) development at a later age. CP/CPPS and PCa manifest with altered sex hormone signaling and inflammatory dysregulation. Extensive characterization of the PCa stroma showed that tumor-associated macrophages (TAM), mast cells and cancer-associated fibroblasts (CAF) significantly influence disease progression. Tissue biopsies of CP/CPPS patients however are rare, and consequently the stromal contributions to CP/CPPS are less understood.

In this study, we examined liquid biopsies (blood and ejaculate) for CP/CPPS-associated changes of estradiol (E2), testosterone and their cognate receptors ER $\alpha$  and ER $\beta$  (genes: *ESR1*, *ESR2*) as well as the androgen receptor (*AR*). To examine the role of stromal cells for CP/CPPS and PCa pathogenesis, we characterized mast cell lines (HMC-1/LAD2), *in vitro* differentiated macrophages (THP-1) and cancer-associated fibroblasts (CAF) from prostatectomy tissue.

Our results demonstrated that CP/CPPS associates with elevated E2 concentrations in seminal plasma (SP), as well as systemic (blood) and local (ejaculate) *ESR1* downregulation. Stratification of CP/CPPS patients by age could additionally show that testosterone, E2 and their receptors (ER $\alpha$ , ER $\beta$  and AR) undergo systemic downregulation in older patients (>40 years). The two mast cell lines (HMC-1/LAD2) differed considerably regarding their estrogen receptor (ER $\alpha$ , ER $\beta$ ) expression, their basal inflammatory gene expression and their response to E2-stimulation. Macrophage polarization with conditioned media (CM) showed that mast cells and primary CAF affect the macrophage response. Mast cell CM suppressed macrophage expression of transcripts from the tumoricidal M1-response (*TNF* and *HLA-DQA1*). CAF CM induced macrophage transcripts (*IL-1 $\beta$*  and *IL-10*) with known associations to prostate carcinogenesis. Our co-culture experiments suggest that macrophages influence stromal/epithelial interactions and facilitate directed cell migration.

Altogether, our study helps to clarify the roles of steroid sex hormones and stromal interactions for chronic inflammatory diseases of the prostate.

# Table of Contents

<b>COPYRIGHT NOTICE</b> .....	<b>3</b>
<b>DECLARATION OF AUTHORSHIP</b> .....	<b>4</b>
<b>ZUSAMMENFASSUNG</b> .....	<b>5</b>
<b>ABSTRACT</b> .....	<b>6</b>
<b>TABLE OF CONTENTS</b> .....	<b>7</b>
<b>LIST OF TABLES</b> .....	<b>10</b>
<b>LIST OF FIGURES</b> .....	<b>10</b>
<b>INTRODUCTION</b> .....	<b>12</b>
1) Chronic prostatitis/chronic pelvic pain syndrome (CP/CPPS).....	12
2) CP/CPPS presents a risk factor for prostate carcinoma (PCa) .....	13
3) The role of sex hormones for CP/CPPS and PCa.....	13
4) Stromal fibroblasts in CP/CPPS and PCa .....	15
5) Mast cells influence CP/CPPS and PCa.....	17
6) Macrophages in CP/CPPS and PCa .....	18
7) Oxidative stress and its role for prostate diseases .....	19
8) The epigenetic effects of inflammation and oxidative stress .....	21
9) The relevance of epigenetics for CP/CPPS and PCa.....	24
10) Summary: Basic research on CP/CPPS and the link to PCa is needed.....	25
<b>AIMS</b> .....	<b>25</b>
1) Investigation of the mast cell response to estradiol stimulation.....	26
2) Analysis of clinical routine parameters from CP/CPPS patients .....	27
3) Isolation of somatic cells from human semen samples .....	28
4) Detection of leukocyte-specific transcripts in somatic cells from semen .....	28
5) Detection of CP/CPPS-related changes of steroid sex hormone signaling .....	29
6) Studies of the stromal influence on macrophage polarization .....	30
7) Investigation of macrophage interactions with the prostate tumor stroma .....	31
8) Summary of study aims .....	32

<b>MATERIAL &amp; METHODS .....</b>	<b>33</b>
1) Collection and clinical routine analysis of liquid biopsy samples .....	33
2) Isolation of circulating white blood cells and ejaculated somatic cells .....	36
3) Isolation of human primary prostate fibroblasts (NPF/CAF).....	37
4) Culture of primary fibroblasts (NPF/CAF) and immortalized cell lines.....	37
5) Preparation of Conditioned Media .....	39
6) Macrophage differentiation and polarization from THP-1 cells .....	39
7) Estradiol stimulation of mast cell lines and macrophages .....	41
8) Nucleic acid isolation .....	42
9) Gene expression analysis .....	43
10) Gene promotor CpG methylation analysis .....	45
11) Western Blot of CCL18 in E2-treated THP-derived macrophages.....	48
12) Chromatin immunoprecipitation .....	49
13) Co-Culture Assays.....	51
14) Fluorescence imaging of co-culture assays.....	52
15) Quantification of fluorescent imaging data.....	52
16) Statistical Analysis .....	53
<b>RESULTS .....</b>	<b>54</b>
1) Estradiol affects the mast cell response.....	56
2) CP/CPPS affects patient semen parameters .....	66
3) Density gradient allows isolation of somatic cells from semen .....	68
4) Somatic cells from semen show leukocyte-specific gene transcription.....	69
5) CP/CPPS associates with aberrant steroid sex hormone signaling .....	71
6) Stromal cells affect the macrophage response .....	80
7) Macrophages affect stromal/epithelial interactions during co-culture.....	92
8) Summary of results.....	102
<b>DISCUSSION .....</b>	<b>103</b>
1) Intra-prostatic acidosis might trigger inflammation in CP/CPPS .....	104
2) Zinc depletion in CP/CPPS could present a risk factor for PCa .....	105
3) CP/CPPS patients display signs of macrophage activation in their semen....	106
4) Mast cell lines allow mechanistic studies of estrogen signaling.....	108
5) Decline of ER $\alpha$ signaling presents a potential CP/CPPS pathomechanism...	110
6) Prostatic estradiol might promote prostate cancer initiation in CP/CPPS .....	113
7) Ageing CP/CPPS patients experience a sex hormone decline .....	115

8) The role of E2 signaling for inflammation is contextual .....	117
9) The CAF-induced interleukins <i>IL1B</i> and <i>IL-10</i> are associated with PCa .....	119
10) Epithelial cells affect the macrophage phenotype.....	121
11) CAF from high grade prostate tumors induce macrophage <i>CCL18</i> .....	121
12) CAF-secreted <i>SFRP-1</i> likely affects macrophage WNT signaling.....	123
13) Mast cells suppress the pro-inflammatory macrophage response.....	124
14) Co-culture assays support a CAF-mediated epithelial transformation.....	125
15) Macrophages disturb prostate tissue integrity and stimulate cell migration	127
<b>LIMITATIONS &amp; FUTURE PROSPECTS .....</b>	<b>130</b>
1) Our liquid biopsy analysis is limited to Pyrosequencing and RT-qPCR .....	130
2) Androgen signaling in CP/CPPS patients is not fully characterized.....	130
3) <i>BMP7</i> inactivation could imply loss of TGF- $\beta$ signaling in CP/CPPS.....	131
4) Extended characterization of leukocytes from semen.....	132
5) Isolation and analysis of fibroblasts from expressed prostatic secretions.....	132
6) Conditioned media experiments affect activated macrophages differently ...	133
7) More detailed analysis of Wnt signaling in CAF-educated macrophages .....	134
8) Macrophage polarization with seminal plasma from CP/CPPS patients .....	135
9) Interrogate the effect of benign-associated fibroblasts on macrophages .....	135
10) Characterization of macrophages after co-culture experiments.....	135
11) Repetition of mast cell culture experiments.....	136
<b>LIST OF REFERENCES .....</b>	<b>137</b>
<b>LIST OF ABBREVIATIONS .....</b>	<b>153</b>
<b>LIST OF EQUIPMENT, CHEMICALS AND LABWARE .....</b>	<b>157</b>

## List of Tables

Table 1: Clinical routine parameters from CP/CPPS patients and healthy donors. ....	35
Table 2. Primers used for quantitative reverse transcription PCR (RT-qPCR). ....	44
Table 3. CpG assays for promotor CpG methylation analysis. ....	46
Table 4. Methylation analysis of gene promotor CpG sites in HMC-1 and LAD2 cells. ....	58
Table 5. Basal inflammatory gene expression in unstimulated HMC-1 and LAD2 cells. ....	63
Table 6. E2-regulated gene candidates in HMC-1 or LAD2 cells. ....	65
Table 7. Clinical parameters of CAF-origin tumors. ....	87
Table 8. Stratification of educated macrophages by confidence of CAF identity/activation...	89

## List of Figures

Figure 1. Gene silencing by hypermethylation of promotor CpG islands. ....	21
Figure 2. Chronic inflammation promotes <i>de novo</i> DNA methylation and cancer.....	23
Figure 3. Schematic of the experiments with mast cell lines. ....	26
Figure 4. Schematic of clinical routine diagnostics in the case-controlled CP/CPPS study....	27
Figure 5. Schematic of the semen separation into sperm cells and somatic cells. ....	28
Figure 6. Schematic of the steroid sex hormone profiling of liquid biopsy samples. ....	29
Figure 7. Schematic of the conditioned media experiments. ....	30
Figure 8. Mast cell conditioned media affects co-cultured BPH-1 cells.....	31
Figure 9. Experimental outline of co-culture experiments.....	31
Figure 10. Recovery of ejaculated somatic by density gradient centrifugation. ....	36
Figure 11. Schematic of macrophage polarization experiments. ....	40
Figure 12. The concept behind pyrosequencing of gene promotor CpG sites. ....	45
Figure 13. HMC-1 and LAD2 cells display different epigenetic states of <i>ESR1</i> and <i>ESR2</i> . ...	56
Figure 14. <i>De novo</i> methylated genes are downregulated in E2-treated HMC-1 cells.....	60
Figure 15. Pyrosequencing of <i>TLR2</i> CpG sites from the methylation profiler array. ....	61
Figure 16. HMC-1 and LAD2 show different basal gene expression and E2-responses.....	62
Figure 17. E2-responsive genes undergo different regulations in HMC-1 and LAD2 cells....	64
Figure 18. Cohort age and semen parameters of CP/CPPS patients and healthy volunteers...	67
Figure 19. Pyrosequencing of separated sperm cells and somatic cells from human semen...	68

Figure 20. Ejaculated somatic cell populations of CP/CPPS patients are affected.....	69
Figure 21. <i>BMP7</i> is E2-responsive and hypermethylated in CP/CPPS ejaculate. ....	70
Figure 22. Blood and semen E2 levels correlate with blood testosterone and each other .....	72
Figure 23. CP/CPPS associates with aberrant systemic and organ-confined E2-signaling. ....	73
Figure 24. Semen estradiol concentrations correlate with urinary tract symptoms. ....	74
Figure 25. <i>ESR1</i> transcript levels in circulating WBC and ejaculated SC correlate.....	74
Figure 26. CP/CPPS patient age correlates with testosterone, estradiol and IL-8 levels.....	76
Figure 27. CP/CPPS patients >40 years show systemic decline of testosterone and E2. ....	78
Figure 28. Some aberrations of <i>ESR1</i> , <i>ESR2</i> , <i>AR</i> happen in exclusively patients >40years....	79
Figure 29. LPS/IFN $\gamma$ and IL-4/IL-13 produce distinct macrophage phenotypes.....	81
Figure 30. LAD2 cells suppress macrophage expression of <i>TNF</i> and <i>HLA-DQAI</i> . ....	82
Figure 31. CAF-educated macrophages upregulate <i>IL-1B</i> , <i>IL-10</i> and downregulate <i>CD206</i> . .	83
Figure 32. CAF-specific marker gene expression in CAF and NPF.....	85
Figure 33. Pairwise comparison of high and low confidence CAF with matched NPF. ....	86
Figure 34. Stratification of CAF and patient-matched NPF by CAF-origin tumor grade. ....	88
Figure 35. NPF/CAF expression of <i>SFRP1</i> correlates with macrophages marker transcripts. 90	
Figure 36. E2-mediated <i>CCL18</i> upregulation in M2 macrophages is directed by ER $\alpha$ .....	91
Figure 37. Binarization allows quantification of confocal images.....	92
Figure 38. Co-cultures with CAF display an increased F-Actin homogeneity and density.....	92
Figure 39. M2 macrophages disrupt the F-Actin staining in co-culture with NPF.....	93
Figure 40. Macrophages induce significant changes of F-Actin staining and BPH-1 cells.....	94
Figure 41. Live cell imaging results support CAF-specific effects on BPH-1 circularity. ....	95
Figure 42. CAF promote directed BPH-1 migration.....	96
Figure 43. Live cell imaging confirms that M2 macrophages increase BPH-1 circularity.....	97
Figure 44. M2 macrophages do not increase the proliferation of co-cultured BPH-1 cells.....	98
Figure 45. Highly motile BPH-1 cells have a high average circularity. ....	99
Figure 46. M2 macrophages affect the frequencies of motile BPH-1 cells. ....	100
Figure 47. M2 macrophages increased the BPH-1 motility more than M1 macrophages. ....	101

# Introduction

CP/CPPS is a debilitating, chronic inflammatory condition with high disease burden that warrants extensive basic and clinical research. Up to 16% of men develop chronic prostatitis/chronic pelvic pain syndrome (CP/CPPS) during their lifetime [1]. CP/CPPS significantly increases the risk for the development of prostate carcinoma (PCa) [2] and may also increase the chance for benign prostatic hyperplasia (BPH), another highly prevalent prostate condition that ~90% of men develop by the age of 80 [3]. Around 11.6% of all men develop PCa [4], with an estimated 1.1 million men worldwide diagnosed with PCa in 2012 and about 307,000 PCa deaths in the same year [5]. This makes PCa the fifth leading cancer death among men. The high prevalence and morbidity of CP/CPPS, as well as the possible link to BPH and PCa stresses the need for the development of reliable molecular markers and treatment strategies.

## 1) Chronic prostatitis/chronic pelvic pain syndrome (CP/CPPS)

CP/CPPS is characterized by ongoing pelvic pain and urinary tract symptoms without detectable pathogens or identifiable aetiology, and various other signs and symptoms that assign the syndrome to the class of chronic inflammatory and perhaps autoimmune disorders [6]. There is currently no reliable biomarker for CP/CPPS. Instead, classification as inflammatory (IIIa: leukocytes) or non-inflammatory (IIIb: no leukocytes) CP/CPPS is based on the presence or absence of leukocytes in expressed prostatic secretions (EPS) of post prostatic massage urine [7]. However, this classification does not have implications for differential treatment [8], nor does the presence of leukocytes in prostatic secretions correlate with the severity of symptoms [9]. Instead, it was the introduction of a multimodal treatment system (UPOINT) with symptom-specific patient stratification that has led to significant advances in disease management [10, 11], indicating that multiple disease entities could be concealed behind the diagnosis CP/CPPS. Nevertheless, there are no reliable biomarkers for CP/CPPS, and the underlying pathophysiology is still poorly understood, so the syndrome is still treated in a phenotype-directed manner. Prostate biopsies in patients with CP/CPPS are not routinely performed, which further complicates the study of this heterogeneous disease.

Since primary patient material is typically limited to clinical liquid biopsies, multiple animal models have been developed in order to study the pathophysiology. These include autoimmune mouse models where prostatic inflammation is induced by the immunization with prostate antigen (PAG) [12] or manipulations of the steroid sex hormones [13, 14].

## **2) CP/CPPS presents a risk factor for prostate carcinoma (PCa)**

A meta-analysis of 16 studies about the link of chronic bacterial (NIH-II) and abacterial prostatitis (NIH-III; CP/CPPS) with PCa concludes that chronic inflammation of the prostate significantly increases the likelihood for PCa development [2]. Even though prostate-specific antigen (PSA) screening and treatment strategies with prostatectomy, radiotherapy and androgen-deprivation therapy (AdT) allow a 5-year PCa survival rate around 98% [15], PCa is still responsible for 6.6% of overall male fatalities [5]. This discrepancy between promising short-term survival rates and overall death toll comes from the fact that ~30% of cancers eventually progress in spite of prostatectomy [16]. Advanced PCa is usually treated with AdT, but merely 5-10% of patients with advanced PCa survive for 10 years in spite of castration therapy [17]. Although castration therapy allows significant short-term PCa remission, it promotes cellular reprogramming with epithelial-mesenchymal transition (EMT) and neuroendocrine-like phenotypes, typically preparing a relapse with metastatic castration resistant prostate cancer (mCRPC) [18]. The analogies between CP/CPPS and PCa could help understand the molecular pathogenesis behind CP/CPPS and identify patients with a high risk for malignant transformation of the prostate.

## **3) The role of sex hormones for CP/CPPS and PCa**

Steroid sex hormones, particularly testosterone and estradiol (E2), play key roles in the development and maintenance of the reproductive systems and are significantly involved in normal and abnormal growth of the prostate gland [19]. PCa is a hormone-dependent cancer, and androgen-deprivation therapy (AdT) allows significant short-term improvement with cancer atrophy [20]. Androgen signaling through the androgen receptor (AR) is a central driver of PCa progression, both in treatment-naïve and castration-resistant prostate cancer (CRPC).

Importantly, CRPC remains dependent on AR signaling and relies on continuous AR activation, even when circulating androgen concentrations are diminished after chemical castration. Therapy failure is attributed to mutation and/or duplication events that increase the AR sensitivity to low endogenous androgen levels, or even sensitize it to anti-androgens [21]. Androgen signaling is therefore a main focus of research on prostate diseases.

Cells amplify androgen signaling by expression of 5-alpha-reductase (5AR) and several 5AR isoenzymes, which convert testosterone into dihydrotestosterone, a ligand with approximately tenfold higher potency for the induction of AR signaling [22]. 5AR and its isoenzymes play a role for prostate disease. BPH and PCa tissues overexpress 5AR isoenzymes [23] and the 5AR inhibitor (5ARI) finasteride is successfully used for the management of BPH [22]. In spite of the 5ARI benefits for BPH and the promising finding that finasteride reduces prostate cancer risk by nearly 25%, it is still not proven that 5ARI provide significant survival benefits for PCa patients [24]. Similarly, it is currently not clear whether treatment with 5ARI benefits CP/CPPS patients. Although some promising studies showed significant improvements of CP/CPPS symptoms after 5ARI treatment, the overall body of evidence remains equivocal and 5ARI are currently not recommended for CP/CPPS monotherapy [22].

Besides testosterone, estrogen signaling is known to influence prostate disease. The synthesis of estrogens from androgens is catalyzed by aromatase (*ARO*). Estrogens affect the male at least in two different ways: systemic endocrine effects through the pituitary gland that indirectly lower androgens, and local effects that directly target prostate tissue by estrogen receptors (ER) [19]. A transgenic mouse model with aromatase overexpression (*ARO+*) produces chronic prostatitis and prostate pre-malignancy with increased mast cell infiltration [14], and further examinations link prostatic estrogen dominance to PCa [25]. Moreover, rat models induce chronic prostate inflammation by combined testosterone and E2 treatment [13], stressing the potential of estrogens for initiation and facilitation of prostate inflammation and cancer. The finding that the estrogen receptors ER-alpha ( $ER\alpha$ , *ESR1* gene) and estrogen receptor beta ( $ER\beta$ , *ESR2* gene) frequently undergo epigenetic silencing in PCa [26] further support this.

Studies examining the steroid sex hormones in CP/CPPS are very limited and equivocal. One study reported elevated systemic testosterone and unchanged E2 levels in CP/CPPS patients [27]. Another study reported elevated systemic E2 levels, but unchanged testosterone levels [28] in CP/CPPS patients with a slightly elevated body mass index, so adipose tissue ARO activity could present a cause for estrogen dominance in some CP/CPPS patients. CP/CPPS patients profit from treatment with substances that interfere with estrogen signaling. Patients respond to treatment of Mepartricin, an estrogen reabsorption inhibitor [29], but also to quercetin, a plant isoflavonoid with estrogenic properties and a ~9 fold higher affinity to ER $\beta$  than to ER $\alpha$  [30-32]. It is interesting to note that ER $\beta$  is a potent suppressor of inflammation in multiple tissues/organs, including the brain and bowel [33, 34]. Hence, altered estrogen signaling and/or an aberrant prostatic ER $\alpha$ :ER $\beta$  ratio may contribute to CP/CPPS.

#### **4) Stromal fibroblasts in CP/CPPS and PCa**

The exact mechanisms behind the development of mCRPC are not clear, but multiple studies highlight the importance of paracrine signaling in the prostate tumor microenvironment (TME). The inflammatory response within many cancers is skewed towards a wound healing program with typical fibroblast activation to cancer-associated fibroblasts (CAF). Accordingly, cancers have been aptly described as wounds that do not heal [35].

CAF are regarded as a central remodeler of the tumor microenvironment that helps promote cancer initiation and progression. There are a multitude of ways how CAF create and maintain a tumor cell niche: CAF deposit aberrant extracellular matrix (ECM) proteins, secrete tumor-promoting factors, ECM-disrupting enzymes and influence ECM and cancer cells by direct contact [36]. The corruptive influence of prostate CAF is supported by transplantation experiments. Primary prostate CAF cause transformation of benign epithelial prostate cells (BPH-1) when co-transplanted into athymic mice, while non-malignant fibroblasts (NPF) do not have this effect [37]. The differential effects of CAF and NPF on BPH-1 cells are also observable *in vitro* during co-culture experiments [38].

An important CAF-secreted factor is the stromal cell-derived factor 1 (SDF-1, also called CXCL12), which influences cancer cells and immune cells likewise. Prostate CAF induce tumorigenesis by secreted CXCL12, which affects BPH-1 cells through its cognate receptor CXCR4 [39]. Breast CAF also promote carcinogenesis with secreted CXCL12, which synergizes with other factors to attract and inactivate of T lymphocytes [40].

Apart from signaling through secreted factors, CAF also modulate the ECM to promote cancer progression. Matrix metalloproteases (MMP) are capable to disintegrate the stiff ECM of the tumor microenvironment and thus enable cancer cell migration, a requirement for cancer metastasis [36]. MMP2 and MMP9 are frequently overexpressed in several cancers [36], including PCa [41]. PCa cell derived IL-6 induced MMP2 and MMP9 secretion of *in vitro* cultured primary prostate fibroblasts [42], supporting the idea that activated fibroblasts are a source of MMPs in the prostate tumor microenvironment.

CAF from castration-naïve PCa loose AR expression and simultaneously increase ER $\alpha$  expression [25], so a role of sex steroid hormone signaling for fibroblast activation in the prostate TME appears likely. Prostate cancer cells and CAF are in close proximity and studies of the TME suggest that stromal/epithelial signaling is reciprocal. PCa cell expression of kallikrein-related peptidase-4 (KLK4) leads to CAF activation with characteristic overexpression of alpha-smooth muscle actin ( $\alpha$ -SMA), *ESR1* and secreted frizzled-related protein (*SFRP1*) [43].

While CAF usually originate from local fibroblasts, also other cell types can differentiate into a myofibroblast phenotype, such as smooth muscle cells or pericytes [44]. It is therefore not surprising that the phenotype of CAF not only differs between different types of cancer, but that even different CAF populations within the same tumor entity can be identified [40, 45].

In summary, ample evidence denotes a central role of CAF for prostate carcinogenesis. Prostate CAF attenuate chemotherapy [46] and mediate malignant transformation of epithelial cells [37], but there is still ambiguity about the exact mechanism behind the CAF influence on immune cells. This might be also due to the fact that CAF display a highly variable phenotype that could reflect different fibroblast subpopulations in the tumor microenvironment. Characterization of the variable CAF phenotype and its influence on immune cells could not only clarify the role of CAF for PCa, but also help understand whether prostatic fibroblasts are involved in the CP/CPPS pathogenesis.

### **5) Mast cells influence CP/CPPS and PCa**

Mast cells are leukocytes with myeloid origin and essential for mediating inflammatory processes, regulating a variety of both adaptive and innate immune responses [47]. They differentiate from tissue-resident progenitors, or infiltrate and differentiate from circulating progenitor cells [48]. Mast cell fate progenitors are CD34<sup>+</sup> Kit<sup>+</sup> and distinct from basophil or monocyte progenitors, and kit ligand (KITLG) stimulation induces key effectors of the mast cell repertoire [49]. They execute their function by the explosive release of pre-formed large dense core vesicles (granules), a unique activation pattern called (anaphylactic) degranulation (AND). The AND is usually IgE mediated, high-affinity IgE receptor (FcεR) dependent and very well described regarding its role for allergies and anaphylactic reactions [50]. Apart from the classical, IgE triggered mast cell degranulation, mast cells are capable of selective mediator release without degranulation, also termed “piecemeal degranulation” (PMD). Resembling the process of synaptic transmission, PMD releases mediators such as VEGF and IL-6 through secretory vesicles around 50nm [51] and is hypothesized to benefit tumor cell growth [52].

Prostate cancer lesions contain significantly elevated mast cell numbers at the tumor interface, with the stroma promoting mast cell recruitment and activation [25]. There are pharmaceutical mast cell inhibitors available [50], so the suppression of mast cell activity appears as a tempting adjuvant therapy option for PCa. Treatment of pancreatic cancer with a mast cell inhibitor for example promoted tumor rejection with cancer cell and endothelial cell death [53].

Early works on the rat however suggest that breast cancer cells inhibit mast cell degranulation [54], so the suppression of mast cell activity might also be in favor of the tumor survival. The role of tumor-associated mast cells for PCa progression is still under debate, with conflicting evidence reporting both beneficial and adverse effects [55-57]. Contradictory findings were at least partly resolved by more detailed examination of the spatial mast cell distribution and PCa outcome. When peritumorally located, mast cells facilitate disease progression and metastasis, but intra-tumoral mast cells serve tumor rejection and patient survival supposedly by suppression of angiogenesis and tumor growth [58]. Moreover, the merits of mast cell inhibitors for PCa treatment seem to depend on the tumor stage. While mast cell inhibitors suppressed early stage adenocarcinoma in a PCa mouse model, poorly differentiated foci responded with formation of aggressive lesions with neuroendocrine phenotype, probably because later stage tumors become independent of the mast cell origin matrix metalloproteinases (MMP) [59].

Mast cells are not only involved in PCa, but also in CP/CPPS. Tryptase, a key mast cell protease, is elevated in EPS of CP/CPPS patients [60]. Mast cells express ER [25], and transgenic aromatase (*ARO+*) overexpressing mice develop chronic prostatitis and prostate pre-malignancy with increased mast cell infiltration [14]. These data link an aberrant estrogen signaling to a pathological mast cell response in CP/CPPS and PCa.

## **6) Macrophages in CP/CPPS and PCa**

In PCa, a growing body of evidence supports a vital role of tumor-associated macrophages (TAM) as key mediators of disease progression and hormonal therapy resistance [61-63]. It is proposed that suppression of androgen signaling enables cancer cells not only for macrophage recruitment [61], but also to reeducate them into a tumor-promoting phenotype [63].

Macrophages have a multitude of physiological roles and display a large repertoire of tissue- and context-specific responses. While the pro-inflammatory phenotype is a primary response to insults like pathogens and toxins, resolution of the acute inflammatory response requires a different phenotype with pro-proliferative and tissue-remodeling capacities to allow wound healing [64].

These two opposing macrophage phenotypes are classified upon their capability for T cell recruitment as M1 (Th1 recruitment; pro-inflammatory) or M2 (Th2 recruitment; pro-resolving/immunoregulatory) [64]. The benefits of the M1/M2 dichotomy for cancer research become clear when comparing macrophages in PCa and colorectal cancer. In colorectal cancer, TAM display an M1 phenotype and provide significant survival benefits [65]. In PCa on the other hand, TAM display an M2 phenotype and mediate a poor prognosis, with an elevated TAM frequency observable in advanced tumors with extracapsular extension [66].

The adverse effects of PCa TAM are assumed to stem from a promotion of cancer cell invasion [66] and T-cell suppression [67]. To overcome cancer progression and therapy resistance, targeting TAM with noble metal or short interfering RNA (siRNA) containing nanoparticles appears promising [68], so the potential role of paracrine signaling for the TAM phenotype warrants deeper investigation. There is evidence that macrophages also contribute to CP/CPPS. Patients display elevated systemic levels of macrophage migration inhibitory factor (MIF), tumor necrosis factor (TNF), IL-1 $\alpha$  and IL-1 $\beta$  [69, 70]. Moreover, infiltrating macrophages are detected in the prostate of PAg immunized EAP mice and in the EPS from CP/CPPS patients [12, 71].

An understanding of the macrophage interactions with the prostate TME could help understand how the pathogeneses of CP/CPPS and PCa are connected.

## **7) Oxidative stress and its role for prostate diseases**

Cells usually maintain homeostasis with antioxidant enzymes that tightly balance the oxidative state [72]. Detrimental oxidative stress is buffered by the expression of antioxidant enzymes, such as superoxide dismutase 2 (SOD2) [73]. Unlike prokaryotic cells, mammalian cells maintain their antioxidant defense by a stable, constitutive expression of antioxidant enzymes, and they have a very limited capability to upregulate antioxidant enzyme levels to oxidative challenges [74]. Mammalian cells react to oxidative challenges with a pronounced p53-dependent stress-response instead [74], suggesting that oxidative stress has a profound influence on cell physiology and the potential for disease initiation. Supporting this idea, oxidative stress has been described as a major contributor to prostatic diseases, including BPH, CP/CPPS and PCa [75].

The cellular capability to cope with free radicals might be impaired in prostate disease. In agreement with this idea, prostate disease progression from prostatic intraepithelial neoplasia (PIN) to castration-naïve PCa [76] and eventually castration-resistant prostate cancer (CRPC) has been demonstrated to involve a progressive loss of the antioxidant enzyme SOD2, which displayed a 9-fold downregulation in CRPC when compared to castration-naïve PCa [77]. Strikingly, prostate tumor growth was inhibited during SOD2 overexpression experiments [78], highlighting its functional relevance for PCa. Intracellular ROS production is tightly linked to the malignant phenotype of prostate cancer cells and critical for their migratory capacity, which likely stems from ROS-mediated matrix-metalloproteinase 9 (MMP9) activation [79]. The profound influence of oxidative stress on PCa progression is most likely a result of its effect on the AR, which presents a key driver of PCa progression. *In vitro* experiments on LNCaP cells demonstrated a direct dependence of the AR activity from intracellular oxidative stress levels. Specifically, SOD2 knockdown led to an increased AR activity, which was reversible by the treatment with antioxidants [80]. Supporting *in vitro* experiments showed that the treatment of AR-dependent prostate cancer cell lines with SOD2 mimetics led to a significant decrease of cellular superoxide levels and AR activity likewise, highlighting the therapeutic potential of oxidative stress management for PCa treatment [81].

Some studies suggest that SOD decline precedes cancer initiation and is also detectable in chronic prostate inflammation. In a rat model of CP/CPPS, reduced SOD activity has been measured under experimental prostatitis conditions, although measurements have been performed in the corpus cavernosum of the penis to explain the comorbidities of CP/CPPS and erectile dysfunction [82]. Nevertheless, CP/CPPS significantly associates with an SOD2 polymorphism, providing clinically relevant data supporting that the oxidative stress response is linked to the syndrome [83].

## 8) The epigenetic effects of inflammation and oxidative stress

Gene dysfunctionality in disease is not limited to mutation events that alter the DNA sequence, but also promoted by changes in the secondary DNA organization, which known as chromatin. A well-studied chromatin modification is the methylation of Cytosine (C) in a CpG context, when 5'-C is followed by a 3'-Guanin (G). CpG sites are frequently clustered in “CpG islands” around the transcription start site (TSS) of housekeeper genes, but also of genes with relevance for subtype-specific cell differentiation [84]. Hypermethylation of CpG islands silences gene expression, and various genes undergo hypermethylation in PCa, including the sex steroid hormone receptors *ESR1*, *ESR2* and *AR* [26]. Promotor CpG island methylation is thought to successively increase before and during malignant transformation (**Fig. 1**).

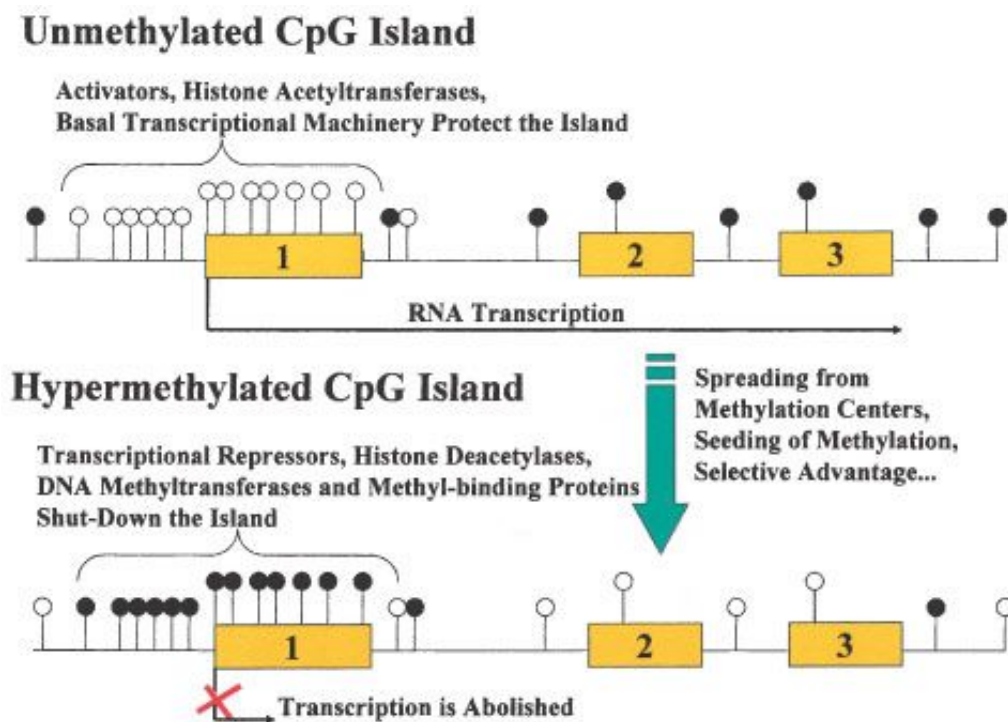


**Figure 1. Gene silencing by hypermethylation of promoter CpG islands.**

While CpG islands are usually free from CpG methylation, their hypermethylation is associated with an altered chromatin configuration and the binding of factors that promote gene silencing. Conversely, CpG methylation in the gene body is associated with an active gene transcription. In cancers, genes with relevance for cell apoptosis, cell cycle, DNA repair and detoxification undergo silencing by promotor CpG methylation. Esteller 2002 [84].

Aging [85] and inflammation [86] are known to facilitate gene promoter CpG methylation, while intergenic CpG methylation is successively lost. The inflammatory response involves the generation of excess reactive oxygen species (ROS), which disrupt the endothelial barrier and promote tissue injury, a process that is postulated to allow the initiation and progression of inflammatory disorders [87]. Moreover, accumulating evidence suggests that oxidative presents a potent epigenetic trigger. Oxidative stress has a documented capability to affect chromatin structure, histone modifications and CpG methylation likewise [88]. There are several mechanisms reported by which oxidative stress might affect DNA methylation, including direct oxidation of 5-mC to 5-hmC, or indirect effects through a changed distribution and activity of DNA methyl-transferases (DNMT), ten-eleven-translocation (TET) proteins and their substrates [88].

The potential of chronic inflammation to prepare cancer initiation is known for chronic *Helicobacter pylori* infections, where *de novo* gene promoter methylation correlates with the risk for gastric cancer development [89] (**Fig. 2**).

Infection-triggered cancers often develop due to the direct interaction of the pathogen with the host genome, as it happens for the human papillomavirus or the hepatitis B virus [89]. Apart from that, the inflammatory host response itself can alter epigenetic patterns, making chronic inflammation also a potential cancer-initiator when pathogens are not present.

CpG methylation increases in ulcerative colitis, a chronic non-infectious inflammatory bowel disease [90, 91], and dextran sulfate sodium (DSS) induced experimental non-infectious colitis also triggers *de novo* CpG methylation events [92]. *De novo* CpG methylation in DSS-induced colitis was associated with IFN $\gamma$ , IL-1 $\beta$  and NOS2 expression and appeared independent of B- and T-cells [92]. Another study demonstrated that nitric oxide (NO) increases DNA methylation by activation of DNA methyl transferase [93]. These findings highlight that chronic inflammation provides a potent agent for epigenetic dysregulation, and that macrophages might play an important role for *de novo* CpG methylation events. Hence, chronic inflammation in CP/CPPS could slowly pave an epigenetic landscape that encourages the development of proliferative inflammatory atrophy (PIA), prostatic intraepithelial neoplasia (PIN) and eventually clinical PCa.

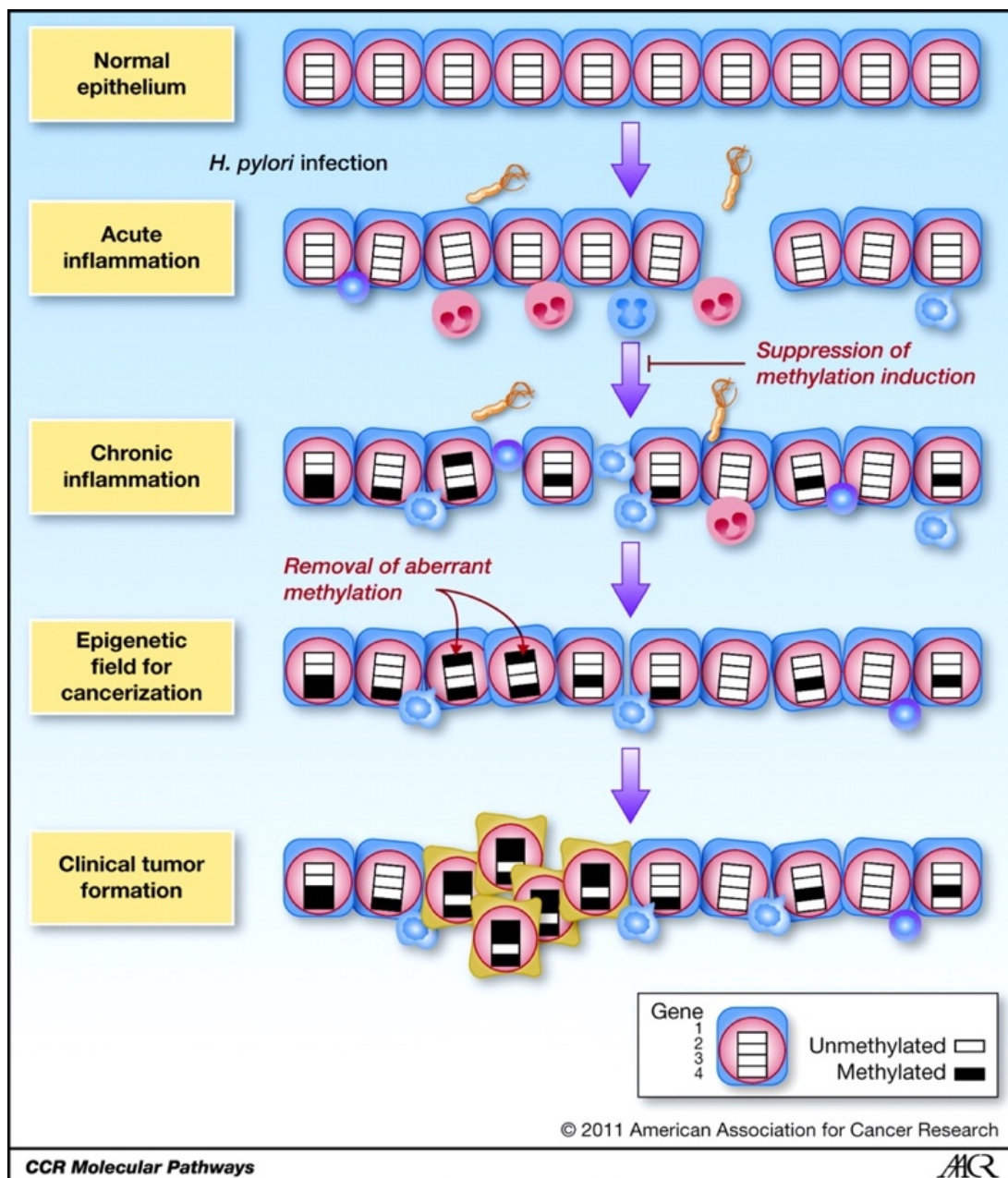


**Figure 2. Chronic inflammation promotes *de novo* DNA methylation and cancer.**

Chronic infection with *H. pylori* encourages *de novo* methylation of gene promoter CpG sites, and the accumulation of these changes presents a risk factor for gastric cancer initiation. The inflammatory host response is assumed to play a central role for *de novo* CpG methylation in chronic *H. pylori* infections. Ushijima & Hattori 2011 [89].

## 9) The relevance of epigenetics for CP/CPPS and PCa

PCa involves a variety of leukocytes, and epigenetic alterations are frequently found in PCa [26]. Laser capture microdissection revealed CpG hypermethylation of the tumor suppressor gene Glutathione S-transferase P (GSTP1) in pre-cancerous prostatic lesions like PIA and PIN [94], indicating that epigenetic changes present an early event of prostate carcinogenesis and likely an important trigger of cancer initiation.

The occurrence of epigenetic changes in PIA of the prostate suggests that these changes might also occur in CP/CPPS, particularly in consideration of the fact that *de novo* CpG methylation happens in other chronic inflammatory diseases like ulcerative colitis. The epigenetic dimension of chronic inflammation is further underlined by the finding that administration of the histone deacetylase (HDAC) inhibitor MS-275 attenuated experimental autoimmune prostatitis (EAP) in a rat model [95]. Gene promoter CpG hypermethylation might simultaneously present cause and result of the inflammatory response, perpetuating chronic inflammation with a positive feedback-loop.

Liquid biopsies seem to allow the detection of epigenetic aberrations in PCa, probably due to mobilization of cell-free circulating DNA and/or intravascular cancer cell death [26]. For instance, *GSTP1* hypermethylation was detectable in blood, ejaculate, urine and EPS from PCa patients [26]. Previous work of our group discovered epigenetic inactivation of the chemokine *CXCR4* (*SDF-1*) in blood and ejaculate from CP/CPPS patients [96], demonstrating that liquid biopsies are also a suitable source for the study of CP/CPPS.

**10) Summary: Basic research on CP/CPPS and the link to PCa is needed**

In the previous paragraphs, steroid sex hormones, the prostate stroma and the inflammatory response have been introduced regarding their function and role for CP/CPPS and PCa. PCa involves leukocytes, stromal cells and an aberrant inflammatory response, which goes along with epigenetic changes that are detectable early on during prostate carcinogenesis. Inflammation and the associated oxidative stress present powerful epigenetic triggers and CP/CPPS presents a risk factor for PCa. Therefore, it appears likely that the chronic inflammatory response in CP/CPPS prepares cancer initiation and is a direct predecessor of the intermediate prostate disease stages PIA and PIN.

However, the connection of CP/CPPS and PCa remains poorly understood due to the lack of tissue biopsies and the high between-subject heterogeneity among CP/CPPS patients [75]. Steroid sex hormone signaling has an influence on the inflammatory response and is affected in CP/CPPS patients. The role of testosterone, estrogen and their receptors for PCa and particularly CP/CPPS are currently still poorly understood. Inflammation is a common denominator of CP/CPPS and PCa, and the role of leukocytes and stromal signaling for both diseases are still not fully understood. This is the reason why the current study aims to investigate steroid sex hormones and inflammatory signaling in CP/CPPS and PCa.

## Aims

The current prospective analytical comparative study aimed to investigate the dysregulation of the steroid sex hormones and inflammatory signaling in CP/CPPS and PCa. Because of limited access to CP/CPPS tissue biopsies, clinical liquid biopsies (peripheral blood and ejaculate samples) were interrogated to detect CP/CPPS-related changes. Obtained results were compared with available clinical routine diagnostic data. Mast cell lines (HMC-1/LAD2), THP-1 derived macrophages and primary patient-derived prostate CAF (and patient-matched NPF) were analyzed to understand the role of stromal cells for CP/CPPS and PCa.

The following paragraphs illustrate the details and rationale behind the core aims of our study:

### 1) Investigation of the mast cell response to estradiol stimulation

Mast cell infiltration and estrogen signaling are interdependent in the pathogenesis of CP/CPPS and PCa [14]. In previous works from our lab, immunohistochemistry (IHC) detection of mast cell tryptase in primary human prostate tissue sections confirmed that mast cells are not exclusively implicated in PCa, but also infiltrate BPH tissue [97]. Detection of elevated mast cell tryptase in EPS from patients supports the implication of mast cells in CP/CPPS [60]. To clarify the role of estrogen signaling for the mast cell physiology, two mast cell lines (HMC-1 and LAD2) were characterized regarding the epigenetic state of the estrogen receptors *ESR1* (ER $\alpha$ ) and *ESR2* (ER $\beta$ ), their inflammatory gene expression profile, and their responsiveness to E2-stimulation. To clarify the relevance of the mast cell physiology for CP/CPPS, the two mast cell lines and their response to estradiol stimulation were compared with each other and findings in the liquid biopsy samples from CP/CPPS patients (Fig. 3).

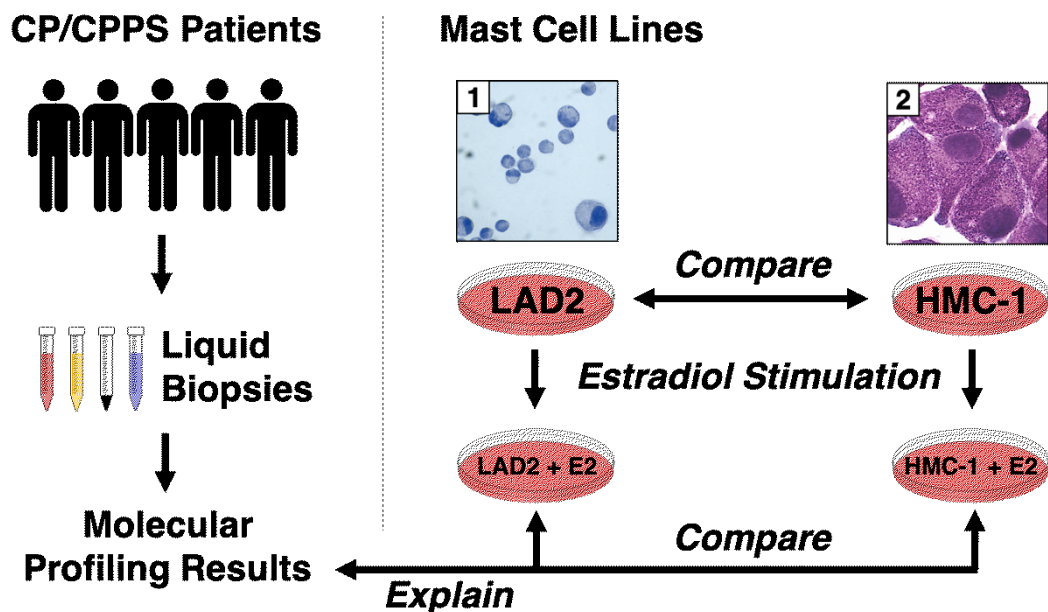


**Figure 3. Schematic of the experiments with mast cell lines.**

The mast cell lines HMC-1 and LAD2 display different phenotypes and require different growth conditions. Both cell lines were characterized before and after stimulation with estradiol. This was done in order to explain the findings in the clinical liquid biopsy samples from CP/CPPS patients. Representative microscopy images from HMC-1 cells (1) and LAD2 cells (2) were taken from Hollander et al. 2003 [98] and Guhl et al. 2010 [99].

## 2) Analysis of clinical routine parameters from CP/CPSS patients

Since CP/CPSS is a disease with unknown etiology, heterogeneous symptoms and probably multiple disease mechanisms, it is crucial to do a thorough examination of all available clinical routine parameters. CP/CPSS is an exclusion diagnosis without reliable markers, so it is likely that patients show a high between-subject variability. It is therefore possible that some or even most of the patients do not show any detectable changes in their liquid biopsies. A thorough interrogation of routine diagnostic parameters has the potential to reveal CP/CPSS-specific changes in the absence of a reliable diagnostic marker and therefore allows helps to gain confidence that CP/CPSS actually manifests in the available liquid biopsy samples. The clinical routine tests are primarily done to establish the CP/CPSS diagnosis and exclude confounding conditions in healthy volunteers. However, stratification of patients by clinical routine parameters could also allow the identification of CP/CPSS sub-pathologies and routine parameters could also be significantly changed when compared to healthy volunteers (Fig. 4). This allows to identify potentially unknown CP/CPSS-related aberrations like the deterioration of semen parameters, which has recently been reported by our group [96].

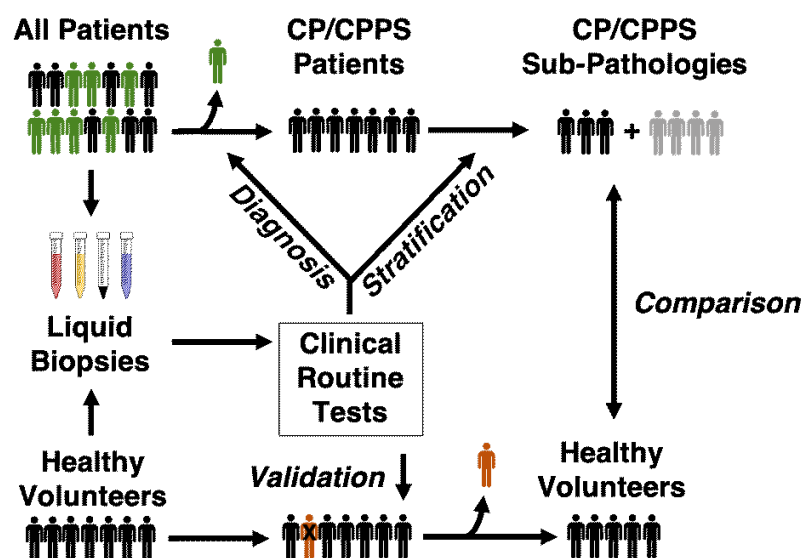


**Figure 4. Schematic of clinical routine diagnostics in the case-controlled CP/CPSS study.**

In the prostatitis outpatient clinic, all prospective CP/CPSS patients and healthy volunteers answered questionnaires and underwent a general examination (not shown). Liquid biopsies (blood, urine and semen) were taken and tested in order to confirm CP/CPSS (e.g. exclusion of infection) in the patients. Patients with other urological conditions were excluded from the cohort (green). Healthy volunteer answered questionnaires to exclude individuals with urological conditions (orange). Clinical routine parameters of patients and healthy volunteers were compared. These parameters were also used to stratify the CP/CPSS patient cohort into subgroups with possible sub-pathologies.

### 3) Isolation of somatic cells from human semen samples

Previous investigations from our research group led to the discovery that ejaculated cells from CP/CPSP patients show epigenetic inactivation of *CXCR4* [96], a chemokine receptor that is dysregulated in 23 different human cancers, including PCa [100]. However, the total ejaculated cell population was analyzed in this study. Besides sperm cells, the human ejaculate also contains immature germ cells and a variety of other somatic cells (SC) like fibroblasts, epithelial cells and infiltrating leukocytes from the male urinary tract, and the composition and/or phenotype of this cell population may change during the development of prostate diseases. We aimed to establish a density-gradient centrifugation (DGC) protocol to separate ejaculated SC from sperm cells and determine which cell population is affected by CP/CPSP-related aberrations (**Fig. 5**).

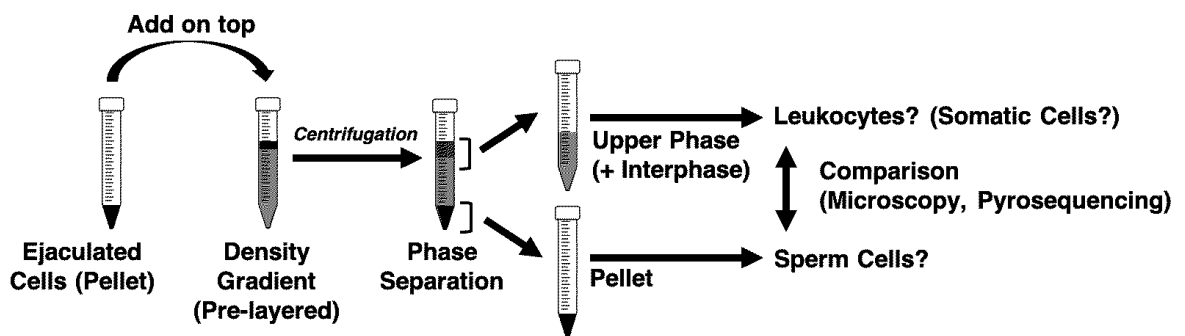


**Figure 5. Schematic of the semen separation into sperm cells and somatic cells.**

Schematic of the procedure for the separation of ejaculated cells into sperm cells and somatic cells. The frozen ejaculated cell pellet was first resuspended in DMEM-F12 and then layered on top of a pre-layered (Histopaque®1077) density gradient. The phenol-red in DMEM-F12 allowed for a visual control of the phase separation before and after the centrifugation. Resulting cell pellet and upper phase (with interphase) were recovered separately after centrifugation. Pyrosequencing and brightfield microscopy were used to control whether the different fractions contain different cell types with a different gene promoter CpG methylation pattern.

### 4) Detection of leukocyte-specific transcripts in somatic cells from semen

CP/CPSP is classified by the presence of prostatic leukocyte infiltrates, but microscopic evaluation of EPS alone has currently no implications for differential treatment [8]. Extended molecular profiling of prostate-infiltrating leukocytes from CP/CPSP patients could help identify individuals that respond well to certain treatment strategies, or that have an increased risk for PCa initiation. We aimed to detect leukocyte-specific transcripts and identify CP/CPSP-associated changes in ejaculated SC obtained by DGC.

## 5) Detection of CP/CPPS-related changes of steroid sex hormone signaling

PCa and probably CP/CPPS involve alterations of androgen and estrogen signaling. We aimed to detect changes of the sex steroid hormone pathways in liquid biopsies of CP/CPPS patients. For this, blood plasma testosterone levels as well as blood and seminal plasma estradiol levels were measured. Gene promoter CpG methylation and transcript levels of the sex steroid hormone receptors ER $\alpha$ , ER $\beta$  and AR (Genes: *ESR1*, *ESR2* and *AR*) were measured in isolated circulating white blood cells (WBC) and ejaculated SC obtained by DGC. A comparison of the CP/CPPS-associated blood (blood cells and blood plasma) and semen (ejaculated cells and seminal plasma) changes was done to understand the relationship of systemic *versus* organ-confined levels of testosterone, estradiol and their receptors (**Fig. 6**).

### Frozen (-80°C) Liquid Biopsy Samples (Healthy Volunteers, CP/CPPS Patients)

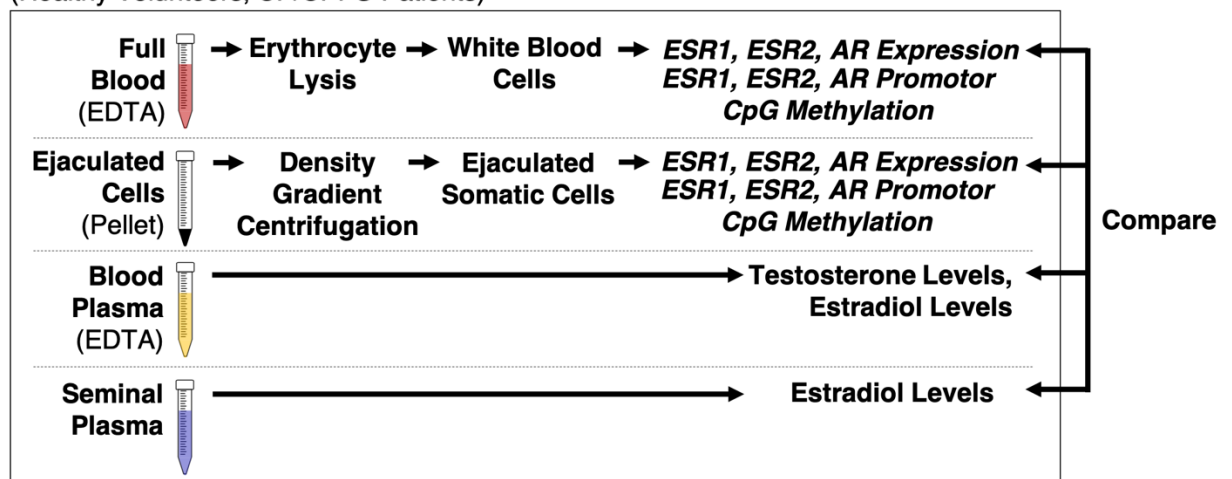


**Figure 6. Schematic of the steroid sex hormone profiling of liquid biopsy samples.**

At the Urology Clinic in Gießen, liquid biopsies were routinely taken for laboratory tests in order to diagnose the patients' condition. The diagnosis was unknown at the time of sampling, so all samples were stored at -80°C first. Samples from confirmed CP/CPPS patients and age-matched healthy volunteers were analyzed for the study. Blood testosterone levels were measured in CP/CPPS patients as a clinical routine parameters, but not measured in the healthy volunteers for economical reasons. Estradiol levels of CP/CPPS patients and healthy volunteers were measured in frozen blood plasma and seminal plasma samples. Frozen full blood (EDTA) samples were used for the isolation of white blood cells (WBC) with an erythrocyte lysis buffer. Frozen ejaculated cell pellets from semen were separated into sperm cells and ejaculated somatic cells (SC) by density gradient centrifugation. Isolated WBC (blood) and SC (semen) were then used for gene expression analysis and promotor CpG methylation analysis of the estrogen receptors (*ESR1*, *ESR2*) and the androgen receptor (*AR*). The levels of Testosterone, Estradiol and their receptors were then compared between different samples (blood, semen) and between individuals (patients and healthy volunteers).

## 6) Studies of the stromal influence on macrophage polarization

TAM are in direct vicinity to other cells from the prostate TME and display type-2-immunity (M2). It is assumed that TAM stem from circulating monocytes that infiltrate the tissue upon chemokine attraction, so epithelial/stromal signaling likely affects the prostatic macrophage count and phenotype in CP/CPPS and PCa. We aimed to polarize THP-1 derived macrophages with conditioned media (CM) from CAF, patient-matched NPF, mast cells and PCa cells to determine how their secretions affect the macrophage phenotype. The CAF phenotype shows between-patient variability and is prone to changes during cell culture, so RNAseq experiments were conducted at Monash-University in order to identify CAF-specific regulated transcripts. These experiments led to the identification of several genes (*HOXD8*, *ESR1*, *SFRP-1*, *SDC2*, *EPHB6* and *PITX2*) that are consistently regulated in CAF when compared to the patient-matched NPF. We aimed to use an RT-qPCR panel with these identified marker transcripts to validate the identity of the CAF from our CM experiments. Furthermore, we aimed to find out whether the gene expression levels of the CAF-specific marker transcripts correlate with the CAF-mediated effects on (CM-treated) macrophages (Fig. 7).

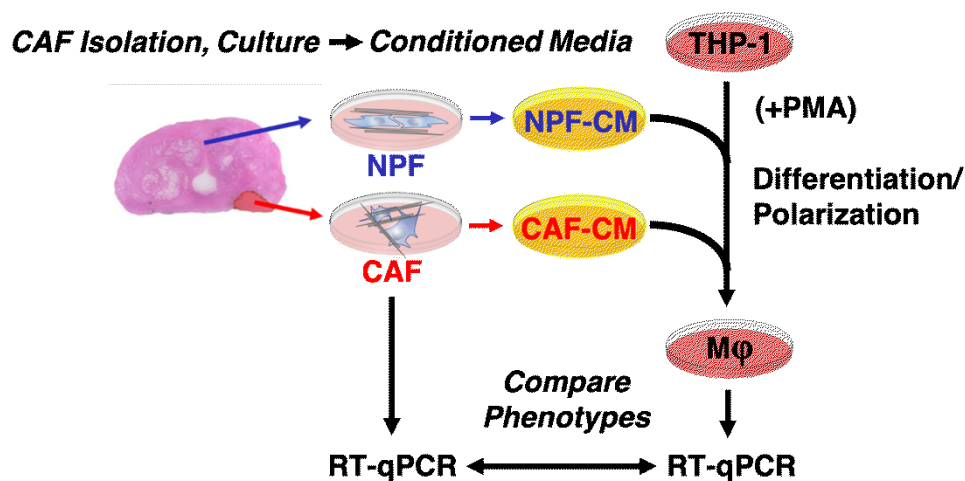


**Figure 7. Schematic of the conditioned media experiments.**

Experimental outline of the conditioned media (CM) experiments. Cancer-associated fibroblasts (CAF) and patient-matched non-malignant fibroblasts (NPF) were first isolated from different areas of the same prostatectomy specimen, then grown in cell culture. Secreted factors from CAF and NPF were prepared and collected as conditioned media samples, which were then used with a well-established macrophage differentiation and polarization protocol (from THP-1 cells). CAF and CAF-educated macrophages were subsequently analyzed by RT-qPCR, using panels with CAF-specific (*HOXD8*, *ESR1*, *SFRP1*, *SDC2*, *EPHB6* and *PITX2*) and macrophage-specific (*TNF*, *IL-1B*, *HLA-DRA*, *HLA-DQA1*, *CD206*, *CCL13*, *CCL18* and *IL-10*) marker genes, respectively.

## 7) Investigation of macrophage interactions with the prostate tumor stroma

Our colleagues at MU established a co-culture system to *in vitro* recapitulate the prostate TME. Compared to patient-matched NPF, CAF were capable to induce a spindle-like elongation of co-cultured benign prostate epithelial cells (BPH-1) [38]. CAF-induced BPH-1 morphology changes indicate EMT, supporting the pro-tumorigenic role that CAF play for PCa. Addition of mast cell (HMC-1) CM or recombinant tryptase to co-culture assays facilitated the CAF-induced BPH-1 morphology changes and led to the formation of characteristic cytoplasmic protrusions (Fig. 8), highlighting the detrimental role of peritumoral mast cells [101].

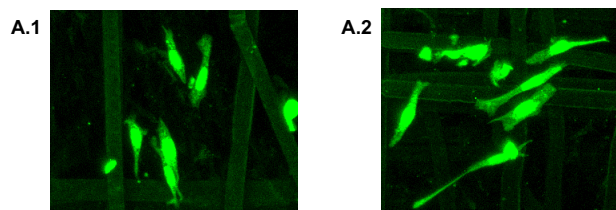


**Figure 8. Mast cell conditioned media affects co-cultured BPH-1 cells.**

BPH-1 assume a characteristic spindle-like shape when co-cultured on a pre-grown CAF layer (A.1). The shown BPH-1 cells were co-cultured on melt-electrospun poly( $\epsilon$ -caprolactone) (PCL) polymer scaffolds. The addition of mast cell (HMC-1) conditioned media or recombinant mast cell tryptase induced the formation of cytoplasmic BPH-1 protrusions that resemble invadopodia [101] (A.2).

In a similar fashion, we aimed to capture macrophage interactions with the TME by addition of THP-1 derived macrophages to the well-established reference co-culture system of BPH-1 cells growing on CAF or NPF (Fig. 9). CAF- and macrophage-mediated BPH-1 morphology changes were to be captured by fluorescent imaging. To find out whether the macrophage polarization has an influence on epithelial/stromal (CAF/BPH-1) interactions, we tested the effects of unpolarized macrophages ( $M\phi$ ) side by side with polarized (LPS/IFN $\gamma$ : M1 or IL-4/IL-13: M2) macrophage populations.

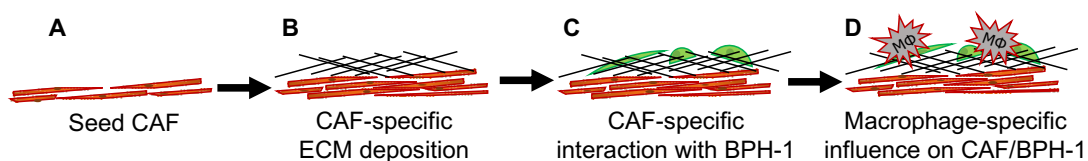


**Figure 9. Experimental outline of co-culture experiments.**

Co-culture experiments were prepared by growing CAF (or NPF) for 5-7 days (A) to allow sufficient ECM deposition (B). For reference co-culture assays, pre-stained BPH-1 cells were seeded onto the pre-grown CAF (or NPF) monolayer (C). To evaluate the effect of macrophages, BPH-1 cells were seeded together with unstained macrophages ( $M\phi$ ).

## 8) Summary of study aims

We aimed to provide a better understanding of the role steroid sex hormones and inflammatory signaling play for CP/CPPS and PCa. The work aimed to fulfil the following core aims:

- (1) Investigation of the mast cell response to estradiol stimulation
- (2) Analysis of clinical routine parameters from CP/CPPS patients
- (3) Isolation of somatic cells from human semen samples
- (4) Detection of leukocyte-specific transcripts in somatic cells from semen
- (5) Detection of CP/CPPS-related changes of steroid sex hormone signaling
- (6) Studies of the stromal influence on macrophage polarization
- (7) Investigation of macrophage interactions with the prostate tumor stroma

Aims 1-5 were followed at Justus-Liebig-University. First, *in vitro* studies of the mast cell lines HMC-1 and LAD2 were done to characterize the inflammatory response of mast cells and their response to estradiol **(1)**. The core concept behind aims 2-5 was to develop an approach for the isolation of leukocytes from frozen clinical liquid biopsies and then show with epigenetic profiling methods that these cells are affected by CP/CPPS. After a successful validation and examination of the study cohorts with available clinical routine parameters **(2)**, a protocol for the isolation of somatic cells from semen was established **(3)**. The presence of leukocytes in the isolated somatic cell population was verified with adequate leukocyte-specific markers **(4)**. An epigenetic profiling of the steroid sex hormone receptors in the somatic cells was done to investigate whether androgen or estrogen signaling are affected in CP/CPPS patients **(5)**.

At the Monash-University, the interaction of stromal fibroblasts, epithelial cells and macrophages was studied in order to understand how stromal signaling affects CP/CPPS and PCa. Conditioned media experiments were done to estimate how the secreted factors from mast cells, fibroblasts and cancer cells affect the macrophage response **(6)**. Co-culture experiments were done to estimate how macrophages interact with the prostate tumor microenvironment **(7)**.

# Material & Methods

## 1) Collection and clinical routine analysis of liquid biopsy samples

The clinical routine analysis of liquid biopsy samples from CP/CPPS patients was done in order to confirm the CP/CPPS diagnosis and disease-related aberrations of clinical routine parameters. In addition, a thorough examination of clinical routine parameters was done to identify possible CP/CPPS sub-pathologies.

The study was approved by the Ethics Commission of the Medical Faculty of the Justus-Liebig-University (JLU) Giessen (ethical votes, AZ.: 55/13; AZ.: 123/12) and all participants provided written informed consent. Whole blood and semen samples were collected from CP/CPPS patients (n=50, median age 36.46, range 17–65) and healthy men (control participants) without any preexisting urological conditions (n=61, median age 36.50, range 20–69) in the Clinic of Urology, Pediatric Urology and Andrology, JLU Giessen, Germany. The control group comprised volunteers (n=38) and men requesting vasectomy (n=23). The latter cohort was added in order to get an age-matched control cohort that allowed exclusion of age-associated effects on the hormonal balance. From patients undergoing vasectomy, we used pre-vasectomy peripheral blood and ejaculates, respectively. The clinical presentation of CP/CPPS patients and healthy volunteers was confirmed according to guidelines [9, 102, 103], including the use of the German version of the Chronic Prostatitis Symptom Index from the National Institute of Health (NIH-CPSI) [104] as we previously described [96]. Infection was excluded with microbiological cultures and gene amplification analysis [104, 105]. Since the classification to inflammatory (IIIa) and non-inflammatory (IIIb) CP/CPPS might present two different stages of the same condition [106], both subcategories were included in our patient cohort. However, only one out of the 50 CP/CPPS patients from our study cohort was diagnosed with inflammatory (IIIa) CP/CPPS.

Blood samples from CP/CPPS patients were routinely analyzed for total testosterone, C-reactive protein (CRP) and prostate-specific antigen (PSA) levels in the central laboratory of our university hospital (ADIVA, Siemens Health Care, Erlangen, Germany). E2 concentrations in blood and seminal plasma (SP) of patients and controls were analyzed separately at the Institute of Laboratory Medicine and Pathobiochemistry, Molecular Diagnostics, UKGM Giessen. Semen parameters of patients and controls were routinely analyzed according to the World Health Organization (WHO) 2010 recommendations [107]. Seminal plasma (SP) was separated from the cellular fraction by centrifugation (5 minutes at 600g) and analyzed for polymorphonuclear elastase, IL-8,  $\alpha$ -glycosidase and zinc with standardized methods [96].

The cellular semen fractions (ejaculate pellets) and EDTA-blood specimen were stored at  $-80^{\circ}\text{C}$  and used for isolation of leukocytes (refer below). CP/CPPS patients and healthy volunteers were examined and evaluated based on CPSI, International prostate symptom score (IPSS) and Hospital Anxiety and Depression Scale (HADS) questionnaires. All clinical and pathological data gathered are summarized in **Table 1**.

**Table 1: Clinical routine parameters from CP/CPSS patients and healthy donors.**

Semen parameters, biochemical ejaculate parameters, biochemical blood parameters, uroflow parameters and CP/CPSS-relevant questionnaires are listed below. Blood testosterone, CRP and PSA, and uroflow data were only collected from CP/CPSS patients, and not from healthy volunteers.

Category	Parameter	Healthy						CP/CPSS						P-Value	
		N	AVG	MED	SD	MIN	MAX	N	AVG	MED	SD	MIN	MAX		
General	Age	61	37.25	36.50	12.85	19.55	69.00	50	39.20	36.46	11.64	17.01	64.54	0.234	
Semen	General	Ejaculate Volume	49	3.29	3.00	1.54	0.50	8.00	50	2.05	1.80	1.39	0.05	6.00	<0.001
	Sperm Count	Spermatozoa/mL	49	76.45	59.90	57.29	6.70	256.50	50	49.05	32.05	58.67	0.00	262.50	<0.001
	Sperm Count	Total Spermatozoa	49	234.42	173.75	186.42	17.42	777.20	50	94.19	55.10	127.29	0.00	592.25	<0.001
	Motility	Type A	49	32.93	36.00	21.56	0.00	72.00	47	17.64	17.00	12.47	0.00	44.00	<0.001
	Motility	Type B	49	22.43	19.00	10.90	3.00	58.00	47	24.89	25.00	9.59	0.00	41.00	0.024
	Motility	Type C	49	9.90	8.00	5.69	1.00	28.00	47	11.19	9.00	7.32	0.00	49.00	0.227
	Motility	Type D	49	35.83	33.00	15.14	13.00	74.00	47	44.47	41.00	15.20	0.00	96.00	<0.001
	Motility	Eosin Test	47	79.14	81.00	10.68	48.00	93.00	47	64.70	71.00	17.19	25.00	91.00	<0.001
	MAR Test	IgG	11	2.67	0.00	4.44	0.00	14.00	36	4.02	0.00	7.20	0.00	37.00	0.742
	MAR Test	IgA	11	2.58	0.00	4.29	0.00	13.00	36	5.32	0.00	8.64	0.00	34.00	0.372
	Morphology	Normal	49	14.14	12.00	10.89	0.00	52.00	43	6.65	5.00	5.31	0.00	19.00	<0.001
	Morphology	Head Defect	49	72.02	73.00	13.26	41.00	99.00	43	80.18	82.00	12.76	51.00	100.00	0.002
	Morphology	Midpiece Defect	49	36.83	41.50	20.98	2.00	69.00	43	11.84	10.00	10.02	1.00	44.00	<0.001
	Morphology	Tail Defect	49	29.45	21.00	19.53	5.00	79.00	43	51.96	48.00	18.77	16.00	90.00	<0.001
	Cytology	Perox(+) Cells	48	0.15	0.05	0.25	0.00	1.40	49	0.31	0.20	0.64	0.00	4.30	0.012
	Cytology	Spermatog. Cells	44	1.40	0.34	2.44	0.00	13.00	38	1.88	0.80	3.41	0.00	18.00	0.162
	Biochemistry	pH	49	7.93	8.10	0.43	7.20	8.70	50	7.62	7.60	0.36	6.90	8.70	<0.001
	Biochemistry	Fructose	24	15.18	15.15	7.92	0.50	38.80	46	16.00	15.80	9.36	0.00	40.40	0.640
	Biochemistry	α-Glucosidase	23	20.93	19.80	11.03	6.70	45.30	45	16.50	13.90	9.55	3.50	50.60	0.086
	Biochemistry	Elastase	23	101.33	73.00	107.54	0.00	312.00	45	175.23	53.50	379.79	0.00	2000.00	0.724
Biochemistry	IL-8	23	3223.93	2341.00	2429.56	805.00	12429.00	46	5444.48	3450.50	6111.73	224.00	25376.00	0.345	
Biochemistry	Zinc	23	5.27	5.20	2.88	1.30	11.20	42	4.63	4.20	3.29	0.70	13.40	0.218	
Biochemistry	Estradiol	46	95.35	93.00	34.59	54.00	261.00	32	100.50	100.50	21.04	60.00	150.00	0.072	
Blood	Biochemistry	Testosterone	N/A	N/A	N/A	N/A	N/A	N/A	49	442	403	224	147	1663	N/A
	Biochemistry	Estradiol	48	40.16	39.00	9.75	27.00	78.00	45	36.45	36.00	11.32	12.00	62.00	0.103
	Biochemistry	CRP	N/A	N/A	N/A	N/A	N/A	N/A	48	2.78	0.75	6.59	0.00	38.00	N/A
	Biochemistry	PSA	N/A	N/A	N/A	N/A	N/A	N/A	46	0.85	0.61	0.88	0.24	5.53	N/A
Urine	Uroflow	MFR	N/A	N/A	N/A	N/A	N/A	N/A	44	18.40	18.10	7.64	6.20	35.20	N/A
	Uroflow	Total Volume	N/A	N/A	N/A	N/A	N/A	N/A	44	310	307	164	38	645	N/A
Questionnaires	NIH-CPSI	Pain	25	0.32	0.00	1.72	0.00	10.00	47	13.08	13.00	3.32	4.00	20.00	<0.001
	NIH-CPSI	UTS	25	1.26	1.00	1.38	0.00	5.00	47	4.77	5.00	2.52	0.00	10.00	<0.001
	NIH-CPSI	QOL	25	0.59	0.00	1.31	0.00	6.00	47	9.33	10.00	2.05	5.00	12.00	<0.001
	NIH-CPSI	Total Score	25	2.12	1.00	3.29	0.00	17.00	47	26.98	27.00	5.75	11.00	36.00	<0.001
	IPSS	Total Score	19	2.43	2.00	2.36	0.00	9.00	47	14.20	14.00	6.63	3.00	33.00	<0.001
	HADS	Anxiety	7	4.86	5.00	2.60	0.00	9.00	24	8.40	7.00	4.96	1.00	18.00	0.028
	HADS	Depression	9	4.43	4.00	4.18	0.00	13.00	24	7.72	8.00	4.38	2.00	19.00	0.011
	HADS	Total Score	7	7.21	7.00	4.76	0.00	17.00	24	16.12	16.00	8.98	4.00	37.00	0.002

N: Case Number; AVG: Average; MED: Median; SD: Standard Deviation; MIN: Minimum; MAX: Maximum; MAR-Test: Mixed Antiglobulin Reaction Test; Cytopl.: Cytoplasmatic; Perox(+): Peroxidase-positive; Spermatog.: Spermatogenesis; CRP: C-Reactive Protein; PSA: Prostate-Specific Antigen; MFR: Maximum Flow Rate; NIH-CPSI: Chronic Prostatitis Symptom Index of the National Institute of Health; UTS: Urinary Tract Symptoms; QOL: Quality of Life; IEF: Index of Erectile Function; HADS: Hospital Anxiety and Depression Scale; SFI: Sexual Function Index. N/A: not applicable. Significance values calculated with Mann-Whitney U-Test.

## 2) Isolation of circulating white blood cells and ejaculated somatic cells

Blood leukocytes and somatic cells from semen were isolated to allow the profiling of inflammatory factors and steroid sex hormone receptors by RT-qPCR and Pyrosequencing.

Frozen EDTA blood samples (3mL) were thawed on ice and incubated for 10 minutes with 5 volumes of red blood cell lysis buffer (15.5mM NH<sub>4</sub>Cl, 1mM KHCO<sub>3</sub> and 0.01mM tetra-sodium EDTA in DEPC-treated deionized water; pH 7.3). Cells were centrifuged (10 minutes at 600g) and pellets were incubated with 1.5mL fresh buffer on ice for another 10 minutes. Blood leukocytes were then obtained by centrifugation (5 minutes at 600g). Ejaculated somatic cells (SC) were isolated from frozen-stored ejaculate pellets by density gradient centrifugation (DGC), a method for isolation of highly motile sperm from ejaculate samples [108]. DGC has successfully been implemented for isolation of ejaculated SC from human and other species [109, 110]. DGC allows for recovery of ejaculated SC, because ejaculated sperm cells have a higher density than SC and travel faster in the density gradient (**Fig. 10**).

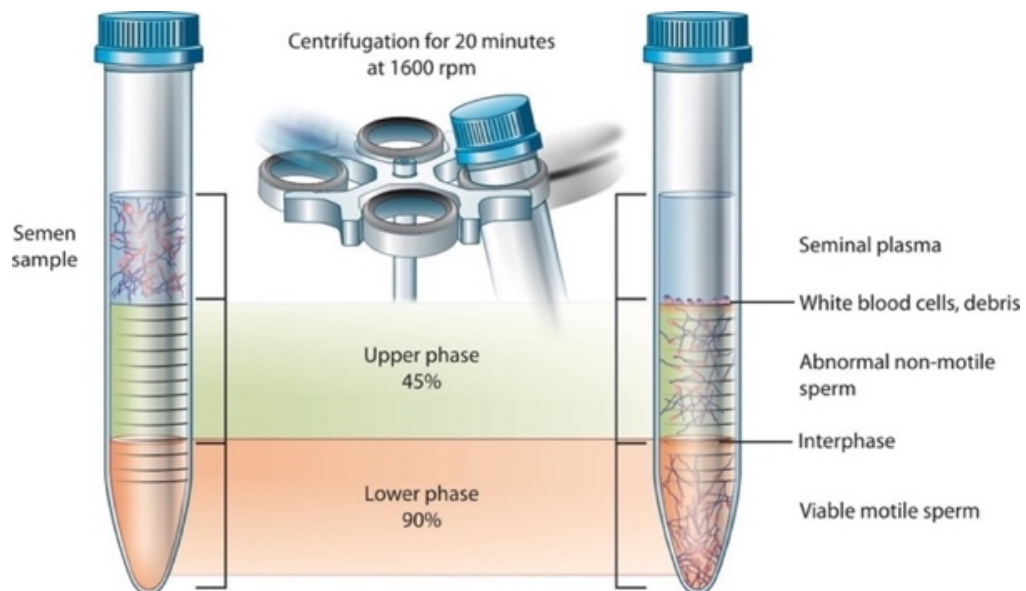


**Figure 10. Recovery of ejaculated somatic by density gradient centrifugation.**

For DGC, a semen sample (or resuspended ejaculated cell pellet) is carefully added on top of a pre-layered density gradient (in our study containing three phases: 90%, 50% and 20%). During low speed centrifugation (400g), cell travel depends on cell density so that highly compact motile sperm cells, abnormal sperm cells and white blood cells accumulate in different fractions. Beydola et al. 2013: Sperm Preparation and Selection Techniques [108].

Briefly, ejaculate pellets were thawed on ice and dissolved in 600 $\mu$ L DMEM-F12 medium (Gibco). Samples were then placed on top of a pre-layered Histopaque®1077 gradient (1.5mL 90% +1.5mL 50% +1.5mL 20%; all solutions at 4° C) in 12mL polypropylene-tubes (Sarstedt) and centrifuged at low speed (30 minutes at 400g). The phenol-red from DMEM-F12 allowed for convenient identification of resulting phases. The upper fraction contained ejaculated SC, and the pellet contained sperm cells. Ejaculated SC in the supernatant were pelleted by centrifugation (2min at 13,000rpm, 4°C). Ejaculated SC and circulating WBC were washed 2x with PBS and frozen at –80° C until DNA and RNA isolations.

### **3) Isolation of human primary prostate fibroblasts (NPF/CAF)**

Primary prostate fibroblasts were isolated in order to study CAF signaling towards macrophages with conditioned media experiments, and to examine how macrophages affect stromal/epithelial interactions with a co-culture system.

NPF/CAF cells were isolated as previously described [38]. In short, a pathologist identified malignant and benign areas of the primary prostatectomy tissue specimen. Identified areas were subsequently cut into pieces of 2-3mm<sup>3</sup> and digested overnight on the rotator (37°C, 15rpm) in digestion media (RPMI-1640 with 10% FCS, 25mM HEPES, 100U/mL penicillin, 100mg/mL streptomycin, 0.5mg/mL fungizone, 100mg/mL gentamicin, 225U/mL Collagenase Type I and 125U/mL Hyaluronidase Type II). Cell suspensions were washed with PBS and immediately seeded in CAF culture media (see below) into T-25 flasks.

### **4) Culture of primary fibroblasts (NPF/CAF) and immortalized cell lines**

Cell lines were cultured for the *in vitro* studies of estradiol effects on the inflammatory response (HMC-1, LAD2, THP-1), for conditioned media experiments that examine how the tumor microenvironment affects macrophage physiology (NPF, CAF, HMC-1, LAD2, PC-3, DU-145, LNCaP, BPH-1, THP-1), and for co-culture experiments that study how macrophages affect the tumor microenvironment (NPF, CAF, BPH-1, THP-1).

Primary cancer-associated fibroblasts (CAF) and patient-matched non-malignant fibroblasts were isolated from primary prostatectomy specimen to study the cancer-specific *in vivo* activation of fibroblasts. PC-3, DU-145 and LNCaP cells represent immortalized prostate cancer cell lines and were studied to get information about prostate cancer cell physiology. In contrast to that, the immortalized cell line BPH-1 represents benign prostate epithelium cells, so this cell line was interrogated to represent benign prostate epithelial cells. THP-1 is an immortalized monocyte cell line that can be differentiated into macrophages, which were used to study macrophage interactions with the prostate tumor microenvironment. HMC-1 and LAD2 cells are two mast cell lines and were used to study the role of mast cells for CP/CPPS and PCa.

Isolated primary NPF or CAF were cultured under low oxygen conditions (37°C, 5% CO<sub>2</sub>, 5% O<sub>2</sub>) in CAF selection media [RPMI-1640 containing 5% heat inactivated FCS (ThermoScientific), 1nM testosterone (Sigma-Aldrich) and 10ng/mL fibroblast growth factor (FGF; Millipore)]. After a few passages, the primary fibroblasts overgrow any other cell type from the original cell suspension, and NPF/CAF are ready for experiments.

All other cell lines were grown under normoxic conditions (37°C and 5% CO<sub>2</sub>). PC-3, DU-145, BPH-1, (each 5% FCS) and THP-1 (10% FCS) were grown in RPMI-1640. LNCaP cells were grown in Dulbecco's Modified Eagle's Medium (DMEM; Gibco) containing 5% FCS. HMC-1 cells (kindly provided by Dr. J. Butterfield; Mayo Clinic, USA) were cultured as previously described [25, 97] in Iscove's Modified Dulbecco's Media (IMDM; ThermoScientific; 10% FCS and 1.2mM 1-Thioglycerol). LAD2 cells (kindly provided by Dr. Kirshenbaum; National Institutes of Health, USA) were propagated as previously described [97, 111] in StemPro™-34 serum-free growth medium (Invitrogen; containing 2mM glutamine and 100ng/mL stem cell factor).

All cell culture media were supplemented with 100U/mL penicillin and 100 mg/mL streptomycin (Gibco).

Detachment of adherent cells was accomplished by incubation for 5min with PBS-EDTA at room temperature (RT) and subsequent incubation with TrypLE™ Express (Gibco) for 5min at 37°C. CAF and NPF were not pre-treated with PBS-EDTA, but immediately incubated with TrypLE™ Express for cell detachment. Suspension cell lines (THP-1, HMC-1, LAD2) were expanded by centrifugation (5min, 500g) and subsequent resuspension in fresh media.

### **5) Preparation of Conditioned Media**

Conditioned media (CM) samples were prepared for primary CAF and NPF, mast cell lines and epithelial cell lines (**Fig. 5**). Mast cell CM was prepared in the respective mast cell (HMC-1 or LAD2) growth media. After media replacement, cells were grown for 48 hours at a density of  $0.5 \times 10^6$  cells/mL, and supernatants were obtained by centrifugation (1000g, 5 min). For preparation of CM from CAF and patient-matched NPF, primary fibroblasts were seeded at a density of  $1.25 \times 10^4$  cells/cm<sup>2</sup> into T-175 flasks to reach confluence overnight. The following day, media was washed out and replaced with 20mL fresh starvation media (RPMI-1640 with 2% FCS). CM of the epithelial cell lines (PC-3, DU-145, LNCaP, BPH-1) was prepared in a similar fashion, but without seeding defined cell densities. Instead, media replacement was done when cell confluence reached ~90%. Epithelial cells, CAF and patient-matched NPF were incubated with starvation media for 48 hours, and supernatants were collected without cell detachment by pipetting. Supernatants were sterile filtered (pore size 20µm) before storage (-20°C).

### **6) Macrophage differentiation and polarization from THP-1 cells**

For macrophage (Mφ) differentiation, THP-1 cells were seeded into THP-1 media (RPMI with 10% FCS) containing 20ng/mL Phorbol-12-Myristate-13-acetate (PMA; Abcam; Cat No. ab120297) at a density of 0.125 Mio. cells/cm<sup>2</sup>. After 24 hours, attached Mφ were washed for 1 hour with PMA-free THP-1 media. For unpolarized Mφ maintenance, cells were subsequently incubated for 48 hours with THP-1 media alone. M1 polarized macrophages were simultaneously obtained under addition of IFNγ (40ng/mL; Peprotech; Cat No. 300-002) and LPS (20pg/mL; Sigma-Aldrich; Cat No. L4391), while M2 macrophages were obtained with IL-4 and IL-13 (each 40ng/mL; Peprotech; Cat No. 200-04 and 200-13).

Alternatively, the polarization step was done with undiluted (thawed and pre-warmed) CM samples (**Fig. 11**). For epithelial cell lines, CAF and NPF, starvation media (RPMI with 2% FCS) served as a CM control. For the mast cell lines (HMC-1/LAD2), their respective growth media served as CM control. After 48 hours of polarization, adherent macrophages were harvested and pelletized (1000g for 5min). Cells for expression analysis were detached for 5min (37°C) with TrypLE™ Express (Gibco) and frozen at -80°C until RNA isolation. Cells for co-culture experiments were incubated with EDTA-PBS (15min at 37°C), detached by gentle pipetting, washed with 1xPBS and immediately seeded into co-culture assays.

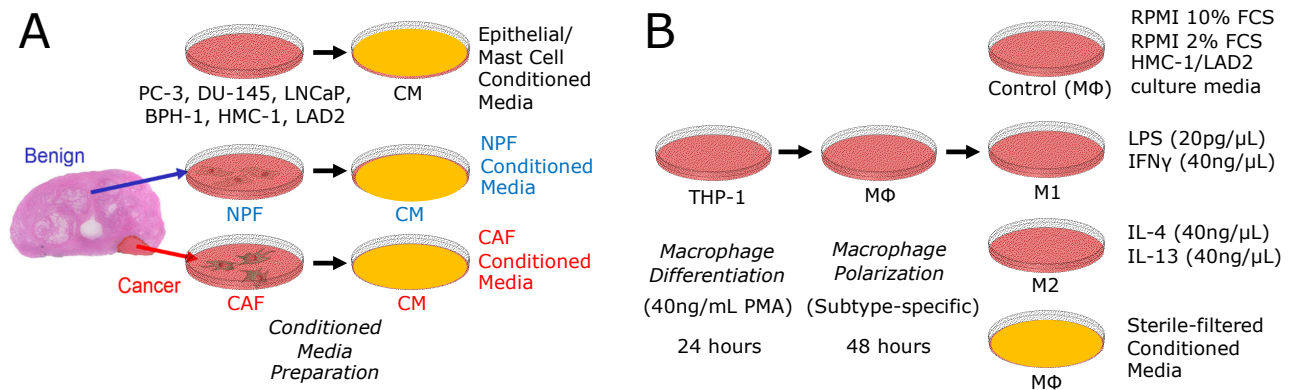


**Figure 11. Schematic of macrophage polarization experiments.**

Conditioned media (CM) samples were collected from immortalized cell lines or primary prostate fibroblasts (NPF/CAF) that have previously been isolated from prostatectomy specimen (**A**). After that, THP-1 derived macrophages were generated using artificial stimuli (LPS/IFN $\gamma$ , IL-4/IL-13) or the previously collected CM samples (**B**). THP-1 derived macrophages were polarized using a two-step protocol. During the first step, THP-1 cells were differentiated with PMA-treatment to macrophages (M $\phi$ ). During the second step, macrophages were polarized with artificial stimuli towards M1 (LPS/IFN $\gamma$ ) or M2 (IL-4/IL-13). Alternatively, macrophages were incubated with CM samples instead. Media without stimuli (RPMI with 10% FCS) was used to retain unpolarized control macrophages (M $\phi$ ). Starvation media (RPMI with 2% FCS) or mast cell culture media were used as CM controls.

## 7) Estradiol stimulation of mast cell lines and macrophages

HMC-1 and LAD2 cells were stimulated with estradiol to investigate how estrogen signaling influences the mast cell response.

Serum estradiol (E2) levels of healthy, fertile men range from 10-82pg/mL [112], corresponding to a concentration of ~0.04-0.3nM. To stimulate the cell lines with excess E2 levels that are still within a physiological range, concentrations of 0.1nM, 1nM, 10nM and 100nM were used. Accordingly, the lowest estradiol concentration from our experiments represents physiological blood serum concentrations and the higher concentrations represent exceeding E2 concentrations.

Mast cells were first seeded into 10cm dishes at densities of  $\sim 0.176 \times 10^6/\text{cm}^2$  (HMC-1;  $1 \times 10^7/\text{dish}$ ) and  $\sim 0.529 \times 10^5/\text{cm}^2$  (LAD2;  $3 \times 10^6/\text{dish}$ ). Treatments with E2 (0.1nM, 1nM, 10nM and 100nM) or the ethanol (EtOH) vehicle control were done for 24 hours, and cells were washed with PBS (5 minutes centrifugation at 400g) before isolation. Cell pellets were resuspended in 50 $\mu$ L PBS for DNA isolation, or in 100 $\mu$ L RNA-later (Sigma) for RNA isolation.

For macrophage stimulation, 100nM E2 was added to the culture media during differentiation (PMA) and polarization (IL-4/IL-13; M2) steps of the protocol. E2 solutions for macrophage stimulation were prepared with dimethyl sulfoxide (DMSO) instead of EtOH, and accordingly DMSO served as vehicle control for these experiments.

## 8) Nucleic acid isolation

DNA and RNA were extracted from cell culture-derived cell pellets and the liquid biopsy-derived cell pellets in order to allow downstream gene expression analysis (RT-qPCR of the RNA) and gene promoter CpG methylation analysis (Pyrosequencing of the DNA).

For DNA extraction from mast cells at JLU, cell pellets were digested for 1 hour with 0.75µg/µL proteinase K (Roth, Karlsruhe) at 56°C. After that, 500µL of Phenol/Chloroform/Isoamylalcohol (25:24:1) were added, samples were mixed by vortexing, and phase separation was acquired by centrifugation (10 minutes at 13.000rpm). DNA was precipitated with 1 volume isopropanol, 1/10 volume sodium acetate (3M) and 5µg glycogen).

RNA from cell pellets was isolated with peqGOLD TriFast™ reagent (Peqlab) following the manufacturer's protocol. The DNA from clinical liquid biopsy cell pellets was recovered from the remaining TriFast™ organic phase (with interphase). DNA recovery was done with a chaotropic "back extraction buffer" (4M guanidine thiocyanate, 50mM sodium citrate and 1M Tris). After rigorous mixing with the "back extraction buffer", phase separation was acquired by centrifugation (15 minutes at 13,000rpm) and DNA was precipitated overnight from the upper phase with 1 volume isopropanol, 1/10 volume sodium acetate (3M) and 5µg glycogen. DNA pellets were digested for 30 minutes with 80µg proteinase K and subsequently purified with Phenol/Chloroform (same method as for mast cells). Isolated RNA was digested in 20µL volume with 1U DNase I, following the manufacturer's (NEB) instructions, purified by TriFast™ extraction and dissolved in 20µL of DEPC-treated nuclease-free water. RNA and DNA concentrations were measured on the NanoDrop-1000 (Thermo Scientific) and stored at -80° C until use.

For RNA isolation from NPF/CAF and macrophages at MU, frozen cell pellets were thawed on ice and total RNA was isolated with the RNeasy Mini Kit (Qiagen; Cat No. 74104) doing on-column DNase I (Qiagen; Cat No. 79254) digestion for 15min at RT.

## 9) Gene expression analysis

At JLU, isolated SC from human ejaculate were analyzed for relative gene expression of *ESR1*, *ESR2*, *AR*, *CMA1*, *PU.1*, *IL-7*, *CD68* and *CCL18* by RT-qPCR (reverse transcription followed by quantitative real-time PCR) using *TUBA1B*, *GAPDH*, *mRPL19* or *ACTB* as reference genes. In isolated circulating WBC, gene expression of *ESR1*, *ESR2* and *AR* was measured. An RNA sample isolated from blood leukocytes of a healthy donor was used as internal standard (calibrator). RNA samples (each 2µg) were reverse transcribed with MMLV-RT (Promega) into cDNA, following the manufacturer's protocol. Subsequent qPCRs were performed using RotorGene SYBR Green PCR Kit (Qiagen) and the CFX96 Touch™ RealTime PCR Detection System (Bio-Rad) with the following thermocycler program:

1. 95°C for 3min (activation of HotStarTaq *Plus* DNA Polymerase)
2. 95°C for 30s (denaturation)
3. 60°C for 30s (annealing)
4. 72°C for 30s (extension)
5. Repeat steps 2-4 for 45 cycles
6. Melt curve acquisition.

At MU, gene expression of *HOXD8*, *ESR1*, *SFRP-1*, *SDC2*, *EPHB6* and *PITX2* was measured in NPF/CAF, and gene expression of *TNF*, *IL-1B*, *HLA-DRA*, *HLA-DQA1*, *CD206*, *CCL13*, *CCL18* and *IL-10* was measured in the macrophages. *GAPDH* served as reference gene. Briefly, 500ng of RNA were reverse transcribed with SuperscriptIII (Invitrogen) in the presence of 40U RNaseOUT™ Recombinant Ribonuclease Inhibitor (Invitrogen). Quantitative PCR measurements were carried out on the “Stratagene Mx3000P qPCR System” (Agilent) using SYBR green (Applied Biosystems) in a reaction volume of 12.5µL and the same PCR program as used at JLU. Primers for RT-qPCR were designed with Primer3 using the online Primer Blast platform (NCBI/NIH), or taken from published articles (**Tab. 2**).

Untreated and E2-stimulated mast cell lines (HMC-1 and LAD2) were analyzed with regard to the relative gene expression of 84 inflammatory factors using the RT<sup>2</sup>Profiler™ “Human Cytokines and Chemokines PCR Array” (Qiagen).

**Table 2. Primers used for quantitative reverse transcription PCR (RT-qPCR).**

For all primers 60°C were used as annealing temperature.

Gene	Upper (5'-3')	Lower (5'-3')	Amplicon (bp)	Reference
<i>ACTB</i>	AACTCCATCATGAAGTGTGACGT	TGATCCACATCTGCTGGAAGGT	235	Self-designed
<i>AR</i>	GCAGGAAGCAGTATCCGAAG	GACACCGACACTGCCTTACA	144	Nesheim et al. 2018 [97]
<i>BCL3</i>	CCGCAGGGTCATCGACATC	AAGACCATTGGAGCTGAGGC	130	Self-designed
<i>CCL13</i>	TGCAGAGGCTGAAGAGCTATG	GTTTGGTTCTGAAGATGACAGCC	72	Self-designed
<i>CCL18</i>	AGCCAGGTGTCATCCTCCTAA	CAGCTTCAGGTCGCTGATGTA	95	Self-designed
<i>CD206</i>	CTACAAGGGATCGGGTTTATGGA	TTGGCATTGCCTAGTAGCGTA	105	Reeves et al. 2015 [113]
<i>CD68</i>	CTTCTCTCATCCCTATGGACA	GAAGGACACATTTACTCCACC	105	Reeves et al. 2015 [113]
<i>CMA1</i>	GTCCCACCTGGGAGAAATGTG	TCTTGCAGAGTGTCTGAGCC	80	Nesheim et al. 2018 [97]
<i>EPHB6</i>	ACAAGATGATCCGCAAGCCA	AGGCAGGTCTCTAGGCTGA	221	Pidsley et al. 2018 [114]
<i>ESR1 (1/2)</i>	TGCAGGGAGAGAGTTTGTG	GGACAGAAATGTGTACACTCCAGA	71	Nesheim et al. 2018 [97]
<i>ESR1 (2/2)</i>	TGATTGGTCTCGTCTGGCGCT	GCACACAACTCCTCTCCCTGC	179	Ellem et al. 2014 [25]
<i>ESR2</i>	GATGAGGGGAAATGCGTAGA	GATCATGGCCTTGACACAGA	120	Nesheim et al. 2018 [97]
<i>GAPDH</i>	GCAAATTCATGGCACCCT	TCGCCCCACTTGATTTTGG	106	Lawrence et al. 2011 [115]
<i>GATA3</i>	GAGATGGCACGGGACACTAC	CTGCAGACAGCCTTCGCTTG	102	Self-designed
<i>HLA-DQA1</i>	GTGGCAAAAACACAACCTGAACA	TGACCTCAGGAACCTCATTGG	76	Self-designed
<i>HLA-DRA</i>	TCCGATCACCAATGTACCTCC	CACTGGTGGGGTGAACCTGT	109	Self-designed
<i>HOXD8</i>	CGGATACGATAACTTACAGAGACAG	TCTTCGTCTACCAGGAGCTTG	184	Pidsley et al. 2018 [114]
<i>IL-10</i>	AAGACCCAGACATCAAGGCG	AATCGATGACAGCGCCGTAG	85	Reeves et al. 2015 [113]
<i>IL-1B</i>	TCGCCAGTGAAATGATGGCT	TGGAAGGAGCACTTCATCTGTT	91	Self-designed
<i>IL7</i>	GTGACTATGGGCGGTGAGAG	AAAGAAACATGGAACATGGTCTGC	90	Self-designed
<i>INH1A</i>	GCTCAACTCCCCTGATGTCC	TGCTACTCTGTGGCAGTTGG	104	Self-designed
<i>mRPL19</i>	TGCCAGTGGAAAAATCAGCCA	CAAAGCAAATCTGCACACCTTG	119	Leach et al. 2015 [116]
<i>PITX2</i>	CAGCCTGAGACTGAAAGCA	GCCCCAGACCTTCTAGCAT	200	Vela et al. 2014 [117]
<i>PU.1</i>	GTGCCCTATGACACGGATCT	CCAGTAATGGTCGCTATGGCT	93	Nesheim et al. 2018 [97]
<i>SDC2</i>	TGGAAACCACGACGCTGAAT	CAGCAATGACAGCTGCTAGG	198	Pidsley et al. 2018 [114]
<i>SFRP1</i>	ATGCAGTTCTTCGGCTTCTACT	AGGGAGGACACACCGTTGTG	136	Joesting et al. 2005 [118]
<i>TLR2</i>	CTGTGCTCTGTTCTCTGCTGA	GATGTTCTGCTGGGAGCTT	133	Self-designed
<i>TNF</i>	GTAGCCCATGTTGTAGCAAACC	TCTCTCAGCTCCACGCCATT	98	Self-designed
<i>TUBA1B</i>	CGTGCCCCGGCTGTGTTT	GCAGCATCTTCTTGCCCTGTGA	117	Nesheim et al. 2018 [97]

Briefly, RNA samples (each 2µg) were reverse-transcribed with the RT2 First Strand Kit (Qiagen). The cDNA samples were purified with the Nucleotide Removal Kit (Qiagen) and analyzed with pre-manufactured RT<sup>2</sup> Profiler™ 96-well plates. Five housekeeping genes (*ACTB*, *B2M*, *GAPDH*, *HPRT1* and *RPLP0*) were included, and those with the most stable expression among conditions (*B2M*, *GAPDH* and *HPRT1*) were chosen as reference for calculation of  $\Delta C_t$  values. All measurements at JLU and MU were done in technical duplicates or triplicates. Relative gene expression values were taken as raw delta Ct value ( $\Delta C_t$ ), calculated into relative expression ( $2^{-\Delta \Delta C_t}$ ), or calculated into gene regulation ( $-\Delta \Delta C_t$ ).

## 10) Gene promotor CpG methylation analysis

Isolated DNA samples were analyzed with pyrosequencing regarding the promotor CpG methylation of the genes *ESR1*, *ESR2*, *AR*, *BMP6*, *BMP7*, *IL-13*, *CXCL2*, *CXCR4* and *CXCL12*. Bisulfite treatment of denatured DNA leads to deamination of unmethylated Cytosine (C) residues to Uracil (U). Methylated C residues standing in a CpG context (5-mC) remain unaffected by this bisulfite conversion. Consequently, bisulfite treatment produces a nucleotide polymorphism of cytosine residue in the CpG site (C or U). The polymerase in the subsequent PCR does not distinguish between Thymine (T) and U, so the induced template DNA polymorphism at the CpG site is amplified (5-mCG stays CG, 5-CG becomes TG). The methylation-dependent polymorphism can be visualized by combined bisulfite restriction analysis (COBRA) or pyrosequencing (**Fig. 12**).

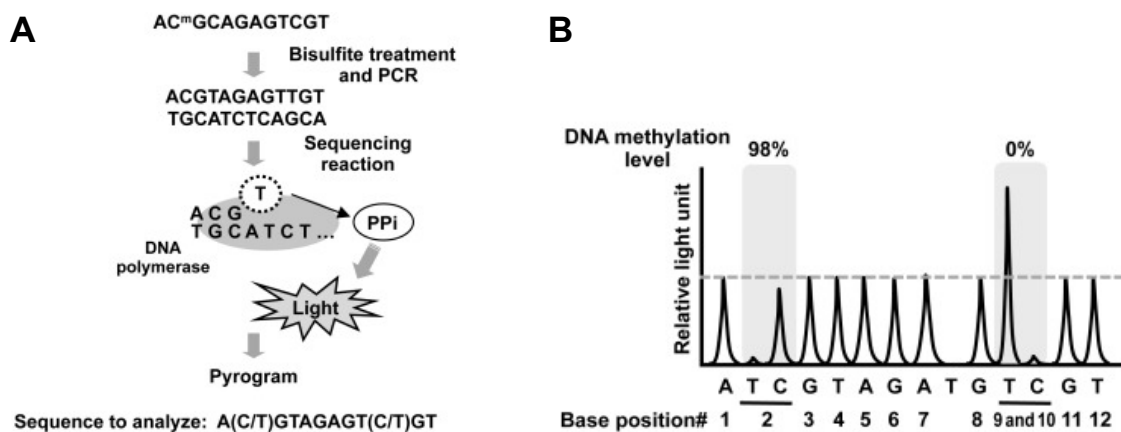


**Figure 12. The concept behind pyrosequencing of gene promotor CpG sites.**

Pyrosequencing can visualize a sequence polymorphism with the photon-generating luciferase reaction. A polymerase reaction generates the substrate for luciferase. Only one dNTP is added to the reaction at once, so that the polymerase is only active when the added dNTP matches the complementary pocket in the nascent template DNA strand (**A**). This results in characteristic signal peaks (**B**). Knowledge of the template DNA sequence with all CpG positions allows to determine the sequence to analyze (**A**), which is then tested during the pyrosequencing reaction (**B**). In case of a CpG related nucleotide polymorphism, the two possible candidate nucleotides are tested (**B**; base position #2) and the signal peak ratio of both tested nucleotides allows for calculation of the CpG methylation percentage at the respective CpG site. Reference: Hattori & Ushijima 2017 [119].

Pyrosequencing employs a PCR reaction that supplies energy for a luciferase reaction. Since DNA polymerase requires double-stranded DNA for synthesis, only the first free nucleotide position of the nascent DNA strand is available for nucleotide incorporation at the same time. In comparison to a conventional PCR, only one nucleotide is added to the reaction at once.

Consequently, the polymerization stops as soon as the following free nucleotide position of the nascent DNA strand does not match the present deoxynucleotide (dNTP), resulting in a characteristic signal peak. Present apyrase leads to degradation of remaining dNTPs and therefore allows to offset the pyrosequencing reaction after each nucleotide addition. With knowledge of the template DNA sequence, an assay-specific nucleotide dispensation order is used to determine nucleotide polymorphisms in the analyzed template DNA.

CpG methylation analysis in the mast cell lines and CP/CPSS patients' liquid biopsies was performed using pre-designed pyrosequencing assays, or a custom pyrosequencing assay was designed using the "PyroMark® Assay Design Software 2.0" in the case of *TLR2* (Tab. 3).

**Table 3. CpG assays for promotor CpG methylation analysis.**

Pyromark assays were either pre-designed (Pyromark CpG Assay; Qiagen) or manually designed using the "PyroMark® Assay Design Software 2.0" (Custom Assay). The PCR amplification and sequencing protocol is identical for all listed CpG assays, including the Custom Assay (*TLR2*).

Gene	Pyromark CpG Assay	Sequence to analyze	CpG #	Amplicon (bp)	Chromosomal Location
<i>ESR1</i>	Hs_ESR1_01_PM (PM00024612)	CGACAGCTGC GGCGCGGGT	4	114	Chromosome 6, BP 1521293XX-1521294XX
<i>ESR2</i>	Hs_ESR2_01_PM (PM00166117)	CGACGGTCTCAGGAAC GCCCGACGCGCGCGT	8	192	Chromosome 14, BP 647611XX-647612XX
<i>AR</i>	Hs_AR_01_PM (PM00134085)	TTTGCAGTCGGGTCCC GCCCCACCGGGCCGGC	5	167	Chromosome X, BP 667638XX-667638XX
<i>AR</i>	Hs_AR_04_PM (PM00134106)	GCCAGGGTACCACACAT CAGGTGCGGTGAAGTCGC	3	110	Chromosome X, BP 667664XX-667665XX
<i>BMP2</i>	Hs_BMP2_01_PM (PM00196763)	TTCCGCTCCAGAGTCCC CGCGAGGGTCCGGCGCGC	6	122	Chromosome 20, BP 67480XX-67480XX
<i>BMP6</i>	Hs_BMP6_01_PM (PM00123529)	CTCCGCGCGCCGACGCC TCCTCAAGCGGAGCGGGC	8	252	Chromosome 6, BP 77265XX-77265XX
<i>BMP7</i>	Hs_BMP7_02_PM (PM00079352)	ACATGGGTGCGAGTTGTGTTGC CCTGGAGGTGCGGGCGGGCGGT	5	210	Chromosome 20, BP 558409XX-558409XX
<i>IL13</i>	Hs_IL13_01_PM (PM00023079)	CCGGAGCCCCGCC GGGTGAGTCAACGC	4	102	Chromosome 5, BP 1319922XX-1319923XX
<i>CXCL2</i>	Hs_CXCL2_01_PM (PM00017773)	TGTGGCCCGGCTCTGTG GCTCTCCGAGAACGGCGA	4	89	Chromosome 4, BP 749648XX-749649XX
<i>CXCR4</i>	Hs_CXCR4_01_PM (PM00009128)	ACTGGGCGGGGCGGAGTG GGGTRGGGGTCAGACGT	3	198	Chromosome 2, BP 1368767XX-1368768XX
<i>CXCR4</i>	Hs_CXCR4_05_PM (PM00009156)	CGTGC GCGCTGCCTCG GGACTCAGACCACCGGT	5	241	Chromosome 2, BP 1368752XX-1368752XX
<i>CXCL12</i>	Hs_CXCL12_04_PM (PM00042343)	GCGGAGTTCGGAGCCCTCGC AGCCTCCTGTTGACCCTCCCG	5	265	Chromosome 10, BP 448818XX-448818XX
<i>TLR2</i>	N/A (Custom Assay)	CGGCCGCGGGGGCTCGCTCGG GGCCACCTGCCTGGAACCTACG	5	149	Chromosome 4, BP 153684087-153684235

The nucleotide sequences of the pre-designed Pyromark CpG Assays (Qiagen) are not disclosed by the vendor. The sequences of the *TLR2* Custom Assay are known: Upper PCR-Primer (5'-3'): GGGAGTTTGTGGGAAGT, Lower PCR-Primer (Biotin-5'-3'): AACCCCCCTCCTTCTAAATAC, Sequencing Primer (5'-3'): GGAGTTTGTGGGAAGTA.

For bisulfite conversion, 1µg of DNA was treated using the EZ DNA Methylation™ Kit (Zymogen). A total amount of 5-30ng bisulfite-treated DNA was subsequently amplified with MyTaq™ HS Polymerase (Bioline) in a PCR reaction volume of 25µL, specific primers and the following thermocycler program:

1. 95°C for 3min (hot-start to activate DNA polymerase)
2. 95°C for 30s (denaturation)
3. 60°C for 30s (annealing)
4. 72°C for 45s (extension)
5. Repeat steps 2-4 for 45 cycles
6. 72°C for 3min (final extension)

PCR products were controlled by separation on a 2% agarose gel (1.8g Agarose, 100mL 1xTAE buffer) in 1xTAE buffer (10x TAE buffer: 48.4g Tris, 11.42mL glacial acetic acid, 20 ml 0.5M EDTA in 1mL deionized water; pH 8.0). PCR products were then pyrosequenced with the PyroMark Q24 System (Qiagen) using the manufacturer instructions. Methylation values were analyzed using PyroMark Q24 Software (Qiagen).

The mast cell lines were analyzed for CpG promoter methylation of 22 inflammatory factors using the EpiTect Methyl II “Human Cytokine Production Signature Panel” (Qiagen). This Kit determines gene promotor CpG methylation without bisulfite conversion of the template DNA by restriction digest with a combination of CpG methylation-sensitive and CpG methylation-dependent restriction enzymes and a quantitative PCR. In case of a successful restriction digest, the PCR template is destroyed and cannot be amplified. Inclusion of controls with unmethylated DNA, fully methylated DNA and a mock digest allowed for  $\Delta$ Ct-based calculation of the relative gene promotor CpG methylation.

Briefly, mast cell DNA samples were incubated for 6 hours (at 37°C) with methylation-dependent and methylation-sensitive restriction enzymes and then amplified on prefabricated 96-well plates using RotorGene SYBR Green PCR Kit (Qiagen) and the CFX96 Touch™ RealTime PCR Detection System (Bio-Rad) with the following protocol:

1. 95°C for 10min (hot-start to activate DNA polymerase)
2. 99°C for 30s
3. 72°C for 1min
4. Repeat steps 2-3 for 3 cycles
5. 97°C for 15s
6. 72°C for 1min
7. Repeat steps 5-6 for 40 cycles
8. Melt curve acquisition.

The “EpiTect Methyl II PCR Array Microsoft Excel based data analysis template” from the Sabiosciences web platform was used for the calculation of relative gene promoter CpG methylation values.

### **11) Western Blot of CCL18 in E2-treated THP-derived macrophages**

To verify that estradiol (E2) upregulates macrophage CCL18 expression on the protein level, a western blot analysis of control cells and E2-treated M2 macrophages was performed.

Frozen (-80°C) cell pellets were thawed on ice and resuspended in lysis buffer (10mM Tris-HCl, 150mM NaCl, 1mM EDTA, 1mM DTT, 1mM PMSF, 1% Triton X-100) containing protease inhibitor. After that, cells were sonicated on ice (3x10sec; 30% intensity) with the Vibra-Cell™ Ultrasonic Liquid Processor (Bioblock scientific). Lysates were centrifuged for 30min (20,000g, 4°C) and pellets were discarded. Protein concentrations of the supernatant were measured with the Pierce BCA Protein Assay Kit.

For sodium dodecyl sulfate polyacrylamide gel electrophoresis (SDS-PAGE), 50µg of protein were cooked for 3min (95°C) in freshly prepared Laemmli buffer (5% β-met) and then separated in a polyacrylamide gel (4% stacking gel, 10% separating gel) in SDS running buffer (25mM Tris, 0.2mM glycine, 0.1% SDS, pH 8.3) using 100V (stacking gel) and 120V (separating gel). Protein separation was controlled on the gels with Coomassie staining (0.1% Coomassie, 10% acetic acid, 20% MeOH), and gels were subsequently de-stained (40% MeOH, 10% acetic acid).

For semi-dry electroblot, the gel was first equilibrated for 5min in transfer buffer (48mM tris, 38mM glycine, 20% MeOH, 0,0375% SDS) under gentle agitation, and the PVDF membrane was activated for 1min in 100% MeOH.

Then a current of 150mA ( $\approx 3\text{mA}/\text{cm}^2$ , max. 25V) was applied for 30min to the saturated (in transfer buffer) sandwich (1. whatman-paper, 2. gel, 3. membrane, 4. whatman-paper) using the Trans-Blot SD Semi-Dry Transfer Cell (Bio-Rad). Protein transfer to the PVDF membrane was controlled with the REVERT™ Total Protein Stain Kit (LI-COR).

After 1 hour blocking of the membrane with Odyssey Blocking Buffer (LI-COR), the membranes were incubated overnight (4°C, 15rpm) in Odyssey Blocking Buffer containing primary antibodies against CCL18 (1:100) or GAPDH (1:2500). The following day, membranes were washed 4x5min with PBS containing 0.1% Tween-20 (PBT) on the rotator (RT, 20rpm). Then, membranes were incubated for 1 hour in the darkness (RT, 20rpm) with secondary fluorescent antibody (IRDye® 800CW Goat anti-Rabbit IgG, LI-COR). Membranes were subsequently washed 4x5min in the darkness with PBT (RT, 20rpm). Image acquisition was done with the Odyssey® Fc Imaging System (LI-COR).

## **12) Chromatin immunoprecipitation**

To assess whether E2-stimulation of THP-1 derived macrophages induced CCL18 expression through estrogen receptor binding of the CCL18 gene promotor, a chromatin immunoprecipitation (ChIP) experiment was done.

Macrophages in 10cm dishes were crosslinked for 10min at 37°C in culture medium containing 1% formaldehyde (FA), and crosslinking was stopped with 125mM glycine for 5min at RT. All solutions of the following steps were prepared with protease inhibitor cocktail (Sigma-Aldrich). Cells were washed 3x with ice cold PBS and scraped in 2mL ice cold lysis buffer (50mM Tris-HCl, pH 8.0; 1mM EDTA, pH 8.0; 10% glycerol, 0.1% NP-40). After 15min incubation on ice with occasional vortexing, cells were centrifuged for 10min at 1,500g (4°C). Pellets were resuspended in 600µL ice cold nuclear resuspension buffer (50mM Tris-HCl, pH 8.0; 1mM EDTA, pH 8.0; 150mM NaCl; 0.1% SDS).

Half the sample (300 $\mu$ L) was sonicated on the Bioruptor® (Diagenode), while the other half was stored at -20°C. Sonication was done using 3 cycles of 30s sonication and 30s pause. Optimal DNA fragment size (~200-550bp) was controlled with agarose gel electrophoresis (2%) of de-crosslinked and phenol/chloroform purified DNA. Soluble chromatin was recovered as supernatant after centrifugation (10min at 16,000g, 8°C) and diluted with 900 $\mu$ L dilution buffer (50mM Tris-HCl, pH 8.0; 1mM EDTA, pH 8.0; 150mM NaCl; 0.5% NP-40; 0.1% Triton X-100).

For chromatin pre-clearing, 20 $\mu$ L magnetic beads from the Dynabeads™ Protein G Immunoprecipitation Kit (Invitrogen) were added and incubated on the rotator for 1 hour (15rpm, 4°C). Magnetic beads were discarded after centrifugation (2min at 100g, 4°C + 1min at 1000g, 4°C) and the supernatant was recovered.

An input control (40 $\mu$ L; 10% volume) of the chromatin solution was stored at -20°C and each (3x) 400 $\mu$ L were used for immunoprecipitation with different antibodies. The chromatin solution was incubated on the rotator (15rpm, 4°C) overnight with 6 $\mu$ L (~4 $\mu$ g) monoclonal mouse ER $\alpha$  antibody (Active Motif, Cat. 61035), 5 $\mu$ L monoclonal rabbit H3K4me3 antibody (Merck/Millipore, Cat. 17-614) and 1 $\mu$ L mouse IgG isotype control (Invitrogen, Cat. 31903). The following day, each 20 $\mu$ L magnetic beads were added and conjugated to the antibody on the rotator (2 hours at 15rpm, 4°C). Beads were then consecutively washed once with low salt wash buffer (20mM Tris-HCl, pH 8.0; 2mM EDTA, pH 8.0; 1% Triton X-100; 0.1% SDS; 0.15M NaCl), high salt wash buffer (20mM Tris-HCl, pH 8.0; 2mM EDTA, pH 8.0; 1% Triton X-100; 0.1% SDS; 0.5M NaCl), LiCl wash buffer (10mM Tris-HCl, pH 8.0; 1mM EDTA, pH 8.0; 1% NP-40; 1% sodium deoxycholate; 0.25M LiCl), and twice with TE buffer (10mM Tris-HCl, 1mM EDTA, pH 8.0), using a magnetic rack for bead immobilization. Chromatin was then eluted 3x with each 250 $\mu$ L elution buffer (0.1M NaHCO<sub>3</sub>, freshly prepared; 1% SDS) for each 15min on the rotator (25rpm, vertical angle, RT). The input control was adjusted with TE buffer to a volume of 750 $\mu$ L, and then de-crosslinked together with the eluates for 4 hours at 65°C after addition of 30 $\mu$ L NaCl (5M).

De-crosslinked DNA was purified with Phenol/Chloroform (same protocol as DNA isolation from mast cells; no Proteinase K digestion) and DNA was resuspended in 20 $\mu$ L water. Specific PCR primers [Upper (5'-3'): GACAACAGCTCATACCCCAGAA; Lower (5'-3'): TGGTGCAGACGAGGACAAGG; Amplicon Size: 132bp] were used for amplification of an estrogen response element (ERE; located at the TSS+29bp) in the *CCL18* gene promoter (Chromosome 17, BP 36064254-36064385). ChIP DNA was amplified in triplicates using RotorGene SYBR Green PCR Kit (Qiagen) and 1 $\mu$ L sample/replicate in a reaction volume of 10 $\mu$ L. We used the CFX96 Touch™ RealTime PCR Detection System (Bio-Rad; same protocol as for RT-qPCR), and enrichment of ER $\alpha$  and H3K4me3 was calculated with the  $\Delta\Delta$ Ct method, normalizing samples to the undiluted input control.

### 13) Co-Culture Assays

Co-culture assays were done to examine the influence of THP-1 derived macrophages on an established reference system with benign prostate epithelium cells (BPH-1) growing on primary patient-derived CAF (and NPF).

First, NPF and CAF were seeded at a density of 1.5x10<sup>4</sup> cells/well into a 24-well plate (BD falcon). NPF/CAF were grown for one week under low oxygen conditions (37°C, 5% CO<sub>2</sub>, 5% O<sub>2</sub>) to allow the development of a confluent monolayer with adequate ECM deposition. For co-culture, 1.5x10<sup>4</sup> BPH-1 cells/well were pre-stained with Cell Tracker green CMFDA (5-chloromethylfluorescein diacetate; Invitrogen), using the manufacturer instructions. Pre-stained BPH-1 cells were then seeded alone or in combination with unstained monocytes/macrophages onto the pre-grown fibroblast layer. Monocytes/macrophages (THP-1, M $\phi$ , M1 or M2) were used with various cell densities (0.75x10<sup>4</sup>, 1.5x10<sup>4</sup> or 3.0x10<sup>4</sup> cells/cm<sup>2</sup>). The results obtained with lower monocyte/macrophage densities (0.75x10<sup>4</sup> and 1.5x10<sup>4</sup>) were less pronounced than results from the highest cell density (3.0x10<sup>4</sup> cells/cm<sup>2</sup>) and are *not shown* in this manuscript. Co-cultures were used immediately (live cell imaging) or grown for 24 hours (37°C, 5% CO<sub>2</sub>) before FA-fixation (confocal imaging).

#### **14) Fluorescence imaging of co-culture assays**

Co-Cultures for confocal imaging were fixed for 10min at RT with 4% FA (Sigma-Aldrich) and subsequently permeabilized for 5min with PBS-TritonX (0.2%; BDH, Poole, UK).

Samples were then washed 2x with PBS and incubated for 25min with PBS containing 8U/mL Phalloidin-Tetramethylrhodamine (TRITC; Invitrogen). Excess dye was removed by washing 2x with PBS and samples were stored in PBS at 4°C. Confocal imaging was done on the Nikon C1 Inverted Confocal Microscope (Nikon Instruments Inc.) with a 100x magnification. Distinct excitation- and emission spectra for Cell Tracker green CMFDA (492/517nm) and phalloidin-TRITC (540/565nm) allowed for multiplexed acquisition in separate channels. Co-Cultures for live cell imaging were not fixed, but instead immediately transferred to the Leica AF6000LX “Integrated Live Cell Workstation” (Mannheim, Germany), where photos were taken every 30min under controlled conditions (37°C, 5% CO<sub>2</sub>). Live cell time lapse images of the growing co-culture assay were captured on the Cell Tracker green CMFDA (492/517nm) channel together with the bright field channel. Minimum exposure intensity and times were used to minimize effects on the cells.

#### **15) Quantification of fluorescent imaging data**

Morphometric quantitation of confocal imaging results was done with FIJI (FIJI Is Just ImageJ), applying a macro script to all acquired image hyperstacks. In short, channel separation preceded background reduction by Gaussian blur (Sigma value 2 pixels) before creation of binary images that allow for software-based cell shape recognition and quantification. Live cell time lapse image stacks were pre-processed with a FIJI macro script (Gaussian Blur, Bleach Correction, Brightness Adjustment, Binary Thresholding) before analysis of BPH-1 cells with CellProfiler 3.0 (Broad Institute).

## 16) Statistical Analysis

Statistical analyses were done with SPSS 24.0 (IBM) and Prism 7.0b (GraphPad). The linear regression model was used to test the relationship of variables for significance. Non-parametric variables were compared using the Mann-Whitney U-test. The paired Students' T-Test was used for the comparison of CAF with patient-matched NPF. All presented p-values were calculated with a two-tailed test. Only p-values  $\leq 0.05$  were considered as statistically significant (\*\*\*\*= $p < 0.0001$ ; \*\*\*= $p < 0.001$ ; \*\*= $p < 0.01$ ; \*= $p < 0.05$ ).

## Results

At Justus-Liebig-University (JLU), we characterized the mast cell lines HMC-1 and LAD2 to assess how estrogen signaling and mast cell activity affect chronic inflammation in CP/CPPS. The mast cell lines were first characterized regarding the epigenetic state of *ESR1*, *ESR2* and various other genes with relevance for the inflammatory response. Then *in vitro* E2-stimulated HMC-1 and LAD2 cells were analyzed to understand the influence of E2 on the mast cell physiology. In consecutive experiments at JLU, liquid biopsies from CP/CPPS patients were analyzed regarding the concentrations of testosterone and E2, the epigenetic state of the sex hormone receptors (*ESR1*, *ESR2*, *AR*) and the expression of some inflammatory genes (*BMP7*, *IL-7*, *CMA1*, *CD68*, *CCL18*).

At Monash-University (MU), THP-1 derived macrophages were educated with CM from different cell types to evaluate the influence of prostatic epithelial and stromal cells on macrophage polarization. Using co-culture experiments, we examined how monocytes (THP-1) and *in vitro* generated macrophage subtypes (M $\phi$ , M1 or M2) influence BPH-1 cells on a pre-grown layer of primary prostate fibroblasts (NPF or CAF).

Our experiments had the following core aims:

- (1) Investigation of the mast cell response to estradiol stimulation
- (2) Analysis of clinical routine parameters from CP/CPPS patients
- (3) Isolation of somatic cells from human semen samples
- (4) Detection of leukocyte-specific transcripts in somatic cells from semen
- (5) Detection of CP/CPPS-related changes of steroid sex hormone signaling
- (6) Studies of the stromal influence on macrophage polarization
- (7) Investigation of macrophage interactions with the prostate tumor stroma

The results from our experiments led to the following observations:

- (1) Estradiol affects the mast cell response (Aim 1)
- (2) Semen parameters of CP/CPPS patients are affected (Aim 2)
- (3) Density gradient centrifugation allows the isolation of ejaculated somatic cells (Aim 3)
- (4) Ejaculated somatic cells from CP/CPPS patients exhibit leukocyte-specific gene transcription changes (Aim 4)
- (5) CP/CPPS associates with aberrant steroid sex hormone signaling (Aim 5)
- (6) Stromal cells affect the macrophage phenotype (Aim 6)
- (7) Macrophages shape the prostate tumor microenvironment (Aim 7)

## 1) Estradiol affects the mast cell response

Estrogens have the potential to modulate inflammatory signaling, so the CP/CPPS pathogenesis might be explained with a dysregulated estrogen signaling. We analyzed the mast cell lines HMC-1 and LAD2 regarding their inherent inflammatory gene expression profile and their susceptibility to estrogens. HMC-1 and LAD2 differ remarkably regarding the epigenetic makeup of the estrogen receptors (*ESR1*, *ESR2*) and their inflammatory gene expression before and after E2-stimulation.

### 1.1) HMC-1 and LAD2 differ regarding *ESR1* and *ESR2*

We measured promotor CpG methylation (Pyrosequencing) and gene expression (RT-qPCR) of the estrogen receptors (ER) *ESR1* and *ESR2* in the mast cell lines HMC-1 and LAD2. LAD2 express both ER, but HMC-1 cells show epigenetically downregulated ER, which is reflected in promotor CpG hypermethylation and diminished transcript levels (**Fig. 13**).

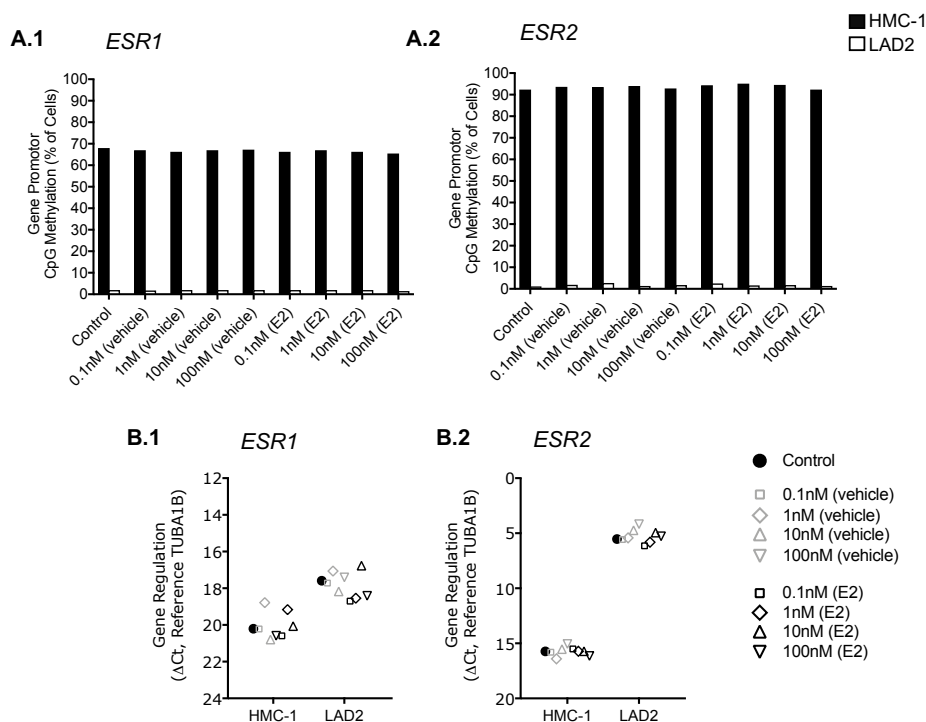


**Figure 13. HMC-1 and LAD2 cells display different epigenetic states of *ESR1* and *ESR2*.**

Promotor CpG methylation (**A**) and gene expression (**B**) of *ESR1* and *ESR2* were measured in untreated and E2-treated HMC-1 and LAD2 cells (n=1). While HMC-1 cells showed promotor methylation of *ESR1* and *ESR2* (**A**; *ESR1*: 68%, *ESR2*: 92% of cells), LAD2 cells were unmethylated in the same CpG sites (**A**; *ESR1*: 2%; *ESR2*: 1% of cells). Accordingly, LAD2 showed higher basal transcript levels of *ESR1* (**B.1**; HMC-1:  $\Delta\text{Ct}$  20.21; LAD2:  $\Delta\text{Ct}$  17.59) and *ESR2* (**B.2**; HMC-1:  $\Delta\text{Ct}$  15.73; LAD2:  $\Delta\text{Ct}$  5.53). Treatment with ethanol (vehicle control) or E2 did not affect *ESR1/ESR2* promotor CpG methylation (**A**), and gene expression was only slightly influenced (**B**).

Treatment with various E2-concentrations (0.1nM, 1nM, 10nM, 100nM) for 24 hours did not affect *ESR1/ESR2* promoter CpG methylation, and *ESR1/ESR2* gene expression levels were only slightly regulated by E2-treatment. *ESR1* expression was slightly suppressed by 1nM, 1nM and 100nM of E2 in both cell lines, but upregulated by 10nM E2. All E2-concentrations downregulated *ESR2* in LAD2, but only the highest concentration (100nM) suppressed *ESR2* expression in HMC-1. Since we did only one repetition for each E2-stimulation (n=1), we have no information about the reproducibility of these expression changes.

### **1.2) HMC-1 and LAD2 differ regarding the CpG methylation of inflammatory genes**

The androgen receptor (*AR*), *BMP6*, *BMP7*, *IL-13*, *CXCL2*, *CXCL12* and *CXCR4* were pyrosequenced in HMC-1 and LAD2 cells. As members of the TGF $\beta$  superfamily, bone morphogenetic proteins (e.g. *BMP6*, *BMP7*) are important regulators of cell differentiation and influence the leukocyte phenotype [120], and signaling through the AR was demonstrated to affect the inflammatory response [121]. The chemokines *CXCL2* and *CXCL12* attract leukocytes, and the *CXCL12/CXCR4* axis was shown to recruit mast cells to PCa lesions [25]. *CXCR4* is epigenetically inactivated in many cancers [100], and our group detected *CXCR4* hypermethylation in ejaculated cells from CP/CPPS patients. *IL-13* is an important T-cell secreted mediator of the anti-inflammatory response, so *IL-13* downregulation has the potential to prime leukocytes for an inadequately pro-inflammatory response. All mentioned genes might be affected in CP/CPPS patients and/or indicate disease progression towards PCa initiation.

The effect of E2-treatment (0.1nM, 1nM, 10nM, 100nM) on promoter CpG methylation of these genes was evaluated. E2-treatment had no obvious effects on gene promoter CpG methylation of pyrosequenced genes, but considerable differences were observable between HMC-1 and LAD2 cells (**Tab. 4**).

**Table 4. Methylation analysis of gene promotor CpG sites in HMC-1 and LAD2 cells.**

Unstimulated (n=1) and E2-treated (0.1nM, 1nM, 10nM, 100nM; each n=1) HMC-1 and LAD2 cells were pyrosequenced in CpG-rich promotor regions of 9 genes with potential relevance for the inflammatory response. A Methylation Profiler Array was used to measure the CpG methylation of 22 genes in unstimulated and E2-stimulated cells (100nM). Promotor CpG methylation values are given as percent of cells (%). Grey values represent a continuous scale from 0-100%.

Cell Line		HMC-1										LAD2																		
Treatment		C					Vehicle Control					E2 Treatment					C				Vehicle Control				E2 Treatment					
Concentration (nM)		0nM	0.1	1	10	100	0.1	1	10	100	0nM	0.1	1	10	100	0.1	1	10	100	0nM	0.1	1	10	100	0.1	1	10	100		
Pyrosequenced Genes	<i>AR (Region 1)</i>	44	46	45	44	44	46	45	45	43	2	2	2	2	2	2	2	2	2	2	2	2	2	2	2	2	2	2		
	<i>AR (Region 4)</i>	42	42	40	40	38	41	41	42	41	4	3	3	3	3	3	3	3	3	3	4	3	3	3	3	3	3	3		
	<i>BMP6 (Region 1)</i>	3	1	2	1	1	2	2	2	2	2	2	2	2	2	2	2	2	2	2	2	2	2	2	2	2	2	2		
	<i>BMP7 (Region 2)</i>	22	29	28	29	28	30	29	30	29	3	4	9	3	4	5	4	4	4	6	3	4	9	3	4	5	4	4	6	
	<i>CXCL2</i>	88	90	88	89	88	89	89	90	89	4	4	4	4	4	4	4	4	4	4	4	4	4	4	4	4	4	4		
	<i>CXCL12</i>	75	78	76	78	78	79	80	79	77	74	73	71	74	73	70	73	74	74	74	73	71	74	73	70	73	74	74		
	<i>CXCR4 (Region 1)</i>	1	1	1	1	1	1	1	1	1	1	1	1	2	1	1	1	1	1	1	1	1	1	2	1	1	1	1	1	
	<i>CXCR4 (Region 5)</i>	2	2	2	2	1	2	2	2	1	2	2	2	2	2	2	2	2	2	2	2	2	2	2	2	2	2	2	2	
	<i>ESR1</i>	68	66	67	66	66	67	66	67	67	2	2	2	2	2	2	2	2	2	2	2	2	2	2	2	2	2	2	2	
	<i>ESR2</i>	92	94	95	95	92	94	94	94	93	1	3	2	2	1	2	3	1	2	1	3	2	2	1	2	3	1	2		
	<i>IL-13</i>	20	18	18	18	17	19	19	21	17	39	38	38	39	41	39	40	39	38	39	38	38	39	41	39	40	39	38		
	Genes measured with Methylation Profiler Array	<i>BCL10</i>	3	N/A	N/A	N/A	N/A	N/A	N/A	N/A	1	0	N/A	0	0	N/A	N/A	N/A	N/A	N/A	N/A	N/A	0							
		<i>BCL3</i>	0	N/A	N/A	N/A	N/A	N/A	N/A	N/A	61	0	N/A	0	0	N/A	N/A	N/A	N/A	N/A	N/A	N/A	0							
<i>ELANE</i>		99	N/A	N/A	N/A	N/A	N/A	N/A	N/A	99	100	N/A	N/A	N/A	N/A	N/A	N/A	N/A	N/A	100	100	N/A	N/A	N/A	N/A	N/A	N/A	N/A	100	
<i>FOXP3</i>		99	N/A	N/A	N/A	N/A	N/A	N/A	N/A	98	99	N/A	N/A	N/A	N/A	N/A	N/A	N/A	N/A	99	99	N/A	N/A	N/A	N/A	N/A	N/A	N/A	99	
<i>GATA3</i>		0	N/A	N/A	N/A	N/A	N/A	N/A	N/A	0	51	N/A	N/A	N/A	N/A	N/A	N/A	N/A	N/A	1	51	N/A	N/A	N/A	N/A	N/A	N/A	N/A	1	
<i>HMOX1</i>		0	N/A	N/A	N/A	N/A	N/A	N/A	N/A	0	1	N/A	N/A	N/A	N/A	N/A	N/A	N/A	N/A	1	1	N/A	N/A	N/A	N/A	N/A	N/A	N/A	1	
<i>IGF2BP2</i>		93	N/A	N/A	N/A	N/A	N/A	N/A	N/A	85	0	N/A	N/A	N/A	N/A	N/A	N/A	N/A	N/A	0	0	N/A	N/A	N/A	N/A	N/A	N/A	N/A	0	
<i>IL12A</i>		0	N/A	N/A	N/A	N/A	N/A	N/A	N/A	1	1	N/A	N/A	N/A	N/A	N/A	N/A	N/A	N/A	1	1	N/A	N/A	N/A	N/A	N/A	N/A	N/A	1	
<i>INHA</i>		72	N/A	N/A	N/A	N/A	N/A	N/A	N/A	70	66	N/A	N/A	N/A	N/A	N/A	N/A	N/A	N/A	28	66	N/A	N/A	N/A	N/A	N/A	N/A	N/A	28	
<i>INHBA</i>		100	N/A	N/A	N/A	N/A	N/A	N/A	N/A	100	100	N/A	N/A	N/A	N/A	N/A	N/A	N/A	N/A	100	100	N/A	N/A	N/A	N/A	N/A	N/A	N/A	100	
<i>IRF1</i>		0	N/A	N/A	N/A	N/A	N/A	N/A	N/A	0	0	N/A	N/A	N/A	N/A	N/A	N/A	N/A	N/A	0	0	N/A	N/A	N/A	N/A	N/A	N/A	N/A	0	
<i>LTB</i>		N/A	N/A	N/A	N/A	N/A	N/A	N/A	N/A	N/A	86	N/A	N/A	N/A	N/A	N/A	N/A	N/A	N/A	85	86	N/A	N/A	N/A	N/A	N/A	N/A	N/A	85	
<i>MALT1</i>		1	N/A	N/A	N/A	N/A	N/A	N/A	N/A	N/A	N/A	N/A	N/A	N/A	N/A	N/A	N/A	N/A	N/A	0	N/A	N/A	N/A	N/A	N/A	N/A	N/A	N/A	0	
<i>MAP3K7</i>		1	N/A	N/A	N/A	N/A	N/A	N/A	N/A	6	0	N/A	N/A	N/A	N/A	N/A	N/A	N/A	N/A	0	0	N/A	N/A	N/A	N/A	N/A	N/A	N/A	0	
<i>MYD88</i>		0	N/A	N/A	N/A	N/A	N/A	N/A	N/A	0	0	N/A	N/A	N/A	N/A	N/A	N/A	N/A	N/A	0	0	N/A	N/A	N/A	N/A	N/A	N/A	N/A	0	
<i>NOD1</i>		N/A	N/A	N/A	N/A	N/A	N/A	N/A	N/A	0	0	N/A	N/A	N/A	N/A	N/A	N/A	N/A	N/A	0	0	N/A	N/A	N/A	N/A	N/A	N/A	N/A	0	
<i>SMAD3</i>		100	N/A	N/A	N/A	N/A	N/A	N/A	N/A	99	100	N/A	N/A	N/A	N/A	N/A	N/A	N/A	N/A	100	100	N/A	N/A	N/A	N/A	N/A	N/A	N/A	100	
<i>SOD1</i>		1	N/A	N/A	N/A	N/A	N/A	N/A	N/A	0	0	N/A	N/A	N/A	N/A	N/A	N/A	N/A	N/A	0	0	N/A	N/A	N/A	N/A	N/A	N/A	N/A	0	
<i>STAT5A</i>		2	N/A	N/A	N/A	N/A	N/A	N/A	N/A	2	82	N/A	N/A	N/A	N/A	N/A	N/A	N/A	N/A	81	82	N/A	N/A	N/A	N/A	N/A	N/A	N/A	81	
<i>TLR2</i>		0	N/A	N/A	N/A	N/A	N/A	N/A	N/A	56	0	N/A	N/A	N/A	N/A	N/A	N/A	N/A	N/A	0	0	N/A	N/A	N/A	N/A	N/A	N/A	N/A	0	
<i>TRAF2</i>		0	N/A	N/A	N/A	N/A	N/A	N/A	N/A	0	0	N/A	N/A	N/A	N/A	N/A	N/A	N/A	N/A	0	0	N/A	N/A	N/A	N/A	N/A	N/A	N/A	0	
<i>TRAF6</i>		0	N/A	N/A	N/A	N/A	N/A	N/A	N/A	0	0	N/A	N/A	N/A	N/A	N/A	N/A	N/A	N/A	0	0	N/A	N/A	N/A	N/A	N/A	N/A	N/A	0	

HMC-1 cells showed hypermethylated CpG sites in the gene promoters of the *AR*, *CXCL2*, and partial CpG methylation of *BMP7*, while these gene promoters were unmethylated in LAD2 cells. Both cell lines were unmethylated for *BMP6* and *CXCR4*, and partially methylated for *IL-13*. The gene promoter of the *CXCR4* ligand *CXCL12* (*SDF-1*) was hypermethylated in both cell lines. These results indicate that both mast cell lines express *CXCR4*, but not its receptor *CXCL12*, and that HMC-1 might possess an inactivated *AR*. However, the regulatory role of the pyrosequenced CpG sites for gene expression still requires confirmation by transcription analysis and functional studies.

The methylation profile of 22 genes with well documented roles in cytokine biosynthesis was evaluated in untreated and E2-stimulated (100nM, 24 hours) mast cells using the Qiagen “EpiTect Methyl II Signature PCR array “Human cytokine production” (Tab. 4).

Four out of 22 genes showed a fully methylated gene promotor (*ELANE*, *FOXP3*, *INHBA* and *SMAD3*; all >98% methylated) in HMC-1 and LAD2, but the majority of candidate genes was unmethylated in both cell lines (*BCL10*, *HMOX1*, *IL12A*, *IRF1*, *MALT1*, *MYD88*, *NOD1*, *SOD1*, *TRAF2*, *TRAF6*; all <4%). *INHA* was the only gene with partial methylation in both cell lines. *IGFBP2* (93%) was exclusively methylated in HMC-1 cells, and *STAT5A* (82%) as well as *GATA3* (51%) were only hypermethylated in LAD2 cells. For *LTB*, *NOD1* (in HMC-1) and *MALT1* (in LAD2), technical errors hindered CpG methylation analysis. Most (17/22) measured gene candidates from the methylation profiler array did not show any changes after E2-stimulation (Tab. 4).

However, E2-treatment increased promotor CpG methylation of *BCL3* (0% to 61%), *MAP3K7* (1% to 6%) and *TLR2* (0% to 56%) in HMC-1 cells, and decreased promotor CpG methylation of *GATA3* (51% to 0%) and *INHA* (66% to 28%) in LAD2 cells (Tab. 4).

Gene promotor CpG methylation of *BCL10* was slightly decreased after E2-treatment of HMC-1 cells (decrease from 3% to 1%). It is interesting to note that E2-promoted *de novo* methylation in HMC-1 cells happened in previously unmethylated promotors, and that E2-mediated CpG demethylation in LAD2 cells happened exclusively for genes (*GATA3* and *INHA*) with previously partially methylated CpG sites, but not for fully methylated genes (Tab. 4; Fig. 9).

Perhaps, the gene promoter has to already be in a bivalent state to be affected by E2-stimulation. Gene expression data supports that E2-mediated hypermethylation of the *BCL3* and *TLR2* gene promoters led to transcriptional downregulation in HMC-1 cells (Fig. 14). In LAD2 cells however, demethylation of the *GATA3* and *INHA* gene promoters was not reflected in re-expression of their respective gene transcripts.

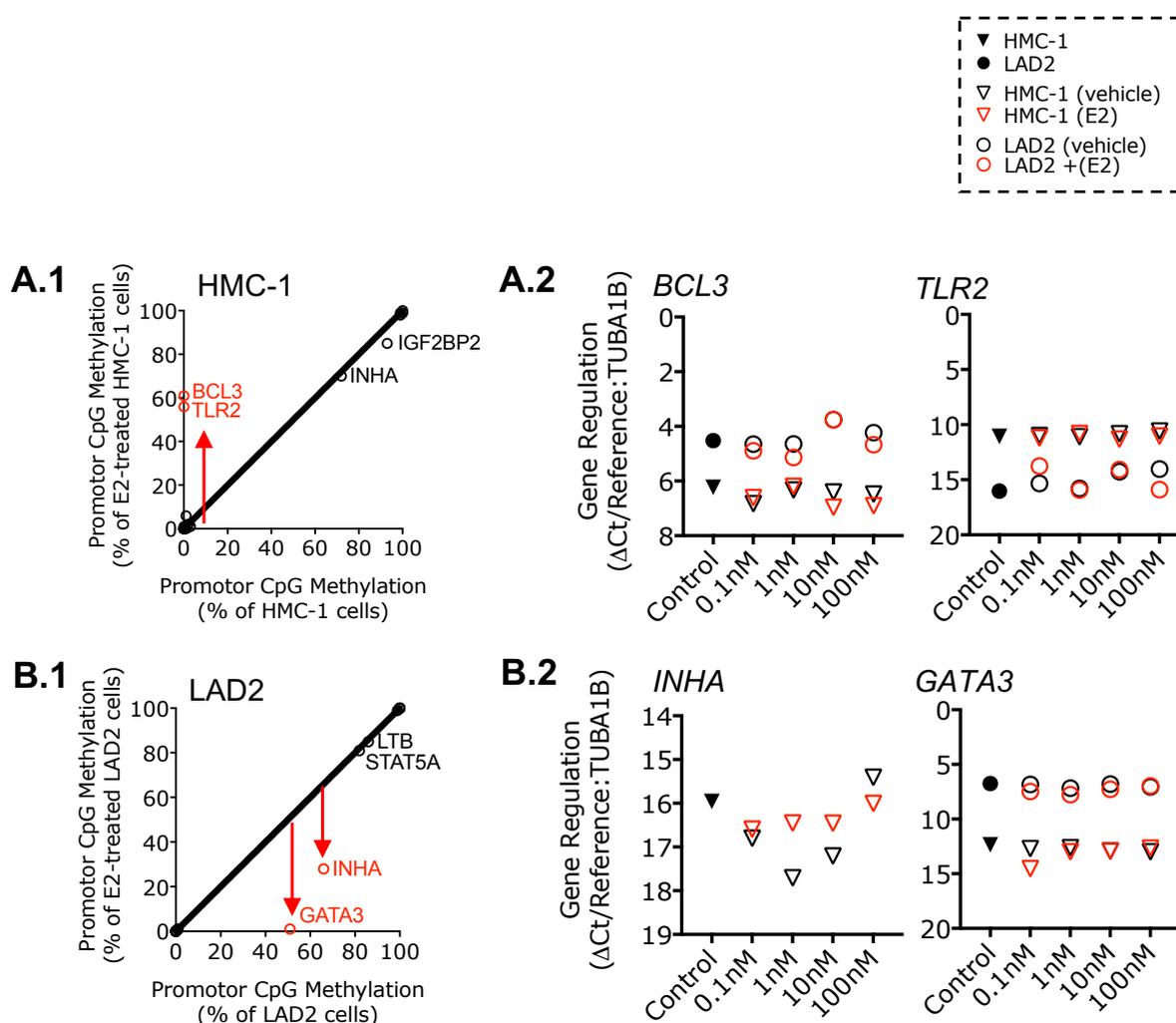


**Figure 14. De novo methylated genes are downregulated in E2-treated HMC-1 cells.**

Untreated (n=1) and E2-treated (n=1) HMC-1 and LAD2 cells were screened with a profiler array for promotor CpG methylation changes of 22 genes (A.1+B.1) and supporting gene expression data of four identified gene candidates was gathered using RT-qPCR (A.2+B.2). Promotor CpG methylation of *INHA*, *GATA3*, *BCL3* and *TLR2* was affected by E2-treatment (A.1+B.1; red arrows). De novo CpG methylation of *BCL3* and *TLR2* in HMC-1 cells coincided with transcriptional downregulation (A.2; *BCL3*:  $\Delta\text{Ct}$  6.48 to 6.91, *TLR2*:  $\Delta\text{Ct}$  10.59 to 11.05), and downregulation was also observable in E2-treated LAD2 cells (A.2; *BCL3*:  $\Delta\text{Ct}$  4.23 to 4.67; *TLR2*:  $\Delta\text{Ct}$  14.02 to 15.90). *GATA3* and *INHA* promotor demethylation in LAD2 cells was not associated with an increased gene expression, and the *INHA* transcript was not detectable in LAD2 (B.2).

To validate the data obtained by the methylation profiler array, we pyrosequenced the CpG sites that showed *de novo* methylation in the *TLR2* promoter of E2-stimulated HMC-1 cells. Pyrosequencing results confirmed *de novo* *TLR2* methylation, but instead of the previously detected +56% (Methyl II Profiler Array), observed methylation increases ranged from +1% to +2% (**Fig. 15**). CpG methylation after E2-treatment was elevated when compared to the vehicle control, but not in comparison to untreated cells.

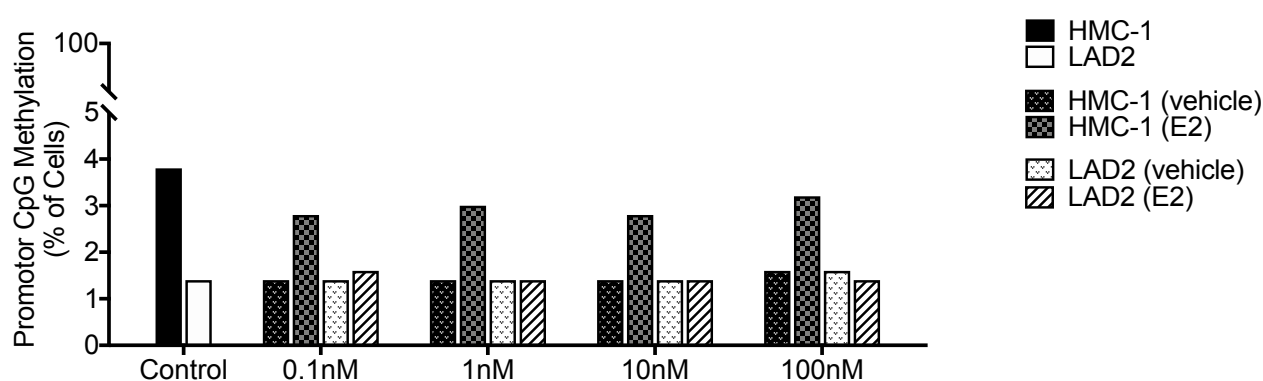


**Figure 15. Pyrosequencing of *TLR2* CpG sites from the methylation profiler array.**

Pyrosequencing of the *TLR2* promoter CpG sites from the “Qiagen Methyl II Profiler Array” in E2-treated HMC-1 cells. A CpG methylation increase was observable across all E2-concentrations, when comparing them to the matched vehicle control samples (n=1). Promotor CpG methylation is given as percent of cells (%).

### 1.3) HMC-1 and LAD2 show different basal inflammatory gene expression

The expression of 84 cytokines and chemokines was examined with the RT2 Profiler PCR array “Human cytokines and chemokines” (Qiagen) in untreated and E2-stimulated (100nM) HMC-1 and LAD2 cells (**Fig. 16**). Untreated HMC-1 cells expressed the majority of genes (52/84, 62%) at high levels ( $\Delta Ct \leq 10$  in qPCR), whereas only a minority of genes (27/84; 32%) showed high transcript levels in untreated LAD2 cells. Most transcripts in LAD2 cells (57/84; 68%) had low levels ( $\Delta Ct > 10$ ) or were not detectable ( $Ct \geq 35$  in qPCR). Both mast cell lines showed high basal transcript levels of *CCL2*, *CXCL5*, *GPI*, *IL18*, *IL1RN*, *LIF*, *MIF*, *TNFSF10* and *VEGFA* ( $\Delta Ct < 5$  in HMC-1 and LAD2), suggesting that these genes play an important role for the mast cell physiology .

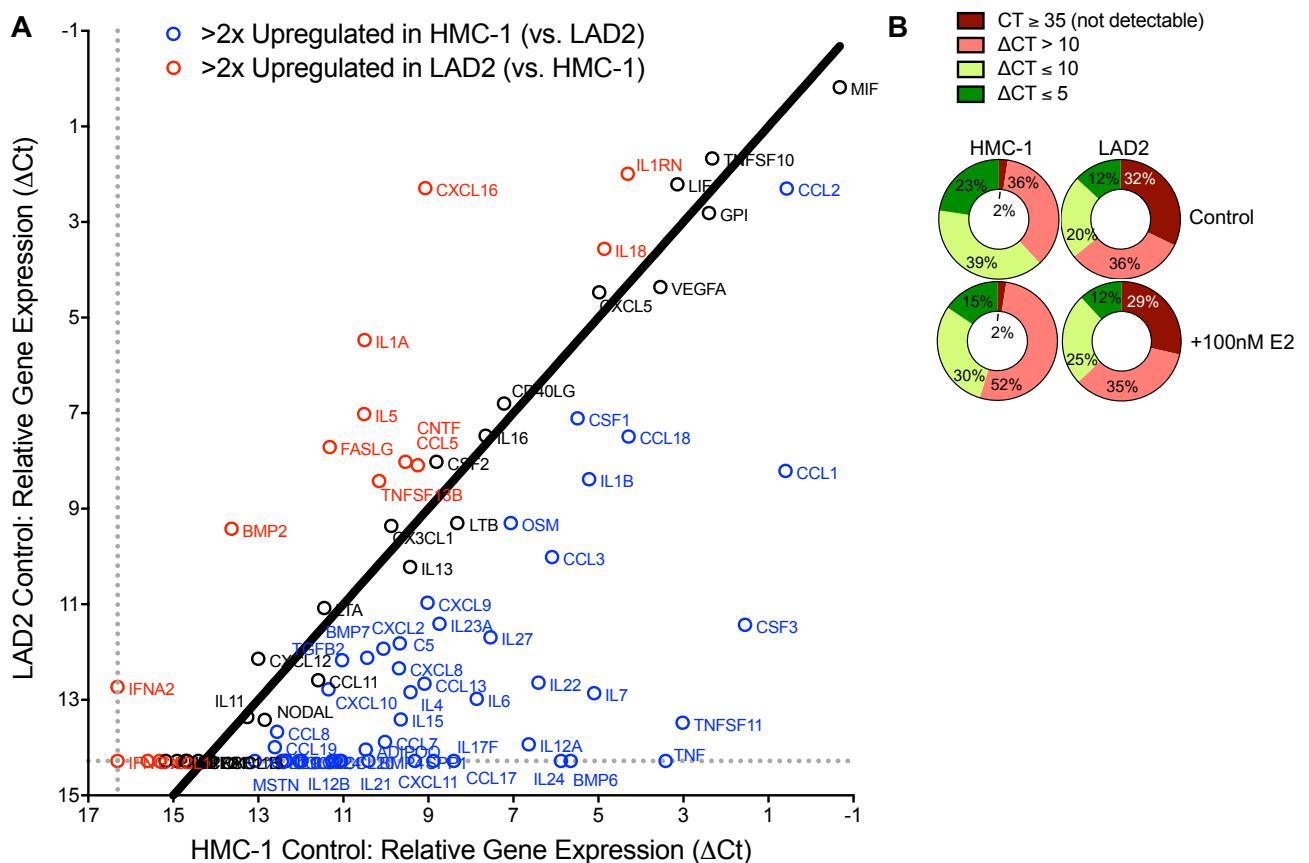


**Figure 16. HMC-1 and LAD2 show different basal gene expression and E2-responses.**

A transcription profiler array was used to evaluate the gene transcription of 84 genes with relevance for leukocyte function in HMC-1 and LAD2 cells ( $n=1$ ). Most inflammatory genes showed higher basal expression in HMC-1 cells (**A**; blue circles), and only a minority showed higher basal transcript levels in LAD2 cells (**A**; red circles). When grouping the inflammatory genes by their  $\Delta Ct$  values in HMC-1 and LAD2 cells (**B**), it becomes obvious that global expression levels are higher in HMC-1 *versus* LAD2 cells. E2-treatment led to downregulation of E2-responsive genes in HMC-1 and upregulated gene expression in LAD2 (**B**). Graph (**B**) represents an excerpt from our published manuscript [97].

HMC-1 cells furthermore express high levels ( $\Delta Ct < 7$ ) of *BMP6*, *CCL1*, *CCL3*, *CCL18*, *CSF1*, *CSF3*, *IL1B*, *IL7*, *IL-12A*, *IL22*, *IL24* as well as *TNF* and *TNFSF11* (also known as *RANKL*), but transcription of these, genes is lower ( $\Delta Ct > 7$ ) or absent (*TNF*, *IL24*) in LAD2 (**Tab. 5**). Only five genes from the panel (*BMP2*, *FASLG*, *IL1A*, *IL5*, *TNFSF13B*) displayed a higher basal expression in LAD2 cells compared to HMC-1, and among these only *IL1A* is expressed at high levels ( $\Delta Ct < 7$ ).

**Table 5. Basal inflammatory gene expression in unstimulated HMC-1 and LAD2 cells.**

Gene expression of the 84 genes from the transcription profiler array was grouped by their  $\Delta Ct$  values in HMC-1 and LAD2 cells (n=1). 22 genes showed high basal gene transcription in both mast cell lines ( $\Delta Ct < 10$ ). 35 genes had low or undetectable gene expression levels in both cell lines ( $\Delta Ct > 10$ ). 22 genes showed high transcription in HMC-1 ( $\Delta Ct < 10$ ), but low transcription in LAD2 cells ( $\Delta Ct > 10$ ). Expression of 5 genes was high in LAD2 ( $\Delta Ct < 10$ ), but low in HMC-1 ( $\Delta Ct > 10$ ). Colors from green to red represent a continuous scale from the lowest (green) to highest (red)  $\Delta Ct$ .

$\Delta Ct < 10$ (both)			$\Delta Ct > 10$ (both)			$\Delta Ct < 10$ (HMC-1)			$\Delta Ct < 10$ (LAD2)		
Gene	HMC-1	LAD2	Gene	HMC-1	LAD2	Gene	HMC-1	LAD2	Gene	HMC-1	LAD2
<i>CCL1</i>	0.60	8.21	<i>ADIPOQ</i>	10.47	14.04	<i>BMP6</i>	5.65	Ct $\geq$ 35	<i>BMP2</i>	13.63	9.42
<i>CCL18</i>	4.29	7.49	<i>BMP4</i>	10.41	Ct $\geq$ 35	<i>C5</i>	9.67	11.82	<i>FASLG</i>	11.32	7.71
<i>CCL2</i>	0.57	2.30	<i>BMP7</i>	10.44	12.12	<i>CCL13</i>	9.09	12.66	<i>IL1A</i>	10.50	5.47
<i>CCL5</i>	9.25	8.09	<i>CCL11</i>	11.59	12.59	<i>CCL17</i>	8.40	Ct $\geq$ 35	<i>IL5</i>	10.51	7.02
<i>CD40LG</i>	7.22	6.80	<i>CCL19</i>	12.61	13.99	<i>CCL3</i>	6.09	10.01	<i>TNFSF13B</i>	10.16	8.42
<i>CNTF</i>	9.54	8.02	<i>CCL20</i>	11.26	Ct $\geq$ 35	<i>CSF3</i>	1.55	11.43			
<i>CSF1</i>	5.49	7.11	<i>CCL21</i>	14.71	Ct $\geq$ 35	<i>CXCL8</i>	9.69	12.34			
<i>CSF2</i>	8.81	8.02	<i>CCL22</i>	12.44	Ct $\geq$ 35	<i>CXCL9</i>	9.02	10.97			
<i>CX3CL1</i>	9.87	9.36	<i>CCL24</i>	12.04	Ct $\geq$ 35	<i>IL12A</i>	6.64	13.93			
<i>CXCL16</i>	9.07	2.29	<i>CCL7</i>	10.02	13.88	<i>IL13</i>	9.43	10.22			
<i>CXCL5</i>	4.98	4.47	<i>CCL8</i>	12.56	13.67	<i>IL15</i>	9.65	13.41			
<i>GPI</i>	2.40	2.81	<i>CXCL1</i>	15.60	Ct $\geq$ 35	<i>IL17F</i>	8.88	Ct $\geq$ 35			
<i>IL16</i>	7.65	7.47	<i>CXCL10</i>	11.35	12.78	<i>IL22</i>	6.41	12.64			
<i>IL18</i>	4.86	3.56	<i>CXCL11</i>	11.09	Ct $\geq$ 35	<i>IL23A</i>	8.74	11.41			
<i>IL1B</i>	5.22	8.38	<i>CXCL12</i>	13.00	12.14	<i>IL24</i>	5.88	Ct $\geq$ 35			
<i>IL1RN</i>	4.31	1.99	<i>CXCL13</i>	14.12	Ct $\geq$ 35	<i>IL27</i>	7.54	11.69			
<i>LIF</i>	3.14	2.21	<i>CXCL2</i>	10.06	11.93	<i>IL4</i>	9.42	12.84			
<i>LTB</i>	8.32	9.30	<i>IFNA2</i>	Ct $\geq$ 35	12.73	<i>IL6</i>	7.86	12.98			
<i>MIF</i>	-0.68	0.18	<i>IFNG</i>	Ct $\geq$ 35	Ct $\geq$ 35	<i>IL7</i>	5.10	12.86			
<i>OSM</i>	7.06	9.30	<i>IL10</i>	12.37	Ct $\geq$ 35	<i>SPP1</i>	9.32	Ct $\geq$ 35			
<i>TNFSF10</i>	2.32	1.67	<i>IL11</i>	13.26	13.36	<i>TNF</i>	3.42	Ct $\geq$ 35			
<i>VEGFA</i>	3.54	4.36	<i>IL12B</i>	11.19	Ct $\geq$ 35	<i>TNFSF11</i>	3.02	13.48			
			<i>IL17A</i>	14.68	Ct $\geq$ 35						
			<i>IL2</i>	15.32	Ct $\geq$ 35						
			<i>IL21</i>	11.05	Ct $\geq$ 35						
			<i>IL3</i>	11.98	Ct $\geq$ 35						
			<i>IL9</i>	12.36	Ct $\geq$ 35						
			<i>LTA</i>	11.45	11.08						
			<i>MSTN</i>	12.34	Ct $\geq$ 35						
			<i>NODAL</i>	12.85	13.42						
			<i>PPBP</i>	15.18	Ct $\geq$ 35						
			<i>TGFB2</i>	11.03	12.17						
			<i>THPO</i>	14.41	Ct $\geq$ 35						
			<i>TNFRSF11B</i>	14.91	Ct $\geq$ 35						
			<i>XCL1</i>	13.08	Ct $\geq$ 35						

#### 1.4) HMC-1 and LAD2 respond differently to estradiol treatment

Having very different basal expression levels of *ESR1* and *ESR2*, HMC-1 and LAD2 responded very differently to E2-stimulation (**Fig. 17**). Inflammatory genes were downregulated by E2-stimulation (100nM) of HMC-1 cells (genes with  $\Delta\text{Ct} > 10$  changed from 36% to 52%) but upregulated in LAD2 cells (genes with  $\Delta\text{Ct} \leq 10$  changed from 20% to 25%; **Fig. 16B**). Only four E2-responsive genes showed the same regulation in HMC-1 and LAD2 cells. Both cell lines upregulated the interferons *IFNA2* and *IFNG* and simultaneously downregulated *BMP7* and *TNFSF11* (*RANKL*) after E2-stimulation (**Tab. 6**). E2-mediated gene regulation of the remaining E2-responsive genes was quite different in HMC-1 and LAD2 cells. In HMC-1 cells, the majority of affected genes (12/15) was downregulated, and only one other gene (*CXCL13*) was upregulated. In LAD2 cells on the other hand, the majority of affected genes was upregulated (14/18), and only *BMP7*, *IL7* and *IL16* were downregulated. Some E2-responsive genes showed opposite regulations in HMC-1 and LAD2 (*CSF3*, *CXCL2*, *IL-17F*), but in the majority cases genes were affected in one cell line not affected in the other one.

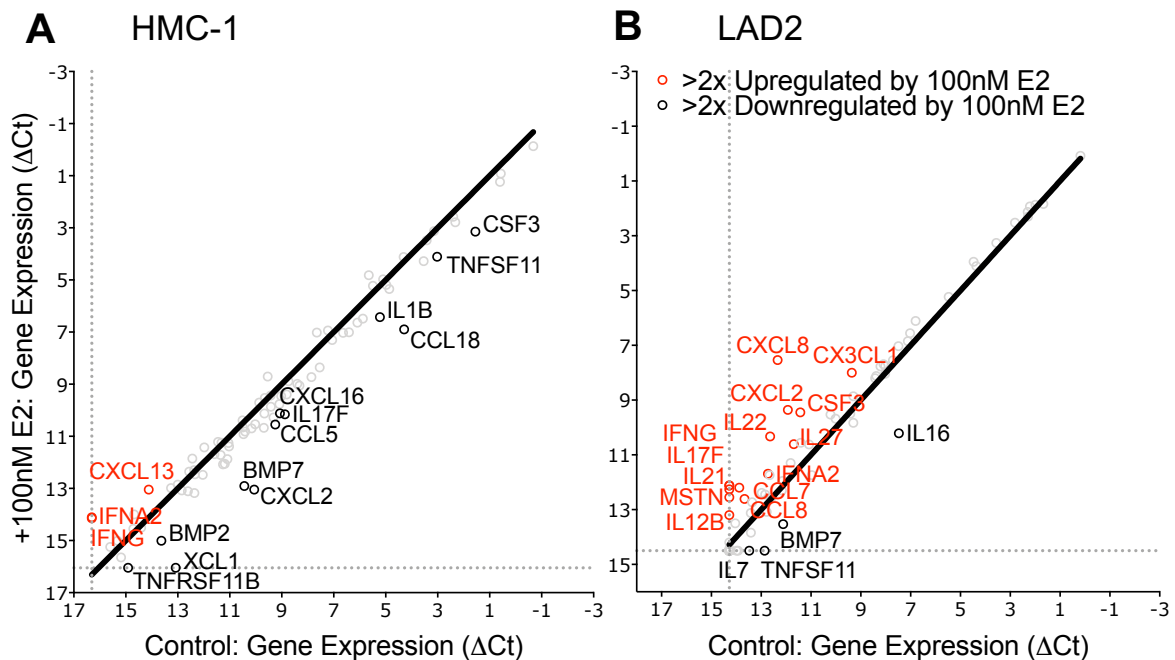


**Figure 17. E2-responsive genes undergo different regulations in HMC-1 and LAD2 cells.**

Scatterplots of E2-mediated (100nM) relative gene expression ( $\Delta\text{Ct}$ ) changes of 84 genes in HMC-1 (**A**) and LAD2 (**B**) cells ( $n=1$ ). Genes were considered regulated when crossing the cutoff value [ $-\Delta\Delta\text{Ct} \geq (+/-)1$ ]. In HMC-1 cells, only 3/15 E2-regulated genes were upregulated (**A**; red circles) and the majority (12/15) of responsive genes was downregulated (**A**; black circles). In LAD2, the majority (14/18) of responsive genes was upregulated (**B**; red circles), and only 4/18 genes were downregulated by the treatment (**B**; black circles).

In HMC-1 cells, downregulated gene candidates were members of the interleukin (*IL1B*, *IL17F*) or chemokine ligand families (*CCL5*, *CCL18*, *CXCL2*, *CXCL16*, *XCL1*). Other downregulated genes included members of the bone morphogenetic gene group (*BMP2*, *BMP7*), *CSF3*, *TNFRSF11B* and *TNFSF11* (*RANKL*). In LAD2 cells, most upregulated gene candidates in E2-stimulated were members of the interleukin (*IL8*, *IL12B*, *IL17F*, *IL21*, *IL22* and *IL27*) and chemokine ligand families (**Tab. 6**; *CCL7*, *CCL8*, *CX3CL1* and *CXCL2*). Other upregulated genes were *CSF3* and *MSTN*. The strongest E2-mediated upregulation in LAD2 cells was detectable for *IL-8* (*CXCL8*:  $\Delta\text{Ct}$  from 12.34 to 7.54; expression increase to 3060%; 4.8-fold upregulation). In HMC-1 cells, *IL-8* expression was downregulated by E2-treatment ( $\Delta\text{Ct}$  from 9.69 to 10.68; below cutoff change  $\Delta\Delta\text{Ct}\geq 1$ ).

**Table 6. E2-regulated gene candidates in HMC-1 or LAD2 cells.**

E2-mediated regulation of 26 candidate genes crossed the cutoff value ( $\Delta\Delta\text{Ct}\geq(+/-)1$ ) in HMC-1 or LAD2 cells (n=1). While the majority of E2-regulated genes in LAD2 cells were upregulated (red), the majority of E2-responsive genes was downregulated (grey) in HMC-1 cells.

Gene	Gene Regulation ( $-\Delta\Delta\text{CT}$ )	
	HMC-1	LAD2
<i>BMP2</i>	-1.38	-0.08
<i>BMP7</i>	-2.47	-1.41
<i>CCL18</i>	-2.61	0.46
<i>CCL5</i>	-1.30	0.40
<i>CCL7</i>	-0.52	1.68
<i>CCL8</i>	0.20	1.06
<i>CSF3</i>	-1.60	1.98
<i>CX3CL1</i>	0.16	1.36
<i>CXCL13</i>	1.07	-0.22 **
<i>CXCL16</i>	-1.05	-0.01
<i>CXCL2</i>	-2.99	2.57
<i>CXCL8 (IL-8)</i>	-0.99	4.80
<i>IFNA2</i>	2.16	1.04
<i>IFNG</i>	2.20	2.02 *
<i>IL12B</i>	-0.87	1.08 *
<i>IL16</i>	0.63	-2.74
<i>IL17F</i>	-1.28	1.73 *
<i>IL1B</i>	-1.21	0.26
<i>IL21</i>	-0.21	2.17 *
<i>IL22</i>	-0.60	2.31
<i>IL27</i>	-0.82	1.08
<i>IL7</i>	0.12	-1.64
<i>MSTN</i>	-0.12	2.16 *
<i>TNFRSF11B</i>	-1.14	-0.22 **
<i>TNFSF11</i>	-1.09	-1.02
<i>XCL1</i>	-2.97	-0.22 **

\*not expressed in control. \*\*not expressed in control or E2-treatment.

## 2) CP/CPPS affects patient semen parameters

We determined clinical routine blood and semen parameters of CP/CPPS patients and compared these with values from age-matched healthy volunteers, when available. We also measured SP E2 concentrations and isolated circulating WBC from frozen EDTA-blood samples and ejaculated SC from semen samples. Then we conducted an epigenetic profiling of *ESR1*, *ESR2* and *AR* in the isolated cell populations with Pyrosequencing and RT-qPCR. Additionally, we measured the expression of some genes with relevance for the inflammatory response in ejaculated SC (*CMA1*, *IL-7*, *CD68*, *CCL18* and *PU.1*). Our results show that CP/CPPS associates with impaired diagnostic parameters of the clinical routine as well as systemic (blood) and organ-confined (semen) aberrations of estrogen signaling. Simultaneously, we traced leukocyte-specific transcription changes in the ejaculated SC from CP/CPPS patients.

Upon comparison with healthy volunteers, we found that CP/CPPS patients' ejaculate had aberrant routine semen parameters. Their ejaculates had decreased overall volume and increased acidity (decreased pH), an increased number of peroxidase-positive cells, a reduced ejaculate volume and consequently also a reduced amount of total ejaculated zinc (**Fig. 18**).

The semen zinc concentration of patients and healthy volunteers showed a high variability. Consistent with this observation, the WHO considers total ejaculated zinc instead of semen zinc concentrations for diagnostics, defining values  $<2.4\mu\text{mol}$  as abnormal. CP/CPPS patients have diminished total ejaculated zinc, with only 4% of healthy volunteer samples (1/23), but 20% of CP/CPPS patient samples (10/49) underneath the WHO threshold. Semen zinc is mainly derived from prostatic secretions and contributes to male fertility. Since CP/CPPS patients have diminished ejaculated zinc and semen volume at the same time, it appears likely that this comes from a reduced prostatic secretory activity. We found a slight positive correlation ( $R^2=0.13$ ;  $p=0.0039$ ) of semen zinc levels with activity of  $\alpha$ -Glucosidase, a male fertility marker that is derived from the epididymis (*not shown*). Average  $\alpha$ -Glucosidase levels were reduced in the semen of CP/CPPS patients, but not significantly lower than in healthy volunteers.

The pH of healthy ejaculate was slightly basic (Median healthy volunteer pH: 8.1), and consequently higher than the pH of blood (pH 7.35-7.45) or interstitial fluid (6.60-7.60), which is highly variable because it contains only few pH-buffering molecules [122]. Zinc solubility increases with acidity, and we find a negative correlation of semen zinc concentrations with semen pH ( $R^2=0.31$ ;  $p<0.0001$ ). Patient ejaculates with low pH have high zinc concentrations, indicating that acidification has the potential for prostatic zinc depletion. Ejaculate pH also shows a weak negative correlation with semen IL-8 levels ( $R^2=0.05$ ;  $p=0.02$ ), and CP/CPSP patients with high semen IL-8 levels ( $>10,000\text{pg/mL}$ ) exclusively have a semen  $\text{pH}<8$ . This indicates that semen acidification associated with the inflammatory processes in the prostate of CP/CPSP patients.

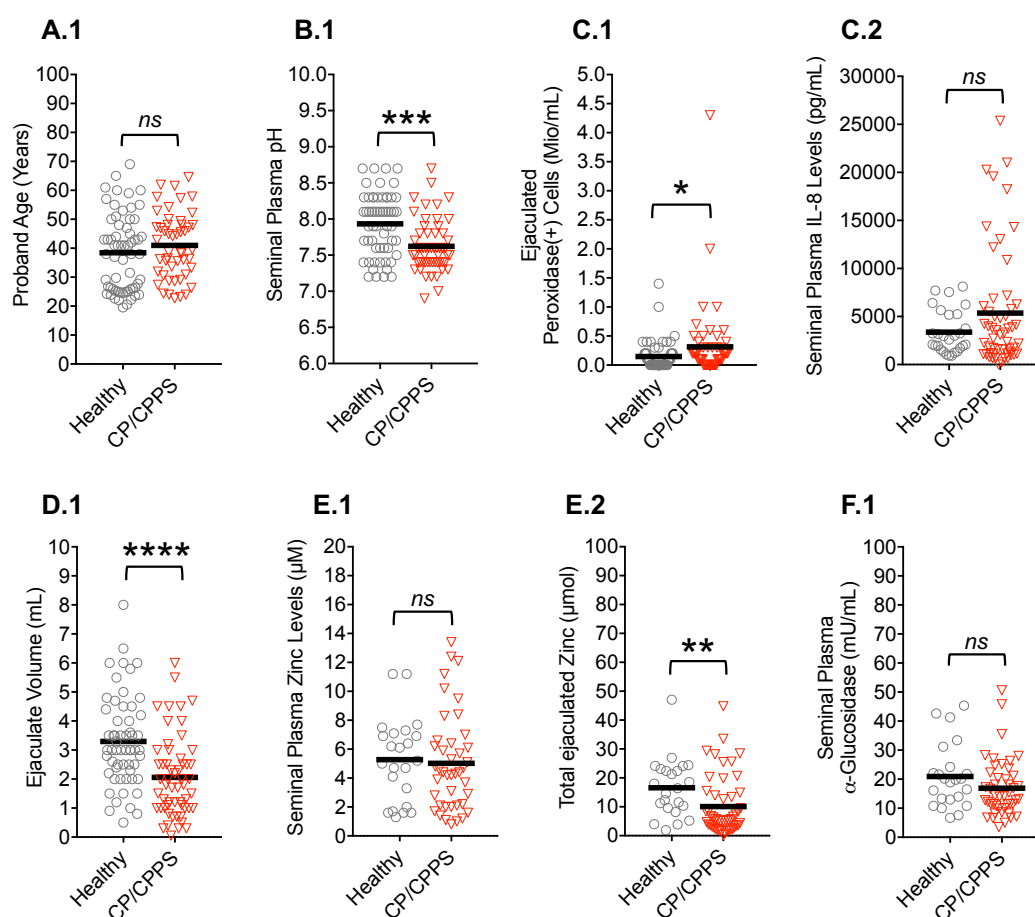


**Figure 18. Cohort age and semen parameters of CP/CPSP patients and healthy volunteers.**

Healthy probands were selected to match the age distribution of the CP/CPSP patient cohort (A.1), and semen parameters were compared with CP/CPSP patients (B-F). CP/CPSP patients have a decreased semen pH (B.1), an elevated count of infiltrating peroxidase-positive cells (C.1), and elevated average seminal plasma IL-8 levels (C.2; *not significant*). At the same time, they have decreased ejaculate volume (D.1) and decreased total ejaculated zinc (E.2; Healthy:  $6.60\pm 10.11\mu\text{mol}$ ; CP/CPSP:  $10.09\pm 10.19\mu\text{mol}$ ;  $n(\text{Healthy/CP/CPSP})=23/42$ ). Semen zinc levels on the other hand were not significantly different from healthy probands (E.1). The average seminal plasma  $\alpha$ -Glucosidase activity of CP/CPSP patients is reduced (F.1;  $p=0.086$ ). Values are given as Mean $\pm$ SD. Significance was tested with Mann-Whitney U. A detailed summary of the plotted variables (Case numbers, median, SD and range) is provided in Table 1.

### 3) Density gradient allows isolation of somatic cells from semen

To clarify whether the CP/CPPS-related epigenetic dysregulation happens in sperm or ejaculated SC, ejaculated cell pellets were separated on a Histopaque-®1077 density gradient to allow separate isolation of sperm cells (high density) and SC (lower density). Microscopic examination confirmed that lower density fractions were free of major sperm cell contamination and contained SC. Sperm cells were predominant in the lowest fraction and the cell pellet (**Fig. 19A**). The low density (SC) fractions (upper 4mL) and the high-density fraction (sperm cell pellet remaining liquid) were pooled separately and used for downstream analysis, respectively. Pyrosequencing of the genes *CXCL12* [25], *ESR2* and *BMP2* in the isolated SC and sperm cell fractions showed that promoter CpG methylation was exclusively detectable in ejaculated SC, but not in sperm cells. *BMP2* methylation was observable in patients and healthy volunteers likewise, but we detected a significant *ESR2* hypermethylation in CP/CPPS patients (**Fig. 19B**).

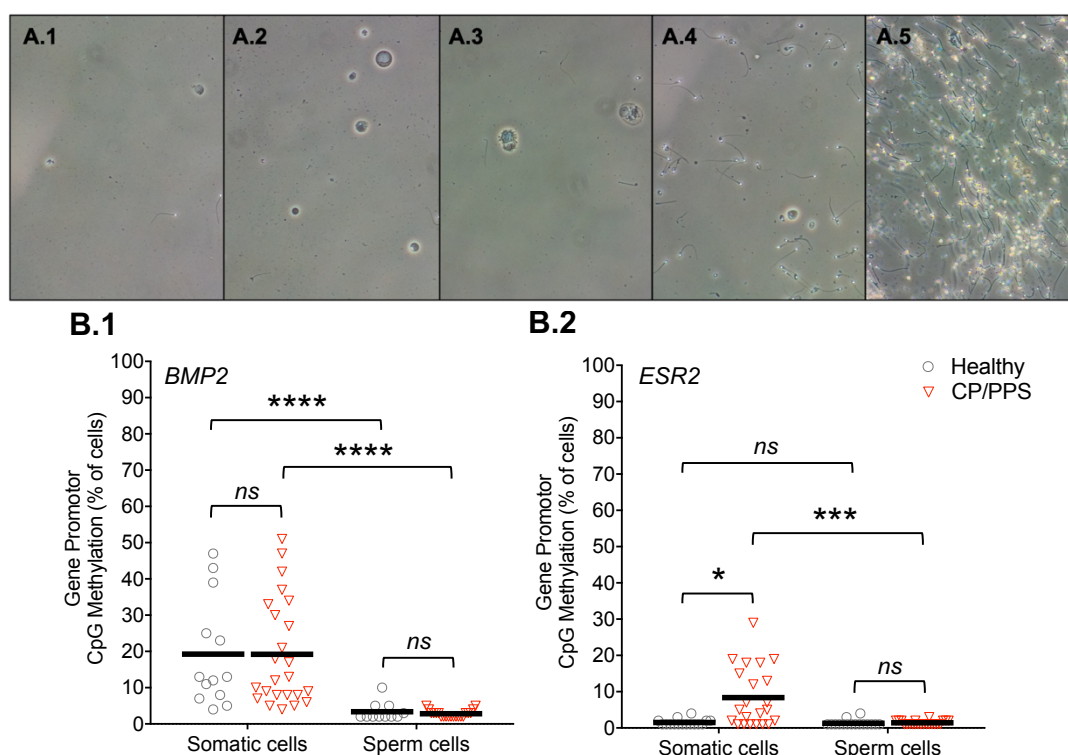


**Figure 19. Pyrosequencing of separated sperm cells and somatic cells from human semen.**

Ejaculated cells were separated by centrifugation on a pre-layered Histopaque®1077 gradient. Five 1mL fractions were taken (from top to bottom) after centrifugation. The first 3 fractions (**A.1**, **A.2**, **A.3**) mainly contained ejaculated somatic cells (SC), the fourth fraction (**A.4**) and pellet (**A.5**) contained sperm cells. Pyrosequencing of CpG sites in the gene promoters of *BMP2* [**B.1**; n(Healthy)=13; n(CP/CPPS)=24] and *ESR2* [**B.2**; n(Healthy)=16; n(CP/CPPS)=22] shows gene promoter CpG methylation in ejaculated SC, but not sperm cells. *ESR2* promoter CpG methylation is significantly elevated in SC from CP/CPPS patients (**B.2**). Significance tested with Mann-Whitney U-Test.

#### 4) Somatic cells from semen show leukocyte-specific gene transcription

Profiling of the isolated SC fraction of CP/CPPS patients revealed that CP/CPPS associates with a changed ejaculated SC population. Routine semen analysis of CP/CPPS patients includes a peroxidase-positivity test to assess granulocyte infiltration. CP/CPPS patients have significantly elevated peroxidase-positive cell counts (**Fig. 18C.1**), indicating an increased prostatic leukocyte infiltration. To test whether this is reflected in the gene expression of ejaculated SC, we characterized leukocyte-specific transcripts by RT-qPCR. Ejaculated SC from CP/CPPS patients and healthy donors transcribed the genes *CMA1*, *IL-7*, *CD68*, *CCL18* and *PU.1* (**Fig. 20**). Previous studies linked CP/CPPS to mast cell infiltration, so we measured mast cell chymase (*CMA1*) in order to detect an increased presence and/or activity of mast cells in CP/CPPS patients. The *IL-7* transcript showed different basal expression levels in the mast cell lines HMC-1 and LAD2 (**Tab. 5**), and E2-treatment suppressed *IL-7* expression in LAD2 (**Tab. 6**). *IL-7* was therefore regarded as a candidate gene with potential for E2-mediated dysregulation in CP/CPPS. Expression levels of *CMA1* and *IL-7* in ejaculated SC from CP/CPPS patients however were not significantly different from isolates out of healthy probands (**Fig. 20A+B**). Macrophages are cells of the myeloid lineage, so we measured gene expression of the myeloid commitment transcription factor *PU.1* as a robust marker for the presence of myeloid origin cells.

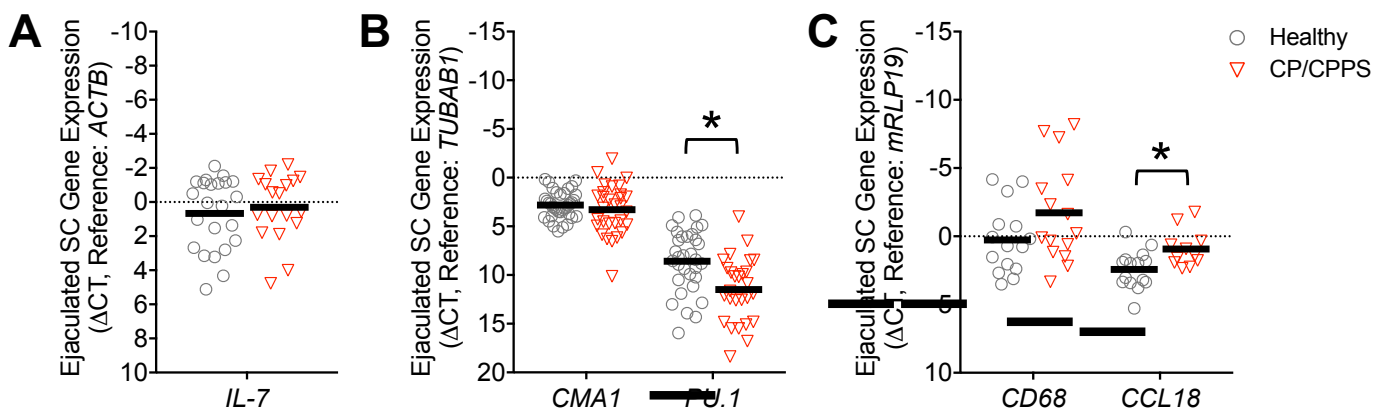


**Figure 20. Ejaculated somatic cell populations of CP/CPPS patients are affected.**

Ejaculated SC were evaluated with RT-qPCR for gene expression of *IL-7* (**A**; n=23/18), *CMA1* (n=21/23), *PU.1*, (**B**; n=32/27), *CD68* (n=15/15) and *CCL18* (**C**; n=15/11). There was no significant CP/CPPS-specific regulation detectable for *IL-7*, *CMA1* or *CD68* (**C**; *CD68*;  $\Delta\text{Ct}[\text{Healthy}]$ :  $0.26 \pm 2.50$ ;  $\Delta\text{Ct}[\text{CP/CPPS}]$ :  $-1.72 \pm 3.70$ ;  $p=0.15$ ), but ejaculated SC from CP/CPPS showed downregulation of the transcription factor *PU.1* (**B**;  $\Delta\text{Ct}[\text{Healthy}]$ :  $8.56 \pm 3.14$ ;  $\Delta\text{Ct}[\text{CP/CPPS}]$ :  $11.48 \pm 3.32$ ) and *CCL18* upregulation (**C**;  $\Delta\text{Ct}[\text{Healthy}]$ :  $2.43 \pm 1.39$ ;  $\Delta\text{Ct}[\text{CP/CPPS}]$ :  $0.92 \pm 1.36$ ). Values are given as Mean  $\pm$  SD. Significance values were calculated with Mann-Whitney U-Test. Case numbers are shown for healthy volunteers first, then CP/CPPS patients [n(Healthy/CP/CPPS)].

Interestingly, *PU.1* was downregulated in ejaculated SC from CP/CPPS patients (**Fig. 20B**). *CD68* on the other hand presents a marker for activated macrophages, and we measured *CD68* expression to detect increased macrophage activation in CP/CPPS patients. Ejaculated SC from CP/CPPS patients showed elevated average *CD68* expression, but transcript levels were highly variable and not significantly different from healthy volunteers (**Fig. 20C**). However, ejaculated SC isolated from CP/CPPS patients showed a significant upregulation of another macrophage-specific transcript, the CC chemokine *CCL18* (**Fig. 20C**). It has to be considered that we used different housekeeper genes as reference for the relative gene expression values of *IL-7* (*ACTB*), *CMA1*, *PU.1* (*TUBAB1*), *CD68* and *CCL18* (*mRLP19*).

E2-treatment downregulated *BMP2* and *BMP7* expression in HMC-1 and LAD2 cells, so we pyrosequenced ejaculated SC to analyze whether these genes are dysregulated in CP/CPPS (**Fig. 21**). Isolates from healthy probands and CP/CPPS patients showed *BMP2* promoter CpG methylation, but there was no significant difference between the cohorts. At the same time, cell isolates from CP/CPPS patients showed an elevated average *BMP7* promoter CpG methylation, but differences from healthy controls were not significant (**Fig. 21B**;  $p=0.09$ ).

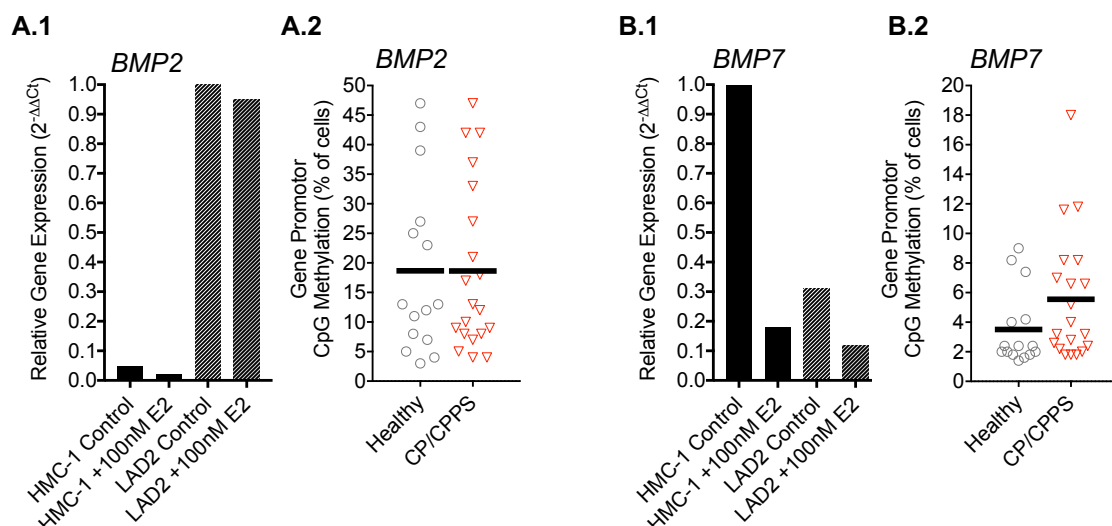


**Figure 21. *BMP7* is E2-responsive and hypermethylated in CP/CPPS ejaculate.**

Gene expression of *BMP2* and *BMP7* was measured by RT-qPCR in E2-stimulated mast cell lines (**A.1+B.1**;  $n=1$ ) and CpG methylation of the corresponding gene promoters was measured in ejaculated SC from CP/CPPS patients by Pyrosequencing (**A.2+B.2**; *BMP2*:  $n=15/20$ , *BMP7*:  $n=15/20$ ). E2-treatment led to *BMP2* downregulation in HMC-1 and LAD2 cells (**A.1**), but promoter CpG methylation in ejaculated SC from CP/CPPS patients and healthy volunteers was not significantly different (**A.2**). E2-stimulation also led to *BMP7* downregulation in HMC-1 and LAD2 cells (**B.1**), and the *BMP7* promoter shows CpG hypermethylation in ejaculated SC from CP/CPPS patients (Healthy:  $3.51\% \pm 2.57$ ; CP/CPPS:  $5.55\% \pm 4.32$ ;  $p=0.09$ ). Significance values calculated with Mann-Whitney U-Test. Case numbers are shown for healthy volunteers first, and then CP/CPPS patients [ $n(\text{Healthy/CP/CPPS})$ ].

## 5) CP/CPPS associates with aberrant steroid sex hormone signaling

Our detection of gene expression changes (e.g. *CCL18*, *PU.1*) in ejaculated SC from CP/CPPS patients indicates that semen is a suitable source for the study of CP/CPPS. The mast cell line HMC-1 displayed epigenetic downregulation of *ESR1*, *ESR2* and concurrent elevated basal inflammatory gene expression levels. Among the highly transcribed inflammatory genes in HMC-1 cells were candidates with possible or confirmed (e.g. *CCL18*, *TNF*, *RANKL*, *VEGFA*) association to CP/CPPS and PCa. Hence, findings in the mast cell lines suggest that the epigenetic inactivation of *ESR1* and *ESR2* could predetermine the inflammatory response and perhaps increase the PCa risk in CP/CPPS patients.

We wanted to determine whether ejaculated SC from CP/CPPS patients resemble HMC-1 cells, or the more differentiated LAD2 cells with a more quiescent inflammatory gene expression profile. CP/CPPS patients suffer from a variety of generalized symptoms like mental health issues and a testosterone deficit, and low testosterone levels in men were associated with elevated systemic CRP levels and increased counts of circulating WBC [123], indicating chronic low-grade systemic inflammation. CP/CPPS might therefore be the result of a changed systemic sex steroid hormone signaling. To analyze systemic CP/CPPS-related changes, we examined blood plasma and isolated circulating white blood cells (WBC).

We had access to systemic testosterone levels of CP/CPPS patients, which are measured during routine clinical diagnostics (refer to **Tab. 1**). There is currently no consensus regarding the threshold value for low testosterone in men [124]. The European Male Ageing Study (EMAS) suggests diagnosis of late onset hypogonadism (in men aged 40-79) when total testosterone is <11nmol/L, free testosterone is <220 pmol/L, and when at least three sexual symptoms are present [125]. Other guidelines suggest a similar value (<12nmol/L) as threshold for testosterone replacement therapy (TRT) [126]. In our study cohort, 30% (17/57) of CP/CPPS patients were below this threshold (11nmol/L $\pm$ 317ng/dL). Low testosterone levels are more predominant in older CP/CPPS patients. While only 15% (5/33) of the young patients (<40years) were below the suggested cutoff value, this was true for 50% (12/24) of older (>40years) patients.

Blood and semen E2 levels of CP/CPPS patients and healthy probands were determined, and both showed a significant correlation with systemic testosterone (Fig. 22A), indicating that testosterone and E2 signaling are inter-dependent. At the same time, blood and semen E2 levels showed a significant correlation among CP/CPPS patients (Fig. 22B).

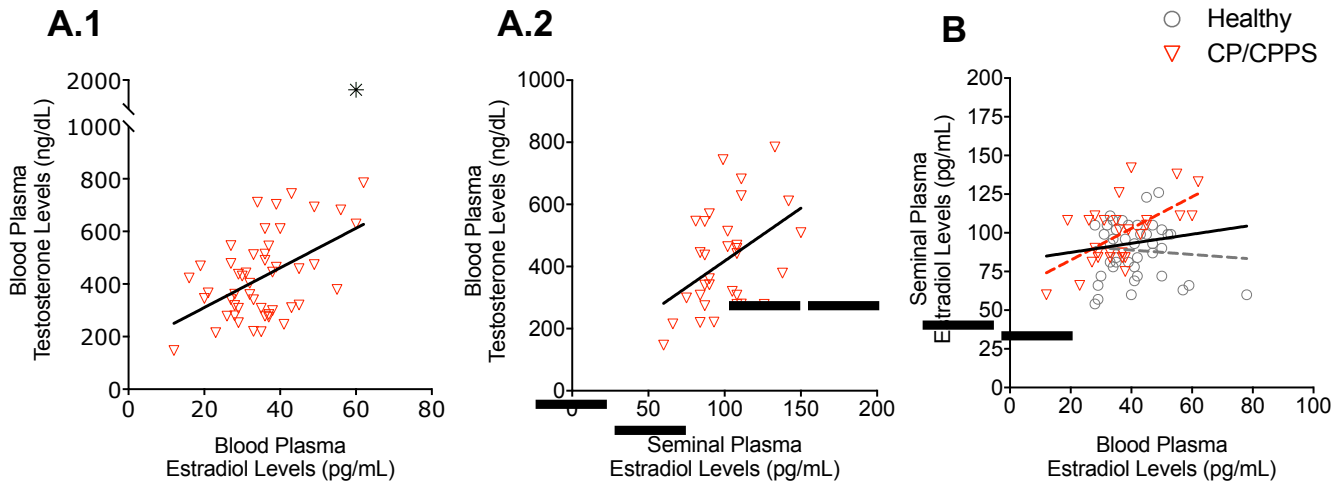


**Figure 22. Blood and semen E2 levels correlate with blood testosterone and each other**

Blood testosterone levels from CP/CPPS patients positively correlated with the concentrations of blood E2 (A.1;  $R^2=0.26$ ;  $p=0.0002$ ) and semen E2 (A.2;  $R^2=0.20$ ;  $p=0.0112$ ). Among CP/CPPS patients, blood plasma E2 concentrations correlated with semen E2 levels (B;  $R^2=0.36$ ;  $p=0.0008$ ). This relationship was not observable among isolated healthy volunteers (B;  $R^2=0.09$ ;  $p=0.0587$ ). Significance tested with linear regression model. \*Outlier; removed from significance calculations. Additional information about the plotted variables is provided in Table 1.

When compared to our healthy volunteer cohort, CP/CPPS patients showed reduced average systemic E2 concentrations ( $p=0.1032$ ) and elevated semen E2 levels (Fig. 23). Complementary to the steroid sex hormone levels, we measured systemic gene promoter CpG methylation (Pyrosequencing) and transcript levels (RT-qPCR) of *ESR1*, *ESR2* and the *AR* in ejaculated SC and circulating WBC (Fig. 23). CP/CPPS patients showed CpG hypermethylation of all receptors (*ESR1*, *ESR2*, *AR*) in ejaculated SC, and systemic (circulating WBC) as well as organ-confined (ejaculated SC) *ESR1* downregulation. The profile of our cell isolates from CP/CPPS patients resembles HMC-1 cells, which possess an epigenetically downregulated ER $\alpha$  (*ESR1*) and show elevated basal inflammatory gene expression when compared to LAD2 cells (Fig. 8+11; Tab. 5). Systemic *ESR1* downregulation in CP/CPPS patients was associated with systemic *ESR1* promoter CpG demethylation, but methylation changes to the healthy volunteer cohort were considerably low (median: -0.25%; avg: -0.01%).

Organ-confined (ejaculated SC) downregulation of the *ESR1* transcript (Fig. 23B.2) in CP/CPPS patients occurred together with hypermethylation of the *ESR1* promoter (Fig. 23B.3), suggesting epigenetic *ESR1* downregulation through *de novo* CpG methylation. Gene expression levels of *ESR2* and the *AR* showed no significant systemic or organ-confined regulation in CP/CPPS patients, but their systemic transcript levels showed a pronounced variability (Fig. 23A.2). Even though the expression levels of *ESR2* and *AR* were not significantly affected in ejaculated SC from CP/CPPS patients (Fig. 23B.2), their corresponding gene promoters were hypermethylated in these cells (Fig. 23B.3).

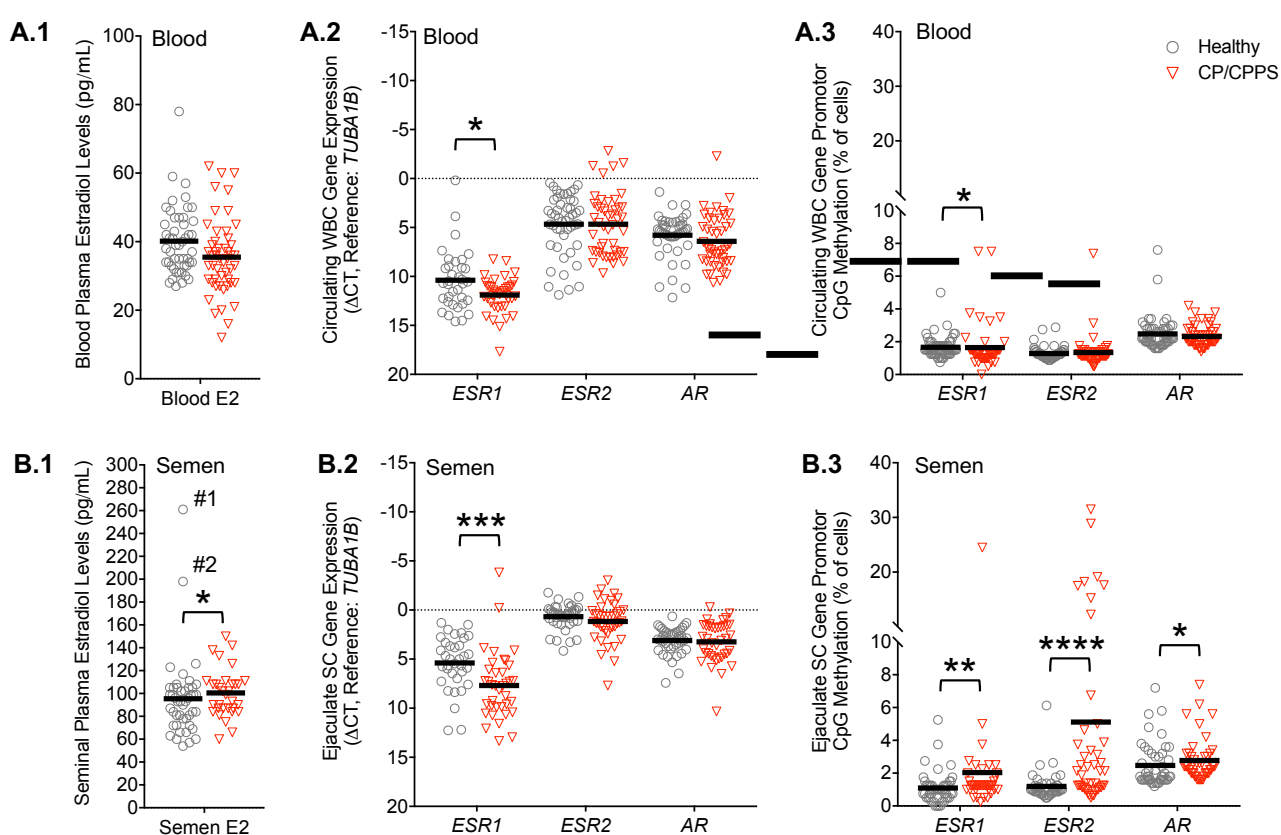


**Figure 23. CP/CPPS associates with aberrant systemic and organ-confined E2-signaling.**

Blood and semen from CP/CPPS patients and age-matched healthy volunteers were analyzed regarding E2 levels and the epigenetic state of *ESR1*, *ESR2* and *AR*. CP/CPPS patients showed reduced blood E2 levels (A.1;  $p=0.1032$ ), but significantly elevated semen E2 concentrations (B.1; two outliers removed;  $p=0.0272$ ). The *ESR1* transcript was downregulated in circulating WBC (A.2;  $\Delta\text{Ct}[\text{Healthy}]: 10.69\pm 3.05$ ;  $\Delta\text{Ct}[\text{CP/CPPS}]: 11.76\pm 1.80$ ;  $n=35/39$ ) and ejaculated SC (B.2;  $\Delta\text{Ct}[\text{Healthy}]: 5.01\pm 2.73$ ;  $\Delta\text{Ct}[\text{CP/CPPS}]: 7.74\pm 3.41$ ;  $n=35/37$ ) from CP/CPPS patients. Expression of *ESR2* and *AR* was not significantly affected in CP/CPPS patients, but among patients a high variability was observable for the systemic expression of *ESR2* (A.2;  $\Delta\text{Ct}$  range  $-2.83$  to  $9.66$ ) and *AR* (A.2;  $\Delta\text{Ct}$  range  $-2.29$  to  $10.64$ ). The *ESR1* gene promoter showed systemic CpG demethylation in CP/CPPS patients ( $n=60/50$ ), but systemic CpG methylation of *ESR2* and *AR* was unaffected (A.3). Ejaculated SC from CP/CPPS patients displayed promoter CpG hypermethylation of *ESR1* (Healthy:  $1.00\%\pm 0.95$ ; CP/CPPS:  $1.25\%\pm 3.70$ ;  $n=48/41$ ), *ESR2* (Healthy:  $1.00\%\pm 0.85$ ; CP/CPPS:  $2.01\%\pm 7.52$ ;  $n=48/46$ ) and the *AR* (B.3; Healthy:  $1.8\%\pm 1.33$ ; CP/CPPS:  $2.4\%\pm 1.31$ ;  $n=47/45$ ). Horizontal line (dotted) represents the reference gene Ct value. Values are given as Mean $\pm$ SD. Significance tested with Mann-Whitney U-Test. #Outlier; removed from significance calculations. Case numbers are shown for healthy volunteers first, and then for CP/CPPS patients [ $n(\text{Healthy}/\text{CP/CPPS})$ ]. Additional information about blood and semen E2 is summarized in Table 1.

Semen E2 levels correlated with reported urinary tract (voiding) symptoms from the NIH-CPSI questionnaire when patients and healthy probands were analyzed together (Fig. 24).

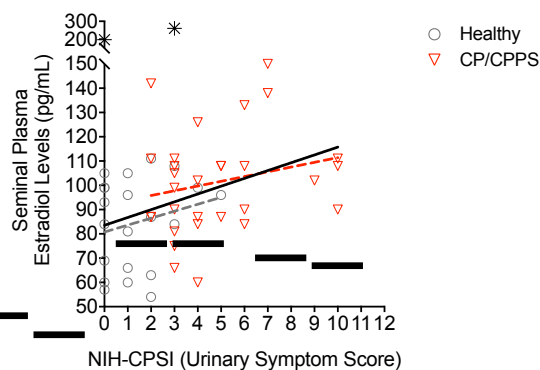


**Figure 24. Semen estradiol concentrations correlate with urinary tract symptoms.**

Semen E2 levels correlate with the reported urinary tract symptoms from the NIH-CPSI questionnaire ( $R^2=0.16$ ;  $p=0.0037$ ). The correlation is only significant when considering CP/CPPS patients and healthy volunteers together. The correlation is not significant in the isolated CP/CPPS cohort ( $R^2<0.05$ ;  $p=0.2353$ ). Significance tested with linear regression model. \*Outliers; removed from significance calculations.

Similar to the observed correlation of blood and semen E2 concentrations among CP/CPPS patients (Fig. 22B), we found that blood and semen *ESR1* expression levels correlate (Fig. 25). This indicates that systemic and local *ESR1* concentration are interdependent and might be a result of prevailing E2 levels.

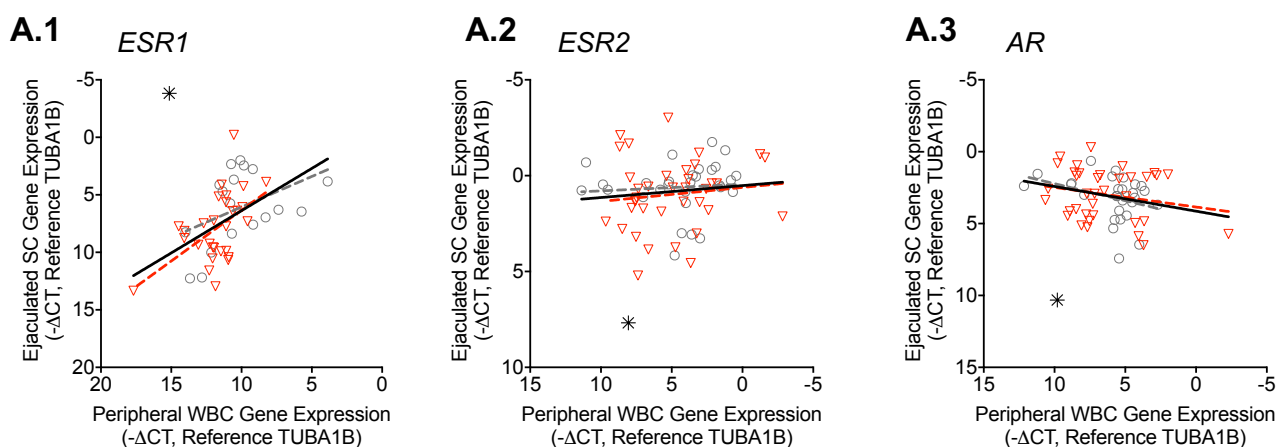


**Figure 25. *ESR1* transcript levels in circulating WBC and ejaculated SC correlate.**

Systemic (circulating WBC) transcript levels of *ESR1*, *ESR2* and *AR* correlate with their respective organ-confined (ejaculated SC) transcript levels. There was a significant correlation of systemic and organ-confined *ESR1* transcript levels (A.1;  $R^2=0.28$ ;  $p=0.0002$ ). Systemic and organ-confined *ESR2* expression did not correlate (A.2;  $R^2=0.01$ ;  $p=0.3632$ ), and there was a weak negative relationship of systemic and organ-confined *AR* transcript levels (A.3;  $R^2=0.07$ ;  $p=0.0372$ ). Significance tested with linear regression model. \*Outlier; removed from significance calculations.

Since the mast cell line LAD2 responded to E2-stimulation with a strong *IL-8* upregulation (**Tab. 6**), we reasoned that semen E2 has the potential to upregulate *IL-8* expression in CP/CPPS patients. However, neither blood or semen E2 levels, nor blood testosterone levels from CP/CPPS patients showed any correlation with SP *IL-8* levels (*not shown*). In order to evaluate whether epigenetic silencing of the *AR* and *ESR2* was masked by individuals without methylated gene promotor CpG sites, we did a linear regression analysis of their gene expression levels and the CpG methylation levels in their corresponding gene promotor. No negative correlation of gene transcription and promotor CpG methylation was revealed for *ESR1*, *ESR2* or *AR* in blood or semen of CP/CPPS patients. On the contrary, those cell isolates with elevated *ESR1* or *ESR2* promotor CpG methylation showed higher levels of the corresponding gene transcript (*not shown*).

### 5.1) CP/CPPS-specific changes are more pronounced in ageing patients

Promotor CpG methylation and gene expression of the steroid sex hormone receptors (*ESR1/ESR2/AR*) showed a high variability among CP/CPPS patients, so we objected to identify possible confounding variables. Regarding the age-dependency of steroid sex hormone decline and the onset of prostate disease, we reasoned that patient age has a strong confounding influence on disease-related parameters. We saw a wide age range among the patients of our study cohort (refer to **Tab. 1**; 19-69 years). PCa develops late in life, with 64% of diagnosed patients >65 years and 23% >75 years [127]. CP/CPPS presents a risk factor for PCa development [2], and ageing itself promotes accumulation of epigenetic changes over time [85]. It appeared therefore likely that older CP/CPPS patients show stronger disease-related aberrations, and that the inflammatory environment in their prostate tissue approaches PCa initiation.

Prostate tissue and liquid biopsies from older CP/CPPS patients might exhibit commonalities with PCa that are not observable in young patients. We stratified patients by age to see whether CP/CPPS-associated changes are more pronounced or exclusive in older patients.

There was no correlation of age with blood E2 levels, but a significant negative correlation of CP/CPPS patient age with blood testosterone and semen E2, and a significant positive correlation with semen IL-8 levels. The age-correlation of semen IL-8 was absent in age-matched healthy volunteers ( $R^2 < 0.01$ ;  $p = 0.6591$ ), indicating that elevated semen IL-8 levels represent age-dependent deterioration of CP/CPPS (Fig. 26A).

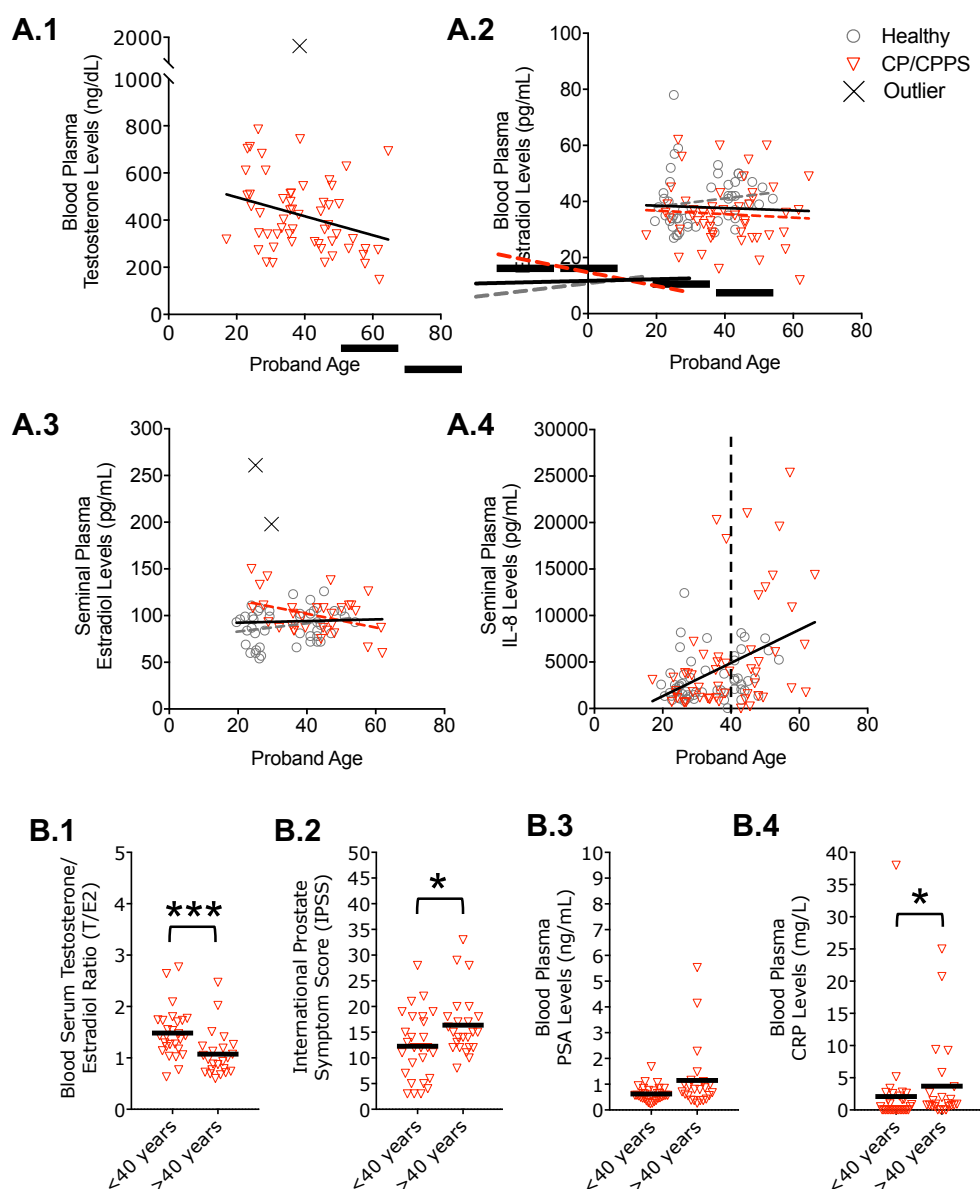


**Figure 26. CP/CPPS patient age correlates with testosterone, estradiol and IL-8 levels.**

CP/CPPS patient age correlates with blood testosterone (A.1;  $R^2 = 0.09$ ;  $p = 0.0210$ ), semen E2 (A.3;  $R^2 = 0.15$ ;  $p = 0.00316$ ) and semen IL-8 (A.4;  $R^2 = 0.19$ ;  $p = 0.0011$ ), but not blood E2 (A.2). Patients with semen IL-8 levels  $> 10,000$  pg/mL were mostly  $> 40$  years (A.4). CP/CPPS patients  $> 40$  years had a reduced blood testosterone to estradiol ratio (B.1; T/E2-ratio;  $\leq 40$  years:  $1.48 \pm 0.48$ ;  $> 40$  years:  $1.07 \pm 0.45$ ), elevated blood PSA (B.2;  $\leq 40$  years:  $0.62 \pm 0.29$ ;  $> 40$  years:  $1.15 \pm 1.26$ ;  $p = 0.0692$ ), and CRP levels (B.3;  $\leq 40$  years:  $2.09 \pm 6.68$ ;  $> 40$  years:  $3.70 \pm 6.49$ ), and score higher in the IPSS questionnaire (B.4;  $\leq 40$  years:  $12.26 \pm 6.59$ ;  $> 40$  years:  $16.38 \pm 6.09$ ). Values are presented as Mean  $\pm$  SD. Significance tested with Mann-Whitney U. (X) Outlier; removed from significance calculations. Case numbers: n(Healthy/CP/CPPS);  $< 40y(31/25)$ ;  $> 40y(37/24)$ .

Given the observed age-dependent decline of blood testosterone, semen E2, and the fact that CP/CPPS patients with excessive semen IL-8 levels ( $>10.000\text{pg/mL}$ ) were almost exclusively  $>40$  years, we grouped our cohorts by age (**Fig. 26B**). Older CP/CPPS patients ( $>40$  years) reported higher scores in the IPSS questionnaire (**Fig. 26B2**), but not in the CP/CPPS-specific NIH-CPSI or the hospital anxiety and depression (HADS) questionnaire (*not shown*).

Age-dependent deterioration of CP/CPPS was supported by available blood parameters. Blood from older patients ( $>40$  years) had a significantly reduced testosterone/estradiol ratio and increased levels of CRP and PSA (**Fig. 26B.3+4**).

Even though CRP levels from most of our CP/CPPS patients remained underneath the clinical cutoff value (WHO 2018:  $10\text{mg/L}$ ), this cutoff value is typically used for the detection of acute infections during clinical routine (peak levels  $\sim 350\text{-}400\text{mg/L}$ ). Apart from that, CRP values  $<10\text{mg/L}$  could still provide a suitable marker for chronic, low grade inflammation. 14% (8/56) of our CP/CPPS patients showed prominent CRP elevation ( $>5\text{mg/L}$ ), and 7% (4/56) actually crossed the cutoff ( $>10\text{mg/L}$ ).

The traditional cutoff for PSA screening is  $4\text{ng/mL}$ , and only one patient from our CP/CPPS cohort crossed that threshold. PSA levels increase with age [128], and adjusted total PSA (tPSA) cutoff values were proposed to reduce false-positives for men between 40-49 (adjusted cutoff:  $2.5\text{ng/mL}$ ) and 50-59 (adjusted cutoff:  $3.5\text{ng/mL}$ ) years of age [129, 130]. tPSA values  $<2\text{ng/mL}$  were suggested as normal for men from 20-40 years [130]. The observable PSA increases in some of the men with CP/CPPS indicate an increased secretory activity and probably a beginning malignant transformation of the prostate, so they could help to identify men with increased risk for PCa development. However, lacking PSA values for our age-matched healthy volunteer cohort make it difficult to interpret the significance of our findings.

Age-stratification of CP/CPPS patients also revealed that aberrations of the steroid sex hormone levels were more pronounced in older (>40 years) patients (**Fig. 27**). Older patients showed significantly reduced systemic testosterone levels when compared younger patients, and significantly reduced blood E2 levels when compared to their age-matched healthy counterparts. Systemic E2-levels increased with age in healthy volunteers, but not in CP/CPPS patients. Even though older CP/CPPS patients (>40 years) have increased semen IL-8 concentrations and report more symptoms, their semen E2 levels are not increased.

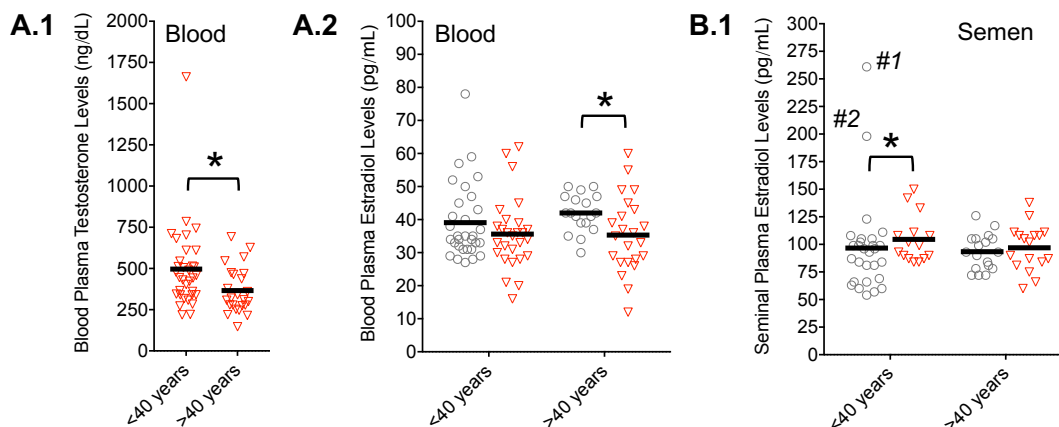


**Figure 27. CP/CPPS patients >40 years show systemic decline of testosterone and E2.**

Blood and semen steroid sex hormones and were separately analyzed for young ( $\leq 40$  years) and older (>40 years) CP/CPPS patients. Blood testosterone levels were significantly decreased in older versus younger patients (**A.1**; <40y:  $496.40 \pm 258.00$ ; >40y:  $366.20 \pm 140.00$ ), and patients >40 years had diminished systemic E2 levels (**A.2**; Healthy:  $42.00 \pm 5.71$ ; CP/CPPS:  $35.30 \pm 11.51$ ). Systemic E2 levels in younger patients were not significantly reduced (**A.2**). Young, but not older (>40 years) CP/CPPS patients displayed significantly elevated semen E2 levels (**B.1**). Values are provided as Mean  $\pm$  SD. Significance was tested with the Mann-Whitney U-Test.

Older CP/CPPS patients (>40 years) also differed from younger patients ( $\leq 40$  years) regarding the epigenetic state of *ESR1*, *ESR2* and the *AR* (**Fig. 28**). Along with systemically diminished testosterone and E2 levels, the older CP/CPPS patients (>40 years) showed systemic (blood) transcriptional downregulation of all three sex steroid hormone receptors (*ESR1*, *ESR2* and *AR*), and this was not observable in younger patients (**Fig. 28A**). The systemic *AR* expression in older CP/CPPS patients (>40 years) was not only reduced when compared to age-matched healthy volunteers, but also lower than in younger CP/CPPS patients (**Fig. 28A.2 versus 28A.1**;  $p=0.0368$ ). Systemic transcriptional downregulation of *ESR1*, *ESR2* and the *AR* mirrors the systemic decline of estradiol and testosterone levels in ageing patients (**Fig. 27**).

Regarding the gene expression in the ejaculated SC from semen, the stratification by age did not reveal any additional CP/CPPS-related changes. CP/CPPS was associated with *ESR1* downregulation in semen, but not with changes of *ESR2* or *AR* levels, no matter which age group was examined (**Fig. 28B**).

Systemic demethylation of the *ESR1* promotor in the blood happened exclusively in young CP/CPPS patients ( $\leq 40$  years), while older patients ( $>40$  years) had rather elevated systemic CpG methylation levels (**Fig. 28C**). In ejaculated SC from the semen, older ( $>40$  years) CP/CPPS patients, but not younger individuals ( $\leq 40$  years), showed gene promotor hypermethylation of *ESR1* and *AR* (**Fig. 28D**). The *ESR2* promotor was hypermethylated in patients from both age groups.

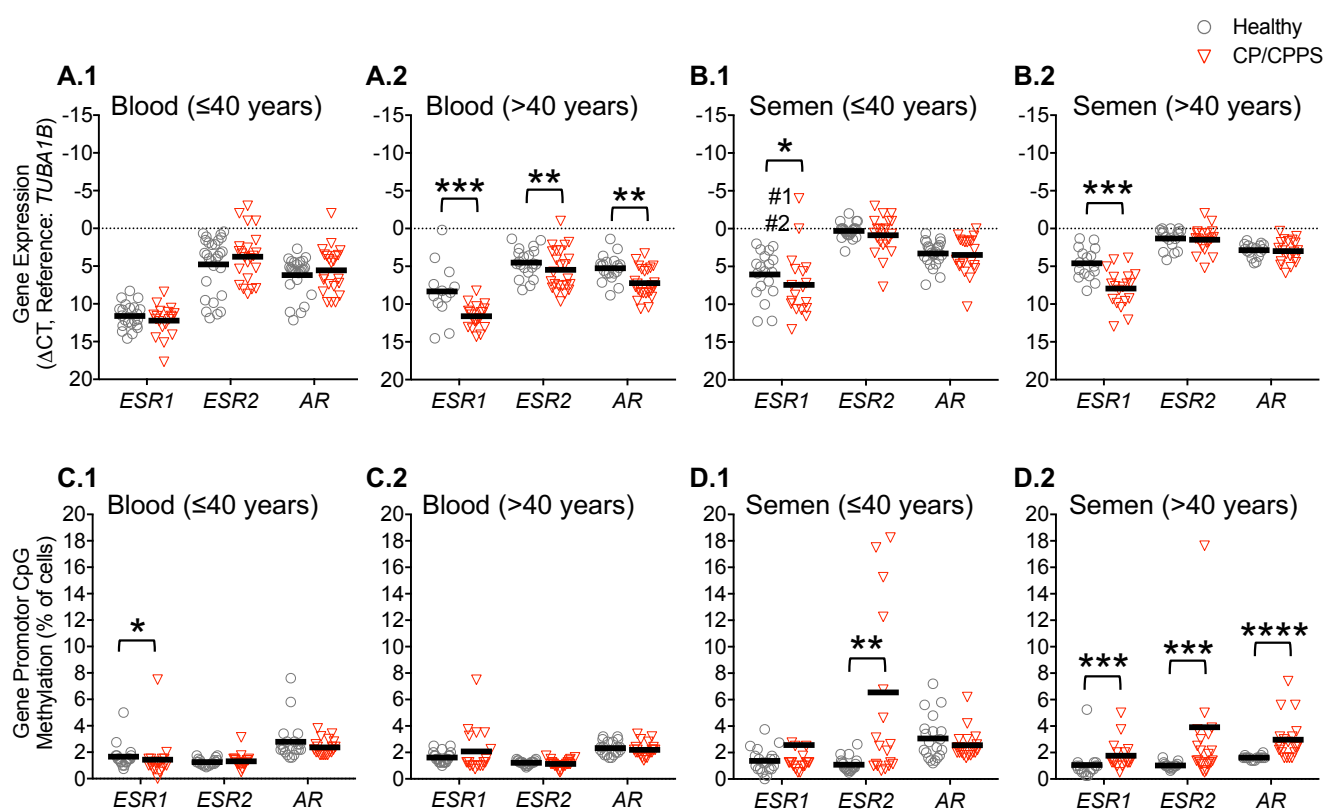


**Figure 28. Some aberrations of *ESR1*, *ESR2*, *AR* happen in exclusively patients >40years.**

Gene expression levels (**A+B**) and promotor CpG methylation (**C+D**) of *ESR1*, *ESR2* and *AR* in circulating WBC and ejaculated SC were separately analyzed for young ( $\leq 40$  years) and older ( $>40$  years) CP/CPPS patients. Systemic expression levels of *ESR1*, *ESR2* and *AR* were diminished in CP/CPPS patients  $>40$  years, but not in younger patients (**A**). CP/CPPS patients of both age groups showed *ESR1* downregulation in ejaculated SC, but no *AR* or *ESR2* regulation in these cells (**B**). Only young patients showed significant *ESR1* demethylation in circulating WBC (**C**), and only old patients showed promotor CpG hypermethylation of *ESR1* and *AR* in ejaculated SC (**D**). Values given as Mean $\pm$ SD. Horizontal line (dotted) represents the reference gene Ct value. Significance tested with Mann-Whitney U-Test.

## 6) Stromal cells affect the macrophage response

We polarized *in vitro* differentiated (THP-1 derived) macrophages for 48 hours with LPS/IFN $\gamma$  or IL-4/IL-13 to generate M1- and M2-polarized macrophages, respectively. Then we used RT-qPCR to measure the macrophage gene expression of polarization-specific markers (M1-specific markers: *TNF*, *IL-1B*, *HLA-DRA*, *HLA-DQA1*; M2-specific markers: *CD206*, *CCL13*, *CCL18*, *IL-10*).

To interrogate the influence of the TME on macrophage polarization, we repeated the polarization protocol with conditioned media (CM) samples from primary CAF and patient-matched NPF, prostate cancer cell lines (PC-3, DU-145, LNCaP), a benign prostate epithelial cell line (BPH-1) and mast cell lines (HMC-1, LAD2) in the absence of artificial polarizing stimuli. To gauge the effect size of CM-produced effects, we compared them with the artificial treatments (LPS/IFN $\gamma$  or IL-4/IL-13). We observed that epithelial cells, NPF, CAF and mast cells affect macrophage marker gene expression.

CAF and NPF display a high inter-individual variability, so we stratified our results with available clinical patient data. CAF-isolation presents a challenging method with the potential for technical errors and isolated fibroblasts have the propensity to change during culture. To counteract these pitfalls, we exclusively used NPF/CAF for our experiments that have been passaged <10 times in culture, and we characterized the expression of CAF-specific marker transcripts (RT-qPCR) as an indicator of CAF activation. Our confidence of CAF identity/activation was taken into account when analyzing the phenotype of CAF-educated macrophages.

### 6.1) LPS/IFN $\gamma$ and IL-4/IL-13 stimulation lead to macrophage polarization

Both polarizing stimuli (LPS/IFN $\gamma$  and IL-4/IL-13) were able to promote a significant macrophage activation with considerable upregulation of M1- and M2-specific marker transcripts (**Fig. 29**). Compared to unpolarized macrophages (M $\phi$ ), the M1-polarized (LPS/IFN $\gamma$  treatment) macrophages showed a significant upregulation of M1-specific marker genes. M2-specific treatment (IL-4/IL-13) also led to a significant induction of M1 markers, but expression was significantly lower than in M1-polarized cells. Similarly, both treatments led to significant upregulation of M2-specific marker genes. An exception was constituted by the M2-specific mannose receptor (*CD206*), which was upregulated by IL-4/IL-13, but slightly downregulated by LPS/IFN $\gamma$  (*not significant*).

Altogether, macrophage-treatment with artificial stimuli rendered sufficient to produce clearly distinct gene expression profiles that were indicative for M1- and M2-polarization, respectively. While M1-specific treatment (LPS/IFN $\gamma$ ) led to a significantly stronger upregulation of M1-specific markers (*IL-1B*, *HLA-DRA* and *HLA-DQA1*), the M2-specific treatment (IL-4/IL-13) led to a significantly stronger upregulation of M2-specific markers (*CD206* and *CCL13*).

The macrophage marker transcripts *TNF* (M1 marker), *CCL18* and *IL-10* (M2 markers) were upregulated by both stimuli, and gene regulations were not significantly different between the treatments.

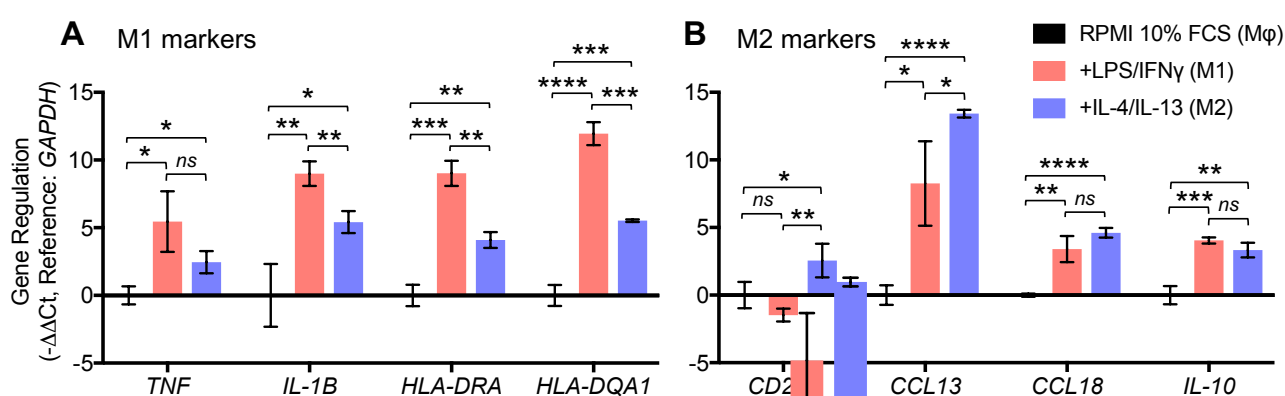


**Figure 29. LPS/IFN $\gamma$  and IL-4/IL-13 produce distinct macrophage phenotypes.**

After 48 hours of treatment with LPS/IFN $\gamma$  (M1-specific) or IL-4/IL-13 (M2-specific), macrophage gene expression of M1- and M2-specific marker genes was measured by RT-qPCR (n=3). Compared to unpolarized macrophages (M $\phi$ ; THP-1 media only), both treatments led to a significant upregulation of M1-markers (**A**), and M2-markers (**B**). In comparison to IL-4/IL-13 treated macrophages, the LPS/IFN $\gamma$  stimulated macrophages expressed significantly higher transcript levels of the M1-specific marker genes *IL-1B*, *HLA-DRA* and *HLA-DQA1* (**A**), and significantly lower levels of the M2-specific marker genes *CD206* and *CCL13* (**B**). The M2-specific marker *CD206* was activated by IL-4/IL-13, but not LPS/IFN $\gamma$  (**B**). Significance was calculated with the unpaired Students' T-Test.

## 6.2) Mast cells suppress macrophage M1 marker transcripts

Macrophages were polarized with CM from the mast cell lines HMC-1 and LAD2 (Fig. 30). HMC-1 and LAD2 culture media differ from THP-1 culture media and contain different additives (e.g. 100ng/mL stem cell factor in LAD2 media). Exchange of THP-1 culture media with mast cell culture media itself has the potential to influence macrophage polarization, so the CM effects on macrophage gene transcription were normalized to a polarization control with mast cell culture media. LAD2 culture media induced macrophage expression of the M1 marker transcripts *TNF*, *IL-1B* and *HLA-DQA1*. LAD2 CM significantly suppressed the media-promoted upregulation of *IL-1B* and *HLA-DQA1* (Fig. 30A).

However, LAD2 CM mediated gene expression was not different from the macrophage THP-1 media control (RPMI with 10% FCS). Hence, LAD2 CM was merely capable to suppress the M1 marker expression that un-conditioned (fresh) LAD2 culture media was able to induce. M2-polarizing effects of CM samples might only be visible when macrophages were properly activated in the first place (e.g. with LPS/IFN $\gamma$ ). Neither HMC-1 culture media, nor HMC-1 CM were capable to provoke any significant gene regulations in macrophages.

The M2-specific macrophage marker genes were neither affected by the mast cell culture media, nor by CM samples from HMC-1 or LAD2 (Fig. 30B).

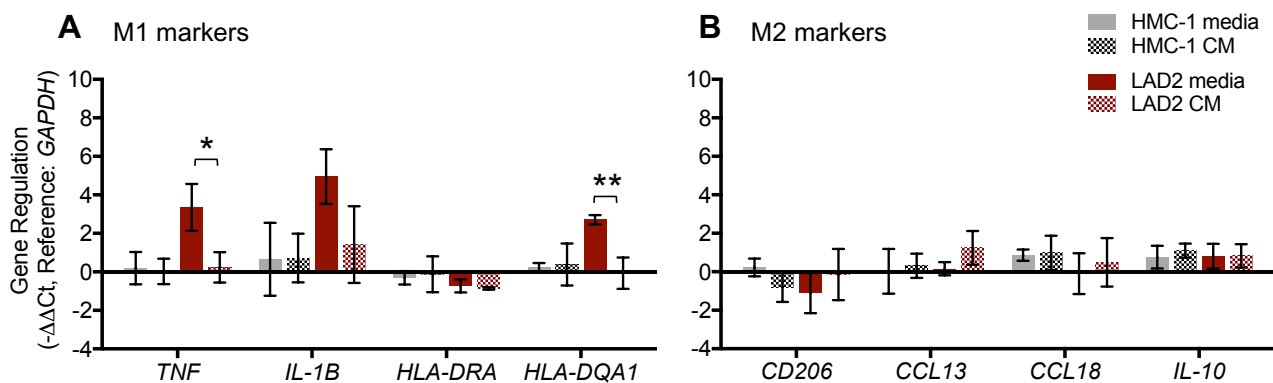


**Figure 30. LAD2 cells suppress macrophage expression of *TNF* and *HLA-DQA1*.**

RT-qPCR measurement of M1-specific (A) and M2-specific (B) marker transcripts in macrophages polarized with mast cell conditioned media (CM: n=3). Mast cell media or CM promoted gene regulations were compared to the relative gene expression in control macrophages that were incubated with THP-1 media only (vertical line at 0). LAD2 media led to macrophage induction of M1-specific markers (*TNF*, *IL-1B* and *HLA-DQA1*), and this effect was significantly suppressed by LAD2 CM in the case of *TNF* and *HLA-DQA1* (A). Gene expression of M2 marker genes was neither affected by mast cell culture media, nor mast cell CM (B). Significance was calculated with the unpaired Students' T-Test.

### 6.3) Epithelial cell lines, CAF and NPF affect macrophage marker transcripts

Conditioned media (CM) from CAF, patient-matched NPF and epithelial cell lines was prepared in THP-1 culture media. To encourage cell secretion of soluble factors into the media, a reduced fetal calf serum (FCS) concentration was used for CM preparation (RPMI with 2% instead of 10% FCS). This harbors the potential to affect the macrophage phenotype, so we normalized our CM experiments to a starvation media control (RPMI with 2% FCS). Comparison with the THP-1 culture media control (RPMI with 10% FCS) showed that starvation media did not significantly alter macrophage gene expression in our experiments (Fig. 31).

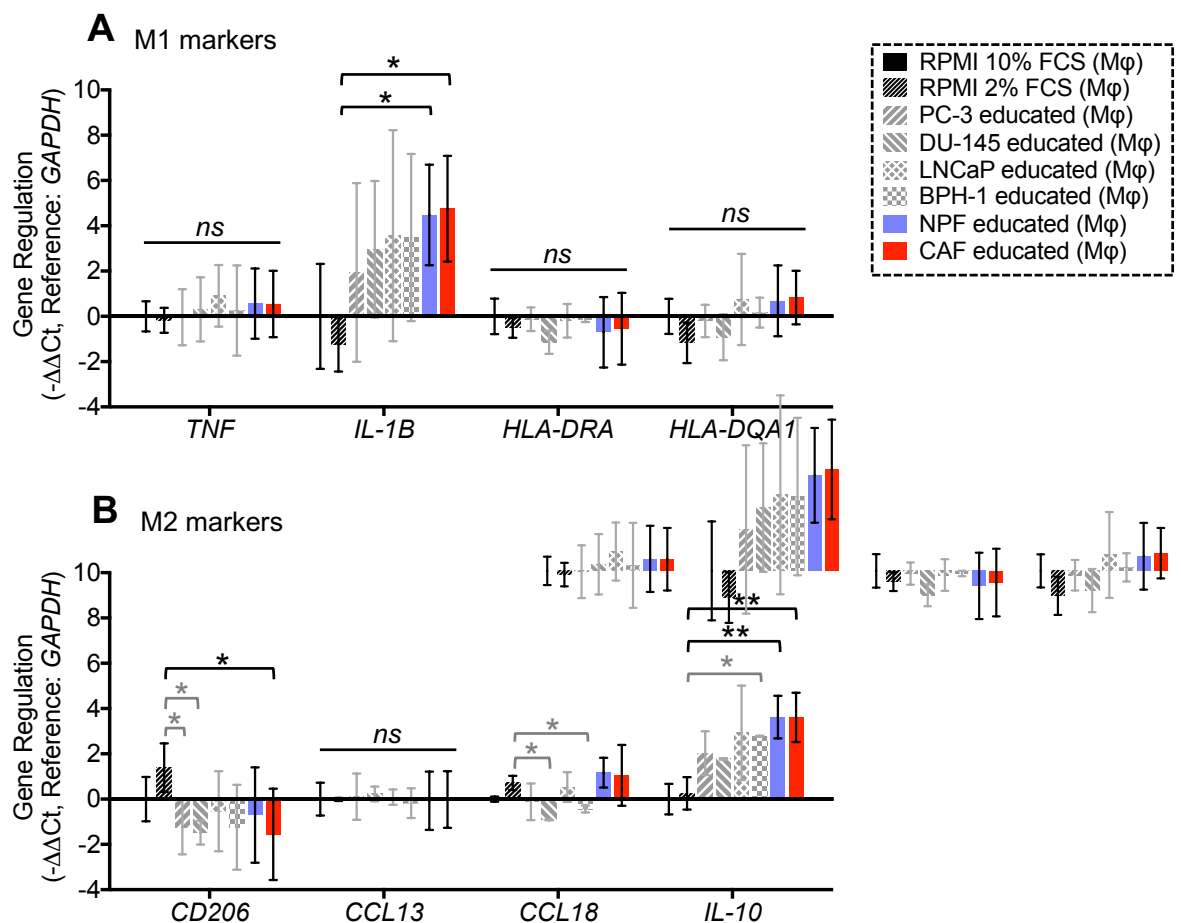


**Figure 31. CAF-educated macrophages upregulate *IL-1B*, *IL-10* and downregulate *CD206*.**

Macrophage expression of M1-specific (A) and M2-specific (B) marker transcripts in macrophages that have been incubated with starvation media (RPMI with 2% FCS; n=3), epithelial CM (PC-3: n=3; DU-145: n=2; LNCaP: n=3; BPH-1: n=2), NPF CM (n=11) or CAF CM (n=11) where compared to an unpolarized THP-1 media control (RPMI with 10% FCS; n=3). Exchange of THP-1 media with starvation media (48 hours) did significantly affect macrophages. Epithelial cell CM affected macrophage expression of *CD206* (downregulated by PC-3 and DU-145), *CCL18* (downregulated by DU-145 and BPH-1) and *IL-10* (B; upregulated by BPH-1). CAF- and NPF-educated macrophages upregulated gene expression of *IL-1B* (A) and *IL-10* (B). CAF-, but not NPF-educated macrophages downregulated gene expression of *CD206* (B). Gene regulations by CM were compared with the starvation media control. Significance of CAF- and NPF-mediated gene regulations was tested with the Mann-Whitney U-Test. Significance of starvation media and epithelial CM effects was calculated with the unpaired Students' T-Test.

Epithelial cell CM did not significantly affect macrophage M1 marker gene expression (**Fig. 31A**), but suppressed the M2 markers *CD206* (PC-3 and DU-145) and *CCL18* (DU-145 and BPH-1), while the M2-marker *IL-10* (BPH-1) was significantly upregulated (**Fig. 31B**). Macrophage expression of *IL-1B* was induced in some iterations of the polarization experiment, but gene expression changes were highly variable and therefore not significant.

CAF- and NPF-educated macrophages significantly upregulated gene expression of *IL-1B* (**Fig. 31A**; fold regulation by NPF: +4.5, by CAF: +4.8) and *IL-10* (**Fig. 31B**; fold regulation by NPF: +3.6, by CAF: +3.6). Importantly, the magnitude of CM effects was similar to the effects that artificial polarizing stimuli had on macrophage expression of *IL-1B* (average regulation after treatment with LPS/IFN $\gamma$ : +9.0 fold, IL-4/IL-13: +5.4 fold) and *IL-10* (average regulation after treatment with LPS/IFN $\gamma$ : +4.0 fold, IL-4/IL-13: +3.3 fold). CAF CM, but not NPF CM, was able to produce a significant macrophage downregulation of the M2-specific marker gene *CD206* (**Fig. 31B**; average regulation by CAF: -1.6 fold). The CAF-mediated *CD206* downregulation was similar to the downregulation after treatment with LPS/IFN $\gamma$  (average regulation: -1.5 fold).

#### 6.4) CAF display a high heterogeneity

CAF-specific marker gene expression was measured by RT-qPCR to estimate whether the CAF from our study show cancer-specific activation. CAF expression of the markers was normalized to patient-matched NPF to account for inter-individual heterogeneity, and to reveal a cancer-specific gene regulation within the patient PCa tissue (**Fig. 32**).

Gene expression of the CAF-upregulated marker *ESR1* correlated positively with expression of the CAF-upregulated markers *HOXD8* and *SFRP1*, and negatively with the CAF-downregulated marker *EPHB6* (**Fig. 32A**). Seven out of 12 NPF/CAF pairs showed a clearly distinguished expression pattern in CAF *versus* the patient-matched NPF (**Fig. 32B**). For the remaining five NPF/CAF pairs, CAF-specific gene regulation in CAF *versus* the patient-matched NPF was less distinct or even opposed the predominant expected trend (NPF/CAF pairs 10-12).

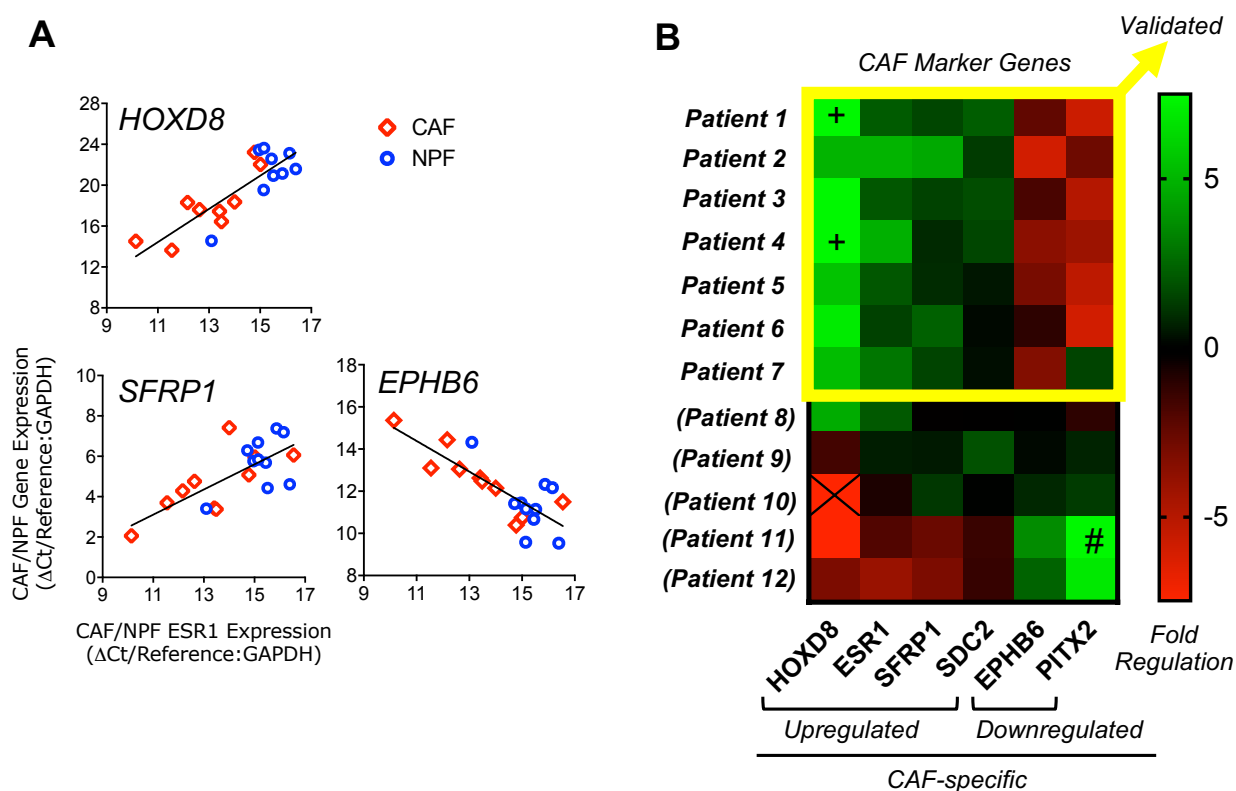


**Figure 32. CAF-specific marker gene expression in CAF and NPF.**

CAF-specific regulated marker genes were measured by RT-qPCR in CAF and patient-matched NPF. CAF-specific upregulation of *ESR1* showed a positive relationship with CAF-specific upregulation of *HOXD8* ( $R^2=0.71$ ;  $p<0.0001$ ) and *SFRP1* ( $R^2=0.51$ ;  $p=0.0004$ ), but a negative relationship with CAF-specific *EPHB6* downregulation (**A**;  $R^2=0.65$ ;  $p<0.0001$ ). High confidence of CAF identity ("validated") was assumed when CAF showed CAF-specific regulation of  $\geq 50\%$  (3/6) from the marker gene panel (**B**). For five NPF/CAF pairs, CAF-specific marker transcript levels were similar in CAF and NPF (Patients 8+9), or NPF appeared more activated than CAF (Patients 10-12). (+) more than 7.5-fold regulation; (#) no detection in NPF; (X) no detection in CAF. Significance was tested with linear regression model.

### 6.5) Pairwise evaluation of low and high confidence CAF

Conditioned media (CM) samples from CAF, but also patient-matched NPF, led to a significant upregulation of *IL-1B* and *IL-10* in educated macrophages. Cancer-specificity of CM effects on macrophages was expected to manifest in a difference between CAF- and NPF-mediated effects. However, no significant differences were observable when comparing CAF- and NPF-mediated effects on educated macrophages (**Fig. 31**; Mann-Whitney U-Test).

Since the high inter-individual variability between NPF/CAF pairs has the potential to mask CAF-specific effects, we did a pairwise comparison of CAF with their patient-matched NPF (**Fig. 33**; Paired Students' T-Test). This comparison revealed that CAF-specific *ESR1* upregulation was stable across most investigated NPF/CAF pairs (**Fig 33A.1**; 9/12 CAF). Moreover, pairwise comparison revealed that CAF *versus* NPF consistently downregulate M2-specific *CD206* expression in educated macrophages (**Fig. 33B.1**; 9/10 CAF). These CAF-specific effects were consistent among nearly all CAF, even though low confidence NPF/CAF pairs were included these pairwise comparisons.

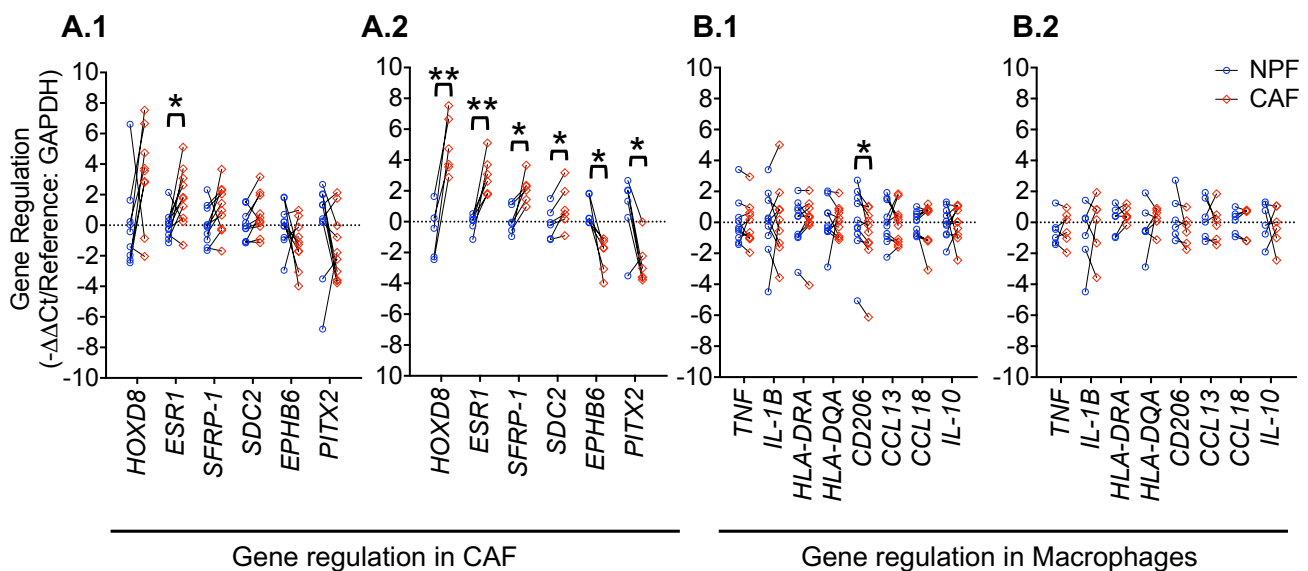


**Figure 33. Pairwise comparison of high and low confidence CAF with matched NPF.**

CAF and NPF expression of CAF-specific marker genes (**A**; n=11/11 NPF/CAF) and M1/M2-specific marker gene expression in CAF-educated macrophages (**B**; n=10/10 NPF/CAF) was measured by RT-qPCR. All NPF/CAF pairs (**A.1+B.1**), or only pairs with high confidence of CAF identity/activation (**B.1+B.2**) were included. The CAF-marker *ESR1* represents the only marker gene with consistent CAF-specific upregulation across all screened NPF/CAF pairs (**A.1**). Simultaneously, CAF-educated macrophages show consistent CAF-specific *CD206* suppression when all screened NPF/CAF pairs are considered (**B.1**). Removal of NPF/CAF pairs with low confidence of CAF identity/activation from the leads to retention of pairs with a distinguished CAF-specific marker profile (**A.2**). This refinement of the study cohort does not reveal any hidden CAF-specific effects on educated macrophages (**B.2**). Significance calculated with Paired Students' T-Test.

To find out whether NPF/CAF pairs with low confidence for CAF identity/activation masked some CAF-specific effects on educated macrophages, we did a separate evaluation without these questionable pairs (**Fig. 33A.2+B.2**). This led to the retention of NPF/CAF pairs with a clearly distinguished gene expression profile (**Fig. 33A.2**), but no other CAF-specific effects on macrophages were concealed behind the high CAF heterogeneity (**Fig. 33B.2**).

## 6.6) CAF-origin tumor grade affects macrophage polarization

The effects of CAF and NPF on CM-educated macrophages showed a high variability, and we observed that outliers affected macrophages that were polarized with CAF and NPF from the same patients (**Fig. 33B.1**). This suggests that CAF and NPF from the same patient share similarities that are distinct from NPF/CAF of the other patients. Furthermore, it could implicate that CAF differences between patients are more pronounced than the differences of CAF and NPF from the same patient. 50% (6/12) of the CAF from our study stem from high grade tumors, and it is difficult to isolate truly benign tissue from high grade prostatectomy specimen. The NPF from our study, especially when isolated from high grade tumor specimen, might also show a cancer-specific fibroblast activation.

Apart from that, the CAF from our study stem from patients with an individual disease pathology, and we had access to relevant clinical disease parameters from these patients (**Tab. 7**).

**Table 7. Clinical parameters of CAF-origin tumors.**

Clinical parameters indicate an increased aggressiveness of higher Gleason Score tumors.

Patient #	ID	Age	PSA	Grade	Vol.	GLE1	GLE2	IDC-P	PI	LI	Node #	SV
Patient 1	128R	56.7	6	pT3b	1.8	7	7	n/a	present	[-]	0/1	left
Patient 2	229R	65	7	pT3bN1	19.7	9	9	yes	extensive	[+]	6/14	bilateral
Patient 3	338R	42	8.1	pT3a	13	7	7	no	extensive	[-]	0/0	n/a
Patient 4	332R	68	11	pT3a	5.4	9	9	yes	extensive	focal	0/2	n/a
Patient 5	156R	73.6	16.8	pT3b	28.6	9	9	no	multifocal	[-]	0/4	bilateral
Patient 6	287R	69	13.1	pT3bN1	23.8	9	9	yes	extensive	[+]	3/7	bilateral
Patient 7	300R	76	7.04	pT2c	2.3	7	7	no	extensive	n/a	0/0	n/a
Patient 8	390R	64	n/a	pT3a	10.6	7	7	no	extensive	[-]	0/0	n/a
Patient 9	180R	67.1	19.3	pT2cN0	4.6	9	9	no	n/a	[-]	0/7	n/a
Patient 10	277R	65	20	pT2cN0	4.8	7	7	no	n/a	[-]	0/1	n/a
Patient 11	275R	66	45	pT3bN0	3.2	8	7	yes	extensive	[-]	0/8	right SV
Patient 12	305R	75	2	pT3bN1	73.4	10	9	yes	extensive	[+]	10/16	bilateral

ID: Internal CAF-origin patient identity; PSA: Prostate-specific antigen (ng/mL); Grade: Tumor staging according to the TNM system; Vol.: Tumor volume (cubic centimeter); GLE1: Gleason Score before tumor resection; GLE2: Gleason Score after tumor resection; IDC-P: Intraductal carcinoma of the prostate; PI: Perineural invasion; LI: Lymph involvement; SV: Seminal vesicle.

Clinical variables like the Gleason Score of the CAF-origin prostate tumor might account for some variability across CAF (NPF) and their effect on educated macrophages. High grade (Gleason 9) tumors had an increased tumor volume, elevated patient blood PSA levels and increased frequencies of intraductal carcinoma of the prostate (IDC-P), seminal vesicle invasion (SVI) and lymph node involvement when compared to Gleason 7 tumors.

We assumed that tumor aggressiveness might be reflected in the CAF phenotype, so we compared our results from high grade (Gleason 9) CAF and NPF to those from low grade (Gleason 7) CAF and NPF. The CAF-specific upregulated marker gene *SFRP1* was significantly upregulated in high grade *versus* low grade CAF (**Fig. 34A**), and high grade CAF skewed CM educated macrophages towards M2 (**Fig. 34B**).

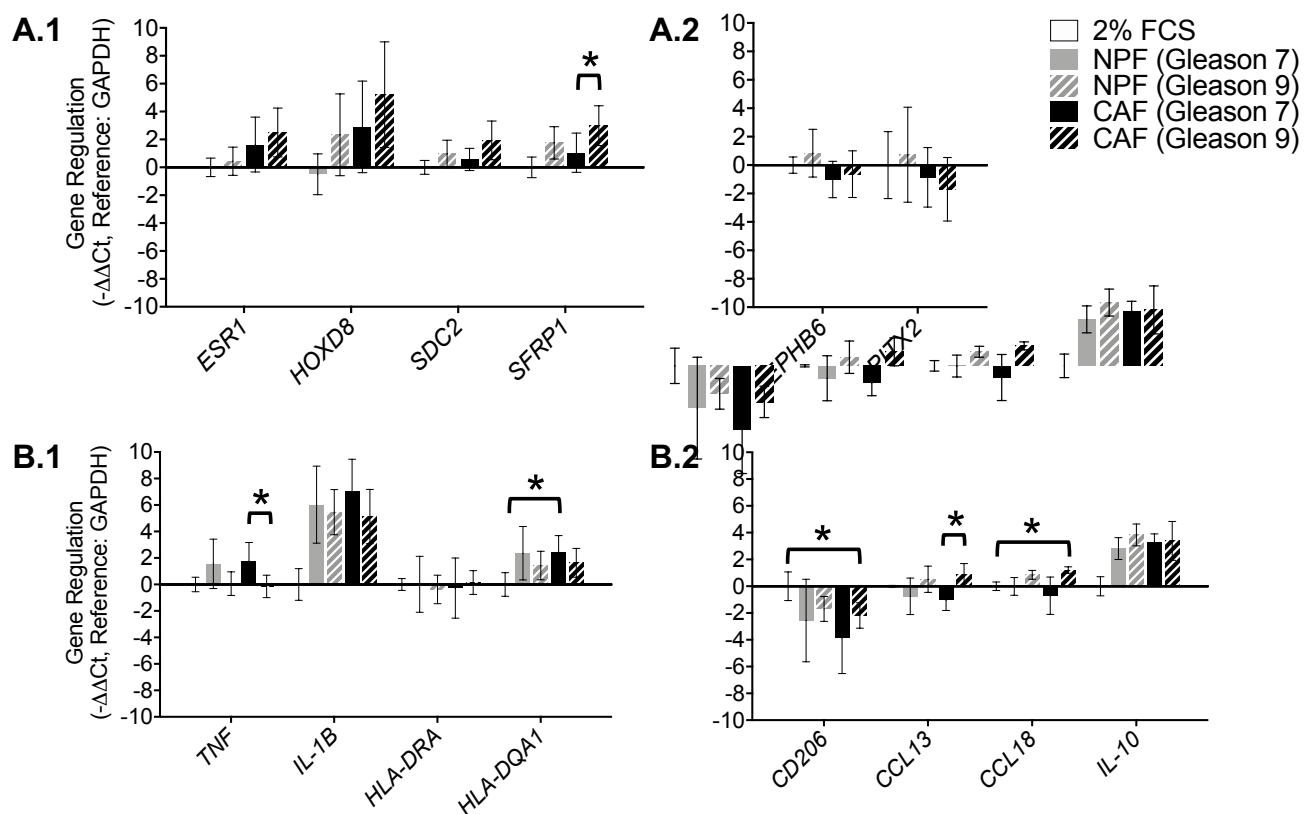


**Figure 34. Stratification of CAF and patient-matched NPF by CAF-origin tumor grade.**

CAF-specific marker gene expression (**A**; Gleason 7: n=4; Gleason 9: n=7) and CAF-mediated macrophage gene regulation (**B**; Gleason 7 n=5; Gleason 9: n=6) was stratified by CAF-origin tumor grade. High grade (Gleason 9) CAF expressed significantly higher levels of CAF-specific upregulated *SFRP-1* than low grade (Gleason 7) CAF (**A.1**). No other CAF-specific regulated markers showed significant regulation with CAF-origin tumor grade (**A1+A.2**). High *versus* low grade CAF promoted *TNF* downregulation (**B.1**) and *CCL13* upregulation in educated macrophages (**B.2**). Only low grade CAF upregulated macrophage expression of *HLA-DQA1* (**B.1**). Only high grade CAF suppressed *CD206* expression while upregulated *CCL18* in educated macrophages (**B.2**). Significance tested with Mann-Whitney U-Test.

Compared to low grade CAF CM, high grade CAF CM induced significantly lower *TNF* and significantly higher *CCL13* transcript levels in educated macrophages. Low grade, but not high grade CAF, induce macrophage expression of *HLA-DQA1*. Conversely, high grade, but not low grade CAF, were capable to induce macrophage *CCL18* and simultaneously suppress *CD206* expression.

These data include NPF and CAF with low confidence of CAF myofibroblast activation. Because of this, we evaluated high confidence NPF/CAF pairs separately (Tab. 8). Isolated consideration of high confidence pairs supports that high grade CAF suppress (M1-specific) *TNF* expression and upregulate (M2-specific) *CCL13* and *CCL18* expression in educated macrophages.

**Table 8. Stratification of educated macrophages by confidence of CAF identity/activation.**

Gene regulation is separately shown for macrophages educated by low grade (Gleason 7) and high grade (Gleason 9) NPF- and CAF. Conditioned media (CM) induced gene expression changes were compared with the starvation media control (RPMI 2% FCS). Separately, effects of high grade CAF were compared with effects of low grade CAF (or NPF *versus* NPF). CM induced gene regulations and significance values are given for each group with all NPF/CAF pairs (Gleason 7: n=5; Gleason 9: n=6), or in isolated consideration of pairs with high confidence of CAF identity/activation (Gleason 7: n=3; Gleason 9: n=4). Significance values were calculated with the Mann-Whitney U-Test. Grey cell background values represent a continuous scale of p-values between 0.01 and 0.1.

		Gene regulation										P-values				P-values	
		Versus THP-1 media (RPMI 10% FCS)										CM vs CM-Control (RPMI 2% FCS)				HG vs LG	
		RPMI 2% FCS		Low Grade NPF		High Grade NPF		Low Grade CAF		High Grade CAF		LG NPF	LG CAF	HG NPF	HG CAF	NPF	CAF
Marker		AVG	SD	AVG	SD	AVG	SD	AVG	SD	AVG	SD	P	P	P	P	P	P
All NPF/CAF pairs	<i>TNF</i>	-0.18	0.55	1.38	1.87	-0.12	0.89	1.59	1.41	-0.32	0.85	0.14	0.14	0.71	0.71	0.25	0.02
	<i>IL-1B</i>	-1.24	1.20	2.96	3.13	4.22	1.71	5.79	2.43	3.89	2.05	0.07	0.04	0.02	0.02	0.54	0.43
	<i>HLA-DRA</i>	-0.50	0.44	-0.49	2.12	-0.88	1.08	-0.78	2.27	-0.36	0.90	0.79	0.79	0.71	0.55	0.43	0.93
	<i>HLA-DQA1</i>	-1.17	0.89	1.19	2.02	0.26	1.08	1.27	1.25	0.47	1.09	0.14	0.04	0.10	0.10	0.27	0.25
	<i>CD206</i>	1.39	1.07	-1.18	3.08	-0.31	0.93	-2.47	2.67	-0.80	0.95	0.13	0.07	0.15	0.05	0.79	0.33
	<i>CCL13</i>	-0.01	0.07	-0.76	1.36	0.51	0.98	-1.04	0.78	0.84	0.85	0.25	0.25	0.71	0.17	0.05	0.02
	<i>CCL18</i>	0.71	0.31	0.70	0.66	1.56	0.33	0.00	1.39	1.92	0.24	0.57	0.25	0.02	0.02	0.07	0.08
	<i>IL-10</i>	0.25	0.72	3.06	0.81	4.09	0.82	3.57	0.59	3.64	1.45	0.04	0.04	0.02	0.02	0.13	0.54
High confidence pairs	<i>TNF</i>	-0.18	0.55	1.87	2.43	0.01	0.47	2.24	1.32	-0.08	0.88	1.00	1.00	0.06	0.06	0.63	0.06
	<i>IL-1B</i>	-1.24	1.20	4.86	4.10	4.23	0.96	6.75	2.62	4.22	2.44	1.00	1.00	0.23	0.63	0.63	0.63
	<i>HLA-DRA</i>	-0.50	0.44	-1.48	2.24	-0.36	0.78	-1.63	2.55	0.06	0.62	1.00	1.00	0.40	0.40	0.86	0.40
	<i>HLA-DQA1</i>	-1.17	0.89	0.49	2.40	0.65	0.59	1.16	1.07	0.89	0.76	1.00	1.00	0.63	0.40	0.86	0.40
	<i>CD206</i>	1.39	1.07	-1.97	3.90	-0.72	0.84	-3.50	2.98	-1.01	1.15	0.70	1.00	0.11	0.23	0.63	0.23
	<i>CCL13</i>	-0.01	0.07	-1.50	0.70	0.94	0.93	-1.41	0.26	0.54	0.89	1.00	1.00	0.06	0.06	0.06	0.06
	<i>CCL18</i>	0.71	0.31	0.46	0.25	1.67	0.37	-0.67	1.09	1.90	0.04	0.10	1.00	0.06	0.06	0.06	0.06
	<i>IL-10</i>	0.25	0.72	2.68	0.87	4.27	0.95	3.26	0.42	3.31	1.71	0.40	1.00	0.23	1.00	0.11	1.00

AVG: Average; SD: Standard Deviation; LG: Low Grade; HG: High Grade; P: P-value.

### 6.7) CAF expression of *SFRP1* correlates with CAF-induced macrophage transcripts

Stratification of CAF and patient-matched NPF by tumor grade indicated that high grade (Gleason 9) CAF upregulate *SFRP1* expression (**Fig. 34A.1**). At the same time, we observed that these CAF affected macrophage expression of marker transcripts (*CD206*, *TNF*, *CCL13* and *CCL18*) differently than low grade CAF (or NPF). Secreted *SFRP1* affects WNT signaling. We tested whether *SFRP1* levels in CAF correlate with macrophage levels of polarization-specific (M1 or M2) marker transcripts. We found a positive correlation of the CAF-expressed *SFRP1* transcript levels with macrophage-expressed (M2-specific) *CCL13* and *CCL18*, and a negative relationship with macrophage-expressed (M1-specific) *TNF* levels (**Fig. 35**).

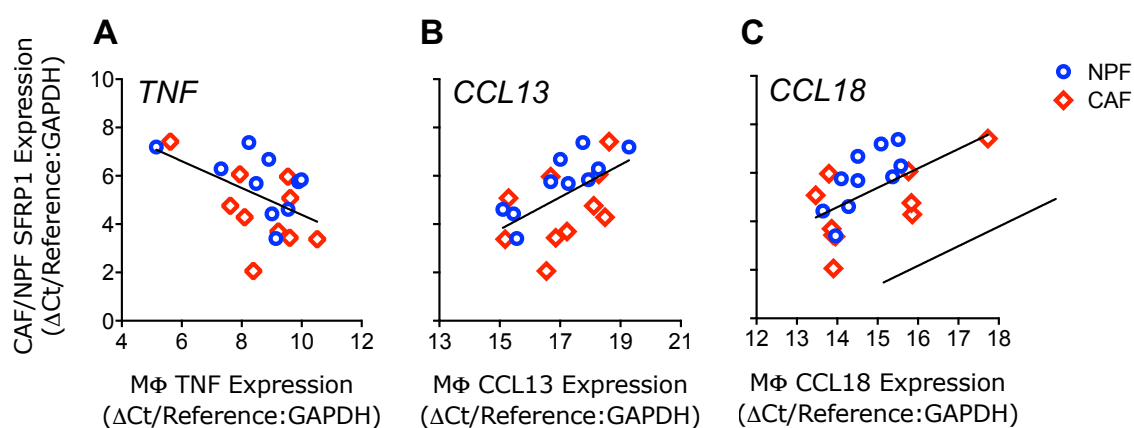


**Figure 35. NPF/CAF expression of *SFRP1* correlates with macrophages marker transcripts.**

NPF and CAF expression of *SFRP1* shows a significant negative relationship with macrophage *TNF* expression (**A.1**;  $R^2=0.26$ ;  $p=0.0216$ ), but not with *CCL13* (**A.2**;  $R^2=0.21$ ;  $p=0.1016$ ) and *CCL18* (**A.3**;  $R^2=0.25$ ;  $p=0.0701$ ). The positive relationship of *SFRP1* with *CCL13* (**A.2**;  $R^2=0.79$ ;  $p=0.0077$ ) and *CCL18* (**A.3**;  $R^2=0.55$ ;  $p=0.0137$ ) is significant when considering NPF only. Significance calculated with linear regression analysis.

### 6.8) Estradiol induces macrophage *CCL18* through ER $\alpha$ signaling

We observed that some CAF-educated macrophages upregulate *CCL18* expression. In ejaculated SC from CP/CPSP patients, we detected elevated *CCL18* transcript levels. *CCL18* is a leukocyte attraction chemokine, and CP/CPSP patients show increased prostatic leukocyte infiltration together with elevated semen E2 levels. We aimed to determine whether E2 affects leukocyte expression of *CCL18*. Since macrophages are present in ejaculated SC from CP/CPSP patients and resemble M2-polarized macrophages in PCa, we stimulated THP-1 derived M2-polarized macrophages with excess (100nM) estradiol and characterized *CCL18* with ChIP, RT-qPCR, Western blot and Pyrosequencing (**Fig. 36**).

With ChIP, we detected increased ER $\alpha$  (and H3K4me3) binding at an estrogen-response element (ERE) in the *CCL18* gene promoter of E2-treated M2-macrophages. *CCL18* upregulation was confirmed on the transcriptional and protein level by RT-qPCR and Western blot. Macrophages (M $\phi$ /M2) show a methylated *ESR2* promoter (M $\phi$ : 71%; M2: 72%) and a demethylated *ESR1* promoter (M $\phi$ : 18%; M2: 17%). This indicates active *ESR1* transcription. Altogether, our data supports that E2-stimulation has the potential to induce *CCL18* expression in macrophages through ER $\alpha$  binding to the *CCL18* gene promoter.

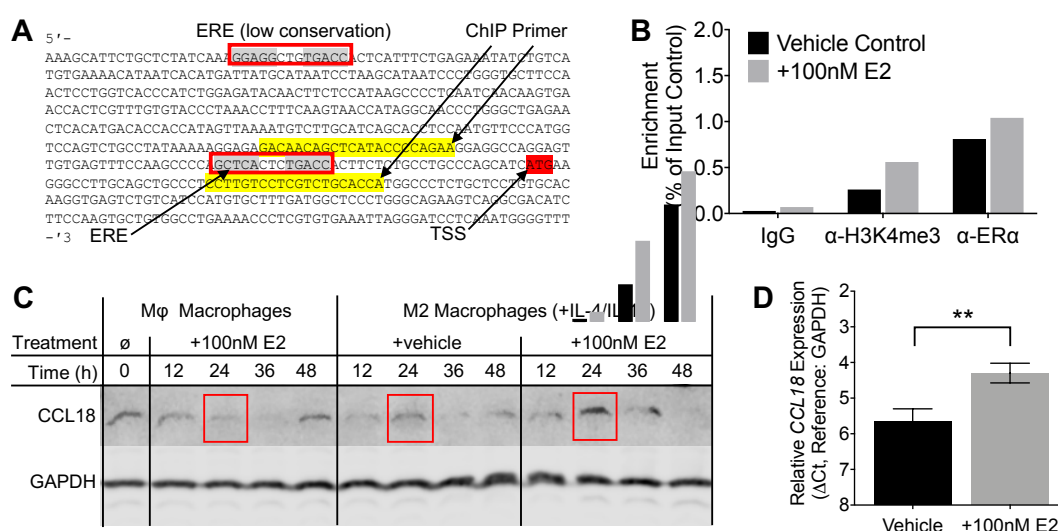


**Figure 36. E2-mediated *CCL18* upregulation in M2 macrophages is directed by ER $\alpha$ .**

E2-stimulated M2 macrophages were analyzed by ChIP (**A+B**), western blot (**C**) and RT-qPCR (**D**). The ChIP PCR covered an estrogen response element (ERE) at the *CCL18* TSS (**A**) and showed enrichment of H3K4me3 and ER $\alpha$  in E2-treated M2 macrophages (**B**; n=1). Western blot confirmed that these cells upregulate *CCL18* on the protein level (**C**; red rectangles; n=1), and RT-qPCR confirmed *CCL18* upregulation on the transcript level (**D**; n=3). Significance was tested with Students' T-Test.

## 7) Macrophages affect stromal/epithelial interactions during co-culture

To evaluate the influence of macrophages on the TME, THP-1 derived macrophages were added to BPH-1 cells growing on a confluent layer of primary CAF or NPF. Undifferentiated THP-1 cells were tested side by side with unpolarized macrophages (M $\phi$ ) and polarized macrophages (M1/M2). BPH-1 cells were pre-stained with Cell Tracker green CMFDA before co-culture, and FA-fixed co-culture assays were stained with the phalloidin-TRITC. Different absorption and emission spectra of CMFDA and TRITC allowed separated acquisition of BPH-1 cells and F-Actin during confocal imaging, and binarized images allowed the quantification of BPH-1 cells and F-Actin positivity (**Fig. 37**).

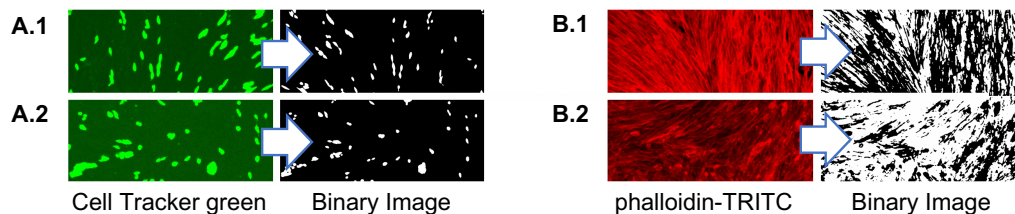


**Figure 37. Binarization allows quantification of confocal images.**

Shown are exemplary images of the cell-tracker green CMFDA (**A**) and Phalloidin-TRITC (**B**) channels in the reference co-culture assay with NPF and BPH-1 cells (**A.1+B.1**), and the same system including 30,000/cm<sup>2</sup> M2 macrophages (**A.2+B.2**). Binary transformation of acquired images allowed morphometric quantification of BPH-1 cells and F-Actin staining.

### 7.1) CAF and NPF produce different F-Actin layers

Confocal imaging of FA-fixed co-culture assays revealed that CAF produced a denser, more homogenous F-Actin staining than patient-matched NPF, and this was reproducible for 4/5 NPF/CAF pairs (**Fig. 38**). Since phalloidin-TRITC is not fibroblast-specific, it also stains F-Actin positive BPH-1 cells. However, most of the labeled area was occupied by the confluent fibroblast layer.

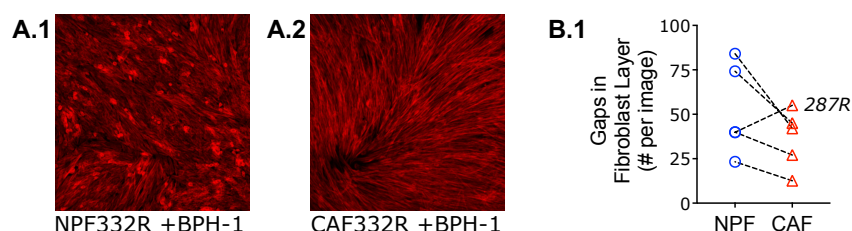


**Figure 38. Co-cultures with CAF display an increased F-Actin homogeneity and density.**

Confocal imaging revealed a different F-actin staining on CAF *versus* patient-matched NPF (n=5). Example images illustrate the F-Actin staining patterns on NPF (**A.1**) and CAF (**A.2**). Quantification confirms a denser F-Actin staining in co-cultures with CAF from 4/5 NPF/CAF pairs (**B.1**).

## 7.2) Macrophages affect F-Actin staining and BPH-1 cell shape in co-culture with NPF

The addition of (undifferentiated) THP-1 cells had no detectable effects on co-culture assays with NPF or CAF and BPH-1 cells, but M2-polarized macrophages led to a consistent disruption of the F-Actin staining when co-culture experiments were done on NPF (**Fig. 39A**). Co-culture experiments were repeated with five high confidence (RT-qPCR validated) NPF/CAF pairs. During brightfield microscopy of co-cultured THP-1 cells with BPH-1 and CAF, THP-1 interactions with the CAF layer could be observed (**Fig. 39B**). Macrophage-mediated F-Actin disruptions were absent or weaker in co-culture assays with CAF (**Fig. 40A**; e.g. 128R, 156R). Morphometric quantification (n=5) indicated that macrophage-mediated F-actin layer density decreases were significant after co-culture with M2 polarized macrophages, while M1-polarized and unpolarized macrophages ( $M\phi$ ) had weaker effects (*not significant*), and undifferentiated THP-1 cells had no observable effect (**Fig. 40A**).

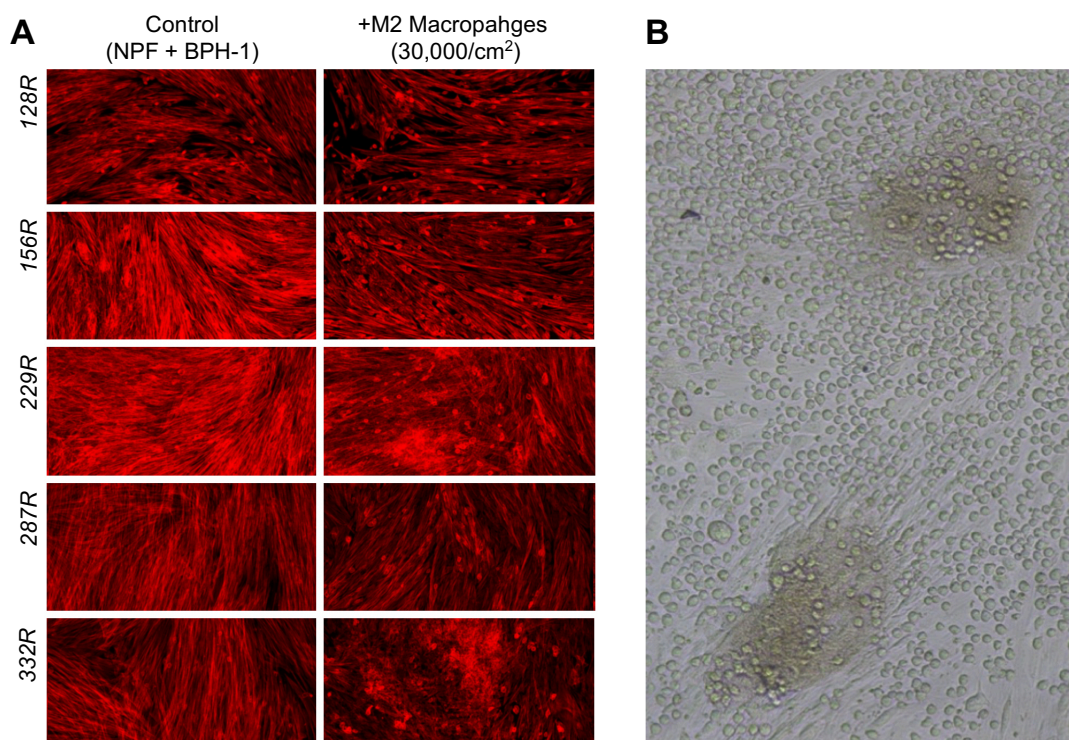


**Figure 39. M2 macrophages disrupt the F-Actin staining in co-culture with NPF.**

In the reference co-culture system (NPF+BPH-1), NPF produced a confluent monolayer with quantifiable F-Actin staining. After addition of M2-polarized macrophages (30,000/cm<sup>2</sup>), the F-actin staining pattern assumed a grainy appearance with increased frequency of areas with absent or decreased dish coverage (**A**; n=5). Brightfield microscopy showed that THP-1 cells form patches on co-cultured CAF (**B**; CAF ID: 180R).

Simultaneously, an increased BPH-1 circularity was observed in co-culture assays with M1- and M2-polarized, but not with unpolarized macrophages (M $\phi$ ) or THP-1 cells on NPF, and again the promoted changes were not significant on CAF. Similar to the macrophage-induced F-Actin layer disruptions, BPH-1 cell circularity increases were strongest in co-culture with M2 macrophages on NPF, suggesting that F-Actin staining and BPH-1 shape might be related (**Fig. 40B**).

Furthermore, addition of macrophages to the co-culture assays led to an increased BPH-1 cell count after 24 hours, which was significant in the case of co-culture assays with M1 macrophages and BPH-1 cells on CAF (**Fig. 40C**).

A major problem of our confocal imaging results was posed by the fact that the BPH-1 cells from our assays did not consistently assume a more elongated, spindle-like shape on CAF *versus* the patient-matched NPF, as it has previously been published [38]. Instead, no consistent CAF-mediated changes on the BPH-1 form factor were observable (**Fig. 40B**; Controls).

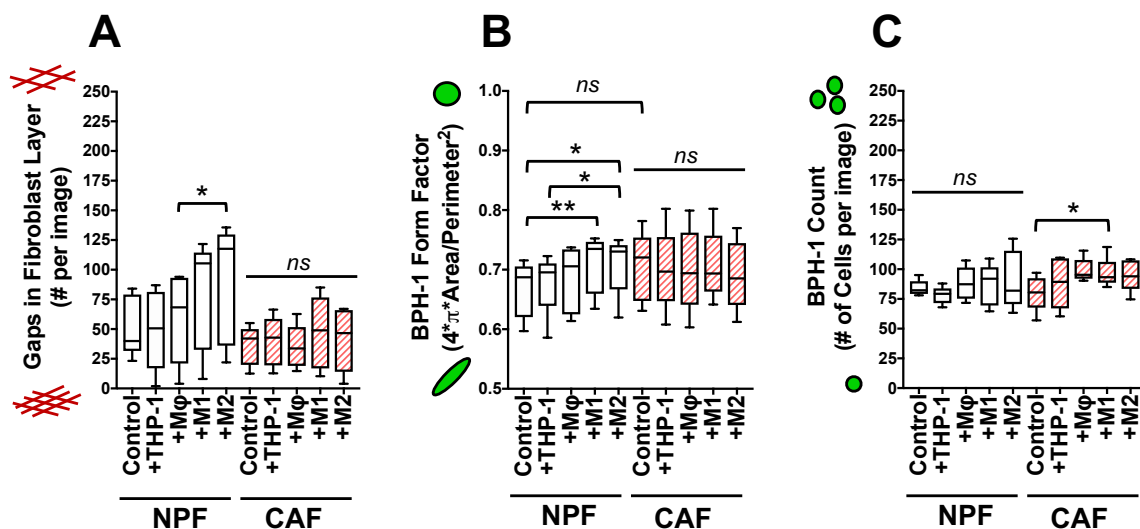


**Figure 40. Macrophages induce significant changes of F-Actin staining and BPH-1 cells.**

THP-1 cells and macrophages (M $\phi$ , M1, M2) were added (30,000 cells/cm<sup>2</sup>) to co-culture assays of CAF or NPF with BPH-1 cells, and fibroblast layer density (**A**), BPH-1 form factor (**B**) and BPH-1 cell count (**C**) after co-culture were quantified on binarized confocal images (n=5 NPF/CAF pairs). Addition of M2 polarized macrophages to co-cultured NPF and BPH-1 cells led to an elevated count of dish areas without fibroblast coverage (**A**). Addition of M1 and M2 macrophages increased BPH-1 circularity in co-culture with NPF (**B**), and M1 macrophages increased the cell count of BPH-1 cells growing on CAF (**C**). Significance tested with Mann-Whitney U-Test.

### 7.3) Live cell imaging supports CAF-mediated BPH-1 form factor changes

A major issue of our current confocal imaging results was posed by the fact that only two out of five (ID: 128R, 332R) NPF/CAF pairs reproduced previously published experiments at MU, which reported that BPH-1 cells assume a more elongated, spindle-like shape during co-culture with CAF when compared to patient-matched NPF [38].

We made live cell time lapse imaging experiments with six NPF/CAF pairs and reproduced the expected CAF-specific BPH-1 form factor changes, with BPH-1 cells assuming a more elongated shape on CAF *versus* NPF during the whole time of the experiment (**Fig. 41**). Pairwise comparison confirmed that CAF-specific BPH-1 changes are significant. Four out of six NPF/CAF pairs from the live cell imaging experiments (ID: 128R, 156R, 229R, 332R; new pairs: 300R, 338R) had previously been used for confocal imaging, so our live cell imaging results contradict previous confocal imaging results (ID: 156R, 229R) and suggest that discrepant findings are the result of technical errors in the preparation steps for the confocal imaging protocol.

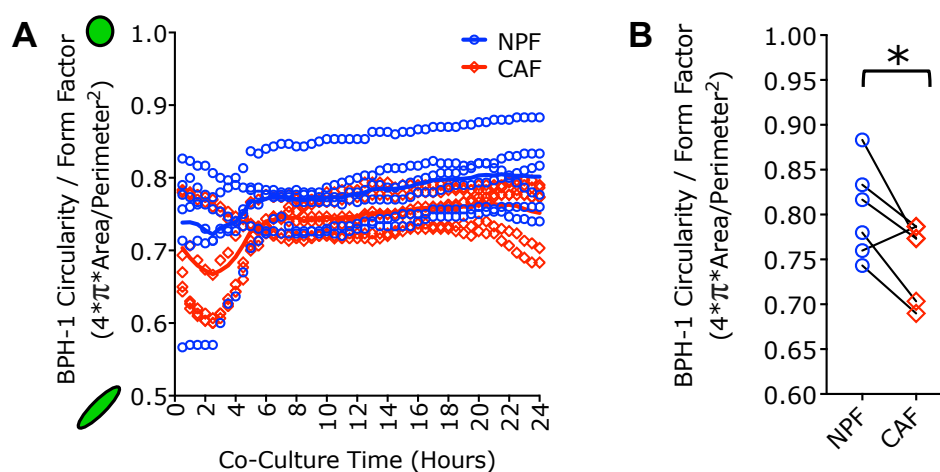


**Figure 41. Live cell imaging results support CAF-specific effects on BPH-1 circularity.**

The circularity of cell-tracker green stained BPH-1 cells was monitored during a 24-hour live cell time lapse imaging experiment. BPH-1 cell circularity was measured every 30min (**A**) and was consistently lower in co-culture assays with CAF (red circles) when compared to NPF (blue circles). Pairwise comparison of the BPH-1 form factor at the end of the live cell time lapse imaging experiment (after 24 hours) confirmed that the circularity of co-cultured BPH-1 cells is significantly lower on CAF *versus* patient-matched NPF (**B**; n=6). Significance tested with paired Students' T-Test.

#### 7.4) Live cell imaging results indicate that CAF increase directed BPH-1 movement

Time lapse imaging allows to quantify the BPH-1 travel path over the course of the co-culture experiment. BPH-1 cells displayed a reduced total motility, but a higher linearity of movement on CAF *versus* patient-matched NPF (Fig. 42). The total BPH-1 motility/cell was quantified every 30 minutes as the sum of cell movement divided by the present cell number. The BPH-1 linearity (directed BPH-1 cell movement) was calculated for each image as the actual cell displacement from the starting position divided by the total travel distance until that time point. The increased directed BPH-1 migration (BPH-1 linearity) on CAF *versus* NPF supports that CAF have a transformative influence on epithelial cells.

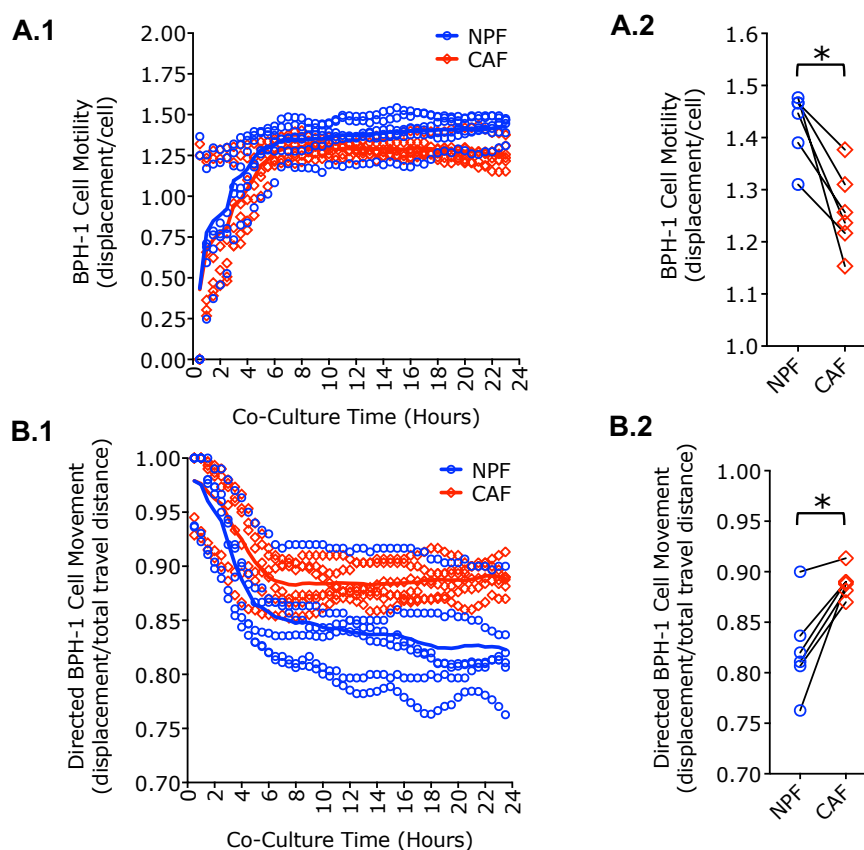


**Figure 42. CAF promote directed BPH-1 migration.**

Live cell imaging of the reference co-culture system with BPH-1 cells growing on CAF *versus* NPF showed that CAF decrease total motility of co-cultured BPH-1 cells (A), but increase their directed migration (B; n=6). Total BPH-1 motility was quantified every 30min (A.1). Quantification of the BPH-1 motility between the last two taken images confirmed that BPH-1 motility was consistently lower on CAF *versus* patient-matched NPF (A.2). The directed BPH-1 movement (BPH-1 linearity) was consistently higher on CAF *versus* patient-matched NPF (B.1). BPH-1 linearity was quantified considering the total displacement of BPH-1 cells from their starting position (after 24 hours) divided by the total BPH-1 travel distance during the (24 hours) experiment. BPH-1 linearity was significantly higher on CAF *versus* NPF (B.2). Significance tested with paired Students' T-Test.

### 7.5) Live cell imaging confirms macrophage-mediated BPH-1 form factor changes

Since our confocal imaging experiments could not reproduce published results from the co-culture reference system [38] (refer to results in **chapter 7.2**), our findings of macrophage-mediated BPH-1 form factor changes were also questionable. To confirm the macrophage-mediated BPH-1 changes, we followed BPH-1 cells in co-culture with M2-polarized macrophages during a 24-hour live cell time lapse imaging experiment.

Indeed, the macrophage-induced BPH-1 form factor changes manifested and remained stable during the whole course of time lapse imaging, suggesting that the previously observed macrophage-mediated BPH-1 form factor changes were not an artifact of the confocal imaging protocol. In our live cell time lapse imaging experiments, macrophage-mediated circularity increases were not limited to co-culture assays with NPF, but also observable with CAF (**Fig. 43**).

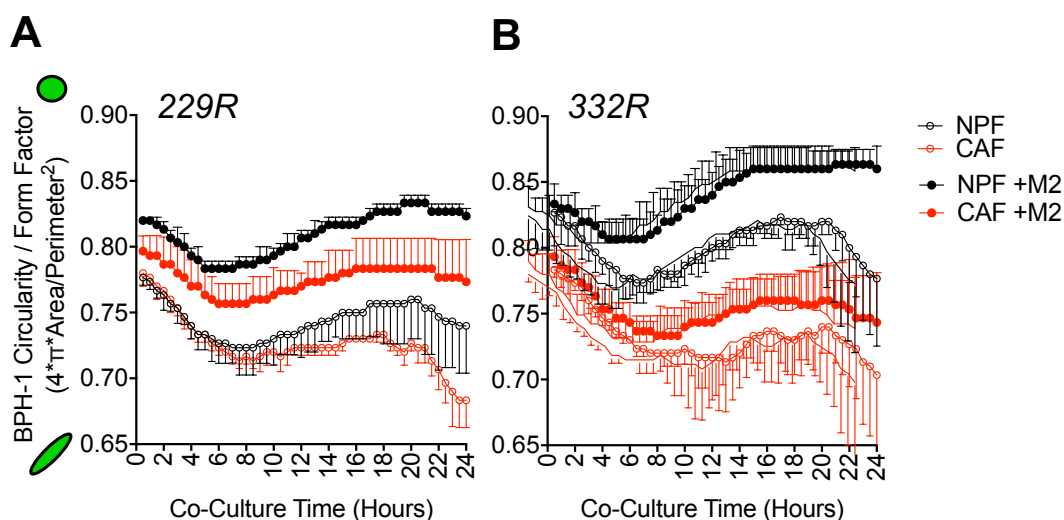


**Figure 43. Live cell imaging confirms that M2 macrophages increase BPH-1 circularity.**

The circularity of cell-tracker green stained BPH-1 cells was monitored during a 24-hour live cell time lapse imaging experiment. BPH-1 cell circularity was measured every 30min. Addition of M2 macrophages ( $30,000 \text{ cells/cm}^2$ ) to co-culture assays increased the circularity of BPH-1 cells growing on NPF, but also on CAF from two patients ( $n=4$ ; **A**: ID 229R and **B**: ID 332R). Error bars represent standard deviation of 3 technical replicates.

## 7.6) Macrophages do not affect the proliferation of co-cultured BPH-1 cells

Confocal imaging results revealed an increased BPH-1 number after 24 hours co-culture with macrophages, suggesting that macrophages might stimulate epithelial cell proliferation. However, time lapse live cell imaging showed that BPH-1 proliferation was not significantly changed in during co-culture with M2 macrophages. Relative increases of the BPH-1 cell count were even higher in the reference system when compared to assays with M2 macrophages (**Fig. 44; not significant**). Instead, the quantification of absolute BPH-1 cell numbers in co-culture revealed that assays with M2 macrophages already had elevated BPH-1 cell counts at the beginning of the time lapse imaging experiment. This could be due to an increased BPH-1 attachment to co-cultured macrophages or fibroblasts, or due to a user-bias when areas for fluorescence imaging were chosen.

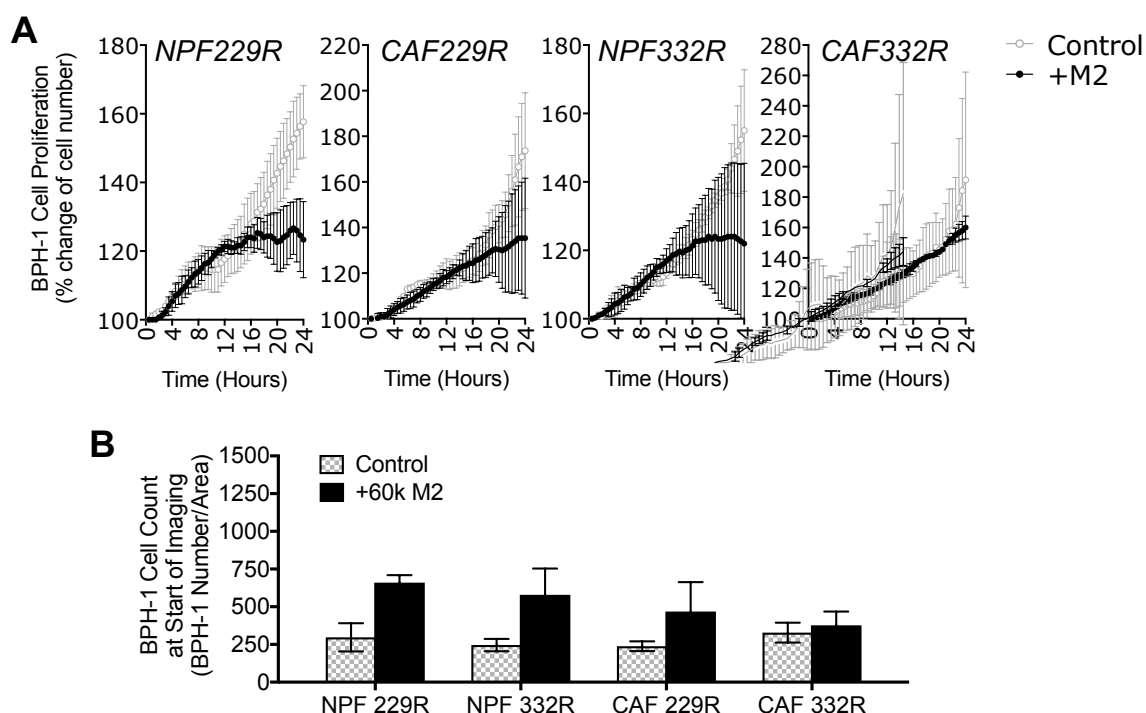


**Figure 44. M2 macrophages do not increase the proliferation of co-cultured BPH-1 cells.**

Live cell imaging allowed BPH-1 recognition every 30min over 24 hours, so BPH-1 proliferation in co-culture with M2 macrophages (30,000 cells/cm<sup>2</sup>) could be calculated as cell count changes over time, which was normalized to the cell number at the beginning of time lapse imaging (% of cell count at start). BPH-1 proliferation in co-culture with M2 macrophages was not higher than proliferation in the reference system, but tendentially lower (**A**). The BPH-1 cell count was already elevated at the beginning of the time lapse imaging experiment (**B**). Live cell imaging experiments with each NPF and CAF line were repeated once (n=1).

## 7.7) Macrophage-mediated BPH-1 circularity changes indicate elevated cell motility

The macrophage-mediated form factor changes of co-cultured BPH-1 cells indicate EMT, a transformation towards an invasive phenotype with decreased cell-adhesion and increased motility [131]. In order to determine whether macrophage-mediated BPH-1 form factor changes associate with an increased cell motility, we determined the total travel distance (displacement) of every individual BPH-1 cell during the 24-hour live cell imaging experiment. Then we grouped the BPH-1 cells by their average form factor during the imaging time (bin width: 0.1) and compared their total travel distance. Results showed that BPH-1 cells with an average form factor of 0.7-0.9 displayed the highest average cell displacement from their original position (**Fig. 45A**). Those BPH-1 cells with the longest travel distance (>30pixels) had the highest form factor value, approaching a completely circular shape (**Fig. 45B**). Curiously, the BPH-1 cell group with a circularity between 0.9-1.0 had a lower average displacement than cells with a circularity between 0.7-0.9 (**Fig. 45A**). We observed that dead cells completely lose contact with the ECM and also assume a highly circular cell shape, so this could explain the (skewed) bell-shaped distribution of the average BPH-1 displacement.

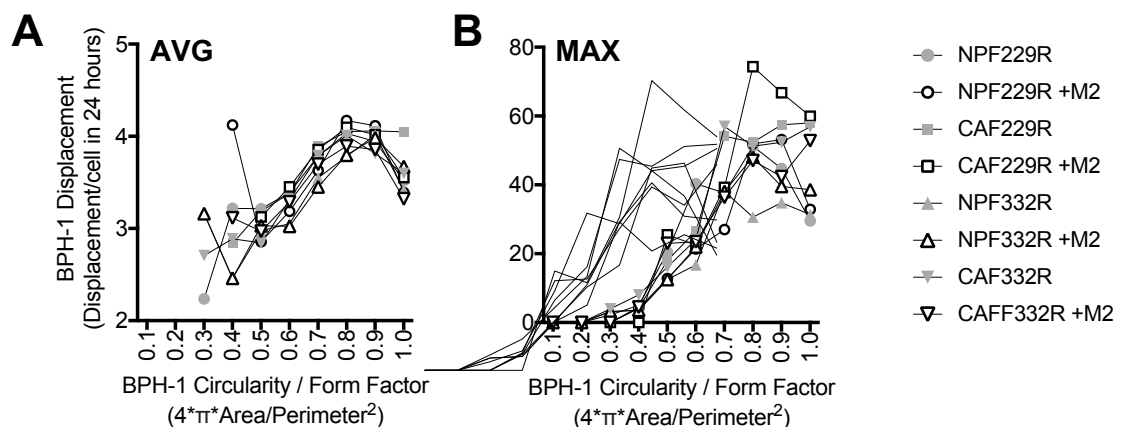


**Figure 45. Highly motile BPH-1 cells have a high average circularity.**

The overall BPH-1 displacement (directed travel distance) during co-culture has a positive relationship with BPH-1 circularity. The relationship of the average BPH-1 displacement (AVG) with their cell circularity follows a skewed bell-shaped distribution (**A**), with BPH-1 cells of high average circularity (*form factor 0.7-0.9*) moving further away from their starting position than elongated, spindle-shaped cells (*form factor 0.3-0.7*). In the case of NPF229R +M2 (**A**; open circle), only one captured cell had an average circularity between 0.3-0.4, so the average value is not adequately represented (outlier). Those BPH-1 cell groups with the highest circularity contain the cells with the highest total travel distance (**B**; MAX). These cells approach a circularity of 1. The data includes BPH-1 cells from reference assays (grey) and co-culture assays with 30,000 M2 macrophages/cm<sup>2</sup> (black).

The occurrence of BPH-1 cells with a maximum displacement of 40-80 pixels in our live cell imaging experiments posed the question whether the frequency of these highly motile cells increases when M2 macrophages are present. We grouped all captured (moving) BPH-1 cells by their total displacement (bin width: 2 pixels of cell displacement) and compared their frequencies in reference co-culture assays and assays containing M2 macrophages (**Fig. 46**).

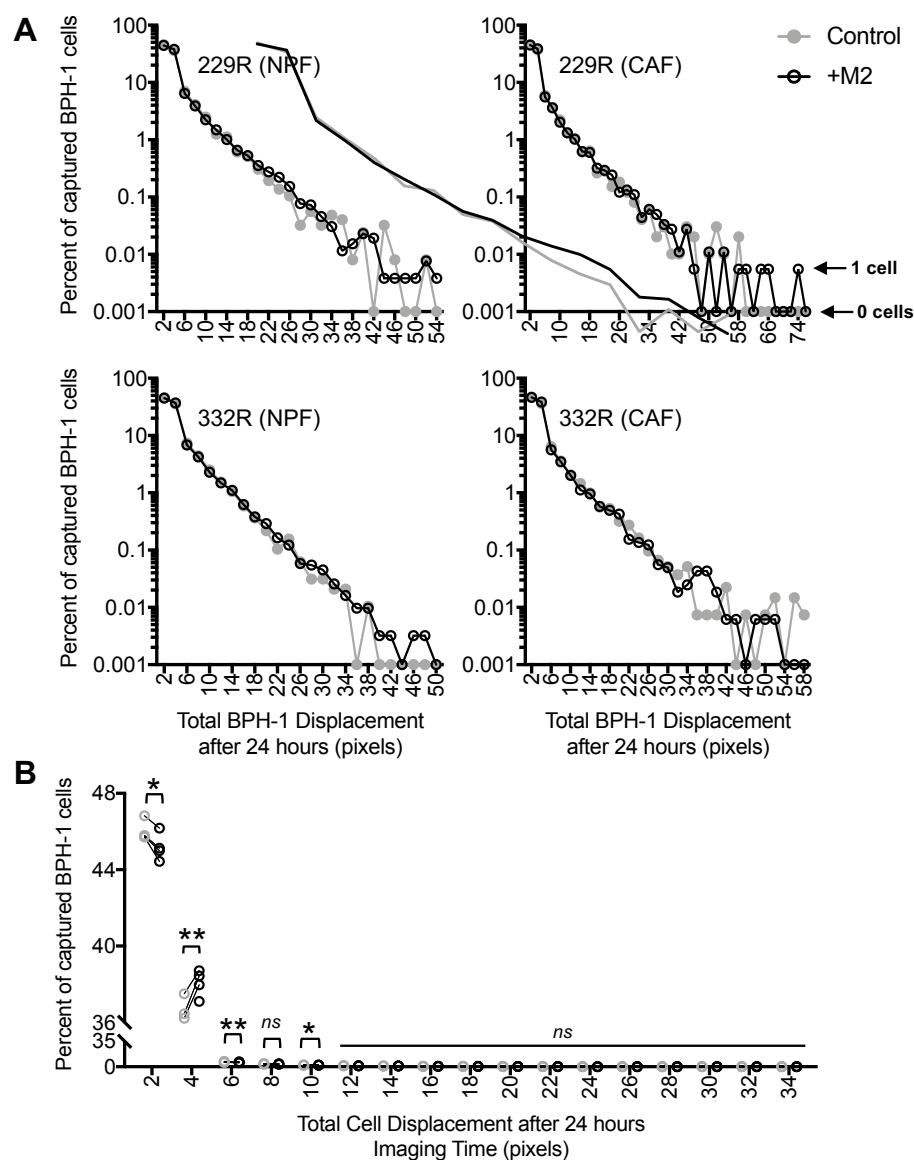


**Figure 46. M2 macrophages affect the frequencies of motile BPH-1 cells.**

Addition of M2 macrophages to co-culture assays with BPH-1 cells growing on of NPF/CAF affects the frequency of motile BPH-1 cells. Motile BPH-1 cells were grouped by their displacement (directed travel distance) from their original position at the end of the co-culture experiment. Addition of M2 macrophages (black circles) increased the frequency of BPH-1 cells with a high directed travel distance when compared to the reference system (**A**; grey circles). Co-culture experiments were repeated with four fibroblast lines (2xCAF, 2xNPF; n=4) from two patients (**A**; 229R and 332R). Pairwise comparison revealed that M2 macrophages decreased the frequency of BPH-1 cells with lower travel distance (**B**; 0-2pixels) and increased the frequency of BPH-1 cells with a higher travel distance (**B**; 2-4pixels). Significance calculated with the paired Students' T-Test.

The frequency of highly motile cells (displacement >34pixels) increased slightly in the presence of M2 macrophages (**Fig. 46A**). Highly motile cells merely comprised a very small fraction of the total captured BPH-1 cell pool. Since our co-culture assays with M2 macrophages contained a higher BPH-1 cell number than our reference assays (refer to **Fig. 44B**), it was difficult for us to calculate the significance of our findings. However, the most frequent BPH-1 populations had a motility between 0-2pixels/24h (46%) and 2-4pixels/24h (36%). After the addition of M2 macrophages to the co-culture assays, the frequencies of these prevailing BPH-1 cell populations changed. The fraction of BPH-1 cells with a lower motility (0-2pixels/24h) decreased from 46 to 45%, and the fraction of BPH-1 cells with a higher motility (2-4pixels/24h) increased from 36% to 38% (**Fig. 46B**).

### 7.8) M2 macrophages increase the BPH-1 motility more than M1 or M $\phi$

In a separate live cell time lapse imaging experiment, we compared the effects of different THP-1 derived macrophage subtypes (M $\phi$ , M1 and M2) on co-cultured BPH-1 cells. BPH-1 motility was measured as previously (**Fig. 47**). BPH-1 cells from assays with M2-polarized macrophages showed a higher motility than cells in co-culture with M1-polarized or unpolarized (M $\phi$ ) macrophages (**Fig. 47A**). Quantification of the total BPH-1 cell movement during the 24-hour co-culture experiment revealed a significantly higher motility in the presence of M2-polarized *versus* M1-polarized or unpolarized (M $\phi$ ) macrophages (**Fig. 47B**).

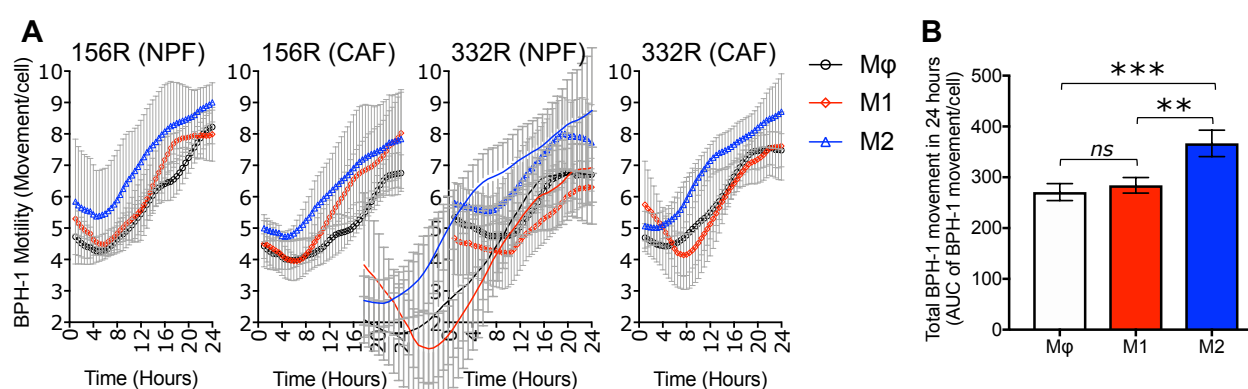


**Figure 47. M2 macrophages increased the BPH-1 motility more than M1 macrophages.**

The effect of unpolarized macrophages (M $\phi$ ) and M1- or M2-polarized macrophages on the BPH-1 motility was tested. BPH-1 cell motility in co-culture with M2 macrophages is consistently higher than in co-culture with M1 or unpolarized macrophages (**A**). The sum of BPH-1 movements/cell during the 24-hour imaging period (AUC: area under curve) was significantly higher in co-culture with M2 macrophages *versus* M1 macrophages or unpolarized (M $\phi$ ) macrophages (**B**; n=4; 2xNPF, 2xCAF; ID: 156R and 332R).

---

## 8) Summary of results

This work intended to study steroid sex hormones and inflammatory signaling in CP/CPPS and PCa with the following core aims:

- (1) Investigation of the mast cell response to estradiol stimulation
- (2) Analysis of clinical routine parameters from CP/CPPS patients
- (3) Isolation of somatic cells from human semen samples
- (4) Detection of leukocyte-specific transcripts in somatic cells from semen
- (5) Detection of CP/CPPS-related changes of steroid sex hormone signaling
- (6) Studies of the stromal influence on macrophage polarization
- (7) Investigation of macrophage interactions with the prostate tumor stroma

Experiments at Justus-Liebig-University (aims 1-5) and Monash-University (aims 6-7) provided corresponding results for each study aim. Results from *in vitro* experiments on the mast cell lines revealed that HMC-1 and LAD2 exhibit very different physiologies with a different epigenetic state of the two estrogen receptors ER $\alpha$  (gene *ESR1*) and ER $\beta$  (gene *ESR2*). The two cell lines responded differently to the stimulation with estradiol **(1)**. Analysis of the clinical routine parameters from patients and healthy volunteers revealed that CP/CPPS associates with impaired clinical routine parameters and elevated semen estradiol levels. High between-patient heterogeneity was observable, and stratification revealed a successive deterioration of clinical routine parameters with age **(2)**. A density gradient centrifugation protocol was successfully used for the isolation of somatic cells from semen **(3)**. Leukocyte-specific transcripts were detected in the isolated somatic cell population and were significantly affected in CP/CPPS patients **(4)**. Epigenetic profiling of blood leukocytes and ejaculated somatic cells revealed a transcriptional ER $\alpha$  downregulation in blood and semen from CP/CPPS patients that coincided with ER $\alpha$  gene promoter CpG hypermethylation in semen. The age-dependency of CP/CPPS-related clinical routine parameters led to a stratification of molecular profiling results by age (threshold 40 years).

Unlike younger patients (<40 years), the older patients (>40 years) showed a marked transcriptional downregulation of all three steroid sex hormone receptors (ER $\alpha$ , ER $\beta$  and AR) in the blood (5). At Monash-University, our conditioned media (CM) experiments demonstrated that primary patient-derived cancer-associated fibroblasts (CAF) and mast cells affect the phenotype of THP-1 derived macrophages (6). The outcomes from our co-culture experiments indicated that M2-macrophages disturb epithelial/stromal interactions and increase the motility of benign epithelial cells (7).

## Discussion

CP/CPPS and PCa are related diseases that both manifest with disturbances of the inflammatory gene regulation and steroid sex hormone signaling. In this study, we interrogated clinical liquid biopsies from CP/CPPS patients, primary prostate fibroblasts and immortalized cell lines. CP/CPPS patients displayed aberrant clinical routine parameters and increased semen estradiol levels. At the same time, our molecular profiling revealed an impaired estrogen signaling through ER $\alpha$  (gene *ESR1*) in the blood and semen from CP/CPPS patients. These findings were complemented by our mast cell lines, which showed that mast cells express estrogen receptors and respond to estradiol. The role of macrophages in the PCa stroma was studied with conditioned media experiments and co-culture experiments. Conditioned media experiments showed that mast cells and fibroblasts affect the macrophage response. Co-culture experiments revealed that macrophages disturb epithelial/stromal interactions and increase cell motility.

Our data led to the following observations:

### 1) Intra-prostatic acidosis might trigger inflammation in CP/CPPS

The semen from CP/CPPS patients showed significant acidification. Extracellular acidosis affects the inflammatory response of endothelial cells [132], fibroblasts [133], and leukocytes including neutrophils, granulocytes, macrophages and lymphocytes [134].

Hence, a reduced prostate pH has the potential to promote inflammatory dysregulation in CP/CPPS and PCa. A pH-reduction happens to suppress killer cell cytotoxicity in favor of tumor survival [135, 136] and alters the physiology of rat, rabbit and mouse macrophages [137-139], even though THP-1 derived human macrophages were not significantly affected by pH changes [138]. Extracellular acidification was described in chronic inflammatory diseases like rheumatoid arthritis [140] and atherosclerosis [141], and these diseases are associated with a dysregulated macrophage response. Fibroblasts and endothelial cells also respond to pH reduction with a pro-inflammatory response [132, 133], and a vital role of fibroblasts is denoted for the initiation and progression of PCa [25, 37, 118, 142, 143]. We observed a negative correlation of the semen pH and IL-8 levels, and that CP/CPPS patients with high SP IL-8 levels (>10,000pg/mL) exclusively had a semen pH below 8 (*not shown*). The inflammatory dysregulation in CP/CPPS could therefore be at least partly the result of prostatic acidification. Whether acidification is the root cause, or a subordinate effect of the inflammatory response, remains to be determined.

## 2) Zinc depletion in CP/CPPS could present a risk factor for PCa

The prostate has the highest zinc concentration of all organs in the body [144], and semen zinc is mainly derived from prostatic secretions. Previous studies found reduced zinc levels in ejaculates of CP/CPPS patients [145], but semen zinc levels from our CP/CPPS patients were not significantly different from the healthy study participants, probably due to the fact that only older (pre-vasectomy) controls were available as reference. Semen samples of our CP/CPPS patients however showed a significant reduction of total ejaculated zinc, indicating a diminished prostatic contribution to the ejaculate, which is also reflected in the reduced semen volume we observed. Ejaculate zinc levels correlate with activity of  $\alpha$ -glycosidase, a marker for epididymis function [146], so reduced prostate activity of CP/CPPS patients could help explain the impaired fertility parameters we previously described [96]. Apart from that, zinc also plays an important role for the immune system [147], and dietary zinc has the potential to alter steroid hormone turnover and modulate testosterone aromatization [148].

Since CP/CPPS, BPH and PCa are linked to an altered steroid sex hormone signaling, zinc abnormalities could be involved in the initiation and progression of these diseases. BPH and PCa tissues have significantly reduced zinc levels compared to normal prostate tissue [149], and cancers have abnormally low pH [134]. We found that semen pH-values negatively correlate with the levels of soluble zinc (*not shown*). The solubility of zinc increases with an increasing acidity, so a chronically acidified environment could be the reason for zinc depletion in CP/CPPS semen and PCa tissue. The potential of zinc deficiency to skew the inflammatory reaction is supported by experiments in pro-myeloid (HL-60) cells, which increase *IL-1B* and *TNF* production after zinc depletion [150]. Strikingly, systemic *IL-1B* and *TNF* levels were significantly elevated, and correlated positively with patient anxiety and depression scores in a large clinical study on CP/CPPS patients [69]. Nucleotide polymorphism studies suggest a role of *IL-1B* in PCa [151]. Zinc helped to alleviate CP/CPPS symptoms, with patients reporting significantly decreased NIH-CPSI scores in the follow-up observation after a 12-week zinc supplementation [152]. Consequently, an immunomodulatory role of zinc for CP/CPPS seems likely.

### 3) CP/CPPS patients display signs of macrophage activation in their semen

Ejaculates from CP/CPPS patients show elevated leukocyte counts, and our transcription profiling revealed that ejaculated SC from semen actively transcribe express genes that are characteristic for leukocytes (e.g. *CCL18*, *CD68*, *CMA1*, *IL-7* and *PU.1*). CP/CPPS associates with a changed expression of some of these genes, so ejaculated SC may serve as a novel source of information about the inflammatory state in the prostate of CP/CPPS and PCa patients. We pyrosequenced ejaculated SC and observed an increased *BMP7* gene promoter CpG methylation in CP/CPPS patients, but the difference from healthy volunteers was below significance ( $p=0.09$ ) and we had no complementary *BMP7* gene expression data. Ejaculated SC from CP/CPPS patients showed increased expression levels of the macrophage-specific transcripts *CD68* ( $p=0.15$ ) and *CCL18* ( $p=0.02$ ), and a simultaneous downregulation of the transcription factor *PU.1*.

Being a cell-fate determinant of myeloid and lymphoid lineage cells [153, 154], *PU.1* is mainly expressed by macrophages, and at several magnitudes lower concentrations, also by B cells [155]. It plays a crucial role for induction and maintenance of the macrophage phenotype by global control of genomic regulatory sites and cooperates with different transcription factors to direct macrophage polarization [156], so *PU.1* transcript levels reflect the presence of macrophages rather than their polarization. However, *PU.1* reduction was shown to suppress anti-inflammatory (Th2) cytokine (IL-5/IL-13) expression in dendritic cells [157], indicating that *PU.1* downregulation might shift immunity towards the pro-inflammatory response in CP/CPPS patients. Another reason for diminished *PU.1* transcript levels could be that macrophages constitute a smaller fraction of ejaculated SC from CP/CPPS patients. This could be due to an increased infiltration with other leukocytes that do not express *PU.1*, such as T cells.

In contrast to that, elevated transcript levels of the macrophage activation markers *CD68* ( $p=0.15$ ) and *CCL18* in ejaculated SC from CP/CPPS patients suggests that the present macrophages display a stronger activation. A variety of pathological processes involve *CCL18* upregulation [158], ranging from chronic inflammatory diseases like arthritis [159], allergic dermatitis [160] and allergic asthma [161] to cancers of the pancreas [162], breast [163, 164] or prostate [165, 166]. This underlines that an inadequate macrophage activation is not only associated with cancer, but chronic inflammatory diseases in general. *CCL18* is secreted by macrophages as a response to immunoregulatory (Th2) cytokines [167], and *CCL18* itself facilitates macrophage M2-polarization [168]. A major role of *CCL18* is constituted by its function as lymphocyte chemoattractant, as it has been demonstrated to guide memory T cells to the skin in atopic dermatitis [169] or (CD4+) T cells to breast cancer tissue [163]. It attracts naïve T-cells [163, 170] rather than cells with myeloid origin, like granulocytes (RefSeq, Sep 2014) or monocytes [171]. Accordingly, we assume that *CCL18* guides infiltrating T cells to the prostate from CP/CPPS patients, which probably mediate autoimmunity of the disease.

An increased T cell infiltration could also explain why the *PU.1* transcript is simultaneously downregulated in the ejaculated SC from CP/CPPS patients.

The idea of an increased T cell infiltration in ejaculated SC from CP/CPPS patients is supported by other studies of CP/CPPS. Prostate antigen immunization promotes infiltration (CD4+) T cells and macrophages in an experimental autoimmune prostatitis (EAP) mouse model [12], and circulating (CD4+) T cells from CP/CPPS patients had an increased reactivity to prostatic alkaline phosphatase and PSA [172].

#### 4) Mast cell lines allow mechanistic studies of estrogen signaling

In order to gain mechanistic insights about the influence of E2-signaling for the inflammatory response, we stimulated the two human mast cell lines HMC-1 and LAD2 with a high concentration of estradiol (100nM). These cell lines are extensively characterized and represent the gold-standard for *in vitro* studies of the mast cell function. A study compared both cell lines with mature skin mast cells (sMC) and reported that LAD2 cells are intermediately differentiated, while HMC-1 cells are very immature, malignantly transformed mast cells [99]. HMC-1 and LAD2 cells also vary considerably in cell properties and culture conditions. LAD2 cells, phenotypically resembling more mature mast cells, grow much slower and are more difficult to culture compared to HMC-1 cells, which are immature and more progenitor-like.

Possessing different expression of the ER (ER $\alpha$  and ER $\beta$ ), they responded very differently to E2-treatment. Untreated HMC-1 cells possessed epigenetically silenced *ESR1* (ER $\alpha$ ) and *ESR2* (ER $\beta$ ). In contrast, *ESR1* and *ESR2* were both actively expressed and had unmethylated promoters in untreated LAD2 cells. At the same time, both cell lines differed remarkably in their basal inflammatory gene expression profile. An elevated basal inflammatory gene expression in HMC-1 cells coincided with downregulated *ESR1* and *ESR2*, suggesting that epigenetic ER silencing is reflective of a pro-inflammatory state. E2-treatment of LAD2 cells mainly led to upregulation of measured immune factors, whereas HMC-1 cells reacted with the downregulation of most inflammatory genes.

Using the Methylation Profiler array, we discovered that E2-treatment led to *de novo* methylation of promotor CpG sites from inflammatory genes in HMC-1 cells, but findings could not be validated by pyrosequencing.

The different outcomes of the two methods (Methylation Profiler Array *versus* Pyrosequencing) might be rooted in methodological differences between the two methods. While pyrosequencing relies on bisulfite conversion of the CpG site, the array makes direct use of CpG methylation-sensitive restriction enzymes. It appears possible that the used restriction enzymes are not only sensitive to 5-mC, but also to 5-hmC. Moreover, the DNA amplification step before Pyrosequencing is prone to contamination with unmethylated DNA (e.g. PCR products from previous PCR), or the PCR might favor unmethylated DNA templates.

The observation that HMC-1 and LAD2 respond so differently to E2 suggests that estrogenic effects are not exclusively pro- or anti-inflammatory but depend on a variety of factors, such as the leukocyte differentiation state, the presence of ER and co-stimulatory factors, or environmental factors like the extracellular pH. HMC-1 and LAD2 cells represent alternative leukocyte differentiation states and present useful model systems for the study of physiological *versus* pathological conditions like CP/CPPS and PCa. The differentiation state of circulating WBC is very different from the leukocyte differentiation state in tissues like the prostate, which we isolated as ejaculated SC from semen by density gradient centrifugation (DGC). We assume that the progenitor-like HMC-1 cells rather represent the (undifferentiated) circulating WBC that we isolated from human peripheral blood, and that the differentiated LAD2 cells rather represent the differentiated leukocytes (e.g. mast cells) that we isolated from human semen.

However, the results from estradiol-stimulated and control mast cell cultures have a very limited informative value because experiments have only been performed once (n=1). The conclusions we made therefore have to be regarded with caution.

## 5) Decline of ER $\alpha$ signaling presents a potential CP/CPPS pathomechanism

We recognized reduced blood E2 levels ( $p=0.1032$ ) and elevated semen E2 levels in CP/CPPS patients, confirming that CP/CPPS associates with alterations of the steroid sex hormones. Furthermore, we traced systemic and local downregulation of the ER $\alpha$  (*ESR1*) transcript in circulating WBC (systemic) and ejaculated SC (organ-confined) from CP/CPPS patients. Supporting epigenetic ER downregulation by promotor CpG methylation, the ejaculated SC from CP/CPPS patients showed promotor CpG hypermethylation of both ER (*ESR1*, *ESR2*) and the *AR*. Complementary experiments from our group on 5-aza-2'-deoxycytidine (AZA) treated PCa cell lines (PC-3, DU-145, LNCaP) provided evidence that the analyzed promotor CpG sites control the gene transcription of *ESR1* and *ESR2* [97].

The significant positive correlation of systemic (isolated circulating WBC) and organ-confined (isolated SC from semen) *ESR1* transcript levels suggests that *ESR1* downregulation in CP/CPPS patients is a global (systemic) phenomenon that also manifests in prostate-infiltrating leukocytes. Together with our previous results on *CXCR4* in ejaculate from CP/CPPS patients [96], these novel findings on the *ESR1* support the notion that semen is a suitable source for the development of diagnostic biomarkers for CP/CPPS. Apart from that, our findings have ramifications for the understanding of the CP/CPPS pathogenesis and might contribute to the development of future treatment options.

Systemic and local ER $\alpha$  (*ESR1*) downregulation has the potential to prime the immune cells of CP/CPPS patients for an immoderate pro-inflammatory response. Our studies of the mast cell lines HMC-1 and LAD2 suggested that ER $\alpha$ /ER $\beta$  (*ESR1*/*ESR2*) downregulation is coupled with a higher basal expression of pro-inflammatory cytokines and chemokines. Similar to the cell isolates from CP/CPPS patients, HMC-1 cells possessed an epigenetically inactivated ER $\alpha$  (*ESR1*). At the same time, they exhibited high expression levels of several interleukins (*IL1B*, *IL7*, *IL-12A*, *IL22*, *IL24*), chemokines (*CCL1*, *CCL3*, *CCL18*) and pro-inflammatory mediators such as *CSF1*, *TNF* or *TNFSF11* (*RANKL*). E2-stimulation of HMC-1 cells led to downregulation several interleukins and chemokines, suggesting potential anti-inflammatory E2-effects on leukocytes with epigenetically downregulated ER $\alpha$ /ER $\beta$ . This could explain why treatment with the ER ligand quercetin helps alleviate symptoms in CP/CPPS patients [31].

The idea that impaired ER $\alpha$  signaling promotes inflammation in CP/PPS patients is backed up ample evidence from studies that postulate anti-inflammatory E2-effects, including epidemiological data about other chronic inflammatory diseases. Even though women have a much higher prevalence for the development of autoimmune disease than men [173], the peak disease onset happens after cessation of the ovarian estrogen production. Women before menopause on the other hand have a lower propensity for chronic inflammatory (not autoimmune) diseases than men [174]. Rheumatoid arthritis (RA) for instance typically develops in women after menopause, and estrogen replacement therapy prove beneficial in these women [175]. E2-supplementation of postmenopausal women also restores an impaired toll like receptor 7 (TLR7)-mediated response through ER $\alpha$  signaling [176].

A lot of valuable insight regarding the role of estrogens for chronic inflammatory diseases was gathered during the studies of multiple sclerosis (MS) and its animal model, the experimental autoimmune encephalomyelitis (EAE) mouse [177]. It is well established that immunosuppressive effects of E2 counteract chronic inflammation in MS, and estrogen treatment rendered promising for MS-treatment [178]. Pregnancy, and the concurrent rise of systemic estrogen levels suppresses the onset of MS and EAE by protective ER $\alpha$  (*ESR1*) signaling [179]. While low physiological E2-levels support the (pathological) pro-inflammatory Th1/Th17 response, high physiological E2-levels during pregnancy prevent the onset of MS by shifting the inflammatory response towards the immunoregulatory (Th2/Treg) side [177, 180]. *ESR1* is expressed in circulating peripheral macrophage and dendritic cell precursors (MDPs) and plays a critical role in the maturation of dendritic cells (DC) [181], which mediate adaptive immunity by antigen-presentation to T cells. Extensive animal research in the EAE mouse model could clarify that the protective, immunosuppressive E2-properties are primarily provided by DC (e.g. M2 macrophages), and that T cells are downstream in the immunomodulatory cascade [182, 183]. Since a role of T cells is also documented for CP/PPS [172], it seems likely that impaired ER $\alpha$  signaling in CP/PPS also predetermines an aberrant signaling from DC towards T cells. *In vitro* experiments confirm that E2 signaling through ER $\alpha$  has anti-inflammatory effects on human DC/macrophages [184], with ER $\alpha$  accelerating the resolution of the pro-inflammatory macrophage response in an IL-10 dependent manner [185].

In DC, ER $\alpha$  signaling sustains and potentiates *GM-CSF* mediated *IRF4* upregulation [186, 187], with *IRF4* being a transcription factor of the immunoregulatory (M2-like) commitment [156].

Impaired estrogen signaling through ER $\alpha$ /ER $\beta$  also provides a satisfying explanation for the development of chronic pain in CP/CPPS. In a rat model of visceral pain, systemic E2-administration led to ER $\beta$ -mediated piecemeal degranulation in intestinal mucosal mast cells, and this response mediated anti-nociceptive effects [188]. Conversely, impaired E2 signaling might enhance nociception in CP/CPPS patients.

Altogether, overwhelming evidence from epidemiological studies and basic research suggests that estrogens, ERs and particularly ER $\alpha$  (*ESR1*) serve the resolution of the inflammatory response and play a beneficial role in chronic inflammatory diseases. Our findings that CP/CPPS associates with systemic and local downregulation of ER $\alpha$  (*ESR1*) therefore presents evidence that impaired signaling through the E2-ER $\alpha$  axis could present a root cause for CP/CPPS development. Low systemic testosterone associates with CP/CPPS symptoms [189], and our results show a significant correlation of systemic testosterone with systemic and organ-confined E2 levels, which is probably the result of ARO turnover. Treatment of testosterone deficiency might therefore also help to restore healthy estrogen signaling in CP/CPPS patients.

Our current data also support the growing body of evidence implicating chronic prostatitis in the development of prostate malignancy. Elevated E2-levels and altered expression of the ER, particularly an altered ER $\alpha$ :ER $\beta$  ratio are associated with PCa. Previous reports proposed that *ESR1* and *ESR2* could have a tumor suppressor role in the prostate gland. For example, the loss of ER $\alpha$  (*ESR1*) transcript and protein by promoter methylation increased with progression of prostatic disease from BPH to low grade and to high grade cancer [190-192]. Most reports on ER $\beta$  (*ESR2*) expression concur, that levels decline in localized PIN through low to high grade Gleason scores [193-196]. The loss of ER $\beta$  expression in organ confined prostate cancer has been shown to be epigenetically regulated by progressive hypermethylation of the *ESR2* promoter [192, 197].

## 6) Prostatic estradiol might promote prostate cancer initiation in CP/CPPS

Our results demonstrate that excess semen E2 levels are characteristic of patients with CP/CPPS, and that semen E2 significantly correlates with perceived urinary tract symptoms. As a marker for local inflammation, semen IL-8 levels are routinely measured in CP/CPPS patients, and increase with age among CP/CPPS patients, but not healthy volunteers. This indicates that the CP/CPPS severity deteriorates with age, and that IL-8 is a suitable marker for the monitoring of disease progression.

Only 2% of healthy volunteers (1/58), but 20% of CP/CPPS patients (11/54) had semen IL-8 concentrations above 10,000pg/mL, rendering this concentration a good cutoff-value for the detection of pathological inflammatory processes in semen. Since the most strongly upregulated cytokine in the E2-treated mast cell line LAD2 was IL-8, we reasoned that excessive semen E2 levels could also affect semen IL-8 levels in CP/CPPS patients. CP/CPPS significantly deteriorates in ageing patients >40 years, which have significantly elevated IPSS scores and semen IL-8 levels. However, this older patient cohort (>40 years) did not show significantly elevated semen E2 levels. Accordingly, there was no correlation of semen E2 and IL-8 levels observable.

Elevated semen E2 levels might be the result of ARO upregulation within the reproductive tissues of CP/CPPS patients. Several ARO gene promotor sites respond to inflammatory mediators (e.g. TNF, IFN $\gamma$ , IL-1, IL-6, cAMP, PGE2) [198], and cytokines (IL-1/IL-6) stimulate ARO activity in breast CAF [199]. ARO is also overexpressed in PCa cells [200] *via* the IL-6 responsive promotor region I.4 [201]. Since elevated prostatic E2 levels recruit and activate mast cells [14], which in turn release inflammatory mediators with the capacity for ARO upregulation [198], it is postulated that this perpetuates a vicious cycle of local estrogen production and inflammation that eventually drives PCa initiation and progression [25]. CP/CPPS presents a risk factor for PCa development [2], and our detection of excess semen E2 levels suggests that the same feedback loop is already established in some CP/CPPS patients. However, we detected a significant correlation of blood and semen E2 levels in the CP/CPPS patient cohort, so it is not clear whether semen E2 increases are a result of ARO activity or systemic E2.

A large body of evidence from the literature and our own findings of CP/CPPS-specific *ESR1* downregulation point in the direction of protective (anti-inflammatory) E2-signaling (refer to discussion **chapter 5**), so it has to be questioned how excess semen E2 relates to the chronic inflammatory processes in CP/CPPS patients. Excess E2 production might constitute a secondary anti-inflammatory (Th2/M2) response with the purpose to resolve the chronic pro-inflammatory reaction in the prostate tissue of CP/CPPS patients.

This idea is also supported by our finding that E2 stimulates expression of the M2-specific marker gene *CCL18*. Since we detected *CCL18* upregulation in ejaculated SC from CP/CPPS patients, we made complementary *in vitro* experiments to probe whether this could be a result of excess prostatic E2 concentrations. *CCL18* is a macrophage origin chemokine, so we stimulated THP-1 derived M2 macrophages with 100nM estradiol (E2) and observed a *CCL18* upregulation on transcriptional and protein level. At the same time, we detected increased ER $\alpha$  binding to an estrogen-responsive element (ERE) of the *CCL18* promotor. Even though *CCL18* is a chemokine of the anti-inflammatory (pro-resolving) phase of the inflammatory response, it is dysregulated in many inflammatory diseases including PCa [158, 165, 166]. Since *CCL18* is a key leukocyte attractant, excess prostatic E2 levels might be indirectly responsible for chronification of CP/CPPS by promoting excess leukocyte recruitment to the prostate tissue. However, other experiments support a pro-inflammatory role of E2 as well. E2-treatment induced ER $\alpha$ -dependent *TNF/IL-1B* upregulation in the mouse model [202]. More research is needed to explain the complicated relationship of estrogen signaling and the inflammatory response.

Together with elevated semen E2 levels, we discovered that CP/CPPS associates with gene promotor CpG hypermethylation of *ESR1/ESR2/AR* in ejaculates SC. The capability of estrogen as a ligand to downregulate ER $\alpha$  is well established [203, 204]. In the breast cancer MCF-7 cell line it has also been shown that the phytoestrogens quercetin and genistein share this capability [32], which makes the use of quercetin in treatment of CP/CPPS questionable, or at least emphasizes the need for an individualized therapy with an involvement of molecular analyses prior to treatment. Similarly, a regulation of ER $\beta$  by estrogens occurs, but this can differ between tissue types.

A study investigating the effect of estrogen on its receptors found estradiol-mediated ER $\beta$  down-regulation in MCF-7 cells, but up-regulation in human aortic smooth muscle cells [205]. These studies and our findings suggest that *ESR1* and *ESR2* hypermethylation in ejaculated SC from CP/CPSP patients might be the result of excess local E2 levels.

### **7) Ageing CP/CPSP patients experience a sex hormone decline**

CP/CPSP is a disease of all ages. An international study including 1,563 CP/CPSP patients reported an average patient age of 47.2 $\pm$ 15.7 years ( $\pm$ SD) [206]. In our study, the included patients were somewhat younger, but generally matched other published cohorts. Age-dependent changes of testosterone levels [207] and other disease-relevant parameters represent a possible confounding factor in a study with a wide age range as ours. Older men with declined testosterone levels have increased systemic CRP levels, suggesting that age-dependent testosterone decline promotes systemic inflammation [123]. We addressed this fact by comparing CP/CPSP patients with an age matched healthy control population. A main obstacle for the understanding of CP/CPSP is its unknown aetiology, with patients presenting very heterogenous and often ambiguous symptoms. Multiple disease mechanisms might lead the diagnosis CP/CPSP, and the pathogenesis is subjected to changes over time. We reasoned that patient stratification by age will help identify possible confounding CP/CPSP progression states or sub-pathologies. Because the semen concentrations of IL-8 showed a positive correlation with patient age and were almost exclusively elevated (>10,000pg/mL) in patients >40 years, we stratified our cohort into younger patients ( $\leq$ 40 years) and older patients (>40 years).

Older patients showed an age-dependent systemic decline of testosterone levels, but not systemic E2 levels, and this manifested as decreased systemic T/E2 ratio in these patients. Moreover, the stratification by age revealed that older CP/CPSP patients showed stronger aberrations of ER $\alpha$ , ER $\beta$  (*ESR1*, *ESR2*) and the *AR* when compared to younger patients. Although ER $\alpha$  (*ESR1*) downregulation happened in ejaculated SC happened from CP/CPSP patients of both age groups, it was more pronounced in older patients.

At the same time, only the older patients (>40 years) showed systemic transcriptional downregulation of ER $\alpha$ , ER $\beta$  (*ESR1*, *ESR2*) and the AR in the circulating WBC that we isolated from peripheral blood. Transcriptional systemic downregulation of *ESR1*, *ESR2* and *AR* was completely absent in the younger patient cohort. At the same time, only older patients showed a significant gene promoter CpG hypermethylation of *ESR1* and *AR* in ejaculated SC from semen.

In summary, our findings from the patient stratification by age indicate that older CP/CPSP patients have a more advanced disease, which is also represented by elevated clinical inflammation markers and a higher IPSS. A deeper understanding of the distinctive pathologies in younger and older CP/CPSP patients might help to understand disease progression, identify patients with the risk for PCa initiation and develop tailored treatment strategies.

The simultaneous systemic reduction of testosterone, E2 and their receptors ER $\alpha$ , ER $\beta$  and AR in ageing CP/CPSP patients (>40 years) indicates that the systemic expression of the sex hormone receptors mirrors the presence of their ligands testosterone and E2. Other recent studies support this assumption. The human circulating leukocyte population mainly consists of neutrophils (40-60%), followed by lymphocytes (20-40%) and monocytes (2-8%), with only a small fraction comprised of eosinophils (1-4%), basophils (0.5-1%) or band cells (0-3%) [208, 209]. Circulating neutrophils therefore represent the majority of isolated circulating leukocytes from our study. Circulating neutrophils from both sexes express ER $\alpha$  and ER $\beta$ , but ER expression in women is increased during the ovulatory phase when systemic E2-levels are elevated [210]. E2-stimulation of isolated circulating neutrophils from female donors promotes ER $\alpha$ /ER $\beta$  upregulation, and ER $\alpha$  upregulation in the case of male donors [210]. This supports that ER $\alpha$ /ER $\beta$  expression of circulating WBC follows the (systemic) presence of their ligand E2, and that CP/CPSP patients downregulate systemic ER $\alpha$ /ER $\beta$  expression in response to reduced systemic E2 levels. There is also evidence supporting that expression of the *AR* follows its ligand testosterone, and consequently that the CP/CPSP-related testosterone decline leads to concurrent *AR* downregulation. Men produce around ~20 times more testosterone than women [211] and ~7-8 times higher circulating testosterone levels [212].

Circulating leukocytes from men in general [213], as well as macrophages in particular [214], express significantly more *AR* when compared to those from women. Female donor leukocytes upregulate the *AR* when suddenly exposed to the elevated testosterone levels of their male bone-marrow transplant (BMT) recipients [213]. However, the picture seems to be more complicated, since *AR* expression of circulating leukocytes increases in men undergoing chemical castration [213]. These conflicting results might be explained with the pharmacological mechanism of antiandrogens.

In summary, the age-stratification of CP/CPPS patients revealed that exclusively older patients (>40 years) suffer from a systemic decline of sex hormone signaling. This could implicate an increased susceptibility of older men for chronic inflammatory diseases, similar to the susceptibility of post-menopausal women to RA [175]. Organ-confined CP/CPPS-related changes were more pronounced in the older CP/CPPS cohort, probably because these patients have a longer history of chronic inflammation that allowed the establishment of measurable epigenetic aberrations. These changes might be indicative for CP/CPPS severity and the risk of PCa initiation. Since expression of the sex hormone receptors mirrors the presence of their ligands, it appears likely that ER $\alpha$  downregulation in CP/CPPS is the result of a sex hormone (T and/or E2) decline.

### **8) The role of E2 signaling for inflammation is contextual**

The results from our study suggest that the influence of estrogen on the inflammatory response is highly contextual and depends the leukocyte differentiation state, the presence of ER, and co-stimulatory molecules in the microenvironment. Our discoveries that ER $\alpha$  is downregulated in CP/CPPS patients, and that mast cells with low ER $\alpha$  levels (HMC-1) respond to E2-stimulation with inflammatory gene suppression, suggests that impaired ER $\alpha$  signaling might lead to CP/CPPS. This is supported by findings about other chronic inflammatory diseases like RA and MS (refer to discussion **chapter 5**).

In contrast to that, we discovered elevated E2 levels in the semen from CP/CPPS patients and demonstrated that LAD2 cells respond to E2-stimulation with the upregulation of inflammatory genes.

The seeming contradictory immunosuppressive and pro-inflammatory roles of E2 might be resolved by the fact that circulating and organ-confined leukocytes populate very different “niches” of the body and have very different differentiation states. A recently proposed “signal strength model” [215] postulates that the lineage commitment potential of leukocyte progenitor cells is determined by a combination of the cellular cytokine receptor profile, instructive signals from the specific local microenvironment (“niche”), and downstream regulatory pathways [216].

This model is supported by experiments that stress the complex role of E2-signaling for the differentiation of dendritic cells (DC) from hematopoietic progenitor cells. Differentiation of DC from hematopoietic progenitors can be triggered by systemic stressors through rising Flt3L levels, or locally through GM-CSF amongst other factors [215]. While physiological E2 concentrations led to a Langerhans-like phenotype of DC that were differentiated with GM-CSF, the same E2-treatment led to a different DC physiology with marked reduction of viable cells when DC were differentiated with Flt3L instead [217]. Pregnant or E2-treated mice have reduced numbers of hematopoietic progenitor populations [215, 218]. Conversely, reduced systemic E2-levels may increase the maturation of DC progenitor cells and thereby promote chronic inflammation in CP/CPPS patients. Increased circulating WBC counts in men with low testosterone (and likely also E2) levels support this idea.

Current works in the field and our own results strongly suggest that E2-signaling has very different effects on circulating leukocyte progenitor populations and differentiated leukocytes, as they occur in the prostate tissue. Our findings underline the complexity of E2-signaling, and why the role of E2 for inflammation is still controversial.

### 9) The CAF-induced interleukins *IL1B* and *IL-10* are associated with PCa

For a variety of cancers, CAF were demonstrated to adversely influence the phenotype of tumor-associated macrophages (TAM). Pancreatic CAF for instance were shown to polarize macrophages in dependency of M-CSF and ROS production towards M2 [219]. Breast CAF on the other hand are capable for macrophage recruitment and M2 polarization *via* Chi3L1 [220].

We educated THP-1 derived macrophages with conditioned media samples (CM) from primary prostate CAF and NPF to find that they upregulate macrophage mRNA levels of the interleukins *IL-1B* and *IL-10*. Simultaneously, comparison with patient-matched NPF revealed CAF-specific suppression of macrophage *CD206* expression. Importantly, the magnitude of CAF-mediated gene expression changes of *CD206*, *IL-1B* and *IL-10* was similar to the gene regulations after treatment with LPS/IFN $\gamma$  or IL-4/IL-13.

The genes *IL-1B* (M1-specific) and *IL-10* (M2-specific) are regarded as specific markers for opposing macrophage polarizations. M1-specific (LPS/IFN $\gamma$ ) and M2-specific (IL-4/IL-13) treatments however led to a significant upregulation of both marker genes, and the magnitude of (M2-specific) *IL-10* induction was not significantly different between the treatments. This could be the result of the long stimulation time (48 hours) of our polarization protocol. It is known that *in vitro* activated macrophages quickly adapt to LPS-stimulation with a compensatory secondary response, which is commonly referred to as endotoxin tolerance [156]. During this process, activated macrophages downregulate LPS-induced (M1-characteristic) genes, but retain expression of M2-characteristic genes like *IL-10*.

Similar to the artificial stimuli, macrophage-education with CAF CM also induced M1- (*IL-1B*) and M2-specific (*IL-10*) marker genes at the same time. It is therefore difficult to judge whether the CAF from our experiments polarized the macrophages towards M1 or M2. However, when comparing the effects of CM and artificial stimuli, the CAF-mediated macrophage gene regulation (upregulation of *IL-1B* and *IL-10*, downregulation of *CD206*) closely resembles the gene expression profile after (M1-polarizing) LPS/IFN $\gamma$  challenge. It is known prostate CAF downregulate the *AR* [25, 221].

Experimental *AR* silencing in CAF upregulates expression of *M-CSF* and *IFN $\gamma$*  in a murine PCa model, and PCa tissue *IFN $\gamma$*  levels correlate with tumor grade [221]. CAF-released *IFN $\gamma$*  could therefore explain CAF-specific macrophage *CD206* downregulation. Our finding that CAF downregulate *CD206* expression of educated macrophages are difficult to explain when considering that PCa tumor tissue contains significantly elevated *CD206*-positive macrophage counts [222]. The TME involves many factors, cell types and exhibits physical properties (like pH, hypoxia, glycolysis products etc.) that might not be adequately represented with our CM experiments.

Nevertheless, CAF CM led to a significant upregulation of macrophage *IL-1B* and *IL-10* expression, and current evidence supports a role of these interleukins for PCa progression. *IL-10* itself is an important mediator of the Th2 (M2) response [223], so the CAF-mediated *IL-10* upregulation in macrophages could mean a CAF-promoted shift towards immunosuppressive immunity.

Polymorphisms of *IL-1B* and *IL-10* were associated with the risk for PCa development [151, 224]. High *IL-1B* levels in prostate tissue increase the chance of biochemical PCa recurrence [225], and functional studies suggest that *IL-1B* promotes skeletal PCa metastasis and neuroendocrine features [226]. Our discovery of CAF-mediated *IL-10* upregulation in macrophages concurs with a very similar study to ours that describes significantly elevated *IL-10* release of LPS-stimulated human macrophages when these have previously been educated with prostate CAF CM [142]. Interestingly, patient-matched NPF were included in the mentioned study to validate primary CAF, but the effect of NPF CM on the macrophage phenotype was not elucidated [142]. Probably, similar to our study, the NPF- and CAF-mediated effects did not significantly differ from each other. Other researchers compared the effect of prostate CAF on macrophages with those from benign-associated fibroblasts (BAF; also referred to as human prostate fibroblasts: HPF) instead of patient-matched NPF. BAF are derived from BPH tissue out of patients without PCa diagnosis. CAF, but not BAF, induced a macrophage M2 phenotype with detectable *IL-10* release [66].

Altogether, our results stand in accordance with other recent advances in the field that highlight the importance of stromal fibroblasts for the establishment of an immunosuppressive TME.

## 10) Epithelial cells affect the macrophage phenotype

The effects of conditioned media (CM) from epithelial cells (PC-3, DU-145, LNCaP and BPH-1) on educated macrophages were similar to CAF-mediated effects. Epithelial CM significantly upregulated macrophage *IL-10* (BPH-1 CM) and downregulated *CD206* (PC-3 and DU-145 CM). While some CAF lines induced *CCL18* expression in macrophages, some epithelial cell lines (DU-145 and BPH-1) led to a *CCL18* suppression instead. Our results resemble findings from a Swedish group that demonstrated the capability of PCa CM to induce macrophage *TGFB2* expression [67].

However, the similarities of epithelial- and CAF-mediated effects on the macrophages from our study raise the question whether CM induced gene regulations are really the result of secreted factors.

Instead, CM effects might stem from other peculiarities of the experimental procedure, like nutrient depletion or FCS degradation during the CM preparation steps. CM samples were prepared with starvation media containing 2% FCS. FCS contains significant amounts of M2-polarizing stimuli like TGF- $\beta$ , so the media composition itself has the potential to influence the macrophage phenotype. However, no significant FCS-influence was observable when comparing the effects of starvation media (RPMI with 2% FCS) and THP-1 media (RPMI with 10% FCS) on the macrophage marker transcripts. CM samples were prepared for 24 hours on a confluent cell layer, and fresh media served as macrophage polarization control. In the case that the CM preparation procedure affected nutrient composition or pH of the media, this might also influence the phenotype of educated macrophages.

## 11) CAF from high grade prostate tumors induce macrophage *CCL18*

The effects of NPF and CAF CM on macrophage *CCL18* expression displayed a high inter-individual variability. Patient-stratification by tumor grade revealed that CAF from high grade (Gleason 9; n=6) tumors induced macrophage *CCL18* expression, while low grade CAF (Gleason 7; n=5) did not affect *CCL18* expression levels. *CCL18* induction was not limited to high grade CAF, but also obtained with high grade (patient-matched) NPF.

Similarly, macrophage-education with high grade, but not low grade CAF and NPF, promoted significant macrophage *CCL13* upregulation. Conversely, M1-specific macrophage expression of *TNF* and *HLA-DQA1* was only upregulated by low grade CAF, and not by high grade CAF. This suggests that high grade CAF skew macrophages towards tumor-promoting M2 immunity, a phenotype with known association to PCa progression and metastasis. Not all NPF/CAF pairs had high confidence of CAF identity/activation. Separated analysis of high confidence NPF/CAF pairs reproduced the tendency of high grade CAF and NPF to induce macrophage *CCL18* expression (each  $p=0.057$ ).

There are several studies supporting that tumor progression goes along with a gradual increase of CAF activation. In our study, high grade CAF showed elevated expression of the CAF-specific marker *SFRP1* when compared low grade CAF. Analogue findings on breast cancer CAF showed that expression of the CAF-markers  $PDGFR\alpha$  and  $PDGFR\beta$  increases with the histologic tumor grade [227].

CAF from high grade (Gleason 9), but not from low grade prostate tumors (Gleason 6+7+8), show *IFN $\gamma$*  upregulation [221]. *IFN $\gamma$*  plays an important role for macrophage recruitment and activation, so these findings underline the importance of CAF-origin tumor grade for the CAF-mediated macrophage phenotype. *CCL18* is key mediator of detrimental macrophage effects on breast cancer, where it is held responsible for Treg-mediated immunosuppression [163]. Blood serum *CCL18* levels were correlated with a poor breast cancer prognosis, indicating a prospective value of *CCL18* for biomarker and for drug development [164]. A role of *CCL18* is also documented in pancreatic cancer, where it supposedly mediates tumor progression [162]. Comparison of PCa tissue with patient-matched BPH samples showed cancer-specific *CCL18* upregulation [165, 228], and blood serum *CCL18* levels were successfully utilized to discriminate PCa from BPH patients [166]. Strikingly, the *CCL18* positivity in PCa tissue increases with tumor grade and co-localizes with the macrophage marker *CD68* [165]. The current body of knowledge blends nicely with our postulated influence of the CAF tumor grade on *CCL18* expression in CAF-educated macrophages. Moreover, it supports that our CM experiments represent disease-relevant stromal interactions.

## 12) CAF-secreted *SFRP-1* likely affects macrophage WNT signaling

In NPF/CAF-educated macrophages, expression of the M1-specific marker transcript *TNF* showed a significant negative correlation with NPF/CAF-expression of *SFRP1*. Conversely, expression of the M2-specific marker transcripts *CCL13* and *CCL18* in these macrophages showed a significant positive relationship with *SFRP1* expression in NPF. High grade (Gleason 9) CAF expressed significantly higher *SFRP1* levels than low grade (Gleason 7) CAF and promoted significantly higher *CCL18* expression levels in educated macrophages. This suggests that the WNT inhibitor *SFRP1* might be a CAF-secreted mediator of the macrophage response to CAF CM.

Through its regulatory role for essential cellular functions like proliferation, differentiation and motility, WNT signaling plays a central role during developmental processes. Disruptions of the WNT pathway are found in several diseases including cancers [229]. PCa is associated with epigenetic downregulation of WNT inhibitors [230].

CAF-secreted *SFRP1* has previously been shown to transform prostate epithelial cells [118], demonstrating its paracrine transformative influence in PCa. Interestingly, contradicting evidence favors a beneficial role of *SFRP1* for PCa patients, with decreased *SFRP1* detection in high grade PCa specimen and a positive association of *SFRP1* with patient survival [231]. The tumor-suppressor role of *SFRP1* might stem from its capability to inhibit osteoclast formation [232], especially in consideration of the fact that fatal PCa usually progresses through bone metastasis. DNA damage and oxidative stress promote *SFRP1* secretion, which mediates cellular senescence via WNT signaling [233], so perhaps *SFRP1* is upregulated by stressors of early carcinogenesis before it is inactivated during later stages of cancer progression. Even though the exact role of *SFRP1* for PCa progression is still not clear, our RT-qPCR results propose that *SFRP1* expression is stimulated in high grade CAF. Since TAM are in close vicinity to stromal CAF, CAF-secreted *SFRP1* could be responsible for the unfavorable M2 polarization of prostate TAM.

Indeed, two independent WNT pathways (non-canonical and canonical) help direct the opposing macrophage polarizations through WNT-5a and WNT-3a [234]. While non-canonical WNT-5a signaling mediates the pro-inflammatory (M1 type) response upon pathogen exposure [235], the canonical WNT-3a signaling causes the anti-inflammatory (M2 type) response through the WNT/ $\beta$ -catenin pathway [234, 236]. WNT5a inhibition with SFRP1 skews human and murine macrophages towards M2 [237, 238], and knockdown *versus* overexpression studies on the WNT-3a component  $\beta$ -catenin demonstrated that WNT-3a signaling activates *CCL18* expression [239]. Hence, other studies from the field advocate for the idea that CAF-secreted SFRP1 might be responsible for the observed *CCL18* upregulation in CAF-educated macrophages. Our results however merely show a correlation of CAF *SFRP1* levels and macrophage *CCL18* levels, rather than a causative relationship. Further experiments will be necessary to gain confidence about the functional relevance of our findings.

Apart from *SFRP1*, prostate CAF also secrete significant amounts of other factors with the potential to influence macrophage polarization, such as *TGF- $\beta$*  [142, 240], *CXCL12 (SDF-1)* [66], *M-CSF* and *IFN $\gamma$*  [221]. It appears likely that *SFRP1* represents just one amongst several involved fibroblast derived factors that allow a fine-tuning of the macrophage response, and that several secreted factors are dysregulated during the fibroblast activation to CAF.

### **13) Mast cells suppress the pro-inflammatory macrophage response**

We demonstrated with our CM experiments that LAD2 cells suppress macrophage expression of *TNF* and *HLA-DRA*, two marker genes of the tumoricidal macrophage M1-polarization. Mast cells produce a variety of factors with potential tumor-promoting as well as tumor-rejecting effects [52]. Tumor promoting mast cell products are thought to stimulate angiogenesis (e.g. histamine, VEGF, heparin, IL-8), facilitate matrix degradation (e.g. MCP-4, MCP-6, MMP9), or act as mitogens (e.g. SCF, NGF, IL-8) to directly stimulate cancer cell proliferation [52, 241]. Many mast cell secreted factors have immunomodulatory effects, such as IL-10 [242], IL-4, IL-13 and TNF [243].

Anaphylactic degranulation (AND) and piecemeal degranulation (PMD) represent different mast cell responses. AND was associated with tumor-rejection and PMD is hypothesized to benefit tumor growth, so the delivery of mast cell secreted factors in our experiment is likely relevant for experimental outcomes. While some protocols accomplish mast cell AND by streptavidin ligation of IgE sensitized cells [244], the CM samples from our mast cell culture were recovered from unstimulated mast cells during the media replacement step of regular cell propagation. Consequently, our mast cell CM samples likely contain constitutively secreted mast cell factors instead of degranulation products, and therefore represent the PMD rather than the AND. Since the products of mast cell PMD are associated with cancer progression, it makes sense that our LAD2 CM led to inhibition of the M1-specific macrophage marker genes.

The transcription profiler array from our study showed that the migration inhibitory factor (MIF) had the highest relative transcript levels of all measured genes in both mast cell lines (HMC-1 and LAD2). Functional studies in the mouse showed that MIF promotes melanoma growth by facilitating macrophage M2 polarization, and that treatment with a MIF-antagonist reduced macrophage M2-polarization, immunosuppression, neo-angiogenesis and tumor outgrowth [245]. Accordingly, MIF represents a promising candidate mediator of immunosuppressive mast cell signaling towards macrophages.

#### **14) Co-culture assays support a CAF-mediated epithelial transformation**

CAF share features of myofibroblasts, a fibroblast phenotype that serves the wound healing process. Fibroblast activation includes the acquisition of contractile fibers with *de novo* expression of  $\alpha$ -SMA and the ED-A splice variant of fibronectin [246], and this leads to the formation of contractile fibers and a significant alteration of the ECM. Breast CAF produce a distinct, more aligned ECM when compared to benign fibroblasts from disease-free mammoreduction surgery specimen, and this altered ECM facilitates EMT of mammary epithelial cells [247]. Similarly, increased deposition of fibronectin by prostate CAF results in a more anisotropic ECM pattern that aids directed cancer cell migration [248].

Previous studies at MU confirmed that primary prostate CAF produce a more anisotropic ECM than patient-matched NPF and showed that co-cultured BPH-1 cells assume a more elongated shape on CAF *versus* NPF [38]. Our co-culture experiments were conducted in the same facilities, using the same protocols and instruments, but did not reproduce previous results from MU. Although our results confirmed that CAF consistently produced a more dense, anisotropic F-Actin staining than patient-matched NPF, co-cultured BPH-1 did not consistently assume a more elongated shape on CAF *versus* NPF. Prostate CAF express lower AR levels than patient-matched NPF [25], and the loss of AR signaling in CAF impairs the attachment of myfibroblasts and epithelial cells [116]. It is therefore possible that the CAF lines from our experiments actually induced the expected BPH-1 (spindle-like) form factor changes, but that handling stresses during the FA-fixation and washing steps before confocal imaging disrupted these fragile stromal/epithelial interactions.

CAF and NPF have inherent growth speed differences and are prone to reach confluence at different time points when the same cell numbers are seeded. For the co-culture assays of our experiments, CAF and NPF were seeded with the same cell numbers and cultured, FA-fixed and imaged simultaneously. This poses the risk that growth speed differences between CAF and NPF override the CAF-specific ECM deposition differences.

We repeated co-culture experiments and used live cell time lapse imaging as a less invasive method to capture the BPH-1 cells on CAF *versus* NPF, and this time our results were conforming with previously published results [38]. Four out of 6 NPF/CAF pairs from the live cell imaging experiments had previously been used for confocal imaging and confirmed the CAF-specific influence on the BPH-1 cell shape this time. Consequently, we have reason to assume that confocal imaging results are invalid due to methodological issues. Quantification of the BPH-1 movement during live cell imaging also revealed an increased directed migration in co-culture with CAF. Consequently, live cell time lapse imaging provided a second parameter to confirm the identity/activation of the CAF from our study. These results underline the versatility of live cell time lapse imaging to visualize the transformative CAF-influence on epithelial cells.

### 15) Macrophages disturb prostate tissue integrity and stimulate cell migration

Recently published work from MU showed that CAF induce morphological changes of co-cultured BPH-1 cells [38], and that mast cell proteases (e.g. tryptase) further pronounce CAF-mediated BPH-1 changes [101]. Conversely, the addition of polarized (M1/M2) macrophages to our co-culture experiments led to an increased BPH-1 circularity. We observed that this was associated with concomitant changes of the F-Actin staining, which we could quantify as gaps in the fibroblast cell layer. Because of our issues to reproduce the CAF-specific influence on co-cultured BPH-1 cells in the reference system, we suspected that the observed macrophage-mediated BPH-1 circularity increase might also stem from methodological issues. However, our live cell imaging experiments confirmed that macrophages increase BPH-1 circularity *in vivo*. Live cell time lapse imaging also revealed that macrophage-mediated BPH-1 circularity increases go along with an increased directed cell migration.

This indicates that macrophages disturb stromal/epithelial interactions and facilitate EMT. The ECM represents an important reservoir for cytokines, chemokines and growth factors, which in turn affect the inflammatory response of infiltrating leukocytes [249]. It is commonly assumed that cancer cells produce their own MMP, which enables them to invade the ECM, penetrate the basement membrane and metastasize [250], but also macrophages secrete MMP that can alter ECM and inflammatory signaling by cleavage of secreted factors [251]. Elevated levels of the protease cathepsin are found in pancreatic cancer, breast cancer and also PCa [252], and TAM-secreted cathepsins are held responsible for tumor growth, angiogenesis and invasion [253]. Another important protease for tissue reorganization is plasmin, the effector protease of the plasminogen activation system, which is intimately connected with carcinogenesis through its effects on angiogenesis and cell migration [254]. Plasmin requires activation by the urokinase-type plasminogen activator (uPA). Macrophages possess the uPA receptor (uPAR) on their cell surface, which allows them to bind uPA and exert spatial control of plasmin activity during tissue remodeling. Breast cancer TAM upregulate uPAR [255], and the plasminogen activation system is also relevant for PCa progression. PCa patients show elevated levels of uPA and its receptor (uPAR) in their blood [256, 257] and prostate tissue [258], and uPA<sup>(-/-)</sup> and uPAR<sup>(-/-)</sup> PCa

mouse models successfully demonstrated the necessity of the plasminogen activation system for macrophage infiltration of the PCa tissue. Aspirin successfully suppressed PCa cell migration in a transwell assay by inhibition of MMP9 and uPA [259]. There are many reports highlighting the importance of macrophage proteases for PCa progression, so we have reason to assume that the disruptive macrophage effects in our co-culture experiments are the result of macrophage-secreted proteases.

In cancers, M2-polarized macrophages are generally assumed to be more detrimental than M1-polarized macrophages, which are assigned a tumoricidal role. M1 and M2 macrophages from our co-culture experiments had very similar disruptive effects on BPH-1 cells and F-Actin staining, suggesting that both subtypes produce copious amounts of proteases.

Our transcript profiling of M1- (LPS/IFN $\gamma$ ) and M2-polarized (IL-4/IL-13) macrophages showed that both polarizations express high transcript levels of M1- and M2-specific markers genes when compared to unpolarized macrophages (M $\phi$ ). Polarization experiments with macrophages from atherosclerotic patients revealed that M1 (IL-1 $\beta$  polarized) macrophages have a higher proteolytic activity with elevated expression of MMP9 amongst others, while M2 (IL-4 polarized) macrophages have a more pro-angiogenic gene expression profile [260]. The tumoricidal properties of activated (M1) macrophages are explained with secreted proteases and family 18 chitinases amongst others [261]. However, macrophage M2-polarization with IL-4 was also sufficient to induce cathepsin expression [253], so there are reports that both macrophages subtypes (M1 and M2) produce proteases with the potential to affect our co-culture experiments.

Live cell time lapse imaging of co-culture experiments was able to resolve differences between M1 and M2 macrophages. The BPH-1 motility in co-culture assays with M2 macrophages was significantly higher than with M1 or unpolarized macrophages. Our findings that M2 macrophages increase the migration of co-cultured BPH-1 cells more than M1 macrophages demonstrate that both subtypes have relevant differences. Increased BPH-1 migration in the presence of M2- *versus* M1-macrophages might stem from pro-tumorigenic M2 signaling, or toxic products (e.g. ROS) of the M1 response might immobilize co-cultured BPH-1 cells.

Interestingly, macrophage-mediated BPH-1 form factor changes and the concomitant F-Actin disruption were exclusively observable in our (confocal imaging) experiments with NPF. Neither M1- nor M2-polarized macrophages significantly affected co-culture assays with CAF. However, live cell imaging results demonstrated that macrophage-mediated BPH-1 circularity increases happen on CAF and NPF layers likewise (as shown for NPF/CAF pairs 229R and 332R). Differences of confocal imaging results might stem from the distinct ECM that CAF and NPF produce. Increased CAF-deposition of proteins like  $\alpha$ -SMA and fibronectin probably makes the ECM more resistant against macrophage-derived proteases.

Apart from that, the composition of the ECM might affect the macrophage phenotype. Integral structural components of the ECM are recognized by macrophage cell surface receptors, similar to pathogen-associated molecular patterns (PAMP) [262]. Some of these molecules, such as tenascin-C, biglycan, versican, and hyaluronan, initiate a toll-like receptor (TLR)-mediated immune response [249]. Hyaluronan accumulates in cancer tissue and accelerates tumor growth [263], and increased levels are also detectable in the PCa stroma [264]. Hyaluronan [265] and biglycan [266] were both demonstrated to induce immunosuppressive macrophages. Perhaps the CAF-produced ECM from our experiments skewed co-cultured macrophages towards an immunoregulatory phenotype so that effects on the quantified F-Actin staining were attenuated.

## Limitations & Future Prospects

Our study revealed that CP/CPPS associates with detectable changes in clinical liquid biopsy samples, and that mast cells as well as primary prostate fibroblasts influence the phenotype of *in vitro* polarized macrophages. The co-culture system allowed us to study the interaction of primary cancer-associated fibroblasts (CAF), benign epithelial cells (BPH-1) and macrophages from the prostate tumor microenvironment (TME). However, the methods we used have their limitations and our findings leave many questions unanswered. These could be addressed by future follow-up experiments.

### **1) Our liquid biopsy analysis is limited to Pyrosequencing and RT-qPCR**

After TriFast™ isolation of DNA and RNA from circulating WBC and ejaculated SC, the remaining organic phase was stored (-80°C) to allow protein isolation in the future. The detection of ER $\alpha$ , ER $\beta$  and AR on the protein level could validate the findings of this study and provide supporting evidence that steroid hormone receptor levels of CP/CPPS patients are actually changed.

### **2) Androgen signaling in CP/CPPS patients is not fully characterized**

We measured E2 concentrations and the gene expression of *ESR1*, *ESR2*, *AR* and in semen from CP/CPPS patients, but have no information about semen testosterone levels. Testosterone levels play a vital role for development and pathogenesis of the male reproductive organs and are intimately connected to the inflammatory response. For instance, testosterone was sufficient to ameliorate experimental autoimmune orchitis (EAO) in a mouse model. Specifically, testosterone substitution prevented macrophage infiltration and significantly decreased the frequency of regulatory T cells at the inflammatory site [121]. CP/CPPS patients frequently suffer from hypogonadism, and a propensity-matched study observed that those patients with low testosterone levels (<3.5ng/mL) had significantly elevated NIH-CPSI scores [189]. In a small clinical study with 45 CP/CPPS patients, testosterone treatment for 12 weeks led to a significant reduction of NIH-CPSI scores [267].

In our study, gene expression of the AR was diminished in circulating WBC from ageing men (>40 years), which also had significantly reduced systemic testosterone levels. Besides that, these older patients reported stronger urinary tract symptoms (IPSS score) and had higher inflammatory marker levels (CRP, IL-8, PSA) than the younger patients ( $\leq 40$  years) from our study. However, we did neither characterize the influence of testosterone on macrophages or mast cells, nor did we measure semen testosterone levels to determine whether CP/CPSP associates with changed prostatic testosterone levels. However, it has to be considered that semen has a high testosterone concentration because of the testicular contribution to the ejaculate, so it might be that CP/CPSP-specific prostatic testosterone levels are overshadowed by the testicular contribution to the ejaculate. It also has to be considered that testosterone fluctuations underlie a circadian rhythm, so an accurate comparison of semen testosterone levels between CP/CPSP patients and healthy volunteers might be challenging.

### **3) *BMP7* inactivation could imply loss of TGF- $\beta$ signaling in CP/CPSP**

Semen samples from CP/CPSP patients showed elevated leukocyte counts, and we observed an increased *BMP7* gene promoter CpG methylation in ejaculated SC from CP/CPSP patients ( $p=0.09$ ). Bone morphogenetic proteins (BMP) are members of the transforming growth factor beta (TGF- $\beta$ ) superfamily and play an important role for cell differentiation processes [268]. *BMP7* treatment led to immunoregulatory macrophage M2 polarization *in vitro* [120], and also *in vivo* in atherosclerotic mice [268]. Epigenetic downregulation of the anti-inflammatory mediator *BMP7* could therefore cause an exaggerated pro-inflammatory response in CP/CPSP patients. Since decreased TGF- $\beta$  signaling through BMP downregulation provides a compelling explanation for a chronic inflammatory response in CP/CPSP, it could be worthwhile to investigate the role of *BMP7* for CP/CPSP with follow-up experiments on clinical samples and *in vitro* cell culture model systems.

#### **4) Extended characterization of leukocytes from semen**

We were able to detect CP/CPPS-specific changes of leukocyte transcripts and the steroid sex hormone receptors (*ESR1*, *ESR2*, *AR*) in ejaculated SC. It remains unclear whether the observed CP/CPPS-related changes happen in ejaculated leukocytes, which represent the majority of SC in semen, or other SC (e.g. epithelial cells from the urogenital tract), which can also be present, even if in low numbers. Our results indicate that the frequency and ratio of macrophages and T cells might be changed. Fluorescence-activated cell sorting (FACS) could present a useful approach to determine which somatic cells are present in ejaculated SC, and whether the frequency or differentiation of these cells is affected by CP/CPPS or PCa. Single-cell sequencing of ejaculated SC could provide insights about the leukocyte differentiation state in the semen from CP/CPPS patients.

The profiling of ejaculated SC could be extended to PCa patients. In a first line of experiments, single cell sequencing could be used to compare ejaculated SC from PCa patients with those from BPH patients and healthy volunteers. When a cancer-specific leukocyte differentiation is detectable in the semen from PCa patients, a second line of experiments could be done, comparing ejaculated SC from PCa patients before and after treatment of the disease. This could allow the tracking of the leukocyte differentiation state over time, without the need for invasive tissue biopsies. A detailed insight into the leukocyte differentiation state before and after treatment could help explain why PCa commonly does not respond well to immunotherapy.

#### **5) Isolation and analysis of fibroblasts from expressed prostatic secretions**

During pilot experiments at JLU, we discovered that the prostate massage urine with EPS contained adhesive cell sheets, and we assumed that these cells were differentiated epithelial cells from the prostate. We tried to culture these cells with culture media from a protocol for the culture of prostate epithelial cells from prostatectomy specimen, published by our MU collaboration partners [269].

Cells did neither grow, nor did they attach to the dish surface properly, leading to a successive loss of cells during media replacement steps.

Instead, it could be observed that single, fibroblast-like cells attached to the dish and were able to divide. The fibroblasts from EPS urine might be successfully cultured and characterized when cell culture conditions are optimized for fibroblast growth (e.g. addition of FGF). The measurement of ARO expression in fibroblasts from EPS urine could clarify whether the measured elevation of E2 levels in the semen from CP/CPPS patients is the result of a fibroblast ARO overexpression. Extended profiling could address the question whether the fibroblasts contained in the EPS from CP/CPPS patients are activated and share features with prostate CAF.

### **6) Conditioned media experiments affect activated macrophages differently**

Our CM experiments revealed that mast cells inhibit M1-specific gene expression in educated macrophages, but this was only observable with LAD2 CM, and not with HMC-1 CM. This may be a consequence of the fact that the LAD2 culture media control led to a significant macrophage induction of *TNF* and *HLA-DRA*, and that the secreted factors from LAD2 suppressed these media-induced gene expression changes.

LAD2 culture media contains considerable amounts of stem cell factor (SCF; 100ng/mL). The SCF receptor c-Kit is classically associated with mast cell maturation and degranulation, but recent works show that also DC express c-Kit, and assign a role of the c-Kit-SCF axis for DC-mediated regulation of adaptive immune responses [270]. SCF was shown to act synergistically with colony stimulating factors that stimulate macrophage differentiation [271]. It is therefore likely that the presence of SCF in LAD2 culture media activated the macrophages in our experiments, and we cannot know whether HMC-1 CM would also suppress macrophage markers in the case that these were activated in the first place. The same goes for CAF-, NPF- and epithelial-educated macrophages, it is possible that the M1-suppressive (and therefore M2-promoting) effects of the secreted factors are more visible when macrophages are activated after education with CM.

The effect of CM on (e.g. LPS/IFN $\gamma$  or IL-4/IL13) activated macrophages would be interesting to examine and could reveal a previously masked influence of prostate CAF, epithelial cells and mast cells on the macrophage phenotype.

## 7) More detailed analysis of Wnt signaling in CAF-educated macrophages

Our CAF-educated macrophages showed a phenotype with a high variability that likely reflects the variable composition of CAF-conditioned media samples. M2-specific *CCL18* expression was significantly elevated in macrophages that have been educated by high grade CAF when compared to low grade CAF. More in-depth analysis revealed a significant correlation of CAF-specific *SFRP1* transcript levels with CAF-mediated *CCL18* (and *TNF*) expression in the macrophages. Since secreted *SFRP1* influences Wnt signaling, which in turn affects the macrophage phenotype, it appears likely that CAF-secreted *SFRP1* is responsible for the observed variability.

However, the SFRP family contains 5 members, and analysis of prostate cancer tissue samples revealed a cancer-specific *SFRP1* downregulation with concurrent DNA hypermethylation and/or H3K27 trimethylation [272]. A pan-cancer analysis of SFRP came to the conclusion that *SFRP1* consistently serves a tumorsuppressor role among cancers, while other members, likely stromal-derived *SFRP2* and *SFRP4*, have cancer-promoting properties [273]. Indeed, *SFRP1* shows a positive association with the survival of PCa patients [231], while *SFRP4* levels are increased in PCa specimen and an independent predictor of biochemical recurrence after prostatectomy [274, 275].

In the current study, *SFRP1* has been selected as a CAF-specific marker gene because of its frequent upregulation in prostate CAF [118]. Regarding the current knowledge about *SFRP1* and its (seemingly protective) role in PCa, it is difficult to interpret the correlation of CAF-secreted *SFRP1* levels and macrophage marker transcript expression. A measurement of *SFRP4* expression in the CAF from our experiments would be useful. Moreover, it has to be considered that our results only show a mere correlation of marker transcripts in CAF and CAF-educated macrophages. It is therefore not clear whether the CAF-secreted factors actually act on Wnt signaling, or influence the macrophage phenotype through other pathways. A detailed examination of downstream Wnt signaling molecules in the CAF-educated macrophages, such as  $\beta$ -catenin, could resolve this question.

### **8) Macrophage polarization with seminal plasma from CP/CPSP patients**

We educated THP-1 derived macrophages with CM from primary prostate CAF and provoked a significant change of the macrophage phenotype. CP/CPSP presents a risk factor for PCa, and inflammatory changes are detectable in the semen of CP/CPSP patients. Seminal plasma presents a protein rich, easy-accessible source with possible diagnostic value, and CP/CPSP patients frequently show elevated semen IL-8 concentrations above 10,000pg/mL. IL-8 was shown to attract TAM to hepatocellular carcinoma (HCC), and polarize them towards the tumor-promoting M2 phenotype [276]. Educating THP-1 derived macrophages with seminal plasma samples from CP/CPSP patients and healthy volunteers could help clarify how inflammatory factors from the semen influence macrophage polarization.

### **9) Interrogate the effect of benign-associated fibroblasts on macrophages**

In our study, the CAF- and NPF-mediated effects on educated macrophages showed a high similarity. It would make sense to prove the cancer-specificity of the CAF-mediated macrophage induction of *IL-1B* and *IL-10*. For this, CAF, NPF and benign-associated fibroblasts (BAF) could be compared regarding their CAF-specific marker gene expression and their effects macrophages. This could clarify whether CAF and patient-matched NPF both undergo significant fibroblast activation during prostate carcinogenesis and might explain why CAF- and NPF-mediated effects on macrophage polarization were not significantly different (exception: *CD206*).

### **10) Characterization of macrophages after co-culture experiments**

Neither M1 macrophages, nor M2 macrophages significantly affected the F-Actin staining on CAF, whereas both macrophages subtypes (M1 and M2) produced a significant F-Actin disruption on co-cultured NPF. This suggests that the CAF-produced ECM is either more resistant to macrophage-derived proteases than the NPF-produced ECM, or that direct macrophage/CAF interactions suppress the macrophage activation that we previously obtained by stimulation with LPS/IFN $\gamma$  or IL-4/IL-13.

Macrophages do not exclusively rely on secreted factors for the adaptation to a changing microenvironment, but continuously sample their surroundings by phagocytosis. Efferocytosis, the macrophage clearance of apoptotic cells from the inflammatory site, skews them towards the wound healing phenotype (M2) during all stages of the inflammatory response, from initial cell attraction up to the post-engulfment state of the resolution phase [277]. The NPF/CAF-derived CM samples from our polarization experiments were sterile-filtered before the macrophage-education step, so the process of efferocytosis is likely not adequately represented by our CM experiments. In the co-culture assays on the other hand, macrophages and CAF are in direct contact with each other. Our finding that co-cultured THP-1 cells form patches on CAF underline the fact that direct cell-cell contact is necessary to capture the full range of macrophage interactions with the TME. It also has to be considered that CM experiments emulate unidirectional signaling from CAF towards macrophages, but not *vice versa* signaling. The *in vivo* establishment of possible feedback loops between CAF, epithelial cells and macrophages is therefore not captured by our CM experiments.

To get a more detailed understanding of the CAF-influence on macrophages, examination of the macrophage phenotype after co-culture with CAF *versus* NPF would be useful. For this purpose, co-cultured macrophages could be recovered and analyzed using cell surface-receptor based cell sorting (e.g. FACS).

### **11) Repetition of mast cell culture experiments**

The results from our mast cell culture experiments with estradiol-stimulated HMC-1 and LAD2 cells have a very limited significance because experiments have only been repeated once (n=1). It would be worthwhile to repeat the estradiol-stimulation experiments to find out whether the opposing responses of HMC-1 and LAD2 to estradiol are actually due to differences of the mast cell physiology and the estrogen receptor expression.

## List of References

1. Collins, M.M., et al., *Prevalence and correlates of prostatitis in the health professionals follow-up study cohort*. J Urol, 2002. **167**(3): p. 1363-6.
2. Perletti, G., et al., *The association between prostatitis and prostate cancer. Systematic review and meta-analysis*. Arch Ital Urol Androl, 2017. **89**(4): p. 259-265.
3. Lepor, H., *Pathophysiology of benign prostatic hyperplasia in the aging male population*. Rev Urol, 2005. **7 Suppl 4**: p. S3-s12.
4. NIH, *National Cancer Institute - Cancer Stat Facts: Prostate Cancer*. 2017.
5. Ferlay J, S.I., Ervik M, Dikshit R, Eser S, Mathers C, Rebelo M, Parkin DM, Forman D, Bray, F, *GLOBOCAN 2012 v1.0. Cancer incidence and mortality worldwide. IARC cancer base no. 11*. International Agency for Research on Cancer, Lyon, France, 2013.
6. Wagenlehner, F., et al., *Prostatitis and andrological implications*. Minerva Urol Nefrol, 2013. **65**(2): p. 117-23.
7. Krieger, J.N., L. Nyberg, Jr., and J.C. Nickel, *NIH consensus definition and classification of prostatitis*. Jama, 1999. **282**(3): p. 236-7.
8. Magistro, G., et al., *Contemporary Management of Chronic Prostatitis/Chronic Pelvic Pain Syndrome*. Eur Urol, 2016. **69**(2): p. 286-97.
9. Schaeffer, A.J., et al., *Leukocyte and bacterial counts do not correlate with severity of symptoms in men with chronic prostatitis: the National Institutes of Health Chronic Prostatitis Cohort Study*. J Urol, 2002. **168**(3): p. 1048-53.
10. Shoskes, D.A., et al., *Clinical phenotyping of patients with chronic prostatitis/chronic pelvic pain syndrome and correlation with symptom severity*. Urology, 2009. **73**(3): p. 538-42; discussion 542-3.
11. Magri, V., et al., *Use of the UPOINT chronic prostatitis/chronic pelvic pain syndrome classification in European patient cohorts: sexual function domain improves correlations*. J Urol, 2010. **184**(6): p. 2339-45.
12. Motrich, R.D., et al., *IL-17 is not essential for inflammation and chronic pelvic pain development in an experimental model of chronic prostatitis/chronic pelvic pain syndrome*. Pain, 2016. **157**(3): p. 585-97.
13. Bernoulli, J., et al., *Histopathological evidence for an association of inflammation with ductal pin-like lesions but not with ductal adenocarcinoma in the prostate of the noble rat*. Prostate, 2008. **68**(7): p. 728-39.
14. Ellem, S.J., et al., *Increased endogenous estrogen synthesis leads to the sequential induction of prostatic inflammation (prostatitis) and prostatic pre-malignancy*. Am J Pathol, 2009. **175**(3): p. 1187-99.
15. Surveillance, E., and End Results (SEER) Program of the National Cancer Institute, *Cancer Stat Facts: Prostate Cancer*. The National Institutes of Health (NIH), 2018.
16. Amling, C.L., et al., *Long-term hazard of progression after radical prostatectomy for clinically localized prostate cancer: continued risk of biochemical failure after 5 years*. J Urol, 2000. **164**(1): p. 101-5.

17. Tangen, C.M., et al., *Ten-year survival in patients with metastatic prostate cancer*. Clin Prostate Cancer, 2003. **2**(1): p. 41-5.
18. Nouri, M., et al., *Therapy-induced developmental reprogramming of prostate cancer cells and acquired therapy resistance*. Oncotarget, 2017. **8**(12): p. 18949-18967.
19. Bonkhoff, H. and R. Berges, *The evolving role of oestrogens and their receptors in the development and progression of prostate cancer*. Eur Urol, 2009. **55**(3): p. 533-42.
20. Huggins C, H.C., *Studies on prostatic cancer II: the effects of castration on advanced carcinoma of the prostate gland*. Arch Surg., 1941(43): p. 209–223.
21. Grossmann, M.E., H. Huang, and D.J. Tindall, *Androgen receptor signaling in androgen-refractory prostate cancer*. J Natl Cancer Inst, 2001. **93**(22): p. 1687-97.
22. Azzouni, F. and J. Mohler, *Role of 5alpha-reductase inhibitors in benign prostatic diseases*. Prostate Cancer Prostatic Dis, 2012. **15**(3): p. 222-30.
23. Ihle, C., et al., *Differences in steroid 5alpha-reductase iso-enzymes expression between normal and pathological human prostate tissue*. J Steroid Biochem Mol Biol, 1999. **68**(5-6): p. 189-95.
24. Hudak, S.J., J. Hernandez, and I.M. Thompson, *Role of 5 alpha-reductase inhibitors in the management of prostate cancer*. Clin Interv Aging, 2006. **1**(4): p. 425-31.
25. Ellem, S.J., et al., *A pro-tumourigenic loop at the human prostate tumour interface orchestrated by oestrogen, CXCL12 and mast cell recruitment*. J Pathol, 2014. **234**(1): p. 86-98.
26. Bastian, P.J., et al., *Molecular biomarker in prostate cancer: the role of CpG island hypermethylation*. Eur Urol, 2004. **46**(6): p. 698-708.
27. Dimitrakov, J., et al., *Adrenocortical hormone abnormalities in men with chronic prostatitis/chronic pelvic pain syndrome*. Urology, 2008. **71**(2): p. 261-6.
28. Byun, J.S., et al., *Chronic pelvic pain syndrome and semen quality of Korean men in their fourth decade*. J Androl, 2012. **33**(5): p. 876-85.
29. De Rose, A.F., et al., *Role of mepartricin in category III chronic nonbacterial prostatitis/chronic pelvic pain syndrome: a randomized prospective placebo-controlled trial*. Urology, 2004. **63**(1): p. 13-6.
30. Miodini, P., et al., *The two phyto-oestrogens genistein and quercetin exert different effects on oestrogen receptor function*. Br J Cancer, 1999. **80**(8): p. 1150-5.
31. Shoskes, D.A., et al., *Quercetin in men with category III chronic prostatitis: a preliminary prospective, double-blind, placebo-controlled trial*. Urology, 1999. **54**(6): p. 960-3.
32. Maggiolini, M., et al., *Estrogen receptor alpha mediates the proliferative but not the cytotoxic dose-dependent effects of two major phytoestrogens on human breast cancer cells*. Mol Pharmacol, 2001. **60**(3): p. 595-602.
33. Saijo, K., et al., *An ADIOL-ERbeta-CtBP transrepression pathway negatively regulates microglia-mediated inflammation*. Cell, 2011. **145**(4): p. 584-95.
34. Jacenik, D., et al., *Estrogen signaling deregulation related with local immune response modulation in irritable bowel syndrome*. Mol Cell Endocrinol, 2018. **471**: p. 89-96.

35. Dvorak, H.F., *Tumors: wounds that do not heal. Similarities between tumor stroma generation and wound healing*. N Engl J Med, 1986. **315**(26): p. 1650-9.
36. Liu, T., et al., *Cancer-Associated Fibroblasts Build and Secure the Tumor Microenvironment*. Front Cell Dev Biol, 2019. **7**: p. 60.
37. Cunha, G.R., S.W. Hayward, and Y.Z. Wang, *Role of stroma in carcinogenesis of the prostate*. Differentiation, 2002. **70**(9-10): p. 473-85.
38. Clark, A.K., et al., *A bioengineered microenvironment to quantitatively measure the tumorigenic properties of cancer-associated fibroblasts in human prostate cancer*. Biomaterials, 2013. **34**(20): p. 4777-85.
39. Ao, M., et al., *Cross-talk between paracrine-acting cytokine and chemokine pathways promotes malignancy in benign human prostatic epithelium*. Cancer Res, 2007. **67**(9): p. 4244-53.
40. Costa, A., et al., *Fibroblast Heterogeneity and Immunosuppressive Environment in Human Breast Cancer*. Cancer Cell, 2018. **33**(3): p. 463-479.e10.
41. Oguic, R., et al., *Matrix metalloproteinases 2 and 9 immunoexpression in prostate carcinoma at the positive margin of radical prostatectomy specimens*. Patholog Res Int, 2014. **2014**: p. 262195.
42. Giannoni, E., et al., *Reciprocal activation of prostate cancer cells and cancer-associated fibroblasts stimulates epithelial-mesenchymal transition and cancer stemness*. Cancer Res, 2010. **70**(17): p. 6945-56.
43. Kryza, T., et al., *Kallikrein-related peptidase 4 induces cancer-associated fibroblast features in prostate-derived stromal cells*. Mol Oncol, 2017. **11**(10): p. 1307-1329.
44. Hinz, B., et al., *The myofibroblast: one function, multiple origins*. Am J Pathol, 2007. **170**(6): p. 1807-16.
45. Li, H., et al., *Reference component analysis of single-cell transcriptomes elucidates cellular heterogeneity in human colorectal tumors*. Nat Genet, 2017. **49**(5): p. 708-718.
46. Cheteh, E.H., et al., *Human cancer-associated fibroblasts enhance glutathione levels and antagonize drug-induced prostate cancer cell death*. Cell Death Dis, 2017. **8**(6): p. e2848.
47. He, A. and G.P. Shi, *Mast cell chymase and tryptase as targets for cardiovascular and metabolic diseases*. Curr Pharm Des, 2013. **19**(6): p. 1114-25.
48. Dahlin, J.S. and J. Hallgren, *Mast cell progenitors: origin, development and migration to tissues*. Mol Immunol, 2015. **63**(1): p. 9-17.
49. Maaninka, K., J. Lappalainen, and P.T. Kovanen, *Human mast cells arise from a common circulating progenitor*. J Allergy Clin Immunol, 2013. **132**(2): p. 463-9.e3.
50. Moon, T.C., A.D. Befus, and M. Kulka, *Mast cell mediators: their differential release and the secretory pathways involved*. Front Immunol, 2014. **5**: p. 569.
51. Theoharides, T.C., et al., *Differential release of mast cell mediators and the pathogenesis of inflammation*. Immunol Rev, 2007. **217**: p. 65-78.
52. Conti, P., et al., *Role of mast cells in tumor growth*. Ann Clin Lab Sci, 2007. **37**(4): p. 315-22.

53. Soucek, L., et al., *Mast cells are required for angiogenesis and macroscopic expansion of Myc-induced pancreatic islet tumors*. Nat Med, 2007. **13**(10): p. 1211-8.
54. Andersson, A.C., et al., *Diamines and polyamines in DMBA-induced breast carcinoma containing mast cells resistant to compound 48/80*. Agents Actions, 1976. **6**(5): p. 577-83.
55. Nonomura, N., et al., *Decreased number of mast cells infiltrating into needle biopsy specimens leads to a better prognosis of prostate cancer*. Br J Cancer, 2007. **97**(7): p. 952-6.
56. Fleischmann, A., et al., *Immunological microenvironment in prostate cancer: high mast cell densities are associated with favorable tumor characteristics and good prognosis*. Prostate, 2009. **69**(9): p. 976-81.
57. Xie, H., et al., *Infiltrating mast cells increase prostate cancer chemotherapy and radiotherapy resistances via modulation of p38/p53/p21 and ATM signals*. Oncotarget, 2016. **7**(2): p. 1341-53.
58. Johansson, A., et al., *Mast cells are novel independent prognostic markers in prostate cancer and represent a target for therapy*. Am J Pathol, 2010. **177**(2): p. 1031-41.
59. Pittoni, P., et al., *Mast cell targeting hampers prostate adenocarcinoma development but promotes the occurrence of highly malignant neuroendocrine cancers*. Cancer Res, 2011. **71**(18): p. 5987-97.
60. Done, J.D., et al., *Role of mast cells in male chronic pelvic pain*. J Urol, 2012. **187**(4): p. 1473-82.
61. Zhu, P., et al., *Macrophage/cancer cell interactions mediate hormone resistance by a nuclear receptor derepression pathway*. Cell, 2006. **124**(3): p. 615-29.
62. Escamilla, J., et al., *CSF1 receptor targeting in prostate cancer reverses macrophage-mediated resistance to androgen blockade therapy*. Cancer Res, 2015. **75**(6): p. 950-62.
63. Wang, C., et al., *Blocking the Feedback Loop between Neuroendocrine Differentiation and Macrophages Improves the Therapeutic Effects of Enzalutamide (MDV3100) on Prostate Cancer*. Clin Cancer Res, 2018. **24**(3): p. 708-723.
64. Mills, C.D., *M1 and M2 Macrophages: Oracles of Health and Disease*. Crit Rev Immunol, 2012. **32**(6): p. 463-88.
65. Forssell, J., et al., *High macrophage infiltration along the tumor front correlates with improved survival in colon cancer*. Clin Cancer Res, 2007. **13**(5): p. 1472-9.
66. Comito, G., et al., *Cancer-associated fibroblasts and M2-polarized macrophages synergize during prostate carcinoma progression*. Oncogene, 2014. **33**(19): p. 2423-31.
67. Lundholm, M., et al., *Secreted Factors from Colorectal and Prostate Cancer Cells Skew the Immune Response in Opposite Directions*. Sci Rep, 2015. **5**: p. 15651.
68. Li, M., et al., *Nanoparticles designed to regulate tumor microenvironment for cancer therapy*. Life Sci, 2018. **201**: p. 37-44.
69. Hu, C., et al., *The role of inflammatory cytokines and ERK1/2 signaling in chronic prostatitis/chronic pelvic pain syndrome with related mental health disorders*. Sci Rep, 2016. **6**: p. 28608.

70. Lundh, D., et al., *Assessing chronic pelvic pain syndrome patients: blood plasma factors and cortisol saliva*. Scand J Urol, 2013. **47**(6): p. 521-8.
71. Nishimura, T., et al., *Study of macrophages in prostatic fluid from nonbacterial prostatitis patients. V. Relation between activation of macrophages and stage of prostatitis*. Urol Int, 1991. **46**(1): p. 15-7.
72. Pohl, S.O., et al., *Cross Talk Between Cellular Redox State and the Antiapoptotic Protein Bcl-2*. Antioxid Redox Signal, 2018. **29**(13): p. 1215-1236.
73. Gelain, D.P., et al., *A systematic review of human antioxidant genes*. Front Biosci (Landmark Ed), 2009. **14**: p. 4457-63.
74. Desaint, S., et al., *Mammalian antioxidant defenses are not inducible by H<sub>2</sub>O<sub>2</sub>*. J Biol Chem, 2004. **279**(30): p. 31157-63.
75. Roumequere, T., et al., *Oxidative stress and prostatic diseases*. Mol Clin Oncol, 2017. **7**(5): p. 723-728.
76. Bostwick, D.G., et al., *Antioxidant enzyme expression and reactive oxygen species damage in prostatic intraepithelial neoplasia and cancer*. Cancer, 2000. **89**(1): p. 123-34.
77. Best, C.J., et al., *Molecular alterations in primary prostate cancer after androgen ablation therapy*. Clin Cancer Res, 2005. **11**(19 Pt 1): p. 6823-34.
78. Venkataraman, S., et al., *Manganese superoxide dismutase overexpression inhibits the growth of androgen-independent prostate cancer cells*. Oncogene, 2005. **24**(1): p. 77-89.
79. Kumar, B., et al., *Oxidative stress is inherent in prostate cancer cells and is required for aggressive phenotype*. Cancer Res, 2008. **68**(6): p. 1777-85.
80. Sharifi, N., et al., *Effects of manganese superoxide dismutase silencing on androgen receptor function and gene regulation: implications for castration-resistant prostate cancer*. Clin Cancer Res, 2008. **14**(19): p. 6073-80.
81. Thomas, R. and N. Sharifi, *SOD mimetics: a novel class of androgen receptor inhibitors that suppresses castration-resistant growth of prostate cancer*. Mol Cancer Ther, 2012. **11**(1): p. 87-97.
82. Hu, Y., et al., *Chronic prostatitis/chronic pelvic pain syndrome impairs erectile function through increased endothelial dysfunction, oxidative stress, apoptosis, and corporal fibrosis in a rat model*. Andrology, 2016. **4**(6): p. 1209-1216.
83. Arisan, E.D., et al., *Manganese superoxide dismutase polymorphism in chronic pelvic pain syndrome patients*. Prostate Cancer Prostatic Dis, 2006. **9**(4): p. 426-31.
84. Esteller, M., *CpG island hypermethylation and tumor suppressor genes: a booming present, a brighter future*. Oncogene, 2002. **21**(35): p. 5427-40.
85. Jones, M.J., S.J. Goodman, and M.S. Kobor, *DNA methylation and healthy human aging*. Aging Cell, 2015. **14**(6): p. 924-32.
86. Niwa, T. and T. Ushijima, *Induction of epigenetic alterations by chronic inflammation and its significance on carcinogenesis*. Adv Genet, 2010. **71**: p. 41-56.
87. Mittal, M., et al., *Reactive oxygen species in inflammation and tissue injury*. Antioxid Redox Signal, 2014. **20**(7): p. 1126-67.
88. Kreuz, S. and W. Fischle, *Oxidative stress signaling to chromatin in health and disease*. Epigenomics, 2016. **8**(6): p. 843-62.

89. Ushijima, T. and N. Hattori, *Molecular pathways: involvement of Helicobacter pylori-triggered inflammation in the formation of an epigenetic field defect, and its usefulness as cancer risk and exposure markers*. Clin Cancer Res, 2012. **18**(4): p. 923-9.
90. Hsieh, C.J., et al., *Hypermethylation of the p16INK4a promoter in colectomy specimens of patients with long-standing and extensive ulcerative colitis*. Cancer Res, 1998. **58**(17): p. 3942-5.
91. Issa, J.P., et al., *Accelerated age-related CpG island methylation in ulcerative colitis*. Cancer Res, 2001. **61**(9): p. 3573-7.
92. Katsurano, M., et al., *Early-stage formation of an epigenetic field defect in a mouse colitis model, and non-essential roles of T- and B-cells in DNA methylation induction*. Oncogene, 2012. **31**(3): p. 342-51.
93. Hmadcha, A., et al., *Methylation-dependent gene silencing induced by interleukin 1beta via nitric oxide production*. J Exp Med, 1999. **190**(11): p. 1595-604.
94. Nakayama, M., et al., *Hypermethylation of the human glutathione S-transferase-pi gene (GSTP1) CpG island is present in a subset of proliferative inflammatory atrophy lesions but not in normal or hyperplastic epithelium of the prostate: a detailed study using laser-capture microdissection*. Am J Pathol, 2003. **163**(3): p. 923-33.
95. Zhang, Z.Y. and H.J. Schluesener, *HDAC inhibitor MS-275 attenuates the inflammatory reaction in rat experimental autoimmune prostatitis*. Prostate, 2012. **72**(1): p. 90-9.
96. Schagdarsurengin, U., et al., *Chronic Prostatitis Affects Male Reproductive Health and Is Associated with Systemic and Local Epigenetic Inactivation of C-X-C Motif Chemokine 12 Receptor C-X-C Chemokine Receptor Type 4*. Urol Int, 2017. **98**(1): p. 89-101.
97. Nesheim, N., et al., *Elevated seminal plasma estradiol and epigenetic inactivation of ESR1 and ESR2 is associated with CP/CPPS*. Oncotarget, 2018. **9**(28): p. 19623-19639.
98. Hollander, C., et al., *Human mast cells decrease SLPI levels in type II - like alveolar cell model, in vitro*. Cancer Cell Int, 2003. **3**(1): p. 14.
99. Guhl, S., et al., *Mast cell lines HMC-1 and LAD2 in comparison with mature human skin mast cells--drastically reduced levels of tryptase and chymase in mast cell lines*. Exp Dermatol, 2010. **19**(9): p. 845-7.
100. Chatterjee, S., B. Behnam Azad, and S. Nimmagadda, *The intricate role of CXCR4 in cancer*. Adv Cancer Res, 2014. **124**: p. 31-82.
101. Pereira, B.A., et al., *Tissue engineered human prostate microtissues reveal key role of mast cell-derived tryptase in potentiating cancer-associated fibroblast (CAF)-induced morphometric transition in vitro*. Biomaterials, 2019. **197**: p. 72-85.
102. Nickel, J.C., L.M. Nyberg, and M. Hennenfent, *Research guidelines for chronic prostatitis: consensus report from the first National Institutes of Health International Prostatitis Collaborative Network*. Urology, 1999. **54**(2): p. 229-33.
103. Lotti, F., et al., *Seminal, clinical and colour-Doppler ultrasound correlations of prostatitis-like symptoms in males of infertile couples*. Andrology, 2014. **2**(1): p. 30-41.

104. Hochreiter, W., et al., [*National Institutes of Health (NIH) Chronic Prostatitis Symptom Index. The German version*]. *Urologe A*, 2001. **40**(1): p. 16-7.
105. Pilatz, A., et al., *Acute epididymitis revisited: impact of molecular diagnostics on etiology and contemporary guideline recommendations*. *Eur Urol*, 2015. **68**(3): p. 428-35.
106. Xiao, J., et al., *Atypical microorganisms in expressed prostatic secretion from patients with chronic prostatitis/chronic pelvic pain syndrome: microbiological results from a case-control study*. *Urol Int*, 2013. **91**(4): p. 410-6.
107. WHO, *WHO Laboratory Manual for the Examination and Processing of Human Semen*. Geneva, 2010.
108. Beydola T, Sharma RK, and A. A, *Sperm Preparation and Selection Techniques*, in *Male Infertility Practice*. Jaypee Brothers Medical Publishers: New Delhi. p. 244-251.
109. Nel-Themaat, L., et al., *Cloned embryos from semen. Part 1: in vitro proliferation of epithelial cells on embryonic fibroblasts after isolation from semen by gradient centrifugation*. *Cloning Stem Cells*, 2008. **10**(1): p. 143-60.
110. Olivier, A.J., et al., *Isolation and characterization of T cells from semen*. *J Immunol Methods*, 2012. **375**(1-2): p. 223-31.
111. Kirshenbaum, A.S., et al., *Characterization of novel stem cell factor responsive human mast cell lines LAD 1 and 2 established from a patient with mast cell sarcoma/leukemia; activation following aggregation of FcepsilonRI or FcgammaRI*. *Leuk Res*, 2003. **27**(8): p. 677-82.
112. Yamamoto, M., et al., *Serum estradiol levels in normal men and men with idiopathic infertility*. *Int J Urol*, 1995. **2**(1): p. 44-6.
113. Reeves, A.R., et al., *Controlled release of cytokines using silk-biomaterials for macrophage polarization*. *Biomaterials*, 2015. **73**: p. 272-83.
114. Pidsley, R., et al., *Enduring epigenetic landmarks define the cancer microenvironment*. *Genome Res*, 2018. **28**(5): p. 625-638.
115. Lawrence, M.G., et al., *Reactivation of embryonic nodal signaling is associated with tumor progression and promotes the growth of prostate cancer cells*. *Prostate*, 2011. **71**(11): p. 1198-209.
116. Leach, D.A., et al., *Stromal androgen receptor regulates the composition of the microenvironment to influence prostate cancer outcome*. *Oncotarget*, 2015. **6**(18): p. 16135-50.
117. Vela, I., et al., *PITX2 and non-canonical Wnt pathway interaction in metastatic prostate cancer*. *Clin Exp Metastasis*, 2014. **31**(2): p. 199-211.
118. Joesting, M.S., et al., *Identification of SFRP1 as a candidate mediator of stromal-to-epithelial signaling in prostate cancer*. *Cancer Res*, 2005. **65**(22): p. 10423-30.
119. Naoko Hattori, T.U., *Analysis of Gene-Specific DNA Methylation*, in *Handbook of Epigenetics: The New Molecular and Medical Genetics (Second Edition)*, T.O. Tollefsbol, Editor. 2017, Elsevier Inc.
120. Rocher, C., et al., *Bone morphogenetic protein 7 polarizes THP-1 cells into M2 macrophages*. *Can J Physiol Pharmacol*, 2012. **90**(7): p. 947-51.
121. Fijak, M., et al., *Testosterone replacement effectively inhibits the development of experimental autoimmune orchitis in rats: evidence for a*

- direct role of testosterone on regulatory T cell expansion.* J Immunol, 2011. **186**(9): p. 5162-72.
122. Marunaka, Y., *Roles of interstitial fluid pH in diabetes mellitus: Glycolysis and mitochondrial function.* World J Diabetes, 2015. **6**(1): p. 125-35.
123. Tsilidis, K.K., et al., *Association between endogenous sex steroid hormones and inflammatory biomarkers in US men.* Andrology, 2013. **1**(6): p. 919-28.
124. Elliott, J., et al., *Testosterone therapy in hypogonadal men: a systematic review and network meta-analysis.* BMJ Open, 2017. **7**(11): p. e015284.
125. Wu, F.C., et al., *Identification of late-onset hypogonadism in middle-aged and elderly men.* N Engl J Med, 2010. **363**(2): p. 123-35.
126. Isidori, A.M., et al., *Outcomes of androgen replacement therapy in adult male hypogonadism: recommendations from the Italian society of endocrinology.* J Endocrinol Invest, 2015. **38**(1): p. 103-12.
127. Bechis, S.K., P.R. Carroll, and M.R. Cooperberg, *Impact of age at diagnosis on prostate cancer treatment and survival.* J Clin Oncol, 2011. **29**(2): p. 235-41.
128. DeAntoni, E.P., *Age-specific reference ranges for PSA in the detection of prostate cancer.* Oncology (Williston Park), 1997. **11**(4): p. 475-82, 485; discussion 485-6, 489.
129. Oesterling, J.E., et al., *Serum prostate-specific antigen in a community-based population of healthy men. Establishment of age-specific reference ranges.* Jama, 1993. **270**(7): p. 860-4.
130. HJ., L., S. JF., and R. H., *Age-Specific Reference Ranges for Prostate-Specific Antigen as a Marker for Prostate Cancer.* EAU-EBU Update Series, 2007. **5**(1): p. 38-48.
131. Heerboth, S., et al., *EMT and tumor metastasis.* Clin Transl Med, 2015. **4**: p. 6.
132. Dong, L., et al., *Acidosis activation of the proton-sensing GPR4 receptor stimulates vascular endothelial cell inflammatory responses revealed by transcriptome analysis.* PLoS One, 2013. **8**(4): p. e61991.
133. Riemann, A., et al., *Acidic environment activates inflammatory programs in fibroblasts via a cAMP-MAPK pathway.* Biochim Biophys Acta, 2015. **1853**(2): p. 299-307.
134. Lardner, A., *The effects of extracellular pH on immune function.* J Leukoc Biol, 2001. **69**(4): p. 522-30.
135. Severin, T., et al., *pH-dependent LAK cell cytotoxicity.* Tumour Biol, 1994. **15**(5): p. 304-10.
136. Loeffler, D.A., P.L. Juneau, and G.H. Heppner, *Natural killer-cell activity under conditions reflective of tumor micro-environment.* Int J Cancer, 1991. **48**(6): p. 895-9.
137. Heming, T.A., et al., *Effects of extracellular pH on tumour necrosis factor-alpha production by resident alveolar macrophages.* Clin Sci (Lond), 2001. **101**(3): p. 267-74.
138. Gerry, A.B. and D.S. Leake, *Effect of low extracellular pH on NF- $\kappa$ B activation in macrophages.* Atherosclerosis, 2014. **233**(2): p. 537-44.
139. Bellocq, A., et al., *Low environmental pH is responsible for the induction of nitric-oxide synthase in macrophages. Evidence for involvement of nuclear factor-kappaB activation.* J Biol Chem, 1998. **273**(9): p. 5086-92.

140. Farr, M., et al., *Significance of the hydrogen ion concentration in synovial fluid in rheumatoid arthritis*. Clin Exp Rheumatol, 1985. **3**(2): p. 99-104.
141. Naghavi, M., et al., *pH Heterogeneity of human and rabbit atherosclerotic plaques; a new insight into detection of vulnerable plaque*. Atherosclerosis, 2002. **164**(1): p. 27-35.
142. Spary, L.K., et al., *Tumor stroma-derived factors skew monocyte to dendritic cell differentiation toward a suppressive CD14(+) PD-L1(+) phenotype in prostate cancer*. Oncoimmunology, 2014. **3**(9): p. e955331.
143. Olumi, A.F., et al., *Carcinoma-associated fibroblasts direct tumor progression of initiated human prostatic epithelium*. Cancer Res, 1999. **59**(19): p. 5002-11.
144. Zaichick, V., T.V. Sviridova, and S.V. Zaichick, *Zinc in the human prostate gland: normal, hyperplastic and cancerous*. Int Urol Nephrol, 1997. **29**(5): p. 565-74.
145. Condorelli, R.A., et al., *Chronic prostatitis and its detrimental impact on sperm parameters: a systematic review and meta-analysis*. J Endocrinol Invest, 2017.
146. Mankad, M., et al., *Seminal plasma zinc concentration and alpha-glucosidase activity with respect to semen quality*. Biol Trace Elem Res, 2006. **110**(2): p. 97-106.
147. Gammoh, N.Z. and L. Rink, *Zinc in Infection and Inflammation*. Nutrients, 2017. **9**(6).
148. Om, A.S. and K.W. Chung, *Dietary zinc deficiency alters 5 alpha-reduction and aromatization of testosterone and androgen and estrogen receptors in rat liver*. J Nutr, 1996. **126**(4): p. 842-8.
149. Christudoss, P., et al., *Zinc status of patients with benign prostatic hyperplasia and prostate carcinoma*. Indian J Urol, 2011. **27**(1): p. 14-8.
150. Wessels, I., et al., *Zinc deficiency induces production of the proinflammatory cytokines IL-1beta and TNFalpha in promyeloid cells via epigenetic and redox-dependent mechanisms*. J Nutr Biochem, 2013. **24**(1): p. 289-97.
151. Yencilek, F., et al., *Investigation of Interleukin-1beta Polymorphisms in Prostate Cancer*. Anticancer Res, 2015. **35**(11): p. 6057-61.
152. Goodarzi, D., et al., *The efficacy of zinc for treatment of chronic prostatitis*. Acta Med Indones, 2013. **45**(4): p. 259-64.
153. Olson, M.C., et al., *PU. 1 is not essential for early myeloid gene expression but is required for terminal myeloid differentiation*. Immunity, 1995. **3**(6): p. 703-14.
154. Nerlov, C. and T. Graf, *PU.1 induces myeloid lineage commitment in multipotent hematopoietic progenitors*. Genes Dev, 1998. **12**(15): p. 2403-12.
155. Klemsz, M.J., et al., *Pillars article: the macrophage and B cell-specific transcription factor PU.1 is related to the ets oncogene*. Cell, 1990. **61**: 113-124. J Immunol, 2008. **181**(3): p. 1597-608.
156. Lawrence, T. and G. Natoli, *Transcriptional regulation of macrophage polarization: enabling diversity with identity*. Nat Rev Immunol, 2011. **11**(11): p. 750-61.
157. Yashiro, T., et al., *PU.1 Suppresses Th2 Cytokine Expression via Silencing of GATA3 Transcription in Dendritic Cells*. PLoS One, 2015. **10**(9): p. e0137699.

158. Schutyser, E., A. Richmond, and J. Van Damme, *Involvement of CC chemokine ligand 18 (CCL18) in normal and pathological processes*. J Leukoc Biol, 2005. **78**(1): p. 14-26.
159. Schutyser, E., et al., *Selective induction of CCL18/PARC by staphylococcal enterotoxins in mononuclear cells and enhanced levels in septic and rheumatoid arthritis*. Eur J Immunol, 2001. **31**(12): p. 3755-62.
160. Goebeler, M., et al., *Differential and sequential expression of multiple chemokines during elicitation of allergic contact hypersensitivity*. Am J Pathol, 2001. **158**(2): p. 431-40.
161. de Nadai, P., et al., *Involvement of CCL18 in allergic asthma*. J Immunol, 2006. **176**(10): p. 6286-93.
162. Ye, H., et al., *Tumor-associated macrophages promote progression and the Warburg effect via CCL18/NF- $\kappa$ B/VCAM-1 pathway in pancreatic ductal adenocarcinoma*. Cell Death Dis, 2018. **9**(5): p. 453.
163. Su, S., et al., *Blocking the recruitment of naive CD4(+) T cells reverses immunosuppression in breast cancer*. Cell Res, 2017. **27**(4): p. 461-482.
164. Sun, J.H., N. Fan, and Y. Zhang, *Correlation between serum level of chemokine (C-C motif) ligand 18 and poor prognosis in breast cancer*. Genet Mol Res, 2016. **15**(3).
165. Chen, G., et al., *CC chemokine ligand 18 correlates with malignant progression of prostate cancer*. Biomed Res Int, 2014. **2014**: p. 230183.
166. Xu, Y., et al., *CC chemokine ligand 18 and IGF-binding protein 6 as potential serum biomarkers for prostate cancer*. Tohoku J Exp Med, 2014. **233**(1): p. 25-31.
167. Vulcano, M., et al., *Unique regulation of CCL18 production by maturing dendritic cells*. J Immunol, 2003. **170**(7): p. 3843-9.
168. Schraufstatter, I.U., et al., *The chemokine CCL18 causes maturation of cultured monocytes to macrophages in the M2 spectrum*. Immunology, 2012. **135**(4): p. 287-98.
169. Gunther, C., et al., *CCL18 is expressed in atopic dermatitis and mediates skin homing of human memory T cells*. J Immunol, 2005. **174**(3): p. 1723-8.
170. Adema, G.J., et al., *A dendritic-cell-derived C-C chemokine that preferentially attracts naive T cells*. Nature, 1997. **387**(6634): p. 713-7.
171. Hieshima, K., et al., *A novel human CC chemokine PARC that is most homologous to macrophage-inflammatory protein-1 alpha/LD78 alpha and chemotactic for T lymphocytes, but not for monocytes*. J Immunol, 1997. **159**(3): p. 1140-9.
172. Kouivaskaia, D.V., et al., *T-cell recognition of prostatic peptides in men with chronic prostatitis/chronic pelvic pain syndrome*. J Urol, 2009. **182**(5): p. 2483-9.
173. Olsen, N.J. and W.J. Kovacs, *Gonadal steroids and immunity*. Endocr Rev, 1996. **17**(4): p. 369-84.
174. Gubbels Bupp, M.R., *Sex, the aging immune system, and chronic disease*. Cell Immunol, 2015. **294**(2): p. 102-10.
175. Islander, U., et al., *Estrogens in rheumatoid arthritis; the immune system and bone*. Mol Cell Endocrinol, 2011. **335**(1): p. 14-29.
176. Seillet, C., et al., *The TLR-mediated response of plasmacytoid dendritic cells is positively regulated by estradiol in vivo through cell-intrinsic estrogen receptor alpha signaling*. Blood, 2012. **119**(2): p. 454-64.

177. Papenfuss, T.L., et al., *Estriol generates tolerogenic dendritic cells in vivo that protect against autoimmunity*. J Immunol, 2011. **186**(6): p. 3346-55.
178. Gold, S.M. and R.R. Voskuhl, *Estrogen treatment in multiple sclerosis*. J Neurol Sci, 2009. **286**(1-2): p. 99-103.
179. Offner, H. and M. Polanczyk, *A potential role for estrogen in experimental autoimmune encephalomyelitis and multiple sclerosis*. Ann N Y Acad Sci, 2006. **1089**: p. 343-72.
180. Polanczyk, M.J., et al., *Enhanced FoxP3 expression and Treg cell function in pregnant and estrogen-treated mice*. J Neuroimmunol, 2005. **170**(1-2): p. 85-92.
181. Laffont, S., C. Seillet, and J.C. Guery, *Estrogen Receptor-Dependent Regulation of Dendritic Cell Development and Function*. Front Immunol, 2017. **8**: p. 108.
182. Liu, H.Y., et al., *Estrogen inhibition of EAE involves effects on dendritic cell function*. J Neurosci Res, 2002. **70**(2): p. 238-48.
183. Polanczyk, M.J., et al., *T lymphocytes do not directly mediate the protective effect of estrogen on experimental autoimmune encephalomyelitis*. Am J Pathol, 2004. **165**(6): p. 2069-77.
184. Ghisletti, S., et al., *17beta-estradiol inhibits inflammatory gene expression by controlling NF-kappaB intracellular localization*. Mol Cell Biol, 2005. **25**(8): p. 2957-68.
185. Villa, A., et al., *Estrogen accelerates the resolution of inflammation in macrophagic cells*. Sci Rep, 2015. **5**: p. 15224.
186. Carreras, E., et al., *Estrogen receptor signaling promotes dendritic cell differentiation by increasing expression of the transcription factor IRF4*. Blood, 2010. **115**(2): p. 238-46.
187. Kovats, S., *Estrogen receptors regulate innate immune cells and signaling pathways*. Cell Immunol, 2015. **294**(2): p. 63-9.
188. Yan, X.J., et al., *Vagal afferents mediate antinociception of estrogen in a rat model of visceral pain: the involvement of intestinal mucosal mast cells and 5-hydroxytryptamine 3 signaling*. J Pain, 2014. **15**(2): p. 204-17.
189. Lee, J.H. and S.W. Lee, *Testosterone and Chronic Prostatitis/Chronic Pelvic Pain Syndrome: A Propensity Score-Matched Analysis*. J Sex Med, 2016. **13**(7): p. 1047-55.
190. Li, L.C., et al., *Frequent methylation of estrogen receptor in prostate cancer: correlation with tumor progression*. Cancer Res, 2000. **60**(3): p. 702-6.
191. Lau, K.M., et al., *Expression of estrogen receptor (ER)-alpha and ER-beta in normal and malignant prostatic epithelial cells: regulation by methylation and involvement in growth regulation*. Cancer Res, 2000. **60**(12): p. 3175-82.
192. Daniels, G., et al., *Decreased expression of stromal estrogen receptor alpha and beta in prostate cancer*. Am J Transl Res, 2014. **6**(2): p. 140-6.
193. Leav, I., et al., *Comparative studies of the estrogen receptors beta and alpha and the androgen receptor in normal human prostate glands, dysplasia, and in primary and metastatic carcinoma*. Am J Pathol, 2001. **159**(1): p. 79-92.
194. Fujimura, T., et al., *Differential expression of estrogen receptor beta (ERbeta) and its C-terminal truncated splice variant ERbetacx as*

- prognostic predictors in human prostatic cancer. Biochem Biophys Res Commun, 2001. 289(3): p. 692-9.*
195. Pasquali, D., et al., *Loss of estrogen receptor beta expression in malignant human prostate cells in primary cultures and in prostate cancer tissues. J Clin Endocrinol Metab, 2001. 86(5): p. 2051-5.*
196. Horvath, L.G., et al., *Frequent loss of estrogen receptor-beta expression in prostate cancer. Cancer Res, 2001. 61(14): p. 5331-5.*
197. Zhu, X., et al., *Dynamic regulation of estrogen receptor-beta expression by DNA methylation during prostate cancer development and metastasis. Am J Pathol, 2004. 164(6): p. 2003-12.*
198. Purohit, A., S.P. Newman, and M.J. Reed, *The role of cytokines in regulating estrogen synthesis: implications for the etiology of breast cancer. Breast Cancer Res, 2002. 4(2): p. 65-9.*
199. Reed, M.J., et al., *Interleukin-1 and interleukin-6 in breast cyst fluid: their role in regulating aromatase activity in breast cancer cells. J Endocrinol, 1992. 132(3): p. R5-8.*
200. Ellem, S.J., et al., *Local aromatase expression in human prostate is altered in malignancy. J Clin Endocrinol Metab, 2004. 89(5): p. 2434-41.*
201. Zhao, Y., et al., *Aromatase P450 gene expression in human adipose tissue. Role of a Jak/STAT pathway in regulation of the adipose-specific promoter. J Biol Chem, 1995. 270(27): p. 16449-57.*
202. Calippe, B., et al., *17Beta-estradiol promotes TLR4-triggered proinflammatory mediator production through direct estrogen receptor alpha signaling in macrophages in vivo. J Immunol, 2010. 185(2): p. 1169-76.*
203. Santagati, S., et al., *Oligonucleotide squelching reveals the mechanism of estrogen receptor autologous down-regulation. Mol Endocrinol, 1997. 11(7): p. 938-49.*
204. Ellison-Zelski, S.J., N.M. Solodin, and E.T. Alarid, *Repression of ESR1 through actions of estrogen receptor alpha and Sin3A at the proximal promoter. Mol Cell Biol, 2009. 29(18): p. 4949-58.*
205. Barchiesi, F., et al., *Differential regulation of estrogen receptor subtypes alpha and beta in human aortic smooth muscle cells by oligonucleotides and estradiol. J Clin Endocrinol Metab, 2004. 89(5): p. 2373-81.*
206. Wagenlehner, F.M., et al., *National Institutes of Health Chronic Prostatitis Symptom Index (NIH-CPSI) symptom evaluation in multinational cohorts of patients with chronic prostatitis/chronic pelvic pain syndrome. Eur Urol, 2013. 63(5): p. 953-9.*
207. Beutel, M.E., et al., *Correlations between hormones, physical, and affective parameters in aging urologic outpatients. Eur Urol, 2005. 47(6): p. 749-55.*
208. Chernecky CC, B.B., *Laboratory Tests and Diagnostic Procedures. 6 ed. Elsevier Saunders. 2013, St Louis, MO. 440-446.*
209. Hutchison RE, S.K., *Henry's Clinical Diagnosis and Management by Laboratory Methods. 23 ed. 2017, St Louis, MO: Elsevier.*
210. Molero, L., et al., *Expression of estrogen receptor subtypes and neuronal nitric oxide synthase in neutrophils from women and men: regulation by estrogen. Cardiovasc Res, 2002. 56(1): p. 43-51.*
211. Southren, A.L., et al., *Mean plasma concentration, metabolic clearance and basal plasma production rates of testosterone in normal young men and women using a constant infusion procedure: effect of time of day and*

- plasma concentration on the metabolic clearance rate of testosterone.* J Clin Endocrinol Metab, 1967. **27**(5): p. 686-94.
212. Torjesen, P.A. and L. Sandnes, *Serum testosterone in women as measured by an automated immunoassay and a RIA.* Clin Chem, 2004. **50**(3): p. 678; author reply 678-9.
213. Sader, M.A., et al., *Androgen receptor gene expression in leucocytes is hormonally regulated: implications for gender differences in disease pathogenesis.* Clin Endocrinol (Oxf), 2005. **62**(1): p. 56-63.
214. McCrohon, J.A., et al., *Androgen receptor expression is greater in macrophages from male than from female donors. A sex difference with implications for atherogenesis.* Circulation, 2000. **101**(3): p. 224-6.
215. Kovats, S., *Estrogen receptors regulate an inflammatory pathway of dendritic cell differentiation: mechanisms and implications for immunity.* Horm Behav, 2012. **62**(3): p. 254-62.
216. Schmid, M.A., et al., *Instructive cytokine signals in dendritic cell lineage commitment.* Immunol Rev, 2010. **234**(1): p. 32-44.
217. Carreras, E., et al., *Estradiol acts directly on bone marrow myeloid progenitors to differentially regulate GM-CSF or Flt3 ligand-mediated dendritic cell differentiation.* J Immunol, 2008. **180**(2): p. 727-38.
218. Medina, K.L., et al., *Identification of very early lymphoid precursors in bone marrow and their regulation by estrogen.* Nat Immunol, 2001. **2**(8): p. 718-24.
219. Zhang, A., et al., *Cancer-associated fibroblasts promote M2 polarization of macrophages in pancreatic ductal adenocarcinoma.* Cancer Med, 2017. **6**(2): p. 463-470.
220. Cohen, N., et al., *Fibroblasts drive an immunosuppressive and growth-promoting microenvironment in breast cancer via secretion of Chitinase 3-like 1.* Oncogene, 2017. **36**(31): p. 4457-4468.
221. Liao, C.P., et al., *Androgen receptor in cancer-associated fibroblasts influences stemness in cancer cells.* Endocr Relat Cancer, 2017. **24**(4): p. 157-170.
222. Chen, P.C., et al., *Prostate cancer-derived CCN3 induces M2 macrophage infiltration and contributes to angiogenesis in prostate cancer microenvironment.* Oncotarget, 2014. **5**(6): p. 1595-608.
223. Mittal, S.K., et al., *Interleukin 10 (IL-10)-mediated Immunosuppression: MARCH-1 INDUCTION REGULATES ANTIGEN PRESENTATION BY MACROPHAGES BUT NOT DENDRITIC CELLS.* J Biol Chem, 2015. **290**(45): p. 27158-67.
224. Horvat, V., et al., *Association of IL-1beta and IL-10 Polymorphisms with Prostate Cancer Risk and Grade of Disease in Eastern Croatian Population.* Coll Antropol, 2015. **39**(2): p. 393-400.
225. Eiro, N., et al., *Analysis of the expression of interleukins, interferon beta, and nuclear factor-kappa B in prostate cancer and their relationship with biochemical recurrence.* J Immunother, 2014. **37**(7): p. 366-73.
226. Liu, Q., et al., *Interleukin-1beta promotes skeletal colonization and progression of metastatic prostate cancer cells with neuroendocrine features.* Cancer Res, 2013. **73**(11): p. 3297-305.
227. Kim, H.M., Y.K. Lee, and J.S. Koo, *Expression of CAF-Related Proteins Is Associated with Histologic Grade of Breast Phyllodes Tumor.* Dis Markers, 2016. **2016**: p. 4218989.

- 
228. Wang, S., et al., *Sex steroid-induced DNA methylation changes and inflammation response in prostate cancer*. Cytokine, 2016. **86**: p. 110-118.
229. Coudreuse, D. and H.C. Korswagen, *The making of Wnt: new insights into Wnt maturation, sorting and secretion*. Development, 2007. **134**(1): p. 3-12.
230. Ying, Y. and Q. Tao, *Epigenetic disruption of the WNT/beta-catenin signaling pathway in human cancers*. Epigenetics, 2009. **4**(5): p. 307-12.
231. Zheng, L., et al., *Diagnostic value of SFRP1 as a favorable predictive and prognostic biomarker in patients with prostate cancer*. PLoS One, 2015. **10**(2): p. e0118276.
232. Hausler, K.D., et al., *Secreted frizzled-related protein-1 inhibits RANKL-dependent osteoclast formation*. J Bone Miner Res, 2004. **19**(11): p. 1873-81.
233. Elzi, D.J., et al., *Wnt antagonist SFRP1 functions as a secreted mediator of senescence*. Mol Cell Biol, 2012. **32**(21): p. 4388-99.
234. Schaale, K., et al., *Wnt signaling in macrophages: augmenting and inhibiting mycobacteria-induced inflammatory responses*. Eur J Cell Biol, 2011. **90**(6-7): p. 553-9.
235. Blumenthal, A., et al., *The Wingless homolog WNT5A and its receptor Frizzled-5 regulate inflammatory responses of human mononuclear cells induced by microbial stimulation*. Blood, 2006. **108**(3): p. 965-73.
236. Zhang, P., J. Katz, and S.M. Michalek, *Glycogen synthase kinase-3beta (GSK3beta) inhibition suppresses the inflammatory response to Francisella infection and protects against tularemia in mice*. Mol Immunol, 2009. **46**(4): p. 677-87.
237. Chen, D., et al., *Wnt5a Deficiency Regulates Inflammatory Cytokine Secretion, Polarization, and Apoptosis in Mycobacterium tuberculosis-Infected Macrophages*. DNA Cell Biol, 2017. **36**(1): p. 58-66.
238. Pereira, C., et al., *Wnt5A/CaMKII signaling contributes to the inflammatory response of macrophages and is a target for the antiinflammatory action of activated protein C and interleukin-10*. Arterioscler Thromb Vasc Biol, 2008. **28**(3): p. 504-10.
239. Yang, C.M., et al., *beta-Catenin promotes cell proliferation, migration, and invasion but induces apoptosis in renal cell carcinoma*. Onco Targets Ther, 2017. **10**: p. 711-724.
240. Gong, D., et al., *TGFβ signaling plays a critical role in promoting alternative macrophage activation*. BMC Immunol, 2012. **13**: p. 31.
241. Maltby, S., K. Khazaie, and K.M. McNagny, *Mast cells in tumor growth: angiogenesis, tissue remodelling and immune-modulation*. Biochim Biophys Acta, 2009. **1796**(1): p. 19-26.
242. Grimbaldston, M.A., et al., *Mast cell-derived interleukin 10 limits skin pathology in contact dermatitis and chronic irradiation with ultraviolet B*. Nat Immunol, 2007. **8**(10): p. 1095-104.
243. Galli, S.J., M. Grimbaldston, and M. Tsai, *Immunomodulatory mast cells: negative, as well as positive, regulators of immunity*. Nat Rev Immunol, 2008. **8**(6): p. 478-86.
244. Kuehn, H.S., M. Radinger, and A.M. Gilfillan, *Measuring mast cell mediator release*. Curr Protoc Immunol, 2010. **Chapter 7**: p. Unit7.38.
-

245. Yaddanapudi, K., et al., *Control of tumor-associated macrophage alternative activation by macrophage migration inhibitory factor*. J Immunol, 2013. **190**(6): p. 2984-93.
246. Cirri, P. and P. Chiarugi, *Cancer associated fibroblasts: the dark side of the coin*. Am J Cancer Res, 2011. **1**(4): p. 482-97.
247. Dumont, N., et al., *Breast fibroblasts modulate early dissemination, tumorigenesis, and metastasis through alteration of extracellular matrix characteristics*. Neoplasia, 2013. **15**(3): p. 249-62.
248. Erdogan, B., et al., *Cancer-associated fibroblasts promote directional cancer cell migration by aligning fibronectin*. J Cell Biol, 2017. **216**(11): p. 3799-3816.
249. Iijima, J., K. Konno, and N. Itano, *Inflammatory alterations of the extracellular matrix in the tumor microenvironment*. Cancers (Basel), 2011. **3**(3): p. 3189-205.
250. Dandekar, R.C., A.V. Kingaonkar, and G.S. Dhabekar, *Role of macrophages in malignancy*. Ann Maxillofac Surg, 2011. **1**(2): p. 150-4.
251. Elkington, P.T., J.A. Green, and J.S. Friedland, *Analysis of matrix metalloproteinase secretion by macrophages*. Methods Mol Biol, 2009. **531**: p. 253-65.
252. Fernandez, P.L., et al., *Expression of cathepsins B and S in the progression of prostate carcinoma*. Int J Cancer, 2001. **95**(1): p. 51-5.
253. Gocheva, V., et al., *IL-4 induces cathepsin protease activity in tumor-associated macrophages to promote cancer growth and invasion*. Genes Dev, 2010. **24**(3): p. 241-55.
254. McMahon, B. and H.C. Kwaan, *The plasminogen activator system and cancer*. Pathophysiol Haemost Thromb, 2008. **36**(3-4): p. 184-94.
255. Hildenbrand, R., et al., *Urokinase plasminogen activator receptor (CD87) expression of tumor-associated macrophages in ductal carcinoma in situ, breast cancer, and resident macrophages of normal breast tissue*. J Leukoc Biol, 1999. **66**(1): p. 40-9.
256. Miyake, H., et al., *Elevation of serum levels of urokinase-type plasminogen activator and its receptor is associated with disease progression and prognosis in patients with prostate cancer*. Prostate, 1999. **39**(2): p. 123-9.
257. Shariat, S.F., et al., *Association of the circulating levels of the urokinase system of plasminogen activation with the presence of prostate cancer and invasion, progression, and metastasis*. J Clin Oncol, 2007. **25**(4): p. 349-55.
258. Li, Y. and P.J. Cozzi, *Targeting uPA/uPAR in prostate cancer*. Cancer Treat Rev, 2007. **33**(6): p. 521-7.
259. Shi, C., et al., *Aspirin Inhibits IKK-beta-mediated Prostate Cancer Cell Invasion by Targeting Matrix Metalloproteinase-9 and Urokinase-Type Plasminogen Activator*. Cell Physiol Biochem, 2017. **41**(4): p. 1313-1324.
260. Roma-Lavisse, C., et al., *M1 and M2 macrophage proteolytic and angiogenic profile analysis in atherosclerotic patients reveals a distinctive profile in type 2 diabetes*. Diab Vasc Dis Res, 2015. **12**(4): p. 279-89.
261. Pan, X.Q., *The mechanism of the anticancer function of M1 macrophages and their use in the clinic*. Chin J Cancer, 2012. **31**(12): p. 557-63.
262. Schaefer, L., *Extracellular matrix molecules: endogenous danger signals as new drug targets in kidney diseases*. Curr Opin Pharmacol, 2010. **10**(2): p. 185-90.

- 
263. Itano, N., L. Zhuo, and K. Kimata, *Impact of the hyaluronan-rich tumor microenvironment on cancer initiation and progression*. *Cancer Sci*, 2008. **99**(9): p. 1720-5.
264. Josefsson, A., et al., *Prostate cancer increases hyaluronan in surrounding nonmalignant stroma, and this response is associated with tumor growth and an unfavorable outcome*. *Am J Pathol*, 2011. **179**(4): p. 1961-8.
265. Kuang, D.M., et al., *Tumor-derived hyaluronan induces formation of immunosuppressive macrophages through transient early activation of monocytes*. *Blood*, 2007. **110**(2): p. 587-95.
266. Chieppa, M., et al., *Cross-linking of the mannose receptor on monocyte-derived dendritic cells activates an anti-inflammatory immunosuppressive program*. *J Immunol*, 2003. **171**(9): p. 4552-60.
267. Ran Pang, J.L., Xinyao Zhou, Xiaosong Gao, Yaqiang Zhang, ***Testosterone replacement therapy for hypogonadal patients with chronic prostatitis / chronic pelvic pain syndrome***. *The Journal of Urology*, 2015. **193**(4S): p. e285.
268. Singla, D.K., R. Singla, and J. Wang, *BMP-7 Treatment Increases M2 Macrophage Differentiation and Reduces Inflammation and Plaque Formation in Apo E<sup>-/-</sup> Mice*. *PLoS One*, 2016. **11**(1): p. e0147897.
269. Niranjana, B., et al., *Primary culture and propagation of human prostate epithelial cells*. *Methods Mol Biol*, 2013. **945**: p. 365-82.
270. Ray, P., et al., *Signaling of c-kit in dendritic cells influences adaptive immunity*. *Ann N Y Acad Sci*, 2010. **1183**: p. 104-22.
271. Brizzi, M.F., et al., *Regulation of c-kit expression in human myeloid cells*. *Stem Cells*, 1993. **11 Suppl 2**: p. 42-8.
272. Garcia-Tobilla, P., et al., *SFRP1 repression in prostate cancer is triggered by two different epigenetic mechanisms*. *Gene*, 2016. **593**(2): p. 292-301.
273. Vincent, K.M. and L.M. Postovit, *A pan-cancer analysis of secreted Frizzled-related proteins: re-examining their proposed tumour suppressive function*. *Sci Rep*, 2017. **7**: p. 42719.
274. Mortensen, M.M., et al., *Expression profiling of prostate cancer tissue delineates genes associated with recurrence after prostatectomy*. *Sci Rep*, 2015. **5**: p. 16018.
275. Sandsmark, E., et al., *SFRP4 gene expression is increased in aggressive prostate cancer*. *Sci Rep*, 2017. **7**(1): p. 14276.
276. Xiao, P., et al., *Neurotensin/IL-8 pathway orchestrates local inflammatory response and tumor invasion by inducing M2 polarization of Tumor-Associated macrophages and epithelial-mesenchymal transition of hepatocellular carcinoma cells*. *Oncoimmunology*, 2018. **7**(7): p. e1440166.
277. Elliott, M.R., K.M. Koster, and P.S. Murphy, *Efferocytosis Signaling in the Regulation of Macrophage Inflammatory Responses*. *J Immunol*, 2017. **198**(4): p. 1387-1394.

## List of Abbreviations

Abbreviation	Meaning
5hmC	5-hydroxymethylcytosine
5mC	5-methylcytosine
A	Adenine
AdT	Androgen-deprivation therapy
AND	Anaphylactic degranulation
AR	Androgen receptor
ARO	Aromatase (Gene: <i>CYP19A1</i> )
BAF	Benign-associated fibroblasts (also referred to as human prostate fibroblasts: HPF)
BPH	Benign prostatic hyperplasia
BPH-1	Benign prostatic hyperplasia 1 (Immortalized benign prostate epithelial cell line)
C	Cytosine
CAF	Cancer-associated fibroblasts
ChIP	Chromatin immunoprecipitation
CM	Conditioned media
CMFDA	5-chloromethylfluorescein diacetate
CO <sub>2</sub>	Carbon Dioxide
COBRA	Combined bisulfite restriction analysis
CP/CPPS	Chronic prostatitis/chronic pelvic pain syndrome
CP/CPPS IIIa	CP/CPPS subcategory with detectable leukocyte infiltration
CP/CPPS IIIb	CP/CPPS subcategory without detectable leukocyte infiltration
CpG site	Nucleotide sequence where cytosine is followed by guanine in 5' to 3' direction
CPSI	NIH-CPSI: Chronic prostatitis symptom index of the NIH
CRP	C-Reactive Protein
Ct value	Cycle threshold value (quantitative PCR)
CXCL12	C-X-C motif chemokine 12 (SDF-1)
CXCR4	C-X-C chemokine receptor type 4; CXCL12 (SDF-1) receptor
DC	Dendritic cell
DEPC	Diethyl pyrocarbonate
DMEM	Dulbecco's modified Eagle's medium

---

DMSO	Dimethyl sulfoxide
DNA	Deoxyribonucleic acid
dNTP	Deoxynucleotide
DGC	Density gradient centrifugation
DSS	Dextran sulfate sodium
DU-145	Immortalized prostate cancer cell line from a central nervous system metastasis
E2	Estradiol
EAP	Experimental autoimmune prostatitis
ECM	Extracellular matrix
EDTA	Ethylenediamine tetraacetic acid
EMT	Epithelial-mesenchymal transition
EPS	Expressed prostatic secretions
ER	Estrogen receptor
ER $\alpha$	Estrogen receptor <i>alpha</i>
ER $\beta$	Estrogen receptor <i>beta</i>
ESR1	Estrogen receptor 1, gene locus of estrogen receptor <i>alpha</i> (ER $\alpha$ )
ESR2	Estrogen receptor 2, gene locus of estrogen receptor <i>beta</i> (ER $\beta$ )
EtOH	Ethanol
F12	Nutrient mixture F-12
FA	Formaldehyde
FACS	Fluorescence-activated cell sorting
FCS	Fetal calf serum
FGF	Fibroblast growth factor
FIJI	FIJI is just ImageJ (ImageJ distribution)
G	Guanine
GSTP1	Glutathione S-transferase P
HADS	Hospital Anxiety and Depression Scale
HEPES	4-(2-hydroxyethyl)-1-piperazineethanesulfonic acid
HMC-1	Human mast cell line-1 (Immortalized mast cell line)
IDC-P	Intraductal carcinoma of the prostate
IFN $\gamma$	Interferon gamma, <i>IFNG</i> gene
IHC	Immunohistochemistry
ILs	Interleukins (e.g. IL-4, IL-13, IL-1 $\beta$ )
IPSS	International prostate symptom score

---

JLU	Justus-Liebig-University
LAD2	Leukocyte adhesion deficiency-2 (Immortalized mast cell line)
LNCaP	Lymph node carcinoma of the prostate (Immortalized prostate cancer cell line)
M1 macrophages	Macrophages polarized (e.g. with LPS/IFN $\gamma$ ) towards type 1 (Th1) immunity (also called classically activated macrophages)
M2 macrophages	Macrophages polarized (e.g. with IL-4/IL-13) towards type 2 (Th2) immunity (also called alternatively activated macrophages)
MeOH	Methanol
MIF	Macrophage migration inhibitory factor
MMP	Matrix metalloproteinase
MS	Multiple sclerosis
MU	Monash-University
M $\phi$	Macrophage
N/A	Not applicable
NIH	National institutes of health
NIH II	NIH classification of prostatitis: Chronic bacterial prostatitis
NIH III	NIH classification of prostatitis: Chronic abacterial prostatitis (CP/CPSP)
NO	Nitric oxide
NOS2	Inducible nitric oxide synthase (iNOS)
NPF	Non-malignant fibroblasts
O <sub>2</sub>	Oxygen
PBS	Phosphate-buffered saline
PBT	Phosphate-buffered saline with Tween-20
PC-3	Immortalized prostate cancer cell line, established from a bone metastasis
PCa	Prostate carcinoma
PCR	Polymerase chain reaction
PIA	Proliferative inflammatory atrophy
PIN	Prostatic intraepithelial neoplasia
PMA	Phorbol 12-Myristate 13-Acetate
PSA	Prostate-specific antigen
RA	Rheumatoid arthritis
RNA	Ribonucleic acid
RPMI	Roswell Park Memorial Institute medium

RT	Room temperature
RT-qPCR	Reverse transcription followed by quantitative real-time PCR
SC	Somatic cells
SCF	Stem cell factor
SDF-1	Stromal cell-derived factor 1 (CXCL12)
SFRP1	Secreted frizzled-related protein 1
SP	Seminal plasma
SD	Standard deviation
SVI	Seminal vesicle invasion
T	Thymine
T/E2 ratio	Testosterone/estrogen ratio
TAM	Tumor-associated macrophages
Th1	Helper T cells (Th) that produce pro-inflammatory cytokines (e.g. IFN $\gamma$ )
Th2	Helper T cells (Th) that produce anti-inflammatory cytokines (e.g. IL-4, IL-13)
THP-1	Immortalized human monocytic cell line (derived from acute monocytic leukemia)
TLR	Toll-like receptor
TME	Tumormicroenvironment
TNF	Tumor necrosis factor
tPSA	Total prostate-specific antigen
TRITC	Tetramethylrhodamine
TSS	Transcription start site
UKGM	Universitätsklinikum Gießen und Marburg
uPA	Urokinase-type plasminogen activator
uPAR	Receptor of the urokinase-type plasminogen activator
UPOINT	CP/CPPS classification system by symptoms (U: Urinary; P: Psychosocial; O: Organ specific; I: Infection; N: Neurologic/Systemic; T: Tenderness)
WBC	White blood cells
WHO	World health organization
$\alpha$ -SMA	Alpha-smooth muscle actin
$\Delta$ Ct	Delta Ct value, Ct(gene of interest)-Ct(reference gene)
$\Delta\Delta$ Ct	Delta $\Delta$ Ct value, $\Delta$ Ct(sample)- $\Delta$ Ct(control)

## List of Equipment, Chemicals and Labware

<b>Part 1: Equipment</b>	<b>Vendor</b>
Benchtop Centrifuge (Universal 320)	Hettich, Germany
Biological Safety Cabinet (MSC-Advantage)	Thermo Fisher Scientific, Germany
Bioruptor®	Diagenode, Belgium
Cell culture CO2 incubator (Heracell150i)	Thermo Fisher Scientific, Germany
CFX96 Touch™ Real-Time PCR Detection System	Bio-Rad, Germany
Eppendorf Thermo Mixer	Eppendorf, Germany
Gel documentation system (BioDocAnalyze)	Biometra, Germany
Heating block (LS 2)	VLM, Germany
Heidolph Reax 2000 shaker	Heidolph, Germany
HERAfreeze™ HFU T Series -86°C Freezer	Thermo Fisher Scientific, Germany
Incubating Mini Shaker	VWR, Germany
Integrated Live Cell Workstation (AF6000LX)	Leica, Germany
Invitrogen Power Ease® 500 Power Supply	Thermo Fisher Scientific, Germany
JB Aqua Plus Unstirred Water Bath	Grant, Germany
Leica ICC50 HD microscope	Leica, Germany
Magnetic Stirrer (BLSH0007)	IKAMAG, Germany
Mastercycler	Eppendorf, Germany
Mettler Toledo AE 240 balance	Mettler Toledo, Germany
Microlitre Centrifuge (MIKRO 220R)	Hettich, Germany
Microwave oven	LG, South Korea
Milli-Q® Direct Water Purification System	Merck KGaA, Germany
Mini-PROTEAN Tetra Cell	Bio-Rad, Germany
NanoDrop ND-1000	PEQLAB, Germany
Nikon C1 Inverted Confocal Microscope	Nikon Instruments, Germany
Odyssey® Fc Imaging System	LI-COR, Bad-Homburg
Phase-contrast inverted microscope (CK2)	Olympus, Germany
Power PAC 200	Bio-Rad, Germany
PyroMark Q24 Cartridge	Qiagen, Germany
Pyromark Q24 instrument	Qiagen, Germany

SevenEasy S20-K pH meter	Mettler Toledo, Germany
Standard Mini-Centrifuge	Fisherbrand, Germany
Stratagene qPCR System (Mx3000P)	Agilent, California
T100™ Thermal Cycler	Bio-Rad, Germany
Trans-Blot SD Semi-Dry Transfer Cell	Bio-Rad, Germany
Vibra-Cell™ Ultrasonic Liquid Processor	Bioblock scientific, Germany

<b>Part 2: Chemicals</b>	<b>Vendor</b>
30% Acrylamide/Bis Solution, 29:1	Bio-Rad, Munich
Acetic acid	Roth, Karlsruhe
Agarose	Roth, Karlsruhe
Ammonium chloride (NH <sub>4</sub> Cl)	Roth, Karlsruhe
Ammonium persulfate (APS)	Sigma-Aldrich, Steinheim
Bovine serum albumin (BSA)	Roth, Karlsruhe
Chloroform	Roth, Karlsruhe
Diethypyrocarbonate (DEPC)	Sigma-Aldrich, Steinheim
Dithiothreitol (DTT)	Roth, Karlsruhe
Ethanol	Sigma-Aldrich, Steinheim
Ethylenediamine tetraacetic acid (EDTA)	Roth, Karlsruhe
Formaldehyde (FA)	Sigma-Aldrich, Steinheim
Glycerol	Roth, Karlsruhe
Glycine	Roth, Karlsruhe
Glycogen	Invitrogen, Karlsruhe
Guanidine thiocyanate	Roth, Karlsruhe
Histopaque®-1077	Sigma-Aldrich, Steinheim
Hydrogen chloride (HCl), 2 N	Roth, Karlsruhe
Isopropanol	Sigma-Aldrich, Steinheim
Lithium chloride (LiCl)	Roth, Karlsruhe
Methanol	Sigma-Aldrich, Steinheim
N,N,N',N'-Tetramethylethylenediamine (TEMED)	Roth, Karlsruhe
Nonidet™ P 40 Substitute	Merck, Darmstadt
Paraformaldehyde (PFA)	Merck, Darmstadt
peqGOLD TriFast™	VWR, Erlangen
Phenol/chloroform/Isoamylalcohol (25:24:1)	Roth, Karlsruhe
Phosphate buffered saline (PBS)	Sigma-Aldrich, Steinheim

Potassium bicarbonate (KHCO <sub>3</sub> )	Roth, Karlsruhe
Protease inhibitor cocktail tablets	Sigma-Aldrich, Steinheim
Sodium acetate (NaOAc)	Roth, Karlsruhe
Sodium bicarbonate (NaHCO <sub>3</sub> )	Merck, Darmstadt
Sodium chloride (NaCl)	Roth, Karlsruhe
Sodium citrate (tri-Sodium citrate dihydrate)	Merck, Darmstadt
Sodium deoxycholate	Merck, Darmstadt
Sodium dodecyl sulfate (SDS)	Roth, Karlsruhe
Sodium hydroxide (NaOH)	Roth, Karlsruhe
Tetrasodium EDTA	Roth, Karlsruhe
Tris-base	Roth, Karlsruhe
Tris-HCl	Roth, Karlsruhe
Triton X-100	Sigma-Aldrich, Steinheim
Tween-20	Roth, Karlsruhe
β-Mercaptoethanol (β-met)	AppliChem, Darmstadt

<b>Part 3: Cell Culture</b>	<b>Vendor</b>
12mL Polypropylene tubes	Sarstedt, Nümbrecht
BD falcon 24-well plates	BD falcon, Franklin Lake, USA
BPH-1 cells	Monash University, Australia
Cell Tracker green-CMFD	Invitrogen, Karlsruhe
Collagenase Type I	Sigma-Aldrich, Darmstadt
Dulbecco's Modified Eagle Medium (DMEM)	Life Technologies, Darmstadt
Dulbecco's Modified Eagle Medium (DMEM)-F12	Gibco, Darmstadt
Dulbecco's PBS (1×) w/o Ca <sup>2+</sup> & Mg <sup>2+</sup>	Gibco, Darmstadt
Estradiol (Cat. No. E8875-1G)	Sigma-Aldrich, Darmstadt
FCS (Monash University)	Thermo Fisher Scientific, Waltham
Fetal calf serum (Justus-Liebig University)	Biochrom AG, Berlin
Fibroblast growth factor (FGF) (Cat. PHG6015)	Life Technologies, Darmstadt
Gentamicin	Life Technologies, Darmstadt
HEPES	Life Technologies, Darmstadt
HMC-1 cells	Mayo Clinic, USA
Hyaluronidase Type II	Sigma-Aldrich, Darmstadt

Iscove's Modified Dulbecco's Media (IMDM) with 1.2mM thioglycerol	Thermo Fisher Scientific, Waltham
LAD2 cells	National Institutes of Health, USA
LPS (Cat. No. L4391)	Sigma-Aldrich, Darmstadt
PC-3, DU-145, LNCaP and THP-1 cells	Deutsche Sammlung von Mikroorganismen und Zellkulturen (DSMZ), Braunschweig
Penicillin/Streptomycin	Gibco, Darmstadt
Phalloidin-TRITC (Tetramethylrhodamine)	Invitrogen, Australia
PMA (Phorbol-12-Myristate-13-acetate) (Cat. No. Ab120297)	Abcam, Cambridge (UK)
Recombinant Human IFN $\gamma$ (Cat. No. 300-02)	Peptidech, Hamburg
Recombinant Human IL-13 (Cat. No. 200-13)	Peptidech, Hamburg
Recombinant Human IL-4 (Cat. No. 200-04)	Peptidech, Hamburg
Roswell Park Memorial Institute (RPMI)-1640 medium	Life Technologies, Darmstadt
RPMI-1640 medium without phenol red	Thermo Fisher Scientific, Waltham
StemPro™-34 serum-free growth medium	Invitrogen, Australia
Synth-a-Freeze cryopreservation	Gibco, Darmstadt
T-25 flasks	Life Technologies, Darmstadt
T-75 flasks	Life Technologies, Darmstadt
T-175 flasks	Life Technologies, Darmstadt
Testosterone, (Cat. No. T1500)	SigmaAldrich, Darmstadt
TrypLE™ Express	Gibco, Darmstadt

**Part 4: Polymerase Chain Reaction****Vendor**

dNTP Mix	Promega, Mannheim
EDTA (0.5 M), pH 8.0	Thermo Scientific, Waltham
GelRed Nucleic Acid Gel Stain	Biotium, Fremont
GeneRuler DNA Ladder Mix	Thermo Scientific, Waltham
M-MLV Reverse Transcriptase	Promega, Mannheim
MyTaq™ mix	Bioline, Taunton
Oligo dT	Promega, Mannheim
Orange G	Merck, Darmstadt
Proteinase K	Roth, Karlsruhe

RNase inhibitor	Promega, Mannheim
RNase-free DNase I (Justus-Liebig-University)	New England Biolabs GmbH, Frankfurt am Main
RNase-free DNase I (Monash-University) (Cat No. 79254)	Qiagen, Melbourne
RNeasy Mini Kit (Cat No. 74104)	Qiagen, Hilden
Rotor-Gene SYBR Green PCR kit	Qiagen, Hilden
RT2 Profiler PCR array “Human cytokines and chemokines”	Qiagen, Hilden

<b>Part 5: Methylation Analysis</b>	<b>Vendor</b>
EpiMark® Bisulfite Conversion Kit	New England Biolabs, Ipswich
EpiTect Methyl II “Human Cytokine Production Signature Panel”	Qiagen, Hilden
PyroMark Annealing Buffer	Qiagen, Hilden
PyroMark Binding Buffer	Qiagen, Hilden
PyroMark Denaturation Solution	Qiagen, Hilden
PyroMark Gold Q24 Reagents	Qiagen, Hilden
PyroMark Wash Buffer	Qiagen, Hilden
Streptavidin-coated Sepharose beads	GE Healthcare, Freiburg

<b>Part 6: Western Blot</b>	<b>Vendor</b>
Coomassie stain	Roth, Karlsruhe
Rabbit polyclonal anti-GAPDH antibody	Sigma-Aldrich, Steinheim
Laemmli sample buffer (6x)	Bio-Rad, Munich
Mouse monoclonal anti-CCL18 (MIP-4) antibody (sc-374438)	Santa Cruz, Dallas
Pierce BCA Protein Assay Kit	Thermo Fisher Scientific, St. Louis, USA
Chameleon™ Duo Prestained Protein Ladder	LI-COR, Bad-Homburg
PageRuler Prestained Protein Ladder	Thermo Fisher Scientific, St. Louis, USA
IRDye® 800CW Goat anti-Rabbit IgG	LI-COR, Bad-Homburg
Odyssey® Blocking Buffer (PBS)	LI-COR, Bad-Homburg
Immobilon®-FL PVDF membrane	LI-COR, Bad-Homburg

Coomassie stain	Roth, Karlsruhe
REVERT™ Total Protein Stain	LI-COR, Bad-Homburg

**Part 7: Chromatin Immunoprecipitation Vendor**

---

Dynabeads™ Protein G Immunoprecipitation Kit	Invitrogen, Karlsruhe
Monoclonal mouse Estrogen Receptor $\alpha$ antibody (Cat. 61035)	Active Motif, Belgium
Monoclonal rabbit H3K4me3 antibody (Cat. 17-614)	Millipore, Darmstadt
Mouse IgG isotype control (Cat. 31903)	Invitrogen, Karlsruhe

